

THE EFFECTS OF CO-ADMINISTRATION OF ANTIRETROVIRAL DRUGS AND/OR
TOPIRAMATE ON THE MIGRATION OF NEURAL CREST CELLS AND NEUROGENESIS IN
AVIAN BRAINS.

UNIVERSITY OF THE
WITWATERSRAND,
JOHANNESBURG



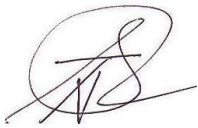
Thabiso Tshabalala

9502128Y

*This thesis is submitted in the fulfillment of the requirements for the degree of Doctor of
Philosophy.*

Declaration

I Thabiso Tshabalala declare that this thesis is my own, original work. It is being submitted for the degree of Doctor of Philosophy in the School of Anatomical Sciences, Faculty of Health Sciences, University of the Witwatersrand, Johannesburg, and has never been submitted before for any degree or examination in this University or any other university.



Thabiso Tshabalala

January 2021

Dedication

This work is dedicated to my mother, **Maria Ketimelwang Tshabalala**. Thank you for making me the man that I am today.

(1957-2006)

May her soul rest in eternal peace.

My brother, **Motsosi Tshabalala**. Thank you for taking care of me when I was sick in 2015. Life has never been the same without you.

(1974-2016)

May his soul rest in peace.

My sister, **Matshidiso Tshabalala**. Thank you for all the motivation and unwavering support.

Presentations arising from this study

Tshabalala T, Nkomozezi P, Ihunwo A, Mbajjorgu F. (2019). The effect of Atripla and Topiramate on the migration of avian neural crest cells (Oral presentation). 48th Annual Conference of the Anatomical Society of Southern Africa, Durban, South Africa (19-22 April 2020)

Abstract accepted but the conference could not take place due to the corona virus.

Publications arising from this study

Tshabalala, T, Nkomozezi, P, Ihunwo, AO, Mbajjorgu, F. Coadministration of ARV (Atripla) and Topiramate disrupts quail cardiac neural crest cell migration. Birth Defects Research. 2021; 113: 485– 499. <https://doi.org/10.1002/bdr2.1871>

Tshabalala T, Nkomozezi P, Ihunwo A, Mbajjorgu F. (2021). **The effects of co-administration of combination antiretroviral therapy and Topiramate on cranial neural crest cell migration: impact on congenital craniofacial anomalies.** Article submitted in Congenital Anomalies Journal (under review)

Tshabalala T, Nkomozezi P, Ihunwo A, Mbajjorgu F. (2021). **Altered prenatal expression of Aquaporin 4 and inhibition of protein synthesis in developing *Gallus gallus domesticus* brains by combination antiretroviral drug and topiramate therapy: clinical implications in hydrocephalus.** Article in progress

Acknowledgements

I would like to express my deep and sincere gratitude to my research supervisors, Professor Felix Mbajorgu, Professor Amadi Ihunwo for providing invaluable guidance throughout the research. I am extremely grateful for their contribution and effort. It was a great privilege to work under their guidance. Also, I would like to thank Dr. Philani Nkomozepe for collaborative work.

Also, I would like to express my heartfelt thanks to Mrs. Hasiena Ali for her technical assistance, particularly for her expertise in quantitative PCR and Immunochemistry. Above all I would like to thank her for her friendship, empathy and for always encouraging me throughout my research. Her efforts did not go unnoticed and are greatly appreciated.

In addition, I would like to thank the Faculty of Health Sciences for their contribution to this work through the enabling grant which allowed me to buy consumables for this research. The completion of this thesis would not have been possible without their generous contribution.

Abstract

The administration of combination antiretroviral drugs (cART) during pregnancy has been shown to cause a myriad of congenital malformations. Birth defects such as cleft lip and palate, ventricular septal defect, neuronal migration disorders and hydrocephalus have been observed in children born to women who are on antiretroviral therapy. However, the mechanism of teratogenicity is unclear and therefore the focus of this study. Some HIV patients on antiretrovirals develop seizures and are therefore placed on antiepileptic drugs such as topiramate, which is also teratogenic. The interactive effects arising from this therapeutic combination may affect their teratogenic propensity. Due to the involvement of cranial and cardiac neural crest cells in the formation of craniofacial and cardiovascular structures, the current study investigated the effect of cART and topiramate on the migration of these two populations of cells. The extent of migration as well as proliferation of neural tube-derived neurons was determined in order to investigate the mechanisms of neuronal migration disorders. In addition, the study investigated the effects of cART and topiramate on the expression of aquaporin 4 during *Gallus gallus* brain development due to the major role played by this gene in the transportation of water in the brain. Appropriately cultured neural crest cells from dissected neural tubes of 32 (cardiac) and 36-hour old (cranial) quail embryos exposed to culture media containing peak plasma levels of Atripla, Topiramate and the combination of both were studied. The migration of neural crest cells was determined using the migration assay and the cells were stained with rhodamine phalloidin to evaluate the cell actin. In addition, cardiac quail neural crest cells were brought into suspension and micro-injected into chick hosts to determine the migration of the cells to the interventricular septum. The differentiation of cranial neural crest cells into melanocytes, osteoblasts and neurites was also evaluated. Neural tube-derived neurons were stained with DCX, while the expression of Rac and Rho were determined using quantitative PCR. The expression of AQP4 and Ribosomal protein S17 was investigated using quantitative PCR. The administration of cART and topiramate inhibited the migration of both cardiac and cranial neural crest cells while it downregulated the expression of DCX and the Rac genes in neural tube-derived neurons and induced the aquaporin 4 expression in early developing brain. These findings indicate that cART and Topiramate cause ventricular septal defects and craniofacial anomalies by inhibiting the migration of neural crest cells while they cause neuronal migration disorders and hydrocephalus by inhibiting the migration of neurons and by inducing the expression of aquaporin 4 respectively. In addition, these findings show that cART and Topiramate inhibit the migration of both cardiac and cranial neural crest cells when administered individually and in combination. The combination with Topiramate showed that Topiramate does not inhibit the activity of cART in most instances. These results suggest that the combination of cART and Topiramate may be ideal for patients who require treatment with antiretrovirals and antiepileptic drugs.

Table of contents	Page no
Title page	I
Declaration	II
Dedication	III
Presentations arising from this thesis	IV
Publications arising from this thesis	IV
Acknowledgements	V
Abstract	VI
Table of contents	VII
List of figures	XII
List of abbreviations	XVII
CHAPTER 1: Introduction and chapter outline	
1.0 Introduction	1
1.1 Ventricular septal defects	4
1.2 Cleft lip and palate	5
1.3 Neuronal migration disorders	7
1.4 Hydrocephalus	8
1.5 Rationale	9
1.6 Aim	9
1.7 Study objectives	9
1.8 Chapter outline	11
CHAPTER 2: Literature review	
2.1.0 Antiretroviral therapy	
2.1.1 Atripla	14
2.1.2 Efavirenz and Pregnancy	15
	VII

2.1.3	Tenofovir during gestation	15
2.2.0	Teratogenic effects of AEDs	16
2.2.1	Topiramate	17
2.3.0	Causes of seizures in HIV	18
2.4.0	The neural crest	19
2.4.1	Factors affecting the migration of neural crest cells	22
2.4.2	Mechanism of neural crest cell migration	23

CHAPTER 3

3.1.0	Introduction	25
3.2.0	Cranial neural crest cells and bone formation	26
3.3.0	Osteoblastic differentiation of cranial neural crest cells	27
3.4.0	The differentiation of melanocytes from neural crest cells and HIV-OMH	28
3.2.0	Material and methods	31
3.2.1	Drugs	31
3.2.2	Ethical clearance	31
3.2.3	Preparation of equipment	32
3.2.4	Embryos	32
3.2.5	Neural tube cultures	32
3.2.6	Measurement of quail neural crest cell migration	33
3.2.7	Actin staining and quantification	34
3.2.8	Determination and quantification of pigmentation	34
3.2.9	Detection of mineralization (Alizarin method)	35
3.2.10	Neurite thickness measurements	35
3.2.11	Statistical analysis	36
3.3.0	Results	37
3.3.1	Migration of neural crest cells	37
3.3.2	Actin cytoskeletal elements at 24 hours	38
3.3.3	Actin cytoskeletal elements after 48 hours	38
3.3.4	Differentiation of neural crest cells into melanocytes	39
3.3.5	Neurite outgrowth	39
3.3.6	Alizarin red for calcium detection	41

3.4.0 Discussion	49
3.4.1 Conclusion	54
CHAPTER 4	
4.1.0 Introduction	55
4.1.1 The origin and migratory pathways of cardiac neural crest cells	56
4.1.2 Cardiac neural crest cells and pharyngeal arch arteries	56
4.1.3 Cardiac neural crest cells and the formation of interventricular and aorticopulmonary septa	57
4.2.0 Material and methods	59
4.2.1 Drugs	59
4.2.2 Embryos and Ethical clearance	59
4.2.3 Preparation of equipment	59
4.2.4 Neural tube cultures	59
4.2.5 Measurement of quail neural crest cell migration	60
4.2.6 Actin staining and quantification	60
4.2.7 Suspension of cultured neural crest cells to obtain cells for micro-injection	60
4.2.8 Transfer of cultured and suspended quail neural crest cells into a chick host	61
4.2.9 The quail neural crest cell experiment	61
4.2.10 Statistical analysis	60
4.3.0 Results	64
4.3.1 Cell migration	65
4.3.2 The <i>in vivo</i> migration of quail neural crest cells into chick hosts	65
4.3.3 Quantitative analysis	67
4.4.0 Discussion	77
4.4.1 Conclusion	80

CHAPTER 5

5.1.0 Introduction	82
5.1.1 The development of neurons	86
5.2.0 Material and methods	90
5.2.1 Drugs	90
5.2.2 Ethical clearance	90
5.2.3 Preparation of equipment	90
5.2.4 Embryos	90
5.2.5 Neural tube cultures	90
5.2.6 Immunocytochemistry	91
5.2.7 Neurite measurements	92
5.2.8 Rhodamine Phalloidin staining	92
5.2.9 MTT assay for cell proliferation	93
5.2.10 RNA extraction	93
5.2.11 Reverse Transcription (cDNA synthesis)	95
5.2.12 Statistical analysis	95
5.2.13 Primer design	96
5.2.14 Quantitative PCR data analysis	97
5.3.0 Results	98
5.3.1 DCX Staining	98
5.3.2 Actin staining	99
5.3.3 MTT Proliferation assay	100
5.3.4 Gene expression	100
5.4.0 Discussion	110
5.4.1 Conclusion	114

CHAPTER 6

6.1.0 Introduction	116
6.1.1 AQP4 Structure	118
6.1.2 Cerebral edema and Hydrocephalus	119
6.1.3 Antiretroviral therapy and ribosomal proteins	119

6.2.0 Material and Methods	124
6.2.1 Drugs	124
6.2.2 The <i>in vivo</i> administration of drugs into chicken embryos.	124
6.2.3 RNA extraction	125
6.2.4 Reverse transcription and quantitative PCR	126
6.2.5 Evaluation of AQP 4 and RPS17 genes expression	126
6.2.6 Statistical analysis	126
6.2.7 Genes and Primers	127
6.3.0 Results	128
6.3.1 Survival rates	128
6.3.2 Aquaporin 4 and RPS17 gene expression in Day 7 brains	129
6.3.3 Aquaporin 4 and RPS17 gene expression in Day 14 brains	129
6.3.4 Aquaporin 4 and RPS17 gene expression in Day 20 brains	129
6.4 Discussion	133
6.5 Conclusion	137
 CHAPTER 7	
7.1.0 Concluding Discussion	138
7.1.1 Efavirenz as a choice for women of child bearing age	139
7.1.2 Dolutegravir vs Efavirenz for women of child bearing age	140
7.1.3 Choice of AED for HIV patients	142
7.1.4 Neural crest cells in congenital anomalies	143
7.1.5 The probable mechanism of cART and TOP cytotoxicity on the actin cytoskeleton	145
7.1.6 Rationale for the choice of neural crest cell migration assay	146
7.1.7 The choice of the avian model for the study	148
7.1.8 Cytochrome P450 activity in avian neural crest cells	149
7.1.9 Limitations and future studies	150
Reference list	151

List of figures

Figure 3.1. Photomicrographs showing the migration of cranial neural crest cells (NCC) from a neural tube (NT) cultured in DMEM only (A), DMSO only (B), DMEM + cART only (C), TOP only (D), and cART/TOP (E) after 24 hours. Neural crest cells (NCC) have migrated a greater distance (orange double-headed arrows) in control explants (A, B) compared to the treated cultures (C, D, E).

Figure 3.2. Photomicrographs showing migration of cranial neural crest cells (NCC) from a neural tube (NT) cultured in DMEM only (A), DMSO only (B), cART only (C), TOP only (D), and cART/TOP (E) after 24 hours. Neural crest cells (NCC) have migrated a greater distance (orange double-headed arrows) in control explants (A, B) compared to the treated cultures (C, D, E). A space in the delamination process (blue arrow) is evident in the Topiramate-treated and cART/TOP-treated neural crest cells (D, E). (Magnification 100X).

Figure 3.3. Fluorescence photomicrographs showing actin filaments in cranial neural crest cells which were cultured in DMEM only (A), DMSO only (B), TOP only (C), cART only (D) and cART/TOP (E) after 24 hours. Control neural crest cells (A, B) are polygonal in shape (blue arrows). A filapodium extension which has detached from a migrating neural crest cell is shown by a white arrow. Actin filaments in treated cultures (C, D, E) are more confined to the extremities of the cells, while the centre appear vacuolated.

Figure 3.4. Fluorescence photomicrographs showing actin filaments in cranial neural crest cells which were cultured in DMEM only (A), DMSO only (B), TOP only (C), cART only (D) and cART/TOP (E) after 48 hours. Control neural crest cells (A, B) appear polygonal in shape (blue arrows). A filapodium extension which has detached from a migrating neural crest cell is shown by a white arrow. All the treated neural crest cells (C, D, E) appear rounded (yellow arrows) and the actin filaments are more restricted to the boundaries of the cells

Figure 3.5. Photomicrographs showing pigment development in cranial neural crest cells cultured in DMEM only (A), DMSO only (B), cART only (C), TOP only (D) and cART/TOP (E) after 96 hours. cART only-treated cells seemed to be producing more pigment as the melanin appeared darker (yellow circle) than in the controls and other treated cultures (yellow arrow). Magnification (200X).

Figure 3.6. Photomicrographs showing neurite development in cranial neural crest cells cultured in DMEM only (A), DMSO only (B), cART only (C), TOP only (D) and cART/TOP (E) after 96 hours. cART only-treated neural crest cells produced more numerous neurites with greater arborization (orange arrows). Neurites cultured in TOP and cART/TOP appeared longer and thinner with less arborization (orange arrows). Control cultures (A, B) exhibited neurites which were less numerous and shorter than neurites of treated cultures (C, D, E) (Magnification 200X).

Figure 3.7. Photomicrographs showing calcium production in cranial neural crest cells (NCC) cultured in DMEM only (A), DMSO only (B), TOP only (C), cART only (D) and cART/TOP (E) after 96 hours. Control neural crest cells (A, B) stained positive with Alizarin red for calcium deposition, while the cART-treated and TOP-treated cells did not stain. Neural crest cells cultured in cART/TOP showed a light shade of red (blue circle), while the neural tube (NT) stained a red colour (Magnification 100X).

Figure 4.1. 1A shows a summary diagram illustrating the *in vitro* neural tube culture technique and the microinjection of quail cardiac neural crest cells into chicken host embryos, while 1B shows photomicrographs of the control neural tube (NT) and migrating neural crest cells (NCC) after 24 (A) and 48 hours (B) in culture. A polygon tool (blue) was used to measure the area migrated by cardiac neural crest cells.

Figure 4.2. Photomicrographs showing neural crest cells cultured in DMEM only (2A), DMSO only (2B), TOP only (2C), cART only (2D), and cART/TOP (2E) after 24 hours. Neural crest cells (NCC) have migrated a greater distance (orange double-headed arrows) in control explants (A, B) compared to the treated cultures (C, D, E). The control and some of the TOP-treated cells were polygonal in shape (A, B and C, black arrows), cART-treated cells appeared to be clustered and mostly rounded (curly brackets). The cells cultured in cART/TOP migrated a greater distance than the cART-treated neural crest cells (Fig 2 E, orange double-headed arrow. Magnification (100X).

Figure 4.3. Photomicrographs showing neural crest cells cultured in DMEM only (3A), DMSO only (3B), TOP only (3C), cART only (3D), and cART/TOP (3E) after 24 hours. Control neural crest cells are mostly polygonal in shape (black arrows) while cART-treated and cART/TOP-treated neural crest cells appear rounded (blue circle). Fig 3A and B (red arrows) shows filapodia which have detached from migrating neural crest cells. Magnification (200X).

Figure 4.4. Photomicrographs showing neural crest cells cultured in DMEM only (4A), DMSO only (4B), TOP only (4C), cART only (4D), and cART/TOP (4E) after 24 hours of culture. Control cells have polygonal cells while cART-treated and cART/TOP cells show rounded profiles with very few cells exhibiting polygonal profiles. Neural crest cells exhibited a pale vesicular nucleus with a prominent nucleolus. While most nuclei had a single nucleolus (red circles) some had 2 nucleoli (yellow circles). (Magnification 400X).

Figure 4.5. Photomicrographs showing neural crest cells cultured in DMEM only (A), DMSO only (B), TOP only (C), cART only (D) and cART/TOP (E) after 24 hours. Migration of neural crest cells (NCC) cultured in cART, TOP and cART/TOP appear inhibited to some extent (Magnification 40X). 5F shows the difference in the radius ratio of cardiac neural crest cells. Migration in the treated cultures was significantly lower than in the control cultures

Figure 4.6. Fluorescence photomicrographs showing neural crest cells which were cultured in DMEM only (A), DMSO only (B), TOP only (C), cART only (D) and cART/TOP (E) after 48 hours. Control neural crest cells show the criss-crossing of actin filaments at right angles (A and B, yellow circles). Filapodial extensions which have detached from migrating neural crest cells appear to be more abundant in the control cultures (B, white arrows). Actin filaments are more confined to the extremities of the cells in treated cultures (C-E). 6F shows the actin CTCF of treated and untreated cardiac neural crest cells. The CTCF in TOP only-treated neural crest cells was significantly lower than that of all other cultures.

Figure 4.7. A Feulgen-stained photomicrograph showing a section through an adult quail liver (A, positive control) and a chicken interventricular septum (B) showing large and small nucleoli respectively. The nuclei in quail liver are pale and exhibit big prominent nucleoli (black arrows). (Mag 1000X, Oil immersion).

Figure 4.8. A photomicrograph showing a longitudinal section through the heart of a chicken host embryo (A) stained with the Feulgen-Rossenbeck method. The section shows the thick interventricular septum (IVS), the left (LV), right ventricles (RV) and the higher magnification of the interventricular septum where the quail nuclei (red circles) of micro-injected cells were located (Mag 200X, A; 1000X, B).

Figure 4.9. Photomicrographs stained with the Feulgen-Rossenbeck method showing quail cardiac neural crest cells injected into chick hosts embryos (black arrows), while the orange arrows show the nuclei of chick hosts embryo. 4.9 A shows neural crest cells which were cultured in DMEM only, while 4.9 B shows neural crest cells cultured in DMSO only. 4.9C shows neural crest cells cultured in TOP, while 4.9 D and E show neural crest cells cultured in cART only and cART/TOP respectively (Mag 1000X, Oil immersion). 4.9F shows the numerical density of injected quail cardiac neural crest cells into chicken host embryos. The numerical density in the treated-samples was significantly reduced when compared to the controls.

Figure 5.1. Photomicrographs showing neural tubes (NT) and neurites (white arrows) cultured in DMEM only (A), DMSO only (B), cART only (C), TOP only (D) and cART/TOP (E) after 96 hours of culture (Mag 100X). Neurites which were cultured in cART only appeared short and thick, while TOP only-treated neurites appeared long and thin (white arrows). Neurites cultured in CART/TOP were shorter and showed greater arborization.

Figure 5.2. Photomicrographs showing DCX-stained neural tubes (NT) and neurites (white arrows) cultured in DMEM only (A), DMSO only (B), cART only (C), TOP only (D) and cART/TOP (E) after 96 hours of culture (Mag 100X). Neurites which were cultured in cART only appeared short and thick, while TOP only-treated neurites appeared long and thin (white arrows).

Figure 5.3. Control fluorescent photomicrographs showing DAPI-positive nuclei. Figure 4A shows a control section where the primary antibody was omitted while Figure 4B shows a control section where the secondary antibody was omitted. The DAPI-positive cells nuclei stained a blue colour.

Figure 5.4. A graph showing the thickness of DCX-positive neurites which were cultured in cART, TOP and cART/TOP. The thickness of the cART-treated neurites was significantly greater than that of the controls as well as the other experimental cultures.

Figure 5.5. A graph showing the CTCF of DCX-positive neural tube-derived neurons which were cultured in cART, TOP and cART/TOP. The CTCF of the cART-treated neurons was significantly lower than the controls as well as the other treated cultures.

Figure 5.6. Fluorescent photomicrographs showing Rhodamine phalloidin-stained neurons cultured in DMEM only (A), DMSO only (B), cART only (C), TOP only (D) and cART/TOP (E). Cells cultured in cART only, TOP only and cART/TOP showed a disarray in the cytoskeleton (blue arrows) and appeared vacuolated in certain parts of the cell (blue circles). Prominent dendrites were evident in the control cultures (A, B, white arrows), while dendrites were short or absent in the cART only and cART/TOP-treated cultures.

Figure 5.7. A graph showing the CTCF of neural tube-derived neurons which were cultured in cART, TOP and cART/TOP and stained with Rhodamine phalloidin. The CTCF of cART only-treated cells was significantly lower than the control cultures and other experimental cultures.

Figure 5.8. An MTT graph showing the rate of proliferation of neural tube-derived neurons in culture. The treated neurons show the highest rate of proliferation compared to the two control cultures. The TOP-treated cultures showed the lowest rate of proliferation out of all the treated cultures.

Figure 5.9. A graph showing the relative quantities (RQ) of Rac1 and RhoB in neural tube-derived neurons cultured in cART, TOP and cART/TOP. Rac1 is downregulated in cART and the DMSO control while it is upregulated in TOP and cART/TOP cultures. RhoB is upregulated in all the cultures.

Figure 5.10. A graph showing the relative quantities (RQ) of Rac1 and RhoB in neural tube-derived neurons cultured in cART, TOP and cART/TOP. Rac1 is downregulated in cART and the DMSO control while it is upregulated in TOP and cART/TOP cultures. RhoB is upregulated in all the cultures.

Figure 6.1. *A diagram showing the general structure and the interhelical loops of aquaporins (Huret, 2019)*

Figure 6.2. A graph showing the relative quantities (RQ vs Sample) of AQP4 and RPS17 in 7-day-old chick brains which were exposed to cART, TOP and cART /TOP. AQP4 is not expressed in the control cultures; however, its expression is induced by cART, TOP and ATP/TOP. However, the expression of RPS17 is downregulated by the administration with the treatment drugs.

Figure 6.3. A graph showing the relative quantities (RQ vs Sample) of AQP4 and RPS17 in 14-day-old chick brains which were exposed to cART, TOP and cART /TOP. The expression of AQP4 is reduced in the cART -treated brain samples, while the other treated samples are little affected. The expression levels of RPS17 are increased remarkably in the cART and cART /TOP-treated brain samples.

Figure 6.4. A graph showing the relative quantities (RQ vs Sample) of AQP4 and RPS17 in 20-day-old chick brains which were exposed to cART, TOP and cART /TOP. The level of expression

of AQP4 is remarkably high in all the brain samples. The expression levels of RPS17 are downregulated in all the treated brain samples.

List of abbreviations

AEDs-	Antiepileptic drugs
ANOVA-	Analysis of variance
AQP-	Aquaporin
ART-	Antiretroviral therapy
ARV-	Antiretrovirals
ASD-	Atrial septal defect
BBB-	Blood-brain barrier
BMPs-	Bone morphogenetic proteins
BSA-	Bovine Serum Albumin
Cart-	Combination antiretroviral therapy
CFC-	Cardoi-Facio-Cutaneous syndrome
CNS-	Central Nervous system
CSF-	Cerebrospinal fluid
CSF-	Cerebrospinal fluid
CTCF-	Corrected total cell fluorescence
CYP 450-	Cytochrome P 450
DCX-	Doublecortin
DDIs-	Drug-drug interactions
DMEM-	Dulbecco's minimal essential medium
DMSO-	Dimethyl Sulfoxide
EFV-	Efavirenz
FDA-	Federation for food and drug administration
FTC-	Emtricitabine
HAART-	Highly Active antiretroviral therapy

HIV-	Human immunodeficiency syndrome
HIV-	OMH HIV Oral melanin hyperpigmentation
IRIS-	Immune reconstitution inflammatory syndrome
IVS-	Interventricular septum
LV-	Left ventricle
MIQE-	Minimum information for publication of quantitative PCR experiments
MITF-	Microphthalmia-associated transcription factor
mRNA-	messenger RNA
MTT-	3-(4,5-dimethylthiazol-2-yl)-2,5-diphenyl-2H-tetrazolium bromide
NCC-	Neural crest cells
NGF-	Nerve growth factor
NHCL-	Ammonium Chloride
NMDs-	Neuronal migration disorders
NNRTIs-	Non-nucleoside reverse transcriptase inhibitors
NRTIs-	Nucleoside reverse transcriptase inhibitors
NT-	Neural tube
OPG-	Osteoprotegerin
PBS-	Phosphate buffered saline
PCR-	Polymerase chain reaction
PIs-	Protease inhibitors
PLWHAs-	People living with HIV/AIDS
PN-	Peripheral neuropathy
PNS-	Peripheral nervous system
RANK-	Receptor activator for nuclear factor kappa β
RANKL-	RANK Ligand
RQ-	Relative quantity
R-	Radius

RR-	Radius ratio
RSP-	Ribosomal protein
RV-	Right ventricle
SA-	South Africa
SCF-	Stem cell factor
SEM-	Standard error of mean
Sema3A-	Class 3 semaporin
TBM-	Tuberculosis Meningitis
TDF-	Tenofovir
TOP-	Topiramate
VSD-	Ventricular septal defect
WHO-	World Health Organization
WS-	Waardenburg syndrome

CHAPTER 1

1.0 INTRODUCTION

HIV is one of the most serious pandemics worldwide and continues to be a health challenge to individuals living with it. South Africa (SA) currently has the highest prevalence of HIV infections in the world, with a staggering 7, 52 million cases reported in the year 2019 (Mabaso *et al*; 2019). It was estimated that over 20% of the total adult South African population was HIV positive (South African National Aids Council, 2019).

Currently, SA has got the largest antiretroviral (ART) program in the world (South African National Aids Council, 2019). In 2014 just over 3 million people were receiving ART, which equated to about 49% of the HIV positive people in the country. Currently 62% of people living with HIV in SA are on antiretroviral therapy, indicating the magnitude of the ART program which is currently still in effect today (South African National Aids Council, 2019). Women living in rural South Africa have been recorded to have some of the highest HIV prevalence rates in the world and tend to typically be of a lower socioeconomic status – putting them at greater risk for adverse outcomes (Brittain *et al.*, 2017). Not only that they have greater difficulty accessing the appropriate treatment but such mothers are at higher risk for other diseases, such as depression (Brittain *et al.*, 2017) amongst others.

The development of Highly active antiretroviral therapy (HAART), a combination of chemotherapeutic regime for people living with HIV/AIDS (PLWHAs), has enormously improved over the last 2-3 decades with resultant decrease in HIV viral loads to undetectable levels and reduction in the incidence of HIV related opportunistic infections among people living with HIV/AIDS [PLWHAs] (Ford *et al.*, 2018). Consequently, a significant increase in life expectancy among HIV-

infected patients has been recorded, but with a major drawback of adverse effects and organ (e.g. brain) toxicities (Bertrand and Toborek; 2015).

In addition, it has been reported that a considerable number of PLWHAs may develop seizures due to the viral attack on the central nervous system (Ssetongo, 2019). These patients may show symptoms of peripheral neuropathy and require treatment with antiepileptic drugs (Wilner, 2012; Ssetongo, 2019; Zaporojan *et al*; 2019; Siddiqi *et al*; 2017; Siddiqi and Bierbeck; 2013).

Peripheral neuropathy affects more than fifty percent of PLWHAs (Wilner, 2012). Thus patients who present with both seizures and HIV/AIDS related infections require co-treatment with antiepileptic drugs (AEDs) and antiretrovirals (ARVs) (Ssetongo, 2019; Kim *et al*; 2015). Though, combination antiretroviral therapy (cART) has decreased the prevalence of the most severe forms of these neurodegenerative disorders such as extreme dementia (Ghosh *et al*; 2017; Carroll and Brew, 2017), the interaction of the two drugs is a great concern, particularly due to the p450 system enzyme, which is activated by the AEDs (Zaporojan *et al*; 2019). The non-nucleoside reverse transcriptase inhibitors (NNRTIs) and the protease inhibitors (PIs) are also metabolized by the same enzyme and may result in decreased efficacy of antiretroviral drugs by AEDs due to drug–drug interaction which is usually associated with a modification of drug action, with resultant attenuation, increase or otherwise the adverse and/or the desired/beneficial effects of one or all of the drugs (Zaporojan *et al*; 2019; Walubo, 2007).

Reports indicate that both therapeutics antiretroviral drugs and Topiramate (AED) lead to development of cleft palate, cleft lip and cardiac ventricular septal defects (Williams *et al*; 2015; Prieto *et al*; 2014; Margulis *et al*; 2012; Brogly *et al*; 2010) if administered during pregnancy. However, the mechanisms behind these effects are unknown. Data is lacking on how these drugs

bring about these effects, and the present study is designed against this backdrop to study the possible mechanisms and document such. We proposed to carry out this study using both *in vitro* and *in vivo* techniques to monitor the migration of neural crest cells and further determine their possible effects separately and in combination on neurite formation. This study apart from throwing light on possible impact of these drugs either alone or in combination on embryogenesis of the neural crest cells will sought to reveal whether neural crest cells are involved in the development of these defects, which has remained speculative.

The neural crest cells appear to be an important factor in the formation of craniofacial and cardiac anomalies as they play a major role in the formation of these two systems (Tarr *et al*; 2018; Yu and Ornitz, 2011; Crane & Trainor, 2006). All facial prominences are derived from cranial neural crest-derived mesenchyme, while cardiac neural crest cells form specific structures of the heart (Tarr *et al*; 2018; Yu and Ornitz, 2011; Crane & Trainor, 2006). Cardiac structures such as the interventricular septum and the aorticopulmonary septum depend largely on the normal migration of cardiac neural crest cells to various areas within the heart, particularly the truncal ridges (Keyte and Hutson, 2012). Failure of cardiac neural crest cells to migrate to these areas will result in the formation of congenital heart defects (Keyte and Hutson, 2012; Crane & Trainor, 2006) such as interventricular septal defects. In addition, failure of the migration of cranial neural crest cells to the facial prominences prior to the development of the face will result in craniofacial malformations such as cleft lip and palate (Cordero *et al*; 2011). Therefore, we propose to explore and investigate the migration patterns of neural crest cells with the co-administration of combination antiretroviral therapy (cART) and Topiramate (TOP). Other studies have reported the development of neuronal migration disorders, (such as pachygyria and the agenesis of the corpus callosum), and

hydrocephaly with the administration of cART during pregnancy, particularly during the first trimester (Ford *et al*; 2014; Sibuide *et al*; 2014).

While the correlation between cART and congenital malformations is known, the mechanism by which cART causes these deleterious effects are blurry. In addition, many countries still use cART in the battle against HIV, therefore it is essential to study the mechanisms by which cART causes these defects. Therefore, this study sought to use the avian model in order to attempt to unravel the mechanisms underlying the formation of four (4) congenital malformations due to the administration of cART and TOP. The congenital malformations of interest in this study were VSD, Cleft lip and palate, Neuronal migration disorders and Hydrocephalus. The antiepileptic drug of interest in this study is Topiramate (TOP), while Atripla was the designated combination antiretroviral drug.

1.1 Ventricular Septal defects

Ventricular septal defects (VSDs) are known to be the most common type of cardiovascular birth anomalies (Dakkak and Oliver, 2019). In some instances, VSDs may occur in isolation, however, other defects such as tetralogy of Fallot, double outlet right ventricle, and transposition of great vessels may be accompanied by VSDs (Dakkak and Oliver, 2019). Isolated VSDs account for 37 % of all congenital cardiovascular malformations. However, these defects occur in 3 out of 1000 births worldwide and the incidence of VSDs does not depend on gender like other congenital malformations (Dakkak and Oliver, 2019). If they persist, VSDs may result in pulmonary arterial hypertension, ventricular dysfunction and a great possibility of arrhythmias (Radhakrishna, 2019). The most common VSDs occur due to the failure of the interventricular foramen to close, resulting in the open communication between the two ventricular chambers (Radhakrishna, 2019).

The interventricular septum consists of two parts, namely pars muscularis (muscular part) and the pars membranacea (membranous part) (Anderson *et al*, 2019; Anderson *et al*, 2003). An interventricular foramen will form between the free edge of the pars muscularis and the fused endocardial cushions (Anderson *et al*, 2019). This foramen is closed by the formation of the pars membranacea in order for the definitive interventricular septum to form (Anderson *et al*, 2019). The pars membranacea has a complex development as it is formed by a contribution of various structures (Anderson, 2019). The downgrowth of the endocardial cushions, truncal ridges and neural crest cells contribute towards the formation of the pars membranacea (Anderson *et al*, 2019). The failure of the pars membranacea to completely close the interventricular foramen will result in a VSD (Privitera *et al*; 2017). Cardiac neural crest cells have been shown to populate the truncal ridges prior to their closure of the interventricular foramen (Privitera *et al*; 2017). Truncation studies have shown that the failure of migration of neural crest cells to the truncal ridges results in the occurrence of VSDs (Hutson and Kirby, 2003; Waldo and Kirby, 1998). We proposed in this study that since cardiac neural crest cells contribute toward the formation of the interventricular septum, the inhibition of these cells may result in the development of VSD.

1.2 Cleft lip and Palate

Cleft lip and palate are the most common birth anomalies which affect the craniofacial area. These congenital anomalies affect approximately 1 in 700 births worldwide (Ahmed *et al*; 2017), while the prevalence in South Africa is 4 percent of live births (Hlongwa *et al*; 2019). Females are generally more affected by this birth defect (Ahmed *et al*; 2017). Affected individuals have impaired facial growth, speech disorders and poor hearing (Nagarajan and

Subramaniyan, 2009). In addition, taking care of a child with craniofacial malformations can bring about psychological distress for parents (De Sousa *et al*; 2009).

Embryonically cleft lip and palate usually occur in the fourth week of development due to the non-fusion of facial prominences which are derived from the neural crest (Tarr *et al*; 2018; Smarius *et al*; 2017; Mishra *et al*; 2015). The mechanism by which antiretrovirals and antiepileptic drugs cause cleft lip and palate is unknown. Since the mesenchyme which forms the facial prominences is derived from neural crest cells, we proposed in this study that the clefting which is observed in children who are born to mothers who are on antiretroviral and antiepileptic therapies may be due to the inhibition of migration of cranial neural crest cells.

In order for normal craniofacial morphogenesis to occur, interactions between neural crest cells and adjacent cell populations should occur (Mishra *et al*; 2015, Jiang *et al*; 2006).

The normal vertebrate face is made up of facial prominences which are derived from ectomesenchyme (Smarius *et al*; 2017; Jiang *et al*; 2006). These are the frontonasal prominence, the paired lateral nasal prominences, the paired medial nasal prominences, maxillary and mandibular prominences (Smarius *et al*; 2017). The derivatives of the frontonasal prominence include the forehead and the bridge of the nose. The medial nasal prominences form the upper lip, philtrum, and the primary palate (Smarius *et al*; 2017; Helms *et al.*, 2005). The philtrum of the upper lip is derived from the fusion of the two medial nasal prominences. If the two processes fail to fuse a medial cleft lip will result (Hu and Helms, 1999). If the medial nasal prominence fails to fuse with the maxillary prominence a unilateral cleft lip will occur. Inductive interactions are required between neural crest cells, the forebrain, and the facial ectoderm in order for the frontonasal prominence to develop properly (Hu and Helms, 1999). The maxillary and mandibular prominences which give

rise to the upper and lower jaws respectively are both derivatives of the first pharyngeal arch (Helms *et al.*, 2005).

The secondary palate is formed by palatine shelves which are derived from the maxillary prominences (Bush and Jiang, 2012). The palatine shelves consist of mesenchyme which is derived from the neural crest (Tarr *et al.*; 2018; Yu and Ornitz, 2011). The palatal shelves are initially projected inferomedially on each side of the tongue. After a week the palatine shelves will elongate and elevate above the tongue into a horizontal position (Yu and Ornitz, 2011). The shelves will approach each other to fuse in the median plane to form a secondary palate. Secondary palatal clefting is attributed to the failure of the neural crest-derived palatine shelves to fuse and the failure of the maxillary prominences to grow and elongate (Bush and Jiang, 2012).

1.3 Neuronal migration disorders

Neuronal migration disorders result due to the disruption of a novel gene called *doublecortin* (DCX) (Yi-Hsuan *et al.*; 2019; Keays, 2007). Mutations in DCX may disturb cortical neuronal migration resulting in a 4-layered cortex in males (Yi-Hsuan *et al.*; 2019; Keays, 2007). In females the mutations in DCX could result in a condition where two populations of neurons exist in the cortex. The result is the formation of a double cortex (Hehr *et al.*; 2019; Kaur *et al.*; 2015). According to Ayanlaja *et al.* (2017) DCX is expressed in migrating neurons. This expression is maintained throughout embryogenesis and also during postnatal development. DCX is expressed in both the CNS and PNS (Ayanlaja *et al.*; 2017). A myriad of symptoms in children born to mothers who are on antiretroviral therapy suggest that cART could be involved in the formation of neuronal migration disorders (de Tejada, 2019; Ford *et al.*; 2014), however there is no evidence which suggests that TOP induces the formation of neuronal migration disorders. The reported neurological defects

observed in children who were born to mothers on cART were ventricular dilatation, partial agenesis of corpus callosum, subependymal cyst and pachygyria (Sibiude *et al.*, 2014). The

mechanism by which cART causes these defects is unclear, and till date no study has been undertaken to determine the mechanisms by which antiretrovirals cause neuronal migration disorders. Therefore, the current study sought to unravel some of the possible mechanisms of action of cART on migrating neurons of the neural tube by examining the structural and molecular development of these neurons.

This study aimed to investigate whether cART and TOP will affect the migration of neural tube-derived neurons and the expression of DCX when administered individually and in combination.

1.4 Hydrocephalus

Hydrocephalus is a congenital malformation which develops as a result of the impairment of the flow and absorption of the cerebrospinal fluid (CSF) (Isaacs *et al.*; 2018; Delbigio and Di Curzio, 2016). The disruption of the flow of CSF results in an increase in volume of CSF in the ventricular systems of the brain (Isaacs *et al.*; 2018; Delbigio and Di Curzio, 2016). The CSF build-up in the ventricular cavities will result in the enlargement of the ventricular cavities, with the subsequent increase in intracranial pressure (Kahle *et al.*; 2016; Fletcher *et al.*; 2000). Several reports have implicated the involvement of aquaporin 4 gene (AQP4) in the formation and development of hydrocephalus during embryonic development due to the role played by this gene in the regulation of water in the brain. Research has also shown that if the expression of AQP4 is impaired, fluid will accumulate and cause the abnormal expansion in the ventricular cavities (Huret, 2020; Verkman *et al.*; 2014; Verkman, 2013). The role of cART and TOP in the occurrence of Hydrocephalus has been suggested (Robertson *et al.*, 2010, Underwood *et al.*, 2015) but this area of research has

never been explored. It is evident that cART AND TOP are able to cross the blood brain barrier (McCormack and Best, 2014) and exert deleterious effects on the components of the central nervous system. However, the mechanism by which cART and TOP mediate neuropsychiatric toxicity has not yet been fully understood. Therefore, the current study sought to investigate the possible involvement of AQP4 in the development of cART- and TOP-induced hydrocephalus.

1.5 Rationale

Though, it has been established that both the therapeutics of cART and TOP lead to the development of cardiac ventricular septal defects, cleft lip, cleft palate, neuronal migration disorders and hydrocephalus, data is lacking on the possible associated mechanism(s). Since the battle against HIV and AIDS is still unabated and the use of cART and TOP is continuing, the need to study and document the possible associated means of their teratogenicity and neuropathology is very crucial. Such information will be invaluable clinically in the management of PLWHAs.

1.6 Aim

To investigate the effect of the co-administration of cART and TOP on the migration of neural crest cells and brain development in quail (*Cortunix cortunix japonica*) and chicken (*Gallus gallus domesticus*) embryos.

1.7 Study objectives

- To investigate whether cART and TOP individually and in combination inhibit and/or misdirect the migration of cardiac neural crest cells *in vitro* and *in vivo* (**Study 1**).
- To investigate the effect of cART and TOP individually and in combination on the migration of cranial neural crest cells when administered *in vitro* (**Study 2**).
- To investigate if the effect of the administration of cART and TOP on DCX (neurogenesis) and the migration of neural tube derived neurons *in vitro* (**Study 3**).

- To investigate if the administration of cART and TOP affect the prenatal expression of Aquaporin 4, and RSP17 genes in *Gallus gallus domesticus* brains (**Study 4**).

Hypothesis

The study hypothesized that both cART and TOP would inhibit the migration of cardiac and cranial neural crest cells and downregulate the DCX and Aquaporin 4 genes. In addition, Topiramate would inhibit the activity of cART when administered in combination.

1.8 Chapter outline

The thesis is organized into several chapters, with each of the four main chapters (chapters 3-6) examining the mechanisms of a specific congenital anomaly.

Chapter 1 gives the background of the study, and it identifies the research question being answered.

Chapter 2 (literature review) presents a synthesis of information from the literature regarding the teratogenicity of combination antiretroviral drugs and AEDs. In addition, this chapter describes the development of neural crest cells and factors affecting their migration.

Chapter 3 investigated the mechanism by which cART and TOP causes the formation of cleft lip and palate in children born to mothers who are on the two therapies. Cranial neural crest cells were obtained from neural tubes of quail embryos which had been cultured for 36 hours. The neural crest cells were cultured in the presence of both cART and TOP. The migration assay was used to determine the extent of migration and the differentiation of cranial neural crest cells into neurites, pigment cells, and bone producing cells was determined. In addition, the actin cytoskeleton of the neural crest cells was evaluated using rhodamine phalloidin. A reduction in the migration of neural crest cells was observed with the administration of cART and TOP. In addition, the two drugs exerted adverse effects on the differentiation of neurites, melanocytes and osteoblasts.

Chapter 4 presents the probable mechanisms by which cART and TOP result in the development of cardiac congenital anomalies like VSDs when administered during pregnancy. In this chapter neural tubes were dissected at cardiac levels from 32 hour-old quail embryos and cultured in the presence of peak plasma levels of cART and TOP individually and in combination. The extent of migration of neural crest cells was determined using the evaluation of the difference in the radius ratio of migrated neural crest cells over 24 and 48 hours. In addition, the neural crest cells were

brought into suspension and micro-injected into chicken host embryos in order to investigate if the injected quail neural crest cells will reach their destination in the heart of the host embryo. The

number of quail neural crest cells which had populated the host chick embryo interventricular septum were counted and expressed as numerical density. Also the neural crest cells were stained with rhodamine phalloidin in order to evaluate the cell actin cytoskeleton. The results show that both cART and TOP inhibit the migration of cardiac neural crest cells and result in the alteration of actin cytoskeleton in these cells.

Chapter 5 presents the mechanism by which cART and TOP result in the formation of neuronal migration disorders in cART and TOP cytotoxicity. Neural tubes were obtained at cranial levels from 36-hour-old quail embryos and cultured in the presence of the two drugs. Migrating neural crest cells were removed from the adjacent neural tubes such that only the neural tube remained in the culture dishes. The outgrowing neurites were stained with DCX and their thickness was measured. The rate of proliferation of the neural tube-derived neurons was determined using the MTT assay. In addition, quantitative PCR was used to determine the effects of cART and TOP on the Rac and Rho GTPases. The CTCF (level of fluorescence) was calculated on the DCX- and rhodamine phalloidin-stained neurons. The results show that cART and TOP decreases the expression of DCX in the neural tube-derived neurons. In addition, the administration of cART upregulates Rho while downregulating Rac.

Chapter 6 investigated the mechanism by which cART and TOP result in the development of hydrocephalus in cART and TOP cytotoxicity. The two drugs were injected *in vivo* into chicken eggs which had been incubated for three days, both individually and in combination. The eggs were returned into the incubator and the brains were dissected out from the developing embryos on days 7, 14 and 20. RNA was extracted from the brains and processed for quantitative PCR. The genes of interest were AQP4 and RPS17. The results show that cART and TOP induces the early expression of AQP 4 in day 7 brains.

Chapter 7 (concluding discussion)

This chapter summarizes the implications and significance of the results obtained in

the studies comprising this thesis and highlights future directions for the choice of antiretroviral and antiepileptic drugs in women of child bearing age.

CHAPTER 2

2.0 Literature review

2.1.0 Antiretroviral therapy

Combination antiretroviral therapy (cART) was first introduced through the discovery of protease inhibitors (PIs), nucleoside reverse transcriptase inhibitors (NRTIs) and non-nucleotide reverse transcriptase inhibitors (NNRTIs) around 1996 with the aim to combat HIV, and this finding led to a significant decline in the mortality due to HIV-1 infections (Bretchtl., *et al* 2001). This treatment however, originally consisted of numerous tablets which had to be taken by individuals on a daily basis (Bogner and Julg, 2008). This manner of distribution was very burdensome as minor slip-ups such as losing or misplacing one drug, could lead to problems in treating the infection effectively. This challenge was counteracted by the introduction of a “one pill daily regimen”- cART.

2.1.1 Atripla (cART)

Atripla is a single pill which is a combination of three compounds: two NRTIs (tenofovir and emtricitabine) as well as an NNRTI (efavirenz). This drug was well accepted due to its high efficacy as well as potency, as it made it for easy daily intake (Horberg *et al*, 2010). Atripla has been long used as monotherapies and each individual drug has its own characteristics which qualify it as the most optimal NRTI or NNRTI in the formulation of the combination drug (Clay, 2008). Efavirenz has a terminal elimination half-life of 50 hours, whereas other ARVs such as dolutegravir and zidovudine have an elimination half- life of 12 and 3 hours, respectively. Many positive properties of the monotherapies formulating Atripla have been discovered. It has been proven that Efavirenz has a high long half-life (45 hours and achieves a steady-state plasma concentration between 6 to

10 days) amongst other NNRTIs (Pau and George, 2014, Eggleton and Nagalli, 2020)). It has also been proven that efavirenz is effective and tolerant in many paediatric patients and has elevated adherence rates needed to sustain long term virologic suppression (Rakhmanina, 2010).

2.1.2 Efavirenz and Pregnancy

Research shows that efavirenz is teratogenic when used during pregnancy, especially if administered during the first trimester (Williams *et al*; 2015; Prieto *et al*; 2014; Margulis *et al.*, 2012; Brogly *et al*; 2010). There have been many case reports on the birth defects observed in infants, and in particular the anomalies of the central nervous system, when efavirenz is administered during the first trimester of pregnancy (Townsend *et al.*, 2006; Ford *et al.*, 2014; WHO, 2019). A study performed on cynomolgus monkeys treated with efavirenz using human equivalent concentrations during the time of organogenesis resulted in congenital defects (Mutlib *et al*; 1999). These defects included anencephaly, microphthalmia, anophthalmia and cleft palate (Mutlib *et al*; 1999). Following this study, there were four other case reports on human infants with neural tube defects consistent with the animal studies (De Santis *et al*; 2002; Saitoh *et al*; 2005). Three cases of human infants with neural tube defects were presented with meningomyocele and one with Dandy-walker malformation (De Santis *et al*; 2002; Saitoh *et al*; 2005).

2.1.3 Tenofovir during gestation

Tarantal *et al.* (2002) studied the effects of tenofovir on simian immunodeficiency virus-infected monkeys and found that some of the infants had bone-related effects. The fetuses were observed using a sonogram as well as through assessing the blood and urine samples of both mother and fetus (Tarantal *et al.*, 2002). Fetal growth was normal, however the weight and the crown-rump

length were reduced when compared to the controls. In addition, circulating insulin-like growth factors and porosity of bone had decreased (Tarantal *et al.*, 2002).

Jao and colleagues (Jao *et al.*; 2016) investigated the effects of tenofovir on the development of long bones by measuring the length of the femur and humerus with the use of a ultrasonogram and found that the length of long bones was not affected by the administration of tenofovir. In addition, no correlation was made between the length of long bones in general and the period of *in utero* tenofovir administration. Gibb *et al.* (2012) assessed the effects of tenofovir taken during and after gestation on HIV positive women. *In utero* tenofovir did not affect the height and weight, as the two parameters were similar to those of the HIV negative population (Gibb *et al.*, 2012). However, Conesa-Buendia *et al.* (2019) showed that tenofovir decreases bone density by decreasing bone production and increasing bone resorption.

2.2.0 Teratogenic effects of AEDs

Although antiepileptic drugs work significantly to combat epileptic seizures, they also have adverse side effects which may be permanent in some cases. Major effects of AEDs include congenital malformations and premature death (Taylor and Meldrum, 1995). Examples of common birth defects includes cleft lip and palate, skeletal abnormalities, neural tube defects such as microcephaly, and ventricular septal defects (Holmes *et al.*, 2001). Other studies showed that AEDs can also result in cognitive impairment, blindness, reduced bone density, loss of hearing and suppression of the immune system (Walton and Treiman, 1992). Studies show that AEDs cause birth defects even when administered at lower doses (Meador *et al.*, 2008) since they are mostly used in polytherapy. However, it was showed that AED's in monotherapy for pregnant women have

a very low potential of causing teratogenic effects when administered at low doses (Meador *et al.*, 2008). Epidemiological studies further added that despite the adverse side effects, withdrawal of AEDs is not an option, especially for pregnant women because seizures could be chronic overtime and could lead to early miscarriages (Holmes *et al.*, 2011).

Although AED's have been shown to be teratogenic during pregnancy, pregnant women with epilepsy require constant treatment with AEDs in order to prevent the occurrence of seizures, (Battino *et al.*, 2013).

2.2.1 Topiramate (TOP)

TOP is an antiepileptic drug which was ratified by the Food and Drug Administration (FDA) for use in patients with epilepsy in the United States in 1996 (Lai *et al.*; 2017; Margulis *et al.*, 2012). In addition to managing seizures, TOP is crucial in the treatment of migraine, bipolar mood disorder and peripheral neuropathy (Molgaard-Nelson, 2011; Margulis, 2012; Ornoy, 2008). The mechanism of action of TOP is not clear, but it is thought to act by blocking Na⁺ channels, L-type calcium channels (Zhang *et al.*; 2000), and α -amino-3-hydroxy-5-methylisoxazole-4-propionic acid (Gibbs *et al.*, 2000). Despite its therapeutic effects during epilepsy, TOP has been shown to be teratogenic when administered during pregnancy, particularly during the first trimester (Hunt *et al.*, 2008; Margulis *et al.*, 2012). A myriad of craniofacial abnormalities has been attributed to the administration of TOP during early pregnancy (Margulis *et al.*, 2012). The consequences include a smaller head circumference and spontaneous abortions (Tomson, & Battino, 2012). The craniofacial abnormalities include cleft lip and palate. A study showed that TOP at high doses during the first trimester increases the risk of oral clefts (Hernandez-Diaz *et al.*; 2017). For this

reason, TOP was placed in Pregnancy Category D by the US FDA. Pregnancy Category D means there are indications that the drug could be harmful during pregnancy but if the benefits surpass the risk then the use of the drug may be acceptable.

Interestingly, some of the teratogenic effects caused by cART during pregnancy are similar to birth defects seen with TOP toxicity (Williams *et al*; 2015; Prieto *et al*; 2014; Margulis *et al.*, 2012; Brogly *et al*; 2010).

2.3.0 Causes of seizures in HIV

As indicated earlier in chapter 1, some HIV patients develop seizures which are caused by the virus and may therefore require treatment with antiepileptic drugs. Treatment of HIV-associated neurocognitive disorders may pose serious challenges, and requires further research into the mechanisms by which these disorders are established.

A myriad of HIV-induced conditions may result in the development of seizures in HIV patients. Tuberculous meningitis (TBM), the most common form of CNS TB is one of the causes of seizures in HIV patients (Abdulaziz *et al*; 2020). In TBM seizures manifest in 10–16% of adults (Abdulaziz *et al*; 2020). In addition to seizures, the symptoms of TBM include chronic headache, florid meningismus and cranial nerve palsies (Abdulaziz *et al*; 2020). The seizures can be both generalized and partial onset. The other cause of seizures in PLWHIV is cryptococcal meningitis (Siddiqi and Birbeck 2013), which occurs when CD4 counts are low. In this condition the seizures are associated with headaches, dilated Virchow-Robin spaces and cryptococcoma. Toxoplasmosis also occurs when CD4 counts are low and has been shown to be the main reason for the onset of seizures in 15-40% of HIV patients (Siddiqi and Birbeck 2013). Other causes of seizures in HIV patients include encephalopathy, EBV-associated primary CNS lymphoma, brain abscess, and

immune reconstitution inflammatory syndrome (IRIS) (Siddiqi and Birbeck 2013). Medication side effects have also been shown to cause seizures in HIV patients, particularly in patients who are placed on several medications due to co-morbidities (Siddiqi and Birbeck 2013; Abdulaziz *et al*; 2020). Hence clinicians are usually advised to be cautious when they select medications that are known to reduce seizures. Interestingly, the supratherapeutic levels of cART have been shown to cause seizures in children and adult patients.

The main objective of treatment in HIV patients who present with seizures is to avoid a recurrent seizure. When clinicians select an AED, the decision should be centered around increasing seizure control, reducing drug side effects, and circumventing underlying medical conditions (Siddiqi and Birbeck 2013). Above all, drug-drug interactions which may negatively affect the control of HIV and seizure control should be avoided. The resolution to initiate treatment, a good choice of the AED and duration of treatment is dependent on whether the clinical presentation is acute or chronic (Siddiqi and Birbeck 2013).

2.4.0 The neural crest

Due to the involvement of the neural crest in the formation of the elements of the craniofacial region and the cardiovascular system, the study sought to investigate if cART and TOP exert adverse effects on the migration and differentiation of cardiac and cranial neural crest cells when administered individually, and in combination.

Neural crest cells (NCCs) are a group of multipotent migratory cells emerging from the dorsal aspect of the neural tube (Takahashi *et al.*, 2013). Once the cells have arrived at their destinations, they will then differentiate into a diverse range of neuronal and non-neuronal derivatives (Selleck

and Bronner-Fraser., 1995). Multipotency is characteristic of NCCs due to their ability to differentiate into various cells types such as neurons of the peripheral nervous system, glial cells, melanocytes, smooth muscle cells as well as precursors of bone and cartilage (Christiansen *et al.*, 2000). The NCCs can be divided into three main groups: the cardiac, cranial, and the trunk neural crest cells. All three groups undergo epithelial-to-mesenchymal transition and migrate throughout the embryo to their final destinations (Selleck and Bronner-Fraser., 1995). Epithelial-to-mesenchymal transition is a regulated process in which cell-cell and cell-extracellular matrix interactions are altered in order to release epithelial cells from the surrounding tissue (Radisky, 2005). Avian cardiac NCCs are considered pluripotent but do not give rise to cartilage, bone and connective tissue; in contrast, the aforementioned derivatives are unique to cranial NCCs which consist of multipotent cell populations (Crane Trainor, 2006).

The neural crest is a precursor cell type of many structures during early embryogenesis (Barrel, 2019), and it is well-documented that failure of migration of this population of cells may lead to an array of birth defects (Trainor 2010; Tobin, 2008). Congenital heart disease has been identified as one of the most common birth defects associated with the migration of cardiac neural crest cells (Trainor 2010; Crane & Trainor, 2006). Other than their ability to differentiate into a wide range of cells, neural crest cells also have the capacity for long-ranged migration (Takahashi *et al.*, 2013). Cranial neural crest cells do not migrate as a single mass but are organised into streams which pour out from the developing brain into the periphery (Graham *et al.*, 2004). Three streams can be identified in the developing head of all vertebrates, namely: trigeminal, hyoid, and post-otic streams (Graham *et al.*, 2004). The trigeminal crest arises from the midbrain and rhombomeres 1 and 2 of the hindbrain. These neural crest cells form the neurons of the trigeminal ganglion as well as the skeleton of the upper and lower jaws (Lumsden *et al.*, 1991; Schilling and Kimmel., 1994; Graham

et al., 2004). The hyoid stream arises from rhombomere 4 of the hindbrain and forms neurons of the proximal facial ganglion as well as the constituents of the second pharyngeal arch (Lumsden *et al.*, 1991; Schilling and Kimmel., 1994; Graham *et al.*, 2004). The post-otic crest arises from rhombomeres 6 and 7 of the hindbrain. These NCCs form the neurons of the proximal and jugular ganglia as well as the skeletal components of the posterior pharyngeal arches (Lumsden *et al.*, 1991; Graham *et al.*, 2004).

A number of craniofacial syndromes and congenital conditions termed neurocristopathies are associated with abnormal migration or reduced survival of cranial neural crest cells (Snider and Mishina, 2014; Watt and Trainor, 2014). Craniofacial defects are evident in neurocristopathies, such as DiGeorge syndrome and Waardenburg syndrome (WS) (Snider and Mishina, 2014; Watt and Trainor, 2014). Waardenburg syndrome which has an incidence of 1 in 4000 births is a classic example of a disease due to changes in CNCC migration (Snider and Mishina, 2014; Watt and Trainor, 2014). The anomalies in this syndrome include a disturbance in the initial formation and the development of the craniofacial complex (Snider and Mishina, 2014; Watt and Trainor, 2014). The accompanying features of this anomaly are hypopigmentation of the eyes, isolated patches of white hair on the anterior scalp, and sensori-neural hearing loss, ranging from total deafness to a progressive loss of hearing (Snider and Mishina, 2014; Watt and Trainor, 2014). Changes in the expression of SOX10 in neural crest cells have been implicated to be a likely cause of the hypopigmentation of the skin, hair, and eyes commonly found in patients with WS (Hou and Pavan, 2008).

2.4.1 Factors affecting the migration of neural crest cells

Other than their ability to differentiate into a wide range of cells, neural crest cells also have the capacity for long-range migration (Takahashi *et al.*, 2013). During this journey, neural crest cells become exposed to a wide range of signals from surrounding microenvironments (Takahashi *et al.*, 2013). These signals vary by developmental stage and site, and have the ability to influence differentiation, morphology and patterning of neural crest derivatives (Takahashi *et al.*, 2013). Migration of the cranial neural crest cells are controlled by a number of factors. Firstly, there are the negative regulators or chemorepulsors, which include the class 3 semaphorin (Sema3A) molecules (Theveneau and Mayor., 2012). Sema3A is a protein secreted by surrounding tissues to guide migrating cells and axons in the developing nervous system (Moret *et al.*, 2007). Sema3A has the ability to inhibit migration as well as to prevent migratory streams from mixing. It is also secreted by neurons during axonal pathfinding (Moret *et al.*, 2007). According to research by Moret *et al* (2007), the Sema3A expressed by neurons is necessary to set the sensitivity of their growth cones to environmental Sema3A. This therefore regulates their pathway choices (Moret *et al.*, 2007). The second set of regulators, the positive regulators, includes permissive factors that generally promote motility (i.e. the extracellular matrix proteins) as well as the chemoattractants that drive NCCs to their locations (Theveneau and Mayor, 2012).

The main protein found in the extracellular matrix which is permissive of migration is fibronectin. Fibronectin is a glycoprotein that binds to membrane-spanning receptor proteins, called integrins (Sakai *et al*; 2003). Fibronectin plays an important role in cell adhesion, growth, migration, and differentiation. It is also important for processes such as wound healing and embryonic development (Sakai *et al*; 2003).

2.4.2 Mechanism of neural crest cell migration

The four main steps of cell migration include the formation of lamellipodia at the cell front, formation of focal adhesions, which facilitates attachment to the extracellular matrix, actomyosin activity in order to generate the necessary energy for the retraction of the rear part of the cell, and lastly the formation of focal adhesions at the rear of the cell will aid in detaching the cell from the extracellular matrix for forward movement (Tang and Gerlach, 2017, Svitkina, 2018). The disruption of any of the four steps could result in the interruption of migratory cells (Tang and Gerlach, 2017). When cells migrate they will move the front forward in order to establish the conduciveness of the environment, and if the environment is not conducive enough, the cell will retract (Hong *et al*; 2016; Tang and Gerlach, 2017). Thus this extension and retraction of the cell constitutes the mechanism by which neural crest cells migrate (Lee, 2013; Tang and Gerlach, 2017). The formation of lamellipodia includes the assembly and the disassembly of actin filaments (Krause and Gautreau, 2014; Tang and Gerlach, 2017). Filament assembly involves branching and elongation of actin filaments. In addition, actin depolymerization occurs in order to facilitate the extension-retraction cycle of migration (Krause and Gautreau, 2014; Tang and Gerlach, 2017). Rhodamine phalloidin binds only to actin in its filamentous form (Chazotte, 2006), therefore another probe DNase-I, which binds to actin in its monomeric form (Cramer *et al*; 2002) would shed more light on specific changes which these cells go through.

This study therefore sought to make use of the parameters of neural crest and neural tube-derived neuronal migration in order to investigate the mechanism by which VSDs, neuronal migration disorders, cleft lip and palate arise during cART and TOP cytotoxicity. In addition, the levels of

AQP4 gene were used to determine the mechanisms by which cART and TOP result in the formation of hydrocephalus during avian brain development.

CHAPTER 3: The effect of cART and TOP on the migration and differentiation of cranial neural crest cells

3.1.0 Introduction

Cranial neural crest cells give rise to a vast number and variety of derivatives during ontogeny including major structures of the ventral head and neck (Knight and Schilling, 2013; Etchevers et al; 2019). The facial and visceral skeleton, peripheral and autonomic nervous systems, connective tissues and melanocytes are dependent on cranial neural crest cell development and migration (Chai *et al*; 2000; Etchevers *et al*; 2019). Cranial neural crest cells migrate to their destinations where they proliferate and differentiate into specific structures following embryonic specification (Trainor *et al.*, 2003; Nie *et al.*, 2006). Any factor resulting in the failure of cranial neural crest cells to migrate and differentiate leads to major abnormalities in the morphology of the face and neck regions (Ito *et al.*, 2003; Kulesa *et al.*, 2010; Wang *et al*; 2019). In addition, abnormal migration as well as differentiation of cranial neural crest cells has been shown to result in the abnormal pigmentation of the skin (Sommer, 2017), and the development of peripheral neuropathy (PN) (Dietrich and Dragatsis, 2016) in newborns. Neural crest cells form most of the neurons and the glia of the peripheral nervous system, which comprises sensory, sympathetic and parasympathetic ganglia and in addition, cranial neural crest cells are sensitive to intrinsic and extrinsic factors such as genetic deletions and some xenobiotics respectively (Karunamuni et al; 2014; Usami et al; 2014; Pallocca *et al*; 2017).

The administration of cART during gestation has been shown to cause congenital craniofacial malformations (Williams *et al*; 2015; Mehta et al, 2019). In particular, non-nucleoside reverse transcriptase inhibitors have been shown to cause cleft lip and palate in children born to HIV positive mothers who use cART during the first trimester (Cartsos *et al*; 2012; James *et al*; 2014).

In addition to its adverse effects on skeletal elements of the craniofacial region, cART has been shown to affect the production and function of melanin in patients with HIV associated oral melanin hyperpigmentation (OMH) (Chandran *et al*; 2014). In this condition, black or brown macules accumulate in the oral mucosa, gingiva, hard palates and tongue due to overproduction of melanin in melanoblasts.

3.1.1 Cranial neural crest cells and bone formation

Cranial neural crest cells are the only type of neural crest cells which give rise to osteoblasts and chondrocytes as they are involved in the formation of cartilage, bone and connective tissue in the craniofacial region (Mishina and Snider 2014; Knight and Schilling, 2013). In addition to the formation of the cranium, these cells are also involved in the formation of the hard and soft palates. Oka *et al*; (2012) showed that the bony palatine shelves which are responsible for the formation of the hard palate, as well as the connective tissue and palatine aponeurosis of the soft palate are derived from cranial neural crest cells. The tissues of the craniofacial area have three sources, namely cranial neural crest, paraxial mesoderm, and lateral mesoderm. Most of the cranial bones and cartilage (anterior portion) are derived from the neural crest, whereas the posterior forming bones are derived from paraxial mesoderm (Mishina and Snider 2014; Knight and Schilling, 2013).

Cranial neural crest cells exhibit three main events, namely formation, migration, and differentiation. Craniofacial abnormalities may arise if one or more of these events are disturbed (Mishina and Snider 2014). As an example, in Treacher Collins syndrome the reduction in the proliferation of cranial neural crest cells results in fewer cells and therefore cranioskeletal hypoplasia (Conley *et al.*, 2016; Dixon *et al.*, 2006; Jones *et al.*, 2008; Sakai *et al.*, 2016).

Neurocranial neural crest cells arise from the level of the mesencephalon and they will pass between the eyes to form the palatal shelves. Cranial neural crest cells which have a viscerocranial destination arise from the hindbrain to populate the pharyngeal arches.

3.1.2 Osteoblastic differentiation of cranial neural crest cells

Cranial neural crest cell- derived osteoprogenitor cells produce bone by intramembranous ossification (Urano-Morisawa *et al*; 2017). These osteoprogenitor cells will proliferate and differentiate into osteoblasts in order to produce the bone matrix.

Intramembranous ossification in cranial neural crest cells is initiated when these cells proliferate and condense into nodules (Abzhanov *et al*; 2007). This condensation of neural crest cells into nodules is induced by the presence of bone morphogenetic proteins (BMPs) which are produced by the epidermis of the head. Under the influence of BMPs, these nodules can either form cartilage or osteoprogenitor cells depending on the concentrations of these growth factors (Abzhanov *et al*; 2007). At this stage the osteoprogenitor cells are under the influence of Runx2 (Urano-Morisawa *et al*; 2017) and they also express mRNA for collagens 2 and 9. Subsequently, these osteoprogenitor cells will express a gene called osteopontin (Abzhanov *et al*; 2007). This gene which gives the osteoprogenitor cell a structure of a typical cartilage producing cell is formed following the downregulation of RUNX2 in these cells (Urano-Morisawa *et al*; 2017; Abzhanov *et al*; 2007). Because the osteoprogenitor cells have a similar structure to cartilage cells they are referred to as chondrocyte-like osteoblasts. In an autocrine mode, these cells will secrete Indian hedgehog as they become definitive osteoblasts. Osteoblasts will produce the bone matrix which consists of the organic and inorganic matrix (Blair *et al*; 2017). The organic component consists of

ground substance and collagen, while the inorganic component consists of calcium and phosphate (Blair *et al*; 2017).

3.1.3 The differentiation of melanocytes from neural crest cells and HIV-OMH

Oral melanin hyperpigmentation is known to occur in HIV patients following a month or more after the commencement of cART (Chandran *et al*; 2016; Ward *et al*; 2006). In certain patients this condition manifests within the first two years after diagnosis of the virus (Chandran *et al*; 2016). Any part of the oral mucosa can be affected by HIV-OMH, although most of the melanin is found in the stratum basale. This condition is thought to occur due to the virus and/or the antiretrovirals affecting cranial neural crest-derived melanocyte function (Chandran *et al*; 2016). In congenital melanocytic nevus the melanosomes are not evenly distributed and the differentiation of melanoblasts from neural crest cells is impaired (Chandran *et al*; 2016).

The differentiation of melanoblasts from neural crest cells is regulated by a number of factors among others Wnt proteins, stem cell factor, BMPs, and ephrins (Mort *et al*; 2015; Thomas and Erickson, 2008). The latter (ephrins) and the former proteins (Wnt) are involved in the activation of the MAPK-signaling pathway which together with the Notch and Wnt signaling pathways are required for melanocyte development (Mort *et al*; 2015). Stem cell factor (SCF) and its receptor c-kit are crucial in the initial stages of melanoblast differentiation. The epidermal and dermal cells are responsible for the production of SCF as the melanoblasts migrate from the neural tube (Mort *et al*; 2015). The survival of melanoblasts depends on the production of SCF.

Microphthalmia-associated transcription factor (MITF) is regarded as the central protein to melanocyte differentiation (Mort *et al*; 2015; Thomas and Erickson, 2008). It is involved in the

proliferation, differentiation and survival of melanocytes. MITF is also responsible for the production of tyrosinase which is the enzyme vital to the production of melanin (Mort *et al*; 2015; Thomas and Erickson, 2008). During melanogenesis, small dark membrane-bound vesicles called melanosomes form in the cytoplasm of the differentiating melanocyte. The melanosomes are responsible for the synthesis and production of melanin (Mort *et al*; 2015; Thomas and Erickson, 2008).

Melanocytes are unable to proliferate once they are differentiated. This is because these cells are highly differentiated and therefore in the adult the only melanocytes which are able to renew are those found in the hair. Once melanin is formed it is distributed for a myriad of functions which include skin pigmentation, reactive oxygen species neutralization and ions storage (Mort *et al*; 2015; Thomas and Erickson, 2008).

There are three types of melanin produced by melanosomes which include pheomelanin and the two types of eumelanin. The latter is dark brown to black in colour and exhibit antioxidant properties, while pheomelanin is red in colour and has phototoxic prooxidant properties (Mort *et al*; 2015; Thomas and Erickson, 2008).

Research has shown that cART is capable of causing PN in HIV patients (Tumusiime, 2014). In addition, the prenatal administration of cART has been shown to cause congenital anomalies (e.g. talipes equinovarus, hip dysplasia, genu valgum) of the nervous system that are associated with PN (Joao *et al*; 2010; Hadianfard and Ashraf, 2012). These findings suggest that cART exerts similar adverse effects on the peripheral nervous system of the developing fetus and adult patients. Therefore, a correlation between the gestational administration of cART and the impairment of neural crest-derived peripheral nerves, with the subsequent development of PN is plausible.

Moreover, HIV patients who suffer epileptic seizures and peripheral neuropathy require treatment with antiepileptic drugs such as topiramate (TOP), in addition to cART (Ssetongo, 2019; Zaporozhan *et al*; 2019). Interestingly, it has been shown that TOP also has similar adverse effects as cART on structures of the craniofacial region such as cleft lip and palate when administered during the first trimester of pregnancy (Margulis *et al*; 2012).

Since the mesenchyme which forms the palate, upper lip and facial skin melanocytes is derived from cranial neural crest cells (Cordero *et al*; 2011), it is hypothesized that gestational co-administration of cART and TOP may lead to the disruption of the migration and differentiation of cranial neural crest cells and contribute to craniofacial abnormalities in the newborn of pregnant women simultaneously exposed to therapy of cART and TOP. Data is lacking on how cART and TOP may bring about these deleterious effects on the craniofacial region of the developing embryo.

This study, apart from throwing light on possible impact of these drugs either alone or in combination on cranial neural crest cells, sought to reveal their (cART and TOP) possible involvement in the development of craniofacial defects in children born to HIV-positive and epileptic mothers on treatment of these conditions. Also, many countries still use cART in the battle against HIV; therefore, it is essential to study the mechanism by which cART causes these defects.

3.2.0 Material and methods

3.2.1 Drugs

A generic tablet of Atripla® (Bristol-Myers Squibb & Gilead Sciences LLC, South Africa) containing 600 mg of efavirenz (EFV), 200 mg of emtricitabine (FTC) and 300 mg of tenofovir disoproxil fumarate (TDF) was used as combination antiretroviral therapy (cART). The tablet was crushed into powder and dissolved in 0.05 % Dimethyl sulfoxide (DMSO, sigma). Topiramate (sigma, CAS NO: 97240-79-7, T0575) was also dissolved in DMSO. A hundred percent solution of 1g/ml in DMSO was prepared for both drugs.

3.2.2 Ethical clearance

All experimental procedures were approved by the University of the Witwatersrand, Animal Research Ethics Committee (Animal Ethics Clearance Number 2019/01/2/A). The quail eggs were obtained through the Wits Research Animal Facility (WRAF), University of the Witwatersrand.

3.2.3 Preparation of equipment

Glassware was dry-heat sterilized at 180°C for 2 hours. Solutions were autoclaved at 121°C at 100 kPa for 30 minutes. Four-well Nunc culture multidishes (Nunclon, Denmark) were layered with fibronectin (Sigma) which was made up in distilled water (1:40 dilution). The dishes containing fibronectin were incubated for one hour at 37°C in a humidified incubator (with 5% CO₂). After incubation, excess fibronectin was removed using a fine pipette. Dulbecco's minimal essential

medium (DMEM, 30 μ l) was added to each well, and the dishes were incubated for a further one hour at 37°C in a humidified incubator (5% CO₂) until use.

3.2.4 Embryos

Fertile Japanese quail (*Cortunix japonica*) eggs were used in this study. The quail eggs were incubated for 36 hours at 37°C in a humidified incubator in order obtain cranial neural crest cells. All experimentation was carried out in a laminar flow hood under aseptic conditions.

3.2.5 Neural tube cultures

The shell of each quail egg was wiped with cotton wool dipped in 70% alcohol (30% distilled water). The egg was cut open, and emptied into an oval dish containing chick Ringer's solution. The blastoderm of stages 12-14 quail embryos (staging according to Hamburger and Hamilton, 1951) was removed from the underlying yolk. The blastoderm was pinned out firmly on the black wax dish. In order to obtain cranial neural crest cells, the neural tube together with adjacent somites, was dissected out between the level of the mid-diencephalon and the fifth somite using a dissecting microscope (Wild Heerbrugg, Leitz). The tissue was placed in 0.0004% collagenase (sigma) in calcium and magnesium-free Tyrode's solution for 20 minutes at room temperature. The tissue was then removed from the collagenase solution and rinsed in Ringer's solution. The neural tube, including neural crest, was separated from the surrounding tissues by microdissection and pipetted on to a fibronectin-coated well (1:40, Sigma) of a 4-well Nunc culture dish.

The explants were randomly allocated to the following treatments: as controls (Groups A & B) the neural tube explants were cultured in 1 ml of DMEM only (n=15), and 1 ml of 0.05% DMSO reconstituted in DMEM (DMSO only, n=15). As experimentals, the explants were cultured in a 1ml DMEM solution containing 3µM topiramate (TOP only, Group C, n=13), 5µM of Atripla® (cART only Group D, n=15) and the combination of the two concentrations of Atripla® and Topiramate (cART/TOP Group E, n=13). The culture medium was made up of the DMEM solution containing 15% chick embryo extract and 10% horse serum (Bronner-Fraser, 1996). The cultures were then placed in an incubator (with 5% CO₂) at 37°C in a humidified atmosphere and were viewed after 24 hours. The cultures were photographed at 24 and 48 hours using an Olympus inverted phase contrast microscope (Olympus CKX41, South Africa) at specific magnifications. In order to maintain the concentrations of the drugs, the culture medium was replaced after 24 hours.

3.2.6 Measurement of quail neural crest cell migration

Only cell cultures where neural crest cells had migrated out around the entire circumference of the neural tube were used to analyze migration. Five cultures (2 DMEM only, 2 DMSO only and 1 cART/TOP) did not have neural crest cells completely surrounding the neural tube, and were thus excluded from the migration assay. The distance migrated by the neural crest cells was calculated as the difference in the radius of the circular spread of the cells between 24 and 48 hours of culture (Usami *et al*; 2014). The outermost NCCs in each of the cultured neural tubes were connected with the polygon tool in a circular fashion, and the pixel count inside the polygon was measured. The radius (R) of the polygon was calculated as follows:

$$R = \sqrt{(\text{number of pixels in a polygon}) / \pi} \dots\dots\dots (1)$$

In order to evaluate the extent of neural crest migration, the radius ratio (RR) was calculated using the following formula:

$$RR = [(R_{48h} - R_{24h}) / R_{24h}] \dots\dots\dots (2)$$

3.2.7 Actin staining and quantification

Control and experimental neural crest cells, which were cultured for 24 and 48 hours *in vitro*, were washed with pre-warmed phosphate-buffered saline (PBS) at pH 7.4. After rinsing, the cells were fixed in 3.7% formaldehyde solution in PBS for 10 minutes at room temperature. After washing extensively in PBS, the cells were layered with 0.1% Triton-X in PBS for 5 minutes, and washed in PBS thereafter. To reduce non-specific background, the fixed cells were pre-incubated with PBS containing 1% BSA for 25 minutes prior to adding the staining solution (Rhodamine Phalloidin, Sigma) to stain for actin. The cells were covered with a solution of rhodamine phalloidin (1:40) in PBS for 20 minutes at room temperature. After extensive rinsing in PBS, the cells were viewed using an Olympus inverted fluorescence microscope (Olympus IX51, South Africa).

In order to determine the level of fluorescence, the corrected total cell fluorescence (CTCF) was calculated using image J® software (National Institutes of Health, USA) as follows:

$$CTCF = \text{Integrated density} - (\text{Area of selected cell} \times \text{Mean fluorescence of background reading}).$$

3.2.8 Determination and quantification of pigmentation

Cranial neural crest cells which were cultured for 96 hours were evaluated for the presence of the black melanin pigment which normally appears in cultured cranial neural crest cells around 72

hours. Image J® software (National Institutes of Health, USA) was used to determine the mean gray values of melanin produced by melanocytes which had differentiated from neural crest cells. The region of interest was randomly selected using a table of random numbers. Ten measurements were recorded for each culture, and the mean of these measurements were regarded as the mean gray value for the specific culture. The area of measurement in which the measurements were made was kept the same.

3.2.9 Detection of mineralization (Alizarin method)

Cranial neural crest cells which were cultured for 48 hours *in vitro*, were washed with pre-warmed phosphate buffered saline (PBS) of pH 7.4 for 5 minutes. The cells were then fixed in 10% formaldehyde at room temperature for 15 minutes after which they were washed twice in distilled water. After washing extensively in distilled water, the cells were stained with 1% Alizarin red of pH 4.2 and incubated at room temperature for 20 minutes with gentle shaking. Following incubation, the cells were washed four times with 1ml distilled water while shaking for 5 minutes.

Excess water was removed by leaving the plates at an angle for 2 minutes and the cells were visualized using an Olympus inverted phase contrast microscope (Olympus CKX41, South Africa). The results were evaluated qualitatively. The results were evaluated qualitatively through the method of scoring. The scale of 0-5 was used, where 0 indicated the absence of staining, and 5 the most intense staining.

3.2.10 Neurite thickness measurements

The relative thickness of neurites was measured using systematic sampling after 96 hours of culture. A double square lattice system and a table of random numbers was used to determine the measurements. The thickness of the neurites was measured using image J® software (National Institutes of Health, USA). A line tool was used to measure the thickness of the neurite between

the two free edges of the neurite. A total number of 25 measurements were obtained for each culture.

3.2.11 Statistical analysis

All statistical analyses were done using Graphpad prism software for windows (Version 5.0, GraphPad Software Inc., San Diego, CA). Measurements for each variable (Radius ratio, CTCF, pigmentation and neurite thickness) were expressed as mean \pm standard error of mean (SEM). Group means for each variable were compared using one-way analysis of variance (ANOVA) followed by Bonferroni's multiple comparison test for post hoc analysis. A significance level of $P < 0.05$ was used.

3.3.0 Results

3.3.1 Migration of neural crest cells

After 24 hours of culture, neural crest cells cultured in DMEM only and DMSO only (Figs. 3.1 A & B) (control groups) appeared to have migrated a greater distance than all the experimental cultures (cART only, TOP only and cART/TOP), while the experimental cultures (Fig. 3.1 C, D, E) appeared to have migrated a shorter distance compared to the control cultures. Most of the control neural crest cells exhibited a typical multipolar shape (Fig 3.2 A, B black arrows), while neural crest cells which were cultured in cART only, appeared stretched (Fig 3.2 C red arrows). In addition, control neural crest cultures were dispersed, whereas the cART-treated neural crest cells appeared more clustered and were in close proximity to the neural tube. Although most of the cART-treated neural crest cells appeared stretched, some of the cells in the migration front appeared multipolar in shape (Fig. 3.2C, black arrow). Cells which were cultured in TOP only and cART/TOP, also appeared multipolar in shape (Fig 3.2 D, E black arrows). In addition, there was a space in the delamination process either separating two populations of neural crest cells (3.2D, blue double-headed arrows) or separating the neural tube from the delaminating neural crest cells (Fig. 3.2 E, blue double-headed arrow) in cultures treated with TOP only and in cultures treated with cART/TOP.

One-way ANOVA showed a significant effect of treatments on the radius ratios (RR) of the cranial neural crest cultures ($F(4, 57) = 26.75, P < 0.0001$, Fig. 3.1 F). Bonferonni's post hoc test revealed that the control cultures (DMEM and DMSO) had significantly higher radius ratios ($p < 0.0001$) compared to all the experimental groups (cART only; TOP only and cART/TOP). However, no significant differences were found among the experimental groups ($P > 0.05$).

3.3.2 Actin cytoskeletal elements at 24 hours

At 24 hours, actin fibres were regularly arranged in the cytoplasm of the neural crest cells of the two control cultures (Fig. 3.3A, B). However, neural crest cells which were cultured in cART, TOP and cART/TOP showed a disarray of the actin cytoskeletal elements (Figures 3.3 C, D, E). The actin filaments in the control cultures spanned the entire length and width of the neural crest cells, with the filaments reaching the filapodia at the end of the cells (Fig 3.3A, B). These actin filaments were arranged in a criss-crossing manner (Fig 3.3B, blue circle), and appeared to be pulling in the same direction. In contrast, neural crest cells, which were cultured in cART only, TOP only and cART/TOP exhibited actin filaments which did not extend the entire length and width of the cells (Fig 3.3 C, D, E). The filaments were confined to the extremities of the cells. The filaments in most of the cells cultured in cART and TOP appeared thinner. The cell bodies of the control cells appeared polygonal (Fig. 3.3A, B, blue arrows), while the treated neural crest cells were more rounded (Figure 3.3C, D, E, yellow circles).

One-way ANOVA showed a significant effect of treatments on the CTCF of actin filaments in the cranial neural crest cultures at 24 hours ($F(4,120) = 31.20, P < 0.0001$, Fig. 3.3 F). Bonferonni's post hoc test revealed that the control cultures (DMEM and DMSO) had significantly higher CTCF values ($p < 0.0001$) compared to all the experimental groups (cART only; TOP only and cART/TOP). However, no significant differences were found among the experimental groups ($P > 0.05$).

3.3.3 Actin cytoskeletal elements after 48 hours

There was no difference in the distribution of actin filaments in the neural crest cells which were cultured for 24 and 48 hours. Neural crest cells which were cultured in DMEM only and DMSO only

after 48 hours of culture exhibited actin filaments which were distributed throughout the entire perimeter of the cell (Fig 3.4 A, 4B). In contrast, actin filaments were concentrated at the lateral cortices of the cells (Fig. 3.4 C, D, E) in neural crest cells which were cultured in cART only, TOP only and cART/TOP. While cells of the control cultures appeared polygonal (Fig 3.4A, B, blue arrows), all treated cells appeared more rounded (Fig 3.4 C-E, yellow arrows).

One-way ANOVA showed a significant effect of treatments on the CTCF of actin filaments in the cranial neural crest cultures at 48 hours ($F(4,120) = 26.54, P < 0.0001$, Fig. 3.4 F). Bonferonni's post hoc test revealed that the control cultures (DMEM and DMSO) had significantly higher CTCF values compared to all the experimental groups (cART only; TOP only and cART/TOP). However, no significant differences were found among the experimental groups ($P > 0.05$).

3.3.4 Differentiation of neural crest cells into melanocytes

Cranial neural crest cells started to differentiate into pigment cells after 72 hours in all the cultures, and a prominent black pigment with varying intensities was evident in all cultures (control and experimental cultures) after 96 hours when the photographs were taken (Figs 3.5A-E, yellow arrows). The black pigment in cART-treated neural crest cells, appeared darker than the pigment in all the other cultures (Fig 3.5C, yellow circle). There was no significant difference in the intensity of pigmentation in the cells cultured in DMEM only and DMSO only (Figs 3.5A& B), although in some cultures, the intensity of pigmentation in DMSO only-treated cells appeared lighter (Fig 3.5B). In addition, both control cultures (Figs 3.5A& B) expressed less pigmentation when compared to the all the experimental cultures (Figs. 3.5 C-E).

One-way ANOVA showed a significant effect of treatments on the mean gray value of the pigmentation of the cranial neural crest cultures ($F(4, 58) = 48.49, P < 0.0001$, Fig. 3.5 F). Bonferroni's post hoc test revealed that the mean gray values of pigmentation of the control cultures (DMEM and DMSO) were significantly higher than all the experimental groups ($P < 0.0001$). In addition, the TOP only and cART/TOP treated cultures were significantly higher than the cART treated ($P < 0.0001$). However, no significant differences were found between the TOP only and cART/TOP groups ($P > 0.05$).

3.3.5 Neurite outgrowth

All cranial neural crest cells in culture developed long processes resembling the processes of neurons (Figs 3.6 A-E, orange arrows). This "neurite" formation occurred only after 96 hours in control cultures (Figs 3.6 A & B), whereas these processes appeared a day earlier (72 hours) in the experimental cultures (Figs. 3.6 C-E). After 96 hours, neurites of the control cultures were less numerous when compared to the experimental cultures. Neural crest cells which were exposed to cART only (Fig 3.6C) yielded more extensive neurites when compared to their control counterparts. Similarly, neurites in the TOP only treated cultures (Fig 3.6D) were more numerous compared to the control cultures (Figs. 3.6 A & B), however TOP only-treated neurites were less numerous than those observed in cART only treated cultures (Fig. 3.6C).

Control cranial neurites (Figs. 6 A & B) appeared shorter than neurites which were exposed to cART only and TOP only, which appeared longer and thicker (Figs 3.6C & D). The neurites in the control cultures were not as developed and were less prominent when compared to the experimental cultures. Neurites which were exposed to cART-only and TOP-only appeared to branch more

extensively. Some branches extended directly from the main neurite (Fig. 3.6D, blue circle), while some fine branches extended from secondary branches (Fig. 6D, yellow circle), forming a neurite tree. The cells cultured in cART/TOP (Fig. 3.6E) showed less neurites when compared to cells cultured in cART only or TOP only.

One-way ANOVA showed a significant effect of treatments on the neurite thickness in the cranial neural crest cultures ($F(4, 95) = 18.81, P < 0.0001$, Fig. 3.6 F). Bonferonni's post hoc test revealed that the neurite thickness of the control cultures (DMEM and DMSO) were significantly lower compared to cART only ($P < 0.0001$) but not different from either the TOP only or cART/TOP treated cultures ($P > 0.05$). In addition, no significant differences were found in the neurite thickness between the cART only and cART/TOP treated cultures ($P > 0.05$).

3.3.6 Alizarin red for calcium detection

Cranial neural crest cells which were cultured in DMEM only and DMSO only after 48 hours showed bright red patches which represented calcium production (Figs 3.7 A& B blue circles), while neural crest cells cultured in cART/TOP showed a lighter shade of red (Fig. 3.7 E, blue circle) or did not stain at all. In contrast, neural crest cells which were cultured in cART only and TOP only did not stain with alizarin red after 48 hours, indicating the absence of calcium. In these cultures, only the neural tubes (NT) stained a red colour.

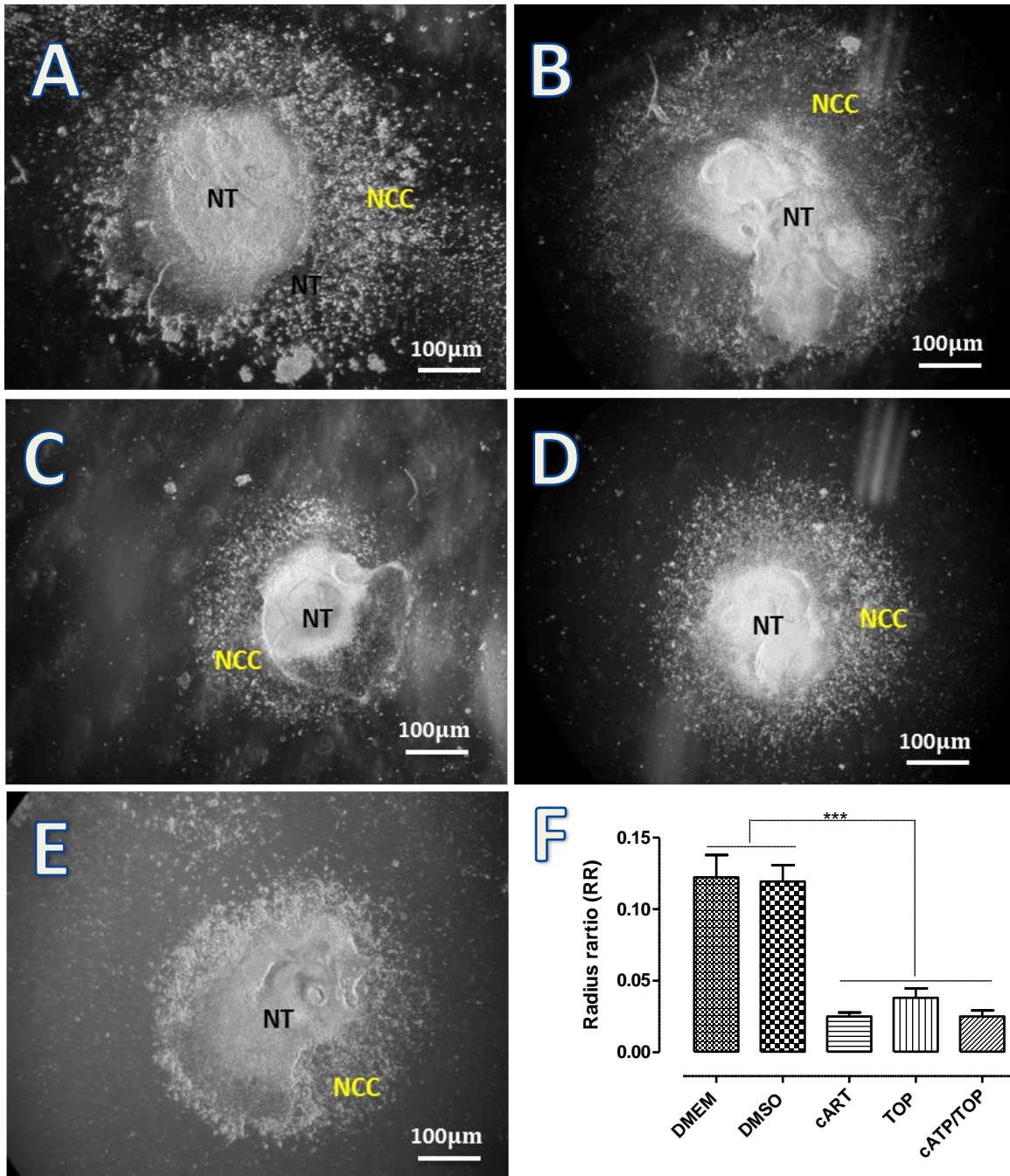


Figure 3.1. Photomicrographs showing the migration of cranial neural crest cells (NCC) from a neural tube (NT) cultured in DMEM only (A), DMSO only (B), DMEM + cART only (C), TOP only (D), and cART/TOP (E) after 24 hours. Neural crest cells (NCC) have migrated a greater distance (orange double-headed arrows) in control explants (A, B) compared to the treated cultures (C, D, E).

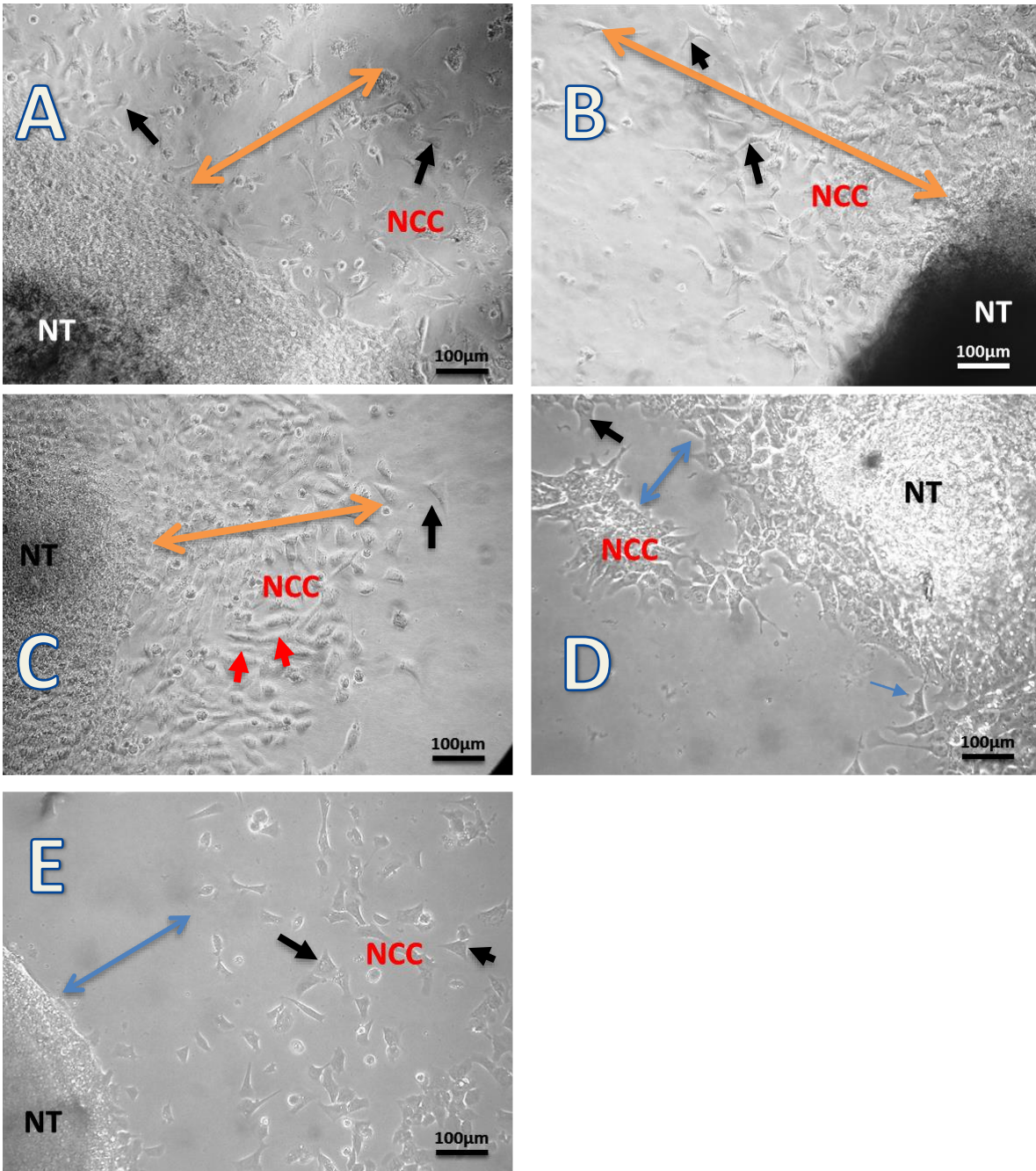


Figure 3.2. Photomicrographs showing migration of cranial neural crest cells (NCC) from a neural tube (NT) cultured in DMEM only (A), DMSO only (B), cART only (C), TOP only (D), and cART/TOP (E) after 24 hours. Neural crest cells (NCC) have migrated a greater distance (orange double-headed arrows) in control explants (A, B) compared to the treated cultures (C, D, E). A space in the delamination process (blue arrow) is evident in the Topiramate-treated and cART/TOP-treated neural crest cells (D, E). (Magnification 100X).

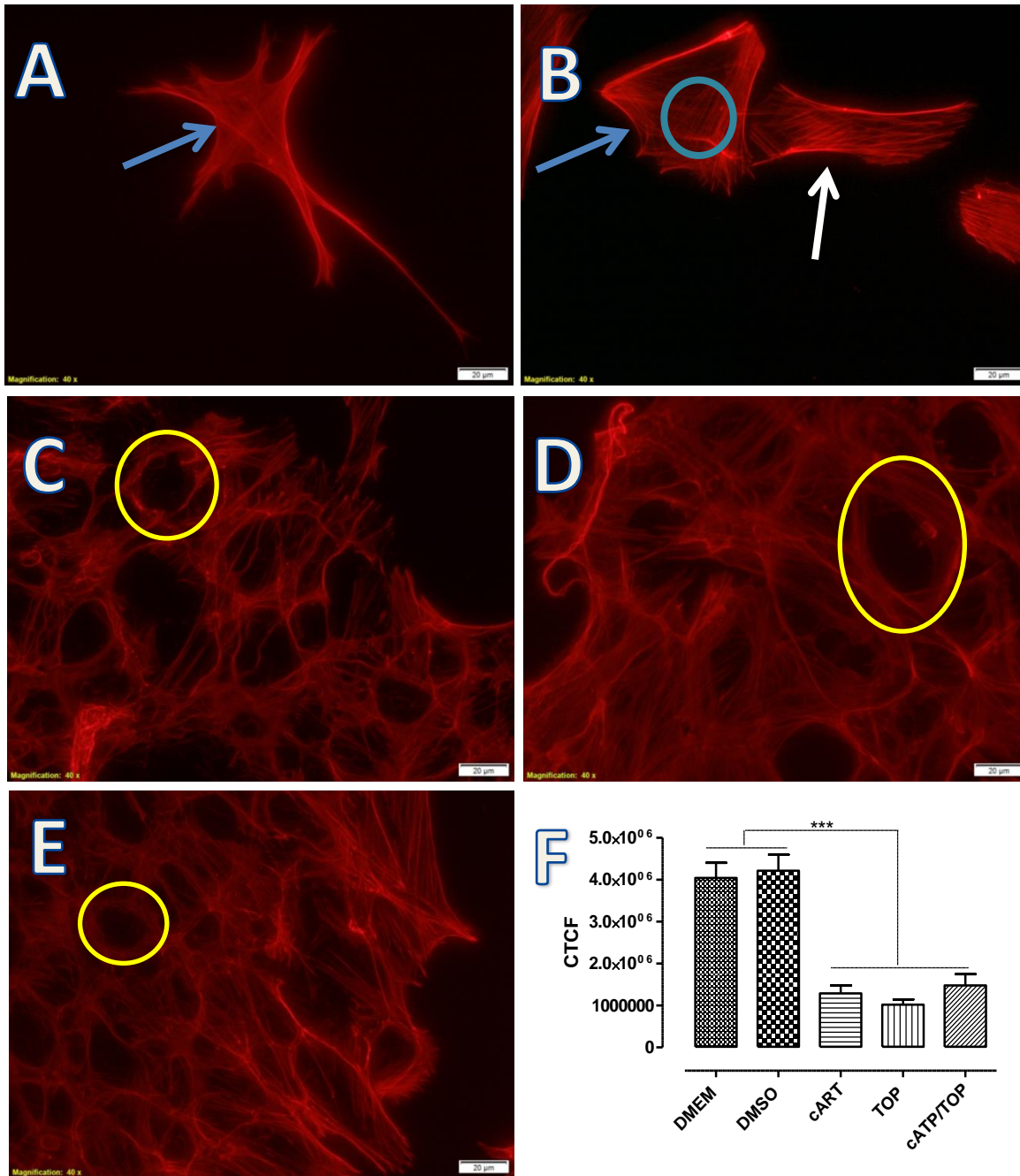


Figure 3.3. Fluorescence photomicrographs showing actin filaments in cranial neural crest cells which were cultured in DMEM only (A), DMSO only (B), TOP only (C), cART only (D) and cART/TOP (E) after 24 hours. Control neural crest cells (A, B) are polygonal in shape (blue arrows). A filopodium extension which has detached from a migrating neural crest cell is shown by a white arrow. Actin filaments in treated cultures (C, D, E) are more confined to the extremities of the cells, while the centre appears vacuolated.

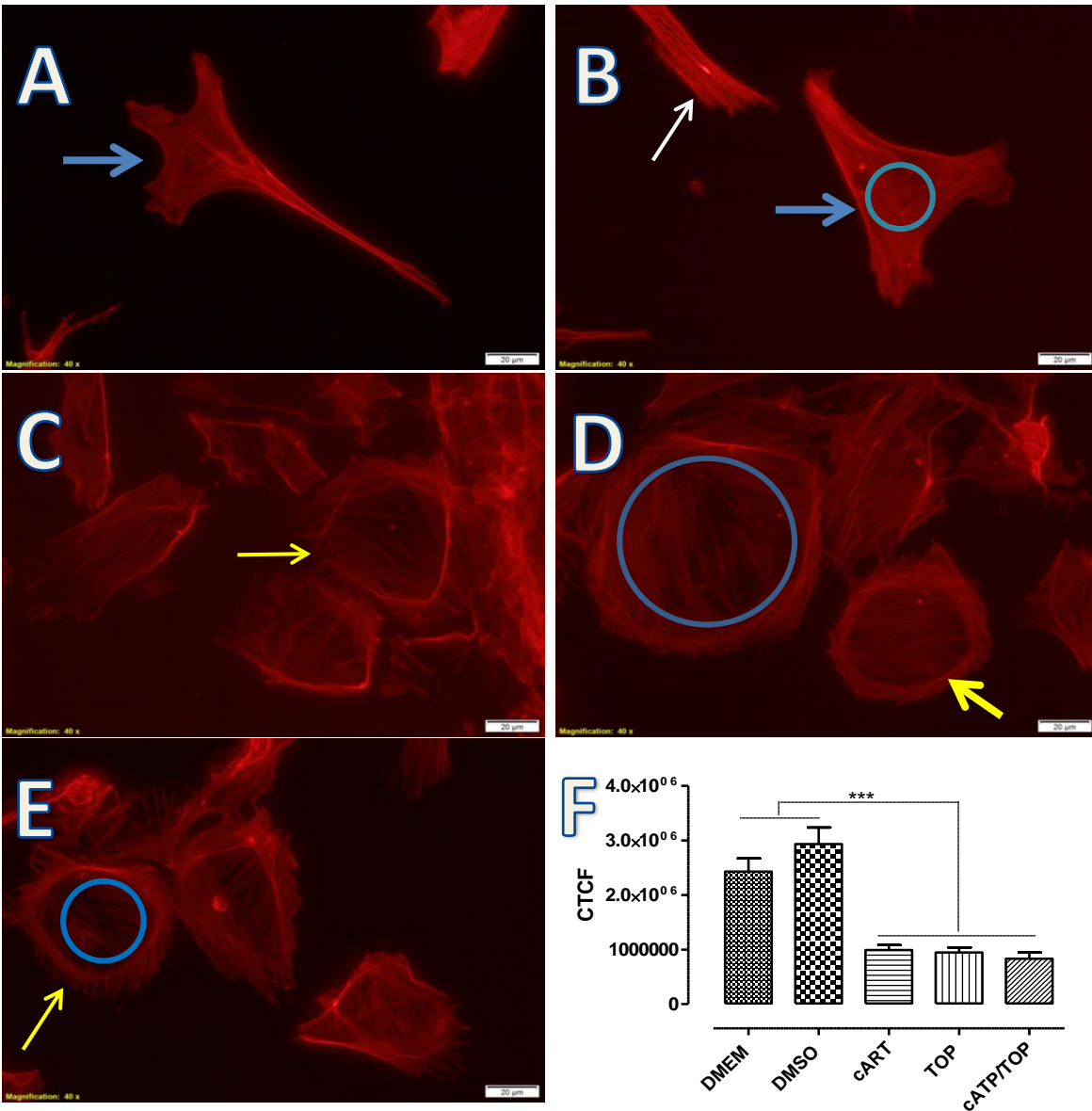


Figure 3.4. Fluorescence photomicrographs showing actin filaments in cranial neural crest cells which were cultured in DMEM only (A), DMSO only (B), TOP only (C), cART only (D) and cART/TOP (E) after 48 hours. Control neural crest cells (A, B) appear polygonal in shape (blue arrows). A filopodium extension which has detached from a migrating neural crest cell is shown by a white arrow. All the treated neural crest cells (C, D, E) appear rounded (yellow arrows) and the actin filaments are more restricted to the boundaries of the cells

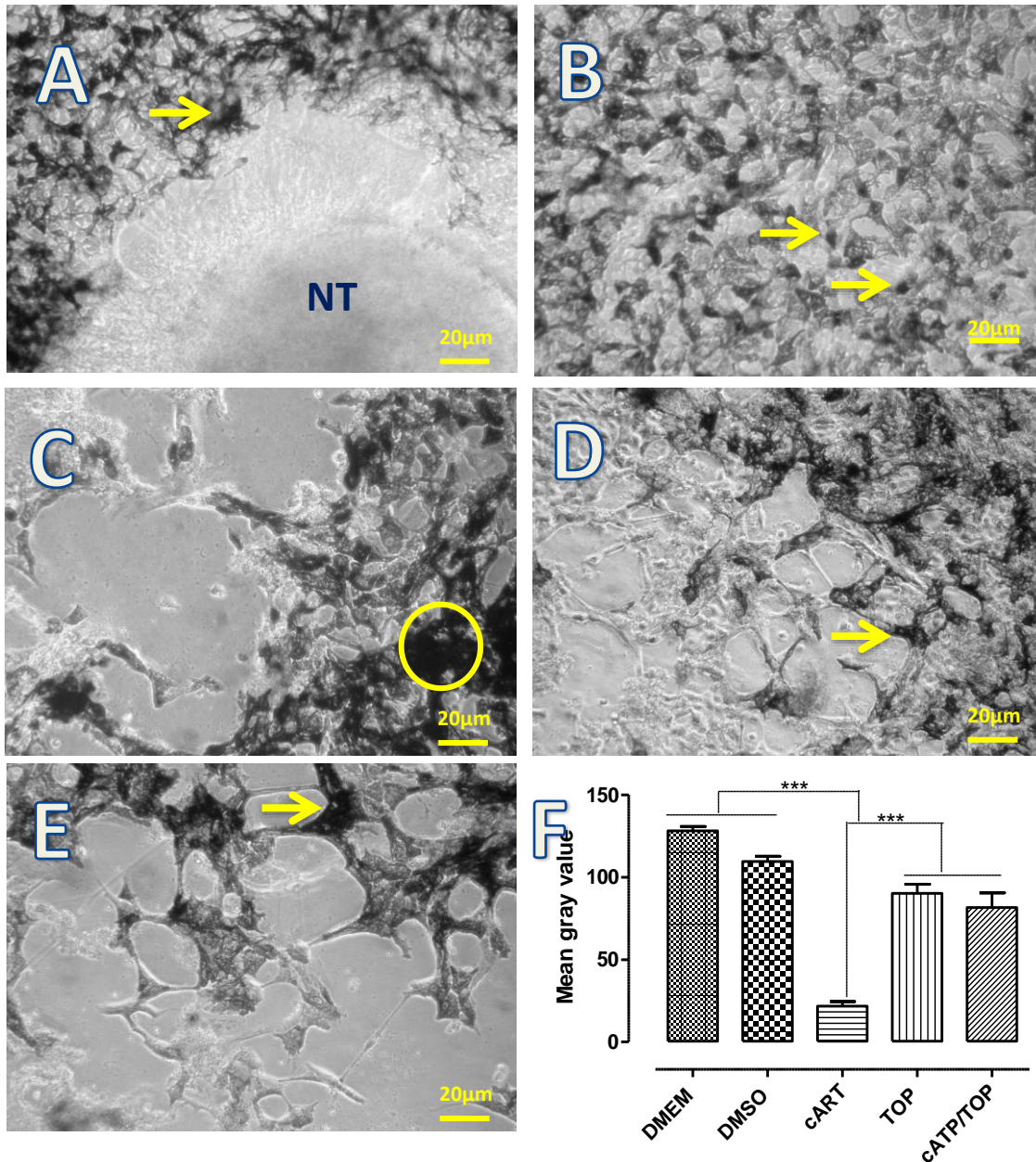


Figure 3.5. Photomicrographs showing pigment development in cranial neural crest cells cultured in DMEM only (A), DMSO only (B), cART only (C), TOP only (D) and cART/TOP (E) after 96 hours. cART only-treated cells seemed to be producing more pigment as the melanin appeared darker (yellow circle) than in the controls and other treated cultures (yellow arrow). Magnification (200X).

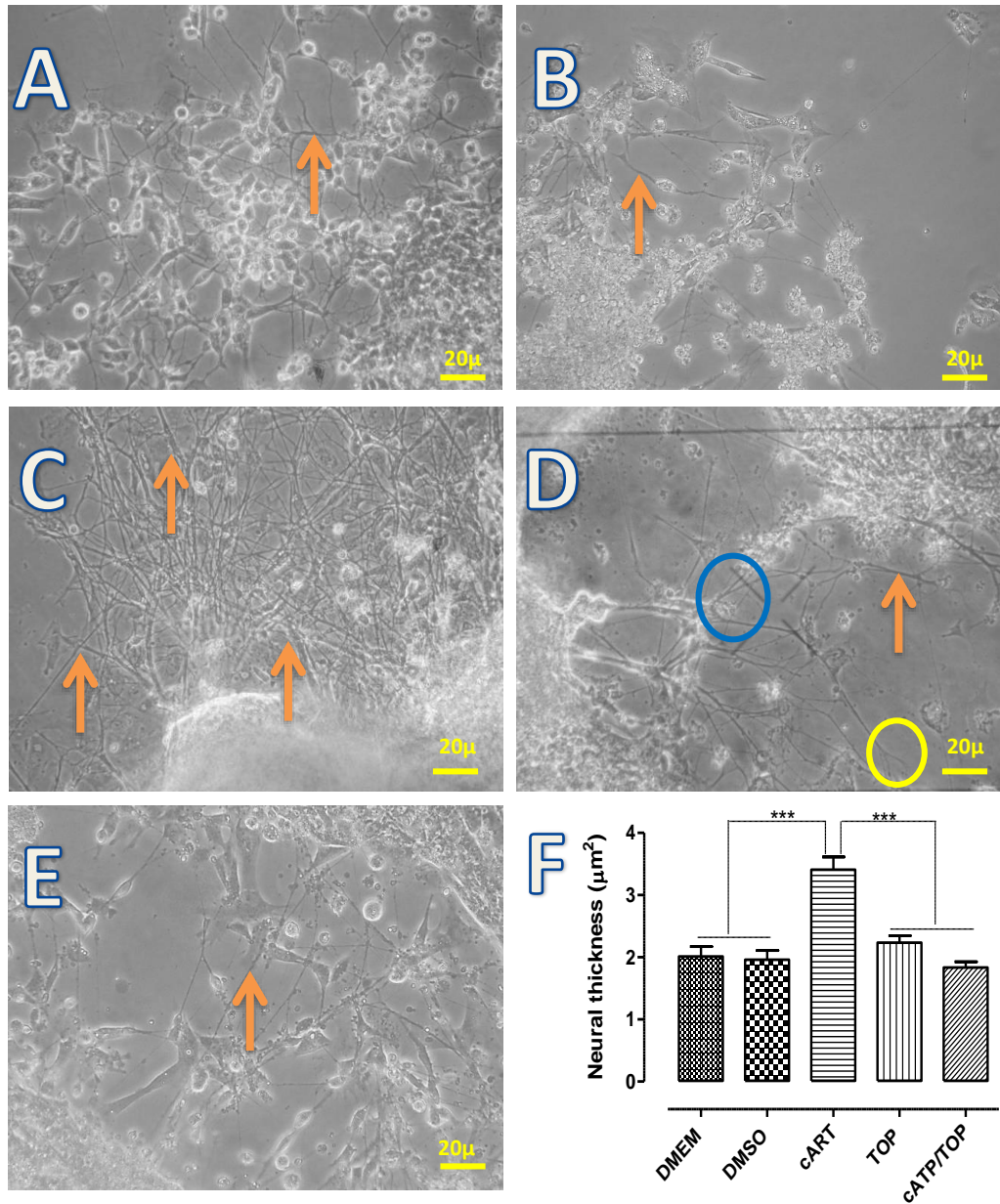


Figure 3.6. Photomicrographs showing neurite development in cranial neural crest cells cultured in DMEM only (A), DMSO only (B), cART only (C), TOP only (D) and cART/TOP (E) after 96 hours. cART only-treated neural crest cells produced more numerous neurites with greater arborization (orange arrows). Neurites cultured in TOP and cART/TOP appeared longer and thinner with less arborization (orange arrows). Control cultures (A, B) exhibited neurites which were less numerous and shorter than neurites of treated cultures (C, D, E) (Magnification 200X).

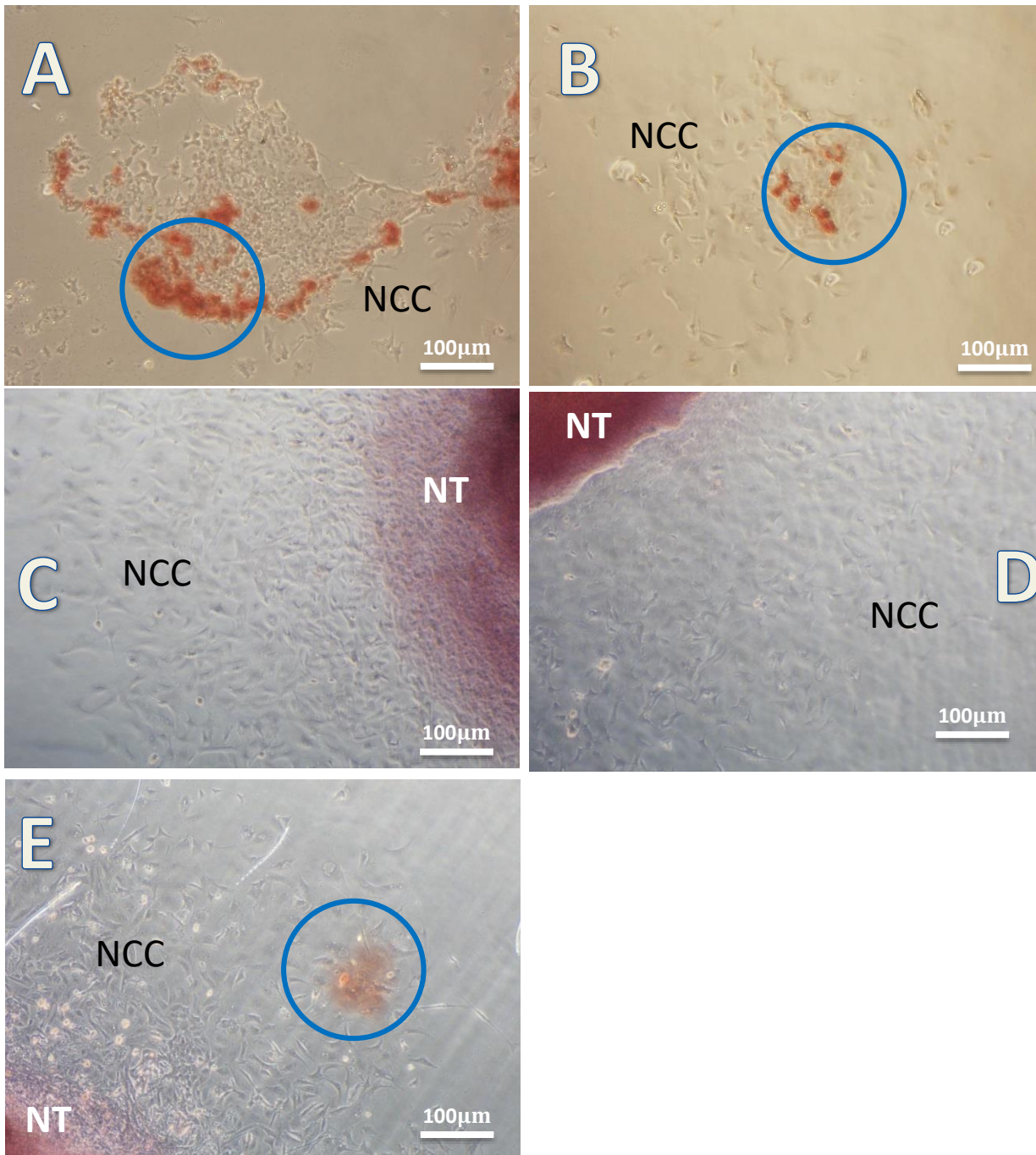


Figure 3.7. Photomicrographs showing calcium production in cranial neural crest cells (NCC) cultured in DMEM only (A), DMSO only (B), TOP only (C), cART only (D) and cART/TOP (E) after 96 hours. Control neural crest cells (A, B) stained positive with Alizarin red for calcium deposition, while the cART-treated and TOP-treated cells did not stain. Neural crest cells cultured in cART/TOP showed a light shade of red (blue circle), while the neural tube (NT) stained a red colour (Magnification 100X).

3.4.0 Discussion

The current study investigated the effects of co-administration of TOP and cART on the migration of cranial neural crest cells in order to establish a possible mechanism by which the two drugs result in the formation of cleft lip and palate when administered during gestation. Research has shown that TOP and cART individually cause cleft lip and palate and other craniofacial malformations when administered prenatally (Margulis *et al*; 2012; James *et al*; 2014), but the mechanism of action of the two drugs is not fully known. The current study therefore used *in vitro* techniques in order to investigate the effects of these two classes of drugs on the migration and differentiation of cranial neural crest cells which are fundamental to the normal development of the craniofacial region. The results of this study show that both TOP and cART inhibit the *in vitro* migration of cranial neural crest cells as indicated by the significant decrease in the extent of migration of cranial neural crest cells which were cultured in the presence of the two drugs, both individually and in combination. As indicated earlier, the inhibition of migration, along with the abnormal proliferation and differentiation of cranial neural crest cells is associated with various malformations of the craniofacial region (Wang *et al*; 2019). Therefore, the significant reduction in migration of cranial neural crest cells observed in this study suggests a possible direct link between the craniofacial malformations and the administration of TOP and cART during gestation. It has been reported (Trainor 2010) that cranial neural crest cells which can survive, proliferate, migrate and differentiate normally are critical to the development of a normal functional craniofacial skeleton. According to Trainor (2010), failure of one or more of the aforementioned processes forms the basis of craniofacial birth defects (Trainor, 2010). The types of defects are dependent on which of the aforesaid processes are perturbed. Anomalies such as cleft palate and micrognathia may arise if the number of neural crest cells is reduced or if the migration is inhibited, such that

neural crest cells fail to reach their destinations (Trainor, 2010; Cordero *et al*; 2011). The migration assay used in this study does not account for the number of cells, therefore it is plausible that the reduced radius ratio in the treated cells could be attributed to a combination of a reduction in number and the inhibition of migration of neural crest cells; however the rounding-up of cells in the evaluation of the actin cytoskeleton suggests that the decrease in the radius ratio in the treated cells is due to the premature cessation of migration of neural crest cells, as this feature of neural crest cells is indicative of stationary cells (Haendel *et al*; 1996).

There was no significant difference in the extent of migration among the three treatments. These results suggest that both TOP and cART inhibit cranial neural crest cells equally, and in addition TOP doesn't affect the activity of cART. Both TOP and cART containing Efavirenz utilize the cytochrome p450 (CYP3A4) enzymatic system (Nallani *et al*; 2003; Xu and Desta; 2013), while cART is metabolized by CYP2B6 (Xu and Desta; 2013) in addition to the CYP3A4 system. The results of the cART/TOP suggest that there may be no competitive inhibition between cART and TOP when administered in combination. The availability of an additional enzyme (CYP2B6) for cART is probably the reason for the lack of competitive inhibition. It is noteworthy to mention that previous studies have shown that Tenofovir and Emtricitabine-(the other two components of cART) which are used in combination with efavirenz do not activate the cytochrome P450 system (Masho *et al*; 2007).

In addition, the current study shows that cART and TOP affect the arrangement and the quantity of the actin cytoskeleton in cranial neural crest cells when administered individually and in combination. The treated neural crest cells in this study showed disarray in the cytoskeletal elements. The actin filaments in these cells were concentrated more in the cortical region of the cells as opposed to the centre which appeared more vacuolated. The cortical region of the cell

plays a major role in migration (Chugh and Paluch, 2018). According to Chugh and Paluch (2018) abnormalities and contractions of cells may occur if alterations in the components of the cortical region take place. The retraction of a migrating cell is facilitated by an increased cortical tension at the rear of the cell (Chabaud *et al*; 2015). This tension can create a cortical flow which helps push the cell forward (Chabaud *et al*; 2015). Two capping proteins CAPZA and CAPZB, and cofilin and profilin regulate the assembly and disassembly of actin filaments (Biro *et al*; 2013; Chugh and Paluch, 2018). A reduction in CAPZB and cofilin 1 results in the increase in the thickness of the cortex, while the cortical tension is reduced (Chugh and Paluch, 2018; Biro *et al*; 2013). Cortical tension is central to the function of the cell cortex. The increase of cortical thickness in the treated neural crest cells in the current study could be due to an alteration in the capping protein CAPZB and cofilin 1. Further studies need to be carried out in order to investigate if cART and TOP affect the activities of the two proteins as a possible mechanism by which actin filaments are confined to the cortical region of the cell as opposed to the centre. In addition, TOP and cART reduced the fluorescence of actin in neural crest cells as indicated by a reduced CTCF over 24 and 48 hours. This reduction in CTCF, coupled with disarray in the cytoskeletal element may suggest the mechanism by which the neural crest cells are inhibited in their migration.

Cranial neural crest cells which were cultured in cART-only produced more melanin compared to both control cultures and other treated explants. The increase in melanin production in the cART only-treated cranial neural crest cells suggests a role of cART in the interruption of the process of melanin production during gestation. These results may provide insight into the mechanisms by which cART affect melanin production in HIV- OMH, congenital melanocytic nevus and trisomy13, 21 which have been observed in children who are born to mothers who are on cART (Joao *et al*; 2010; Hadianfard and Ashraf, 2012). In congenital melanocytic nevus the melanosomes are not

evenly distributed and the differentiation of melanoblasts from neural crest cells is impaired (Chandran *et al*; 2016). It is not clear whether the increase of pigmentation in the cART only-treated cells in the current study as observed involves the distribution, number or the activity of melanosomes. Determining the mechanism of action of melanin production impairment may be challenging as there are many factors which may lead to increased production of melanin (Roh *et al*; 2015; Chandran *et al*, 2016; Yang *et al*; 2017).

In addition to increased pigmentation in neural crest cells, the results show that cART increases the differentiation of neurites from the cranial neural crest cells. The treated neural crest cells showed extensive growth and branching of neurites, a feature which may be associated with defects of the nervous system (Emoto, 2011). According to Dalakas (2001) cART causes specific side effects of the central nervous system which are associated with PN. Toxicity of peripheral nerves is induced exclusively by NRTIs when used individually and when they are used in combination with other classes of antiretrovirals. According to Dalakas (2001), the treatment of HIV infected patients with cART resulted in worsened peripheral neuropathy observed in the patients, suggesting that the antiretroviral drug is toxic to peripheral nerves.

Therefore, the results of the current study suggest a possible correlation between the use of cART during gestation and the development of PN-associated congenital defects like talipes equinovarus and hip dysplasia which have been observed in children born to mothers who are on cART (Joao *et al*; 2010; Hadianfard and Ashraf, 2012). The possible mechanism of action of cART based on the results of this study is through increased branching and reduced thickness of neurons of the peripheral nervous system.

Following the staining of cranial neural crest cells which were cultured for 48 hours with the Alizarin red method, only the control neural crest cells and the cART/TOP-treated produced calcium. In contrast, neural crest cells cultured in cART only and TOP only did not produce any calcium deposits. The increase in calcium translates to the production of bone matrix, as cranial neural crest cells are the only crest cells which are capable of bone formation (Knight and Schilling, 2013; Mishina and Snider 2014). These results are consistent with various studies which show that cART affects bone production and density (Aukrust, 1999; O Hileman *et al*, 2015; Park *et al*; 2017; Vlot *et al*; 2018). According to Aukrust (1999) cART induces changes in osteocalcin and C-telopeptide. These markers of bone remodelling are increased during cART, although the mechanism of this change is unknown (Aukrust, 1999). Park *et al* (2017) showed that elevated levels of osteocalcin were more prominent in patients taking tenofovir. However, the results from the current study suggests that cART and TOP suppresses the activity of osteoblasts during the early stages of development, with the subsequent decline in the production of calcium production.

The formation and resorption of bone during the administration of cART is regulated by RANK (receptor activator for nuclear factor kappa β) and its ligand, RANKL (Ji *et al*; 2009; Moran *et al*; 2017). RANK is a receptor which is expressed on the surfaces of osteoclasts, while RANK ligand is produced by osteoblasts. In order to inhibit the activity of osteoclast, osteoblasts secrete a protein called osteoprotegerin which binds to the RANK ligand in order to prevent bone resorption by osteoclasts (Ji *et al*; 2009; Park *et al*; 2017; Moran *et al*; 2017). Blood levels of RANKL and osteoprotegerin proteins have been shown to increase in patients who are on antiretroviral therapy. The levels of RANKL and OPGs are linked to a change in bone mass density in these patients (Ji *et al*; 2009; Park *et al*; 2017; Moran *et al*; 2017).

Brown *et al*; 2014 showed that the markers of bone resorption and formation increase during the first 6 months of cART introduction, whereas OPG and RANKL and inflammation are negatively affected. The failure and/or reduction of the production of calcium in cranial neural crest cells in this study could involve the activity of RANK and its ligand RANKL, a hypothesis which needs to be explored further.

3.4.1 Conclusion

The teratogenicity of exposure to either cART or TOP during gestation have been well documented. However, the mechanisms by which the two drugs cause craniofacial have been unclear. The current study shows that both cART and TOP inhibit the migration of cranial neural crest cells- the primordium of the face and palate. These results suggest a possible link between the gestational administration of the two drugs and the development of craniofacial malformations, as the mesenchyme responsible for the development of the structures of the head and neck region are derived from cranial neural crest cells. This data may shed light on the causes of congenital abnormalities of the craniofacial region in children who are born to female patients who are being treated for HIV and seizures. Cranial neural crest cells start to migrate out from the neural folds during the third week of development in humans, and therefore it is plausible that the third week could be the critical period for cART and TOP teratogenicity.

CHAPTER 4: The *in vivo* migration of cultured quail cardiac neural crest cells in the chicken interventricular septum

4.1.0 Introduction

The use of cART in the treatment of HIV-infected pregnant women and in the prevention of mother-to-child transmission of HIV has occasioned a significant reduction in the number of infants born with HIV (Williams *et al*; 2015). However, the safety of intrauterine exposure to cART remains a concern, particularly as an increasing number of women are becoming pregnant while already receiving cART (Watts, 2006). While previous studies assessing the risk of congenital anomalies (CAs) related to intrauterine exposure to cART seem to report absence of CAs (Jungmann *et al*; 2001; Heather-Watts *et al*; 2004), recent evidence suggests that intrauterine exposure to cART could increase the risk of congenital cardiac anomalies (Knapp *et al*; 2012, Phiri *et al*; 2014, Williams *et al*; 2015; Mehta *et al*; 2019).

A myriad of cardiovascular abnormalities has been attributed to the administration of cART and TOP during early pregnancy (Margulis *et al.*, 2012, Tennis *et al*; 2015). The cardiovascular effects of TOP teratogenicity include coarctation of the aorta, patent ductus arteriosus, atrial and ventricular septal defects (ASD & VSD) (Tennis *et al*; 2015). Remarkably, some of the aforementioned cardiovascular defects such as VSDs have also been reported in cART teratogenicity (Brogly *et al*; 2010; Prieto *et al*; 2014; Williams *et al*; 2015; Vannappagari *et al*; 2016).

Ablation studies have shown that the failure of migration of cardiac neural crest cells to the truncal ridges and their subsequent failure to contribute towards the closure of the interventricular foramen results in VSDs (Waldo and Kirby, 1998; Hutson and Kirby, 2003) which underscore the important

role of cardiac neural crest cells in the development of a normal interventricular septum in the embryo and subsequently in a definitive adult heart.

4.1.1 The origin and migratory pathways of cardiac neural crest cells

Cardiac neural crest cells arise from the level between the mid-otic placode and the third somite during stage 8 of chick embryo development (Hamburger and Hamilton, 1951). As they migrate, cardiac neural crest cells they will eventually reach the third, fourth and sixth pharyngeal arches. This population of cells plays a role in the formation of the aorticopulmonary septum, cardiac innervation, aortic arch repatterning, and myocardial function (Kirby et al., 1983, 1985; Kirby and Stewart, 1983; Kirby, 2002; Hutson and Kirby, 2003).

4.1.2 Cardiac neural crest cells and pharyngeal arch arteries

Prior to this, the cells migrate ventrally before they temporarily suspend their migration in the circumpharyngeal ridge (Kirby et al., 1983, 1985; Kirby and Stewart, 1983; Kirby, 2002; Hutson and Kirby, 2003). As they navigate their way between pharyngeal ectoderm and endoderm cardiac neural crest cells will populate the endothelial cells of aortic arch arteries (Kirby et al., 1983, 1985; Kirby and Stewart, 1983; Kirby, 2002; Hutson and Kirby, 2003). These aortic arch arteries will eventually be modified such that they become asymmetric great arteries. These include the common carotid artery and the ductus arteriosus. According to Bockman *et al.*; 1987, cardiac neural crest cells play a role in the patterning and not the formation of the aortic arch arteries. However, these cells will form the smooth muscle cells of the tunica media of these great arteries (Bergwerff et al., 1998).

During stage 9 of avian development neural crest cells will migrate from the neural tube as they undergo an epithelial-mesenchymal transition (Boot *et al.*, 2003). These cells will migrate to the

aorticopulmonary septum and the pharyngeal arch arteries. These arteries do not include the dorsal aorta (Boot *et al.*, 2003).

Cardiac neural crest cells which are derived from stages 12 to 13 of avian development only populate the proximal part of pharyngeal arch arteries as they are involved in the remodeling of these arteries. These cells are not involved in the formation of the aorticopulmonary septum (Boot *et al.*, 2003).

4.1.3 Cardiac neural crest cells and the formation of interventricular and aorticopulmonary septa

Following their migration from the dorsal neural tube cardiac neural crest cells will populate the cardiac outflow cushions. This population of neural crest cells will form the aorticopulmonary septum (Waldo *et al.*, 1998; Waldo *et al.*, 1999). The septum will result in the formation of the aorta and pulmonary trunk from the truncus arteriosus (Waldo *et al.*, 1998; Waldo *et al.*, 1999). In addition, the cardiac neural crest cells will migrate into the truncal ridges which contribute towards the formation of the interventricular septum. Cranial neural crest cells will also give rise to all parasympathetic innervation of the heart (Kirby *et al.*, 1983). By stage 15 the cardiac neural crest has stopped producing cardiac neural crest cells (Boot *et al.*, 2003) and these cells have reached aortic arch 3 at stage 17 (Waldo *et al.*, 1996, 1999). Around day 20 ventricular septation will commence, and the interventricular foramen will be visible about 2 stages later (De la Cruz *et al.*, 1983).

Around stage 23 these cells will populate the outflow tract (Waldo *et al.*, 1998; Farrell *et al.*, 1999; Kirby, 2002). The arterial pole (Poelmann *et al.*, 1998) and the venous pole (Poelmann and Gittenberger-de Groot, 1999) are the two entry points to the primitive heart. Three different types of derivatives are found in the arterial pole. These are the outflow tract septum; smooth muscle

cells in the great vessel walls; and ganglionic cells in the outer vessel walls and in the subepicardial space of the heart.

There is a range of defects which have been reported due to cardiac neural crest ablation. These defects include ventricular septal defects, truncus communis, abnormal patterning of the aortic arch arteries and great arteries, abnormal myocardial function (Besson *et al.*, 1986; Bockman *et al.*, 1987; Creazzo *et al.*, 1997; Kirby *et al.*, 1983). In addition, cranial neural crest cells are crucial in the formation of a normal cardiac loop. According to field (Yelbuz *et al.*, 2002), defective looping occurs early on following cardiac neural crest ablation.

In this regard, this study aimed to investigate the individual and combined effects of cART using cART and TOP on the migration of quail cardiac neural crest cells *in vitro*. The study further determined the *in vivo* migration of *in vitro* CART and TOP-treated quail neural crest cells, microinjected into chick embryo *in vivo*.

4.2.0 Material and methods

4.2.1 Drugs

The drugs (cART and TOP) were prepared as described in the previous chapter (chapter 3).

4.2.2 Embryos and Ethical clearance

Sixty (60) fertile Japanese quail (*Cortunix cortunix japonica*) and 60 chicken (*Gallus gallus domesticus*) eggs were used in this study. The quail eggs were incubated for 32 hours at 37°C in a humidified incubator. The chicken eggs were used as hosts and were also incubated at 32 hours in a humidified incubator. All experimentation was carried out in a laminar flow hood under aseptic conditions. All experimental procedures were approved by the University of the Witwatersrand, Animal Research Ethics Committee (Animal Ethics Clearance Number 2019/01/2/A).

4.2.3 Preparation of equipment

Equipment was sterilized as previously described in chapter 3.

4.2.4 Neural tube cultures

The blastoderm of stage 8 quail embryos (staging according to Hamburger and Hamilton, 1951) was removed from the underlying yolk as previously described in chapter 3. In order to obtain cardiac neural crest cells, the neural tube together with adjacent somites, was dissected out

between the level of the mid-otic placode and the third somite. The explants were randomly allocated to the following treatments: as controls (A & B) the neural tube explants were cultured in 1 ml of DMEM only, (n=12), and 1 ml of 0.05% DMSO reconstituted in DMEM (DMEM only, n=12). As experimentals, the explants were cultured in a 1ml DMEM solution containing 3 μ M TOP (Group C, TOP only, n=12), 5 μ M of Atripla® (Group D, cART only, n=12) and the combination of the two concentrations of Atripla® and TOP (Group E, cART/TOP, n=15). The cultures were then placed in an incubator (with 5% CO₂) at 37°C in a humidified atmosphere and were viewed after 8 and 24 hours. The cultures were photographed at 24 and 48 hours using an Olympus inverted phase contrast microscope (Olympus, South Africa) at specific magnifications. In order to maintain the concentrations of the drugs the culture medium was replaced after 24 hours.

4.2.5 Measurement of quail neural crest cell migration

The extent of migration was measured using the determination of the difference in the radius ratio of migrated neural crest cells as previously described in chapter 3.

4.2.6 Actin staining and quantification

Control and experimental neural crest cells were stained with Rhodamine phalloidin for the quantification of actin as previously described (chapter 3).

4.2.7 Suspension of cultured neural crest cells to obtain cells for micro-injection

Migrating quail cranial neural crest cells which had been cultured on fibronectin for 24 hours were brought into suspension using 2.5% trypsin as follows. Both the culture medium and the neural tube were removed from each well, and the neural crest cells were washed with pre-warmed PBS. A 150 μ l of trypsin (Highveld Biological, South Africa, Gauteng) was added to each well and the

adhering neural crest cells were then incubated at 37°C for 3-5 minutes. The trypsin was used neat (undiluted). The action of trypsin was stopped by adding 500µl of DMEM to each well. The suspended cells were transferred into a sterile centrifuge tube and spun for 5 minutes at 1500rpm. The supernatant was poured off and the pelleted cells were used for micro-injection into the cardiac regions of chick embryo hosts which had been incubated for 32 hours. To test for cell viability, a TC20 automated cell counter (BIO-RAD, Country) was used. In addition, neural crest cells were re-plated onto a clean fibronectin-coated four-well Nunc culture multidish. The cells were viewed hourly to determine if they are able to re-adhere to the fibronectin.

4.2.8 Transfer of cultured and suspended quail neural crest cells into a chick host

The quail neural crest cell experiment

Out of 60 chick host embryos, 12 died and 48 embryos (80%) were used for this part of the study and were distributed as follows: DMEM only (n=8); DMSO only (n=9); cART only (n=10); TOP only (n=11) and cART/TOP (n=10). For the microinjections of quail cardiac neural crest cells into the cardiac region of chick hosts, fertile 32-hour chicken host embryos were used. The chick-quail chimaera technique was used because the large quail nucleoli are easily distinguishable from the small nucleoli of chick cells, and hence any neural crest cell which had migrated from the quail donor neural tubes could be easily identified in the chicken host embryo.

In this procedure, each chicken egg (stages 8-9) was wiped with 70% alcohol and placed horizontally onto an egg holder. The blunt end of the egg was punctured using a hack-saw blade to release air from the air sac. Following which, 1.5ml of albumen was aspirated by penetrating the pointed end of the egg, slightly below the equator of the shell with the needle and a syringe. The

needle was pointed downward, almost vertically, as it is passed into the shell to avoid damage to the yolk. To avoid leakage of albumen, the entry point was sealed with clear tape. A window was then cut in the shell, overlying the position of the embryo at the highest point of the egg when lying transversely, and the shell membrane was removed. The embryo was then visible through the window. To keep the blastoderm moist, a few drops of chick Ringer's solution with antibiotics (1µl penicillin and streptomycin, Sigma) was placed on to the chorioallantoic membrane of the embryo. In order to visualize the different regions of the embryo, 100 µl of 1% Pelican India ink was injected below the blastoderm.

The cultured, suspended quail cranial neural crest cells were counted using a TC20 automated cell counter (BIO-RAD, Country). Each cell pellet was diluted using the culture medium until a live cell count reached 1×10^{-3} to ensure that an equivalent number of cranial neural crest cells are injected into the chicken host. The cells were then backfilled into a sterile-pulled thin glass needle of unknown diameter. The needle was connected to an aspirator tube. The tip of the needle was then inserted into the desired region of the embryo. The quail cranial neural crest cells were then micro-injected under the surface ectoderm into the mesenchyme adjacent to the cardiac neural tube (Fig. 4.1A). This procedure was carried out for both the non-treated controls (DMEM only and DMSO only) and the treated groups (cART only; TOP only and cART/TOP). Following micro-injection of the neural crest cells, the egg was sealed with clear cellophane tape and returned to the humidified incubator at 37°C for 14 days. The chicken embryos were removed from the eggs shells, and the hearts were dissected out, and fixed in 10% formalin, processed in an automatic processor (Shandon Citadel 1000), and embedded in paraffin wax. The heart tissue was serially sectioned on a Leica microtome (Leica, South Africa) at 5µm and stained with the Feulgen-Rossenbeck method to identify the large nucleoli of quail neural crest cells. To avoid loss of tissue during

processing, silane-coated slides were used. Light microscopy was used to view the processed tissue.

4.2.9 Feulgen reaction (Feulgen and Rossenbeck, 1924).

The paraffin sections of the chicken hearts samples were brought to distilled water. The sections were briefly rinsed in cold ammonium chloride (NHCL) and transferred to NHCL at 60°C for 8 minutes. As controls, similar sections of each heart tissue were placed in distilled water at 60°C for the same period of time (8 minutes). After washing in distilled water, the sections were transferred to Schiff's reagent for 60 minutes. The sections were rinsed in three changes of sulphite rinse solution, and then in water. The sections were counterstained in 1% aqueous light green for 1 minute, dehydrated, cleared and mounted in entellan. As a positive control for the big quail nucleoli, adult quail liver was used (Fig. 4.7A).

The interventricular septum of the chicken host embryo was assessed under the light microscope (Fig. 1 C, X100, oil immersion) for the presence of quail cranial neural crest cells and the cells were counted using image J® software (National Institutes of Health, USA). The cells were counted using systematic sampling. A double square lattice system and a table of random numbers were used to determine the areas of cell counts. Ten sets of counts were randomly made on each interventricular septum of chicken hosts (given a total count of 80 to 100 per treatment group) and the average was used as a count for each group. The numerical density of quail neural crest cells was expressed as:

$$\left[\frac{\text{Number of counts}}{\text{Area}} \right]$$

4.2.10 Statistical analysis

All statistical analyses were done using Graphpad prism software for windows (Version 5.0, GraphPad Software Inc., San Diego, CA). Measurements for each variable (Radius ratio, CTCF and numerical density) were expressed as mean \pm standard error of mean (SEM). Group means for each variable were compared using one-way analysis of variance (ANOVA) followed by Bonferroni's multiple comparison test for post hoc analysis. A significance level of $P < 0.05$ was used.

4.3.0 RESULTS

4.3.1 Cell migration

The qualitative results of neural crest cell migration are as shown in figure 4.2. The neural crest cells (NCC) started to migrate out of the neural tube (NT) after 12 hours of culture in both the treated and control explants and some good migration distance was covered at 24 hours when the pictures were taken. The neural crest cells of the treated groups (cART only, TOP only and cART/TOP-treated i.e. groups C, D, and E respectively) migrated a lesser distance (Fig. 4.2C, D and E orange double-headed arrows, Fig. 4.5) than the control cultures (Fig. 4.2A and B; orange double-headed arrows). The interruption of migration was pronounced in group D where neural crest cells cultured in cART only were clustered around the epithelial sheath as they delaminate from the neural tube (Fig. 4.2D; curly brackets). However, the TOP only-cultured neural crest cells, were sparse and scattered (Fig. 4.2C), and in addition a gap was observed in delaminating process depicted by the blue double-headed arrow (Figure 4.2C). The distance of migration in cART/TOP-treated neural crest cells was reduced when compared to the control cultures, but was greater than in the cART only-treated neural crest cells (Fig.4. 2E, Fig. 4.5)

In addition, the cART only-treated neural crest cells showed rounded profiles both at low (Fig. 4.2D; curly brackets, 100X) and high magnifications [Figs. 4.3D (200X) and 4.4D (400X)]. However, at low (Fig. 4.3 A, B) and higher magnification (Fig. 4.4A), the migrating neural crest cells of the control groups exhibited a polygonal/stellate shape with filapodial extensions; depicting typical migrating cells (Fig. 4.2A, 4.3A and B, black arrows). The cART/TOP-treated neural crest cells also showed rounded profiles at higher magnification (Figs. 4.3E and 4.4E). Numerous detached filapodial extensions from the migrating neural crest cells could be seen among the migrating neural

crest cells (Fig. 4.3A and B, red arrows). While most of the neural crest cells exhibited a single nucleolus (Fig. 4.4B and D, and E, red circle) some exhibited pale vesicular nuclei with two nucleoli (Fig. 4.4 A and C, yellow circle).

Figure 4.6 (A and B) shows rhodamine phalloidin stained control neural crest cells which were cultured for 48 hours in DMEM only (A) and DMSO only (B). The parallel bundles of actin filaments are seen extending within the entire cell body processes of all the control cells (Fig. 4.6 A, B). Some stress fibers could be seen criss-crossing with the parallel fibers at right angles (Fig. 4.6 A and B, yellow circles). The fluorescence staining also revealed the polygonal shape of control neural crest cells (Fig 4.6 A, B). All the treated cultures showed similar features of the actin cytoskeleton (Fig. 4.6 C-E). The cells were more rounded and smaller than the control cells. The actin filaments appeared to be in disarray, concentrated at the lateral cortices and center was devoid of filaments (Fig. 4.6 C-E). Filopodial extensions, detached from the migrating cells were observed in both the experimental and control cultures (Fig.4.6 B-E, white arrows) but are more numerous in the control cultures than in the treated cultures. The experimental neural crest cells which remained in the vicinity of the neural tube appeared to be attached to each other (Figs. 4.6 C-E).

One-way ANOVA showed a significant effect of treatments on the CTCF of actin in the neural crest cultures ($F(4, 120) = 11.41, P < 0.0001$, Fig. 4.6 B). The CTCF values of control cultures (DMEM only and DMSO only) were not significantly different from that of the cART only group ($P > 0.05$) but significantly different from the TOP only ($P < 0.0001$) and cART/TOP ($P < 0.01$) groups. Furthermore, the mean of CTCF for the TOP only group was significantly lower than the cART only or cART/TOP groups ($P < 0.05$). However, no significant differences were found between the DMEM only and DMSO only groups or between the cART only and cART/TOP groups ($P > 0.05$).

4.3.2 The *in vivo* migration of quail neural crest cells into chick hosts

The nucleolus of quail neural crest cells microinjected onto chick hosts, were distinguishable from the chicken nucleolus by their large size in the interventricular septum of the chick hosts either singly or in groups (Fig.4. 8).

4.3.3 Quantitative analysis

One-way ANOVA showed a significant effect of treatments on the radius ratios of the neural crest cultures, with higher radius ratios in control cultures (DMEM only and DMSO only, A & B) compared to treated groups (cART only; TOP only and cART/TOP, C, D & E) (Bonferroni's post-hoc test $F(4, 64) = 61.68$, $P < 0.0001$, Fig. 4.5F). However, no significant differences were found among the control groups ($P > 0.05$) and among the experimental groups [$P > 0.05$], Fig 5F].

One-way ANOVA showed a significant effect of treatments on the numerical density of quail neural crest cells in the chick heart interventricular septum ($F(4, 31) = 67.12$; $P < 0.0001$, Fig. 4.9F). The control groups (DMEM only and DMSO only) had significantly higher numerical densities of quail neural crest cells in the chick heart interventricular septum compared to the experimental groups; cART only; TOP only and cART/TOP (Bonferroni's post hoc test $F = 67.12$, $P < 0.05$). In addition, no significant difference was found among all the treated groups ($P > 0.05$) and among the control groups [$P > 0.05$], Fig. 4.9F].

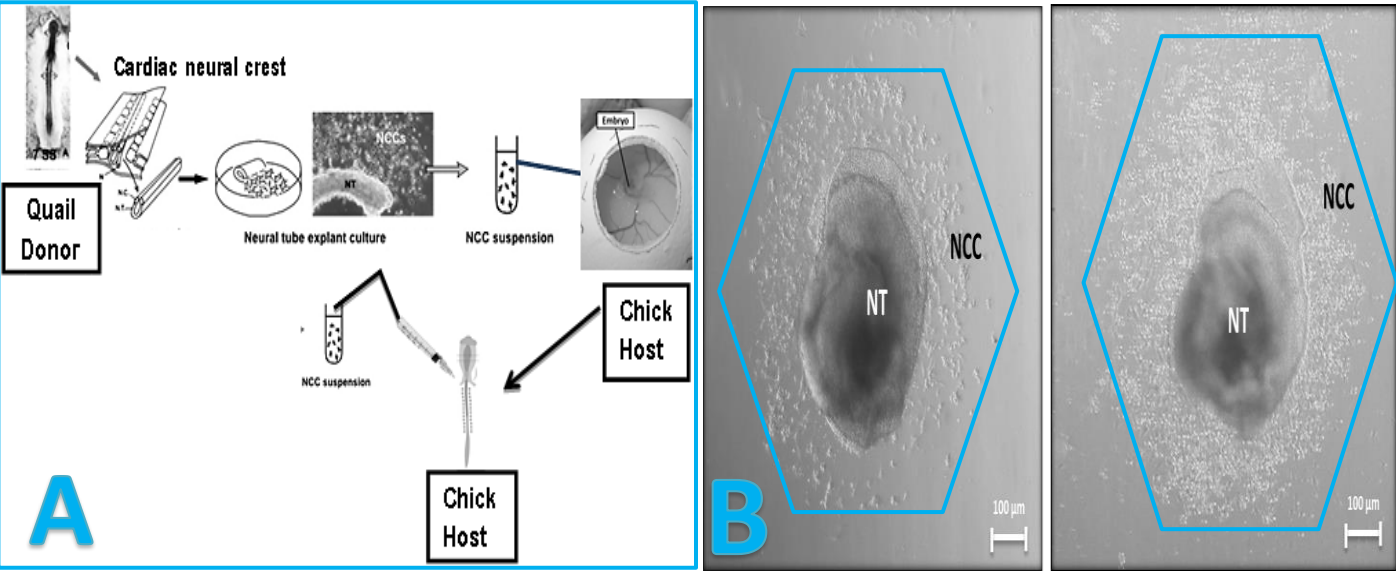


Figure 4.1. 1A shows a summary diagram illustrating the *in vitro* neural tube culture technique and the microinjection of quail cardiac neural crest cells into chicken host embryos, while 1B shows photomicrographs of the control neural tube (NT) and migrating neural crest cells (NCC) after 24 (A) and 48 hours (B) in culture. A polygon tool (blue) was used to measure the area migrated by cardiac neural crest cells.

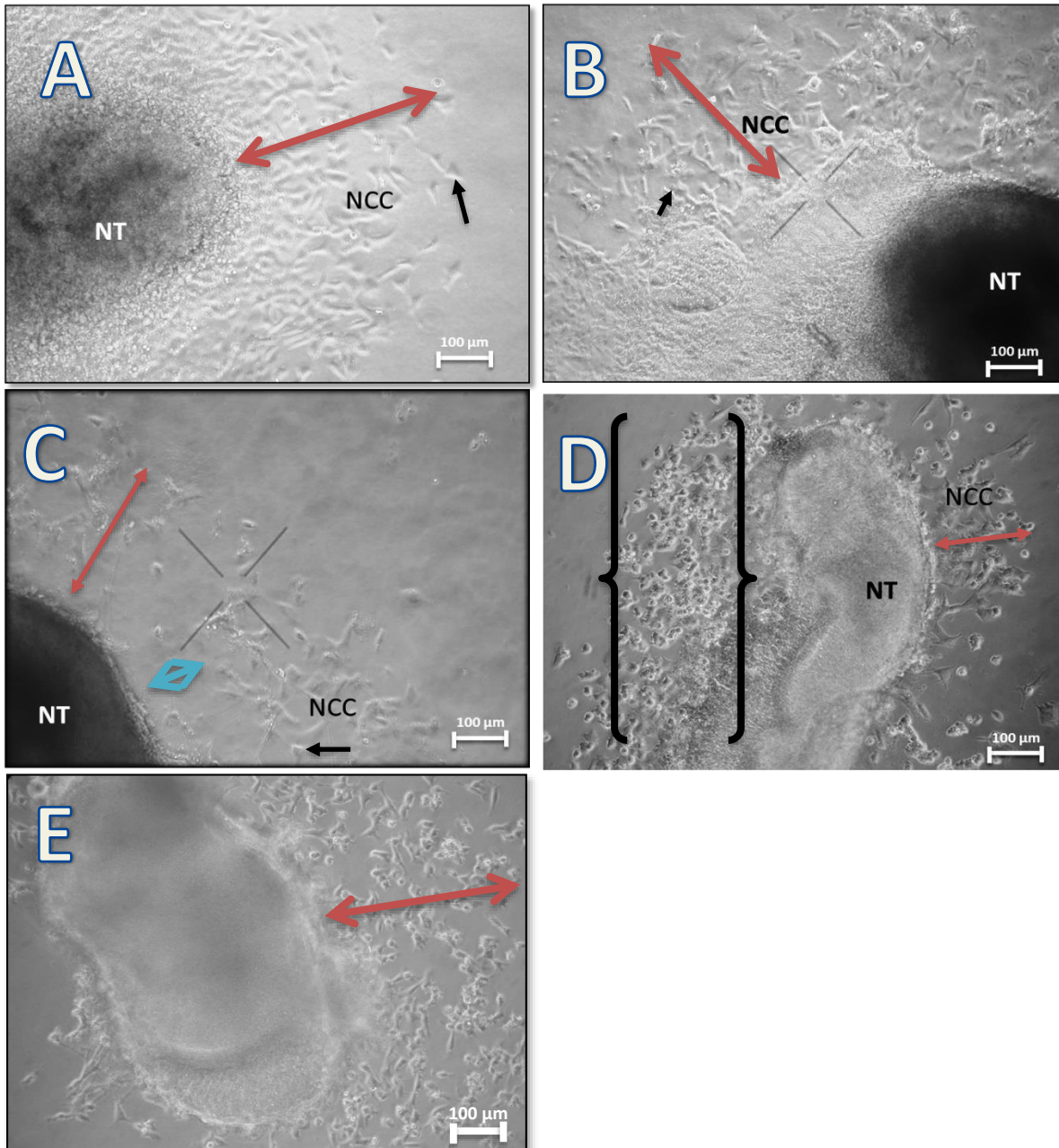


Figure 4.2. Photomicrographs showing neural crest cells cultured in DMEM only (2A), DMSO only (2B), TOP only (2C), cART only (2D), and cART/TOP (2E) after 24 hours. Neural crest cells (NCC) have migrated a greater distance (orange double-headed arrows) in control explants (A, B) compared to the treated cultures (C, D, E). The control and some of the TOP-treated cells were polygonal in shape (A, B and C, black arrows), cART-treated cells appeared to be clustered and mostly rounded (curly brackets). The cells cultured in cART/TOP migrated a greater distance than the cART-treated neural crest cells (Fig 2 E, orange double-headed arrow. Magnification (100X).

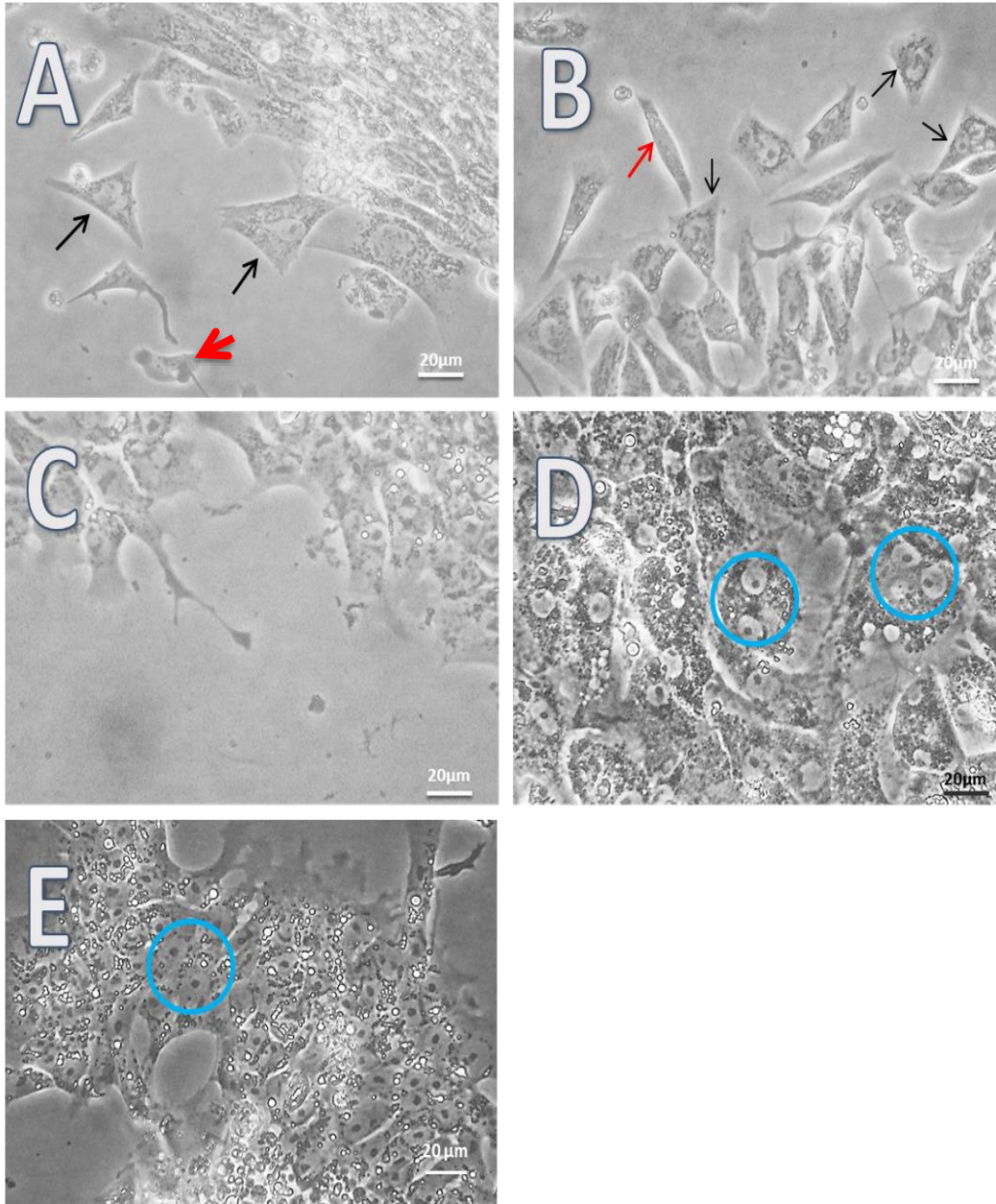


Figure 4.3. Photomicrographs showing neural crest cells cultured in DMEM only (3A), DMSO only (3B), TOP only (3C), cART only (3D), and cART/TOP (3E) after 24 hours. Control neural crest cells are mostly polygonal in shape (black arrows) while cART-treated and cART/TOP-treated neural crest cells appear rounded (blue circle). Fig 3A and B (red arrows) shows filapodia which have detached from migrating neural crest cells. Magnification (200X).

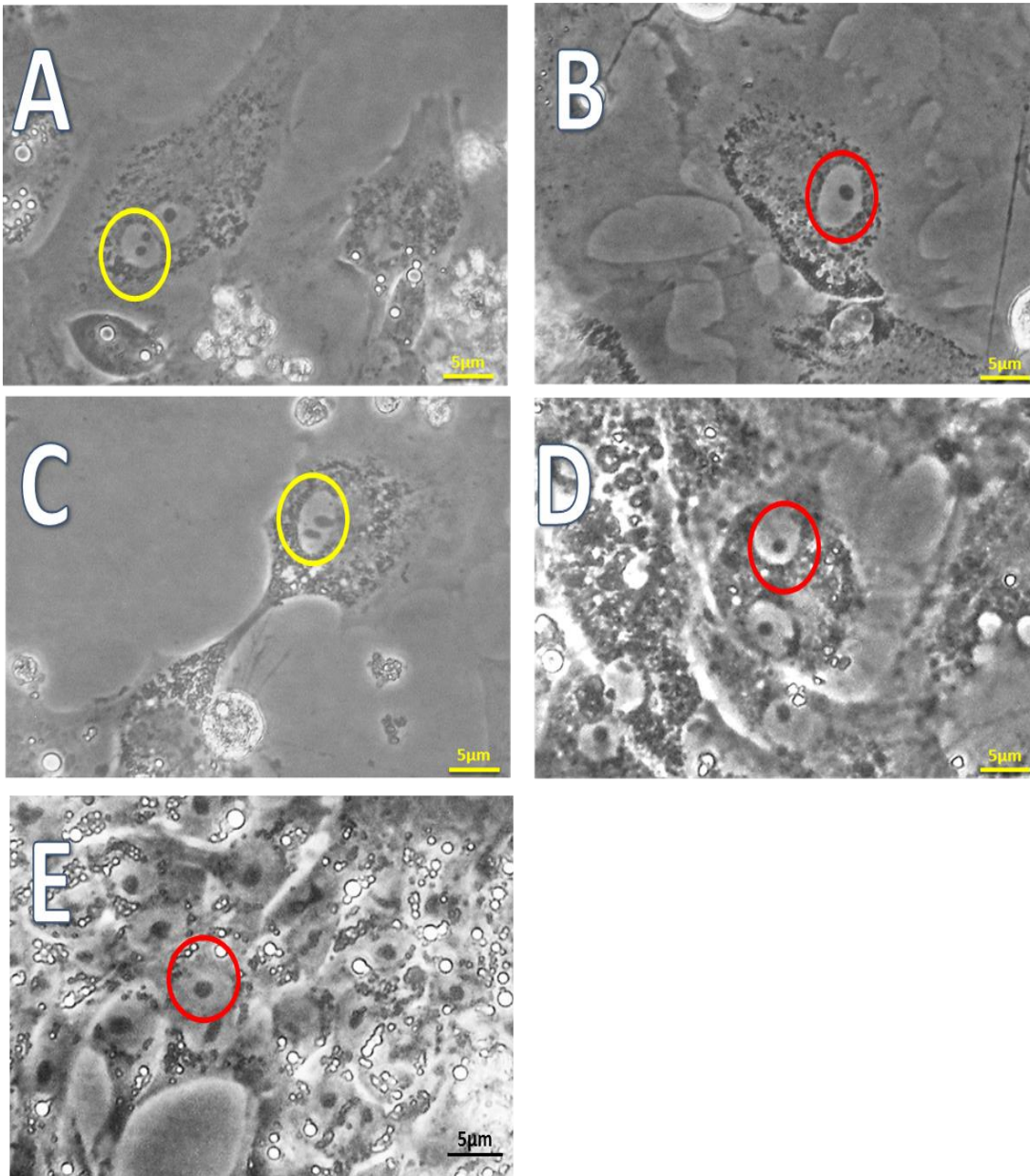


Figure 4.4. Photomicrographs showing neural crest cells cultured in DMEM only (4A), DMSO only (4B), TOP only (4C), cART only (4D), and cART/TOP (4E) after 24 hours of culture. Control cells have polygonal cells while cART-treated and cART/TOP cells show rounded profiles with very few cells exhibiting polygonal profiles. Neural crest cells exhibited a pale vesicular nucleus with a prominent nucleolus. While most nuclei had a single nucleolus (red circles) some had 2 nucleoli (yellow circles). (Magnification 400X).

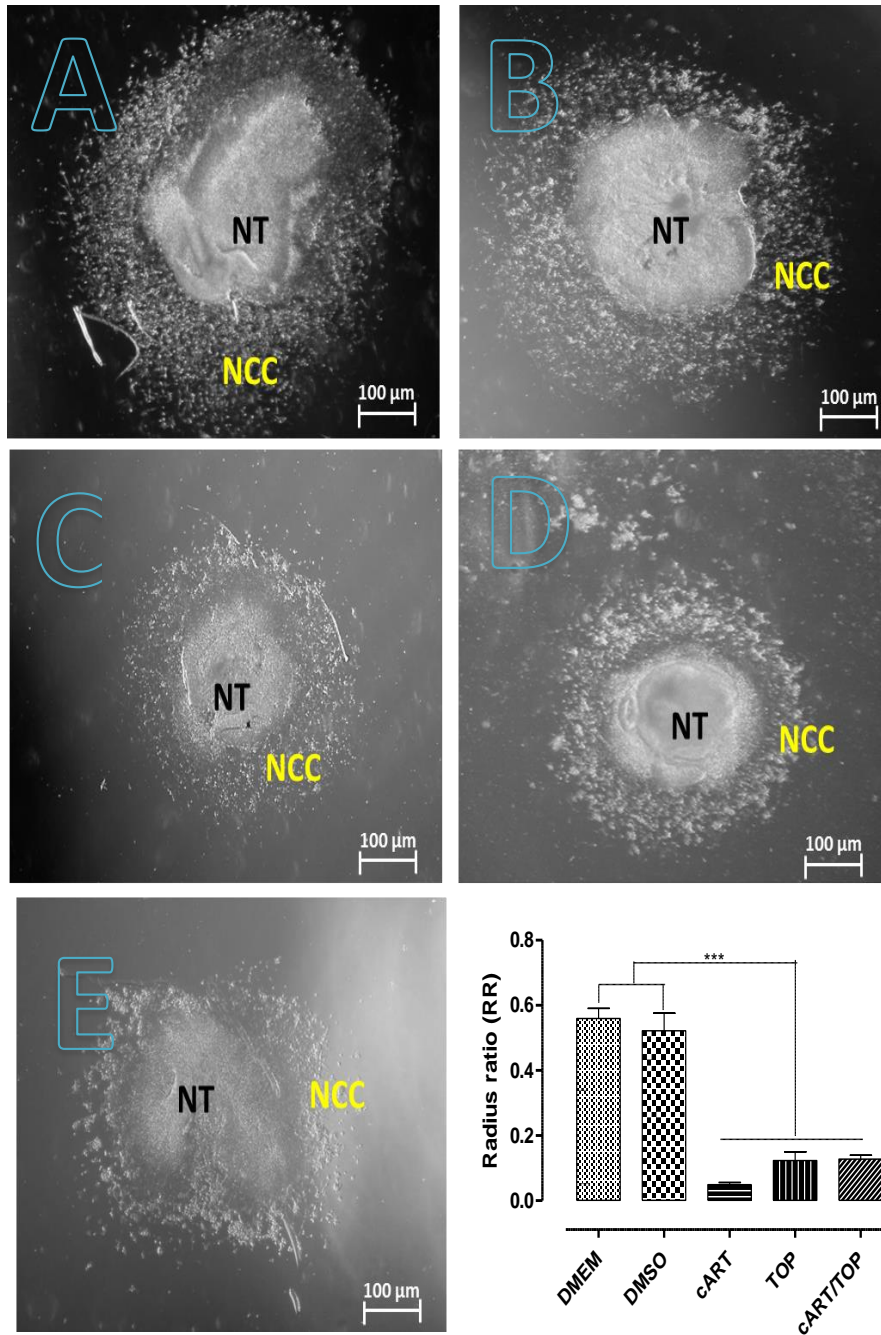


Figure 4.5. Photomicrographs showing neural crest cells cultured in DMEM only (A), DMSO only (B), TOP only (C), cART only (D) and cART/TOP (E) after 24 hours. Migration of neural crest cells (NCC) cultured in cART, TOP and cART/TOP appear inhibited to some extent (Magnification 40X). 5F shows the difference in the radius ratio of cardiac neural crest cells. Migration in the treated cultures was significantly lower than in the control cultures

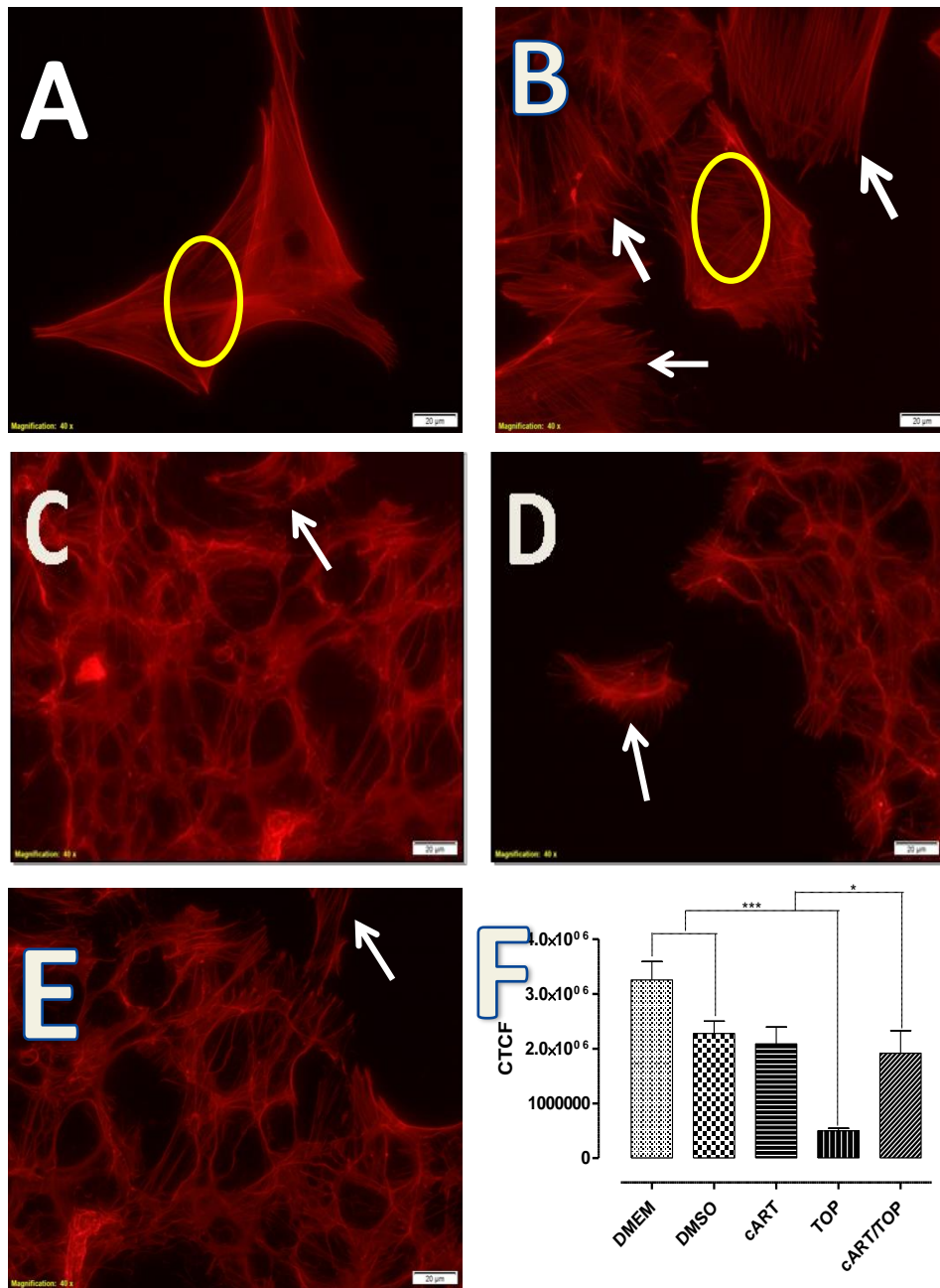


Figure 4.6. Fluorescence photomicrographs showing neural crest cells which were cultured in DMEM only (A), DMSO only (B), TOP only (C), cART only (D) and cART/TOP (E) after 48 hours. Control neural crest cells show the criss-crossing of actin filaments at right angles (A and B, yellow circles). Filopodial extensions which have detached from migrating neural crest cells appear to be more abundant in the control cultures (B, white arrows). Actin filaments are more confined to the extremities of the cells in treated cultures (C-E). 6F shows the actin CTCF of treated and untreated cardiac neural crest cells. The CTCF in TOP only-treated neural crest cells was significantly lower than that of all other cultures.

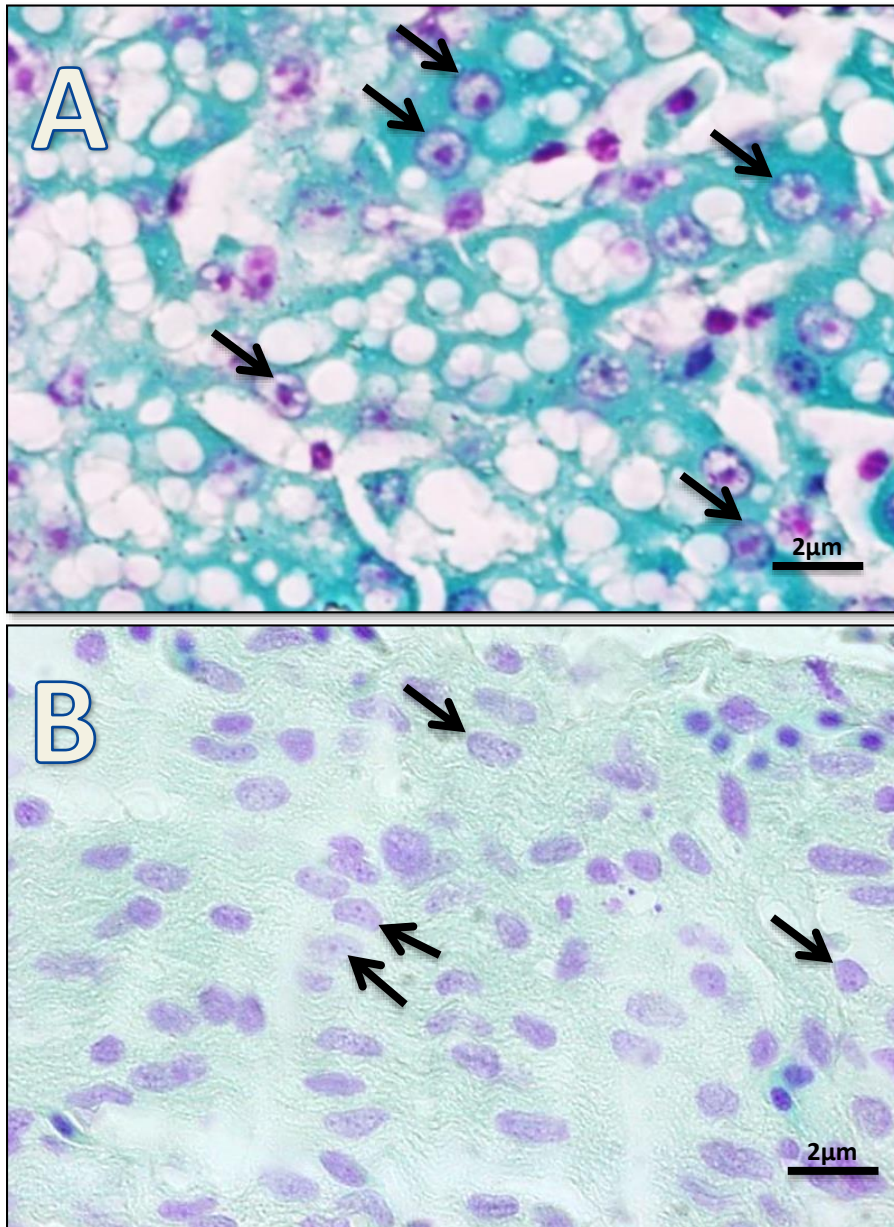


Figure 4.7. A Feulgen-stained photomicrograph showing a section through an adult quail liver (A, positive control) and a chicken interventricular septum (B) showing large and small nucleoli respectively. The nuclei in quail liver are pale and exhibit big prominent nucleoli (black arrows). (Mag 1000X, Oil immersion).

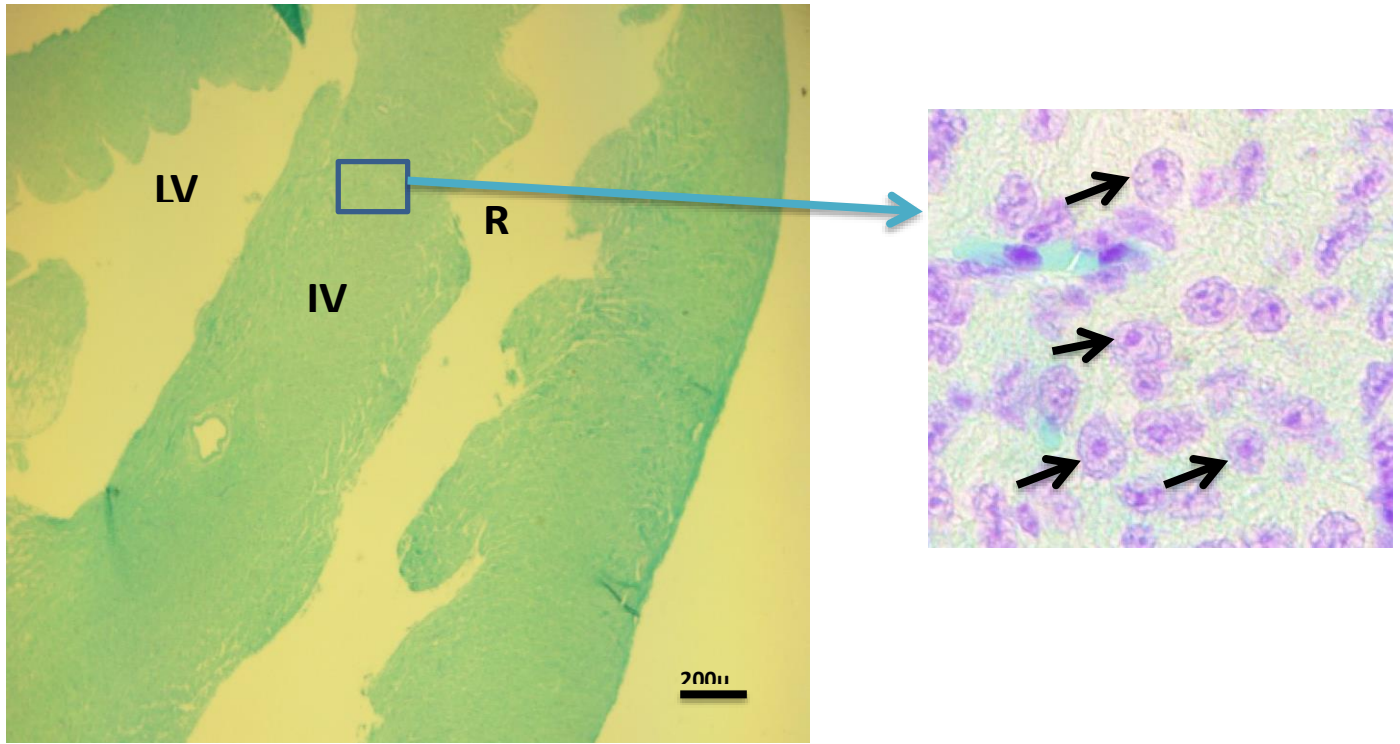


Figure 4.8. A photomicrograph showing a longitudinal section through the heart of a chicken host embryo (A) stained with the Feulgen-Rossenbeck method. The section shows the thick interventricular septum (IVS), the left (LV), right ventricles (RV) and the higher magnification of the interventricular septum where the quail nuclei (black arrows) of micro-injected cells were located (Mag 200X, A; 1000X, B).

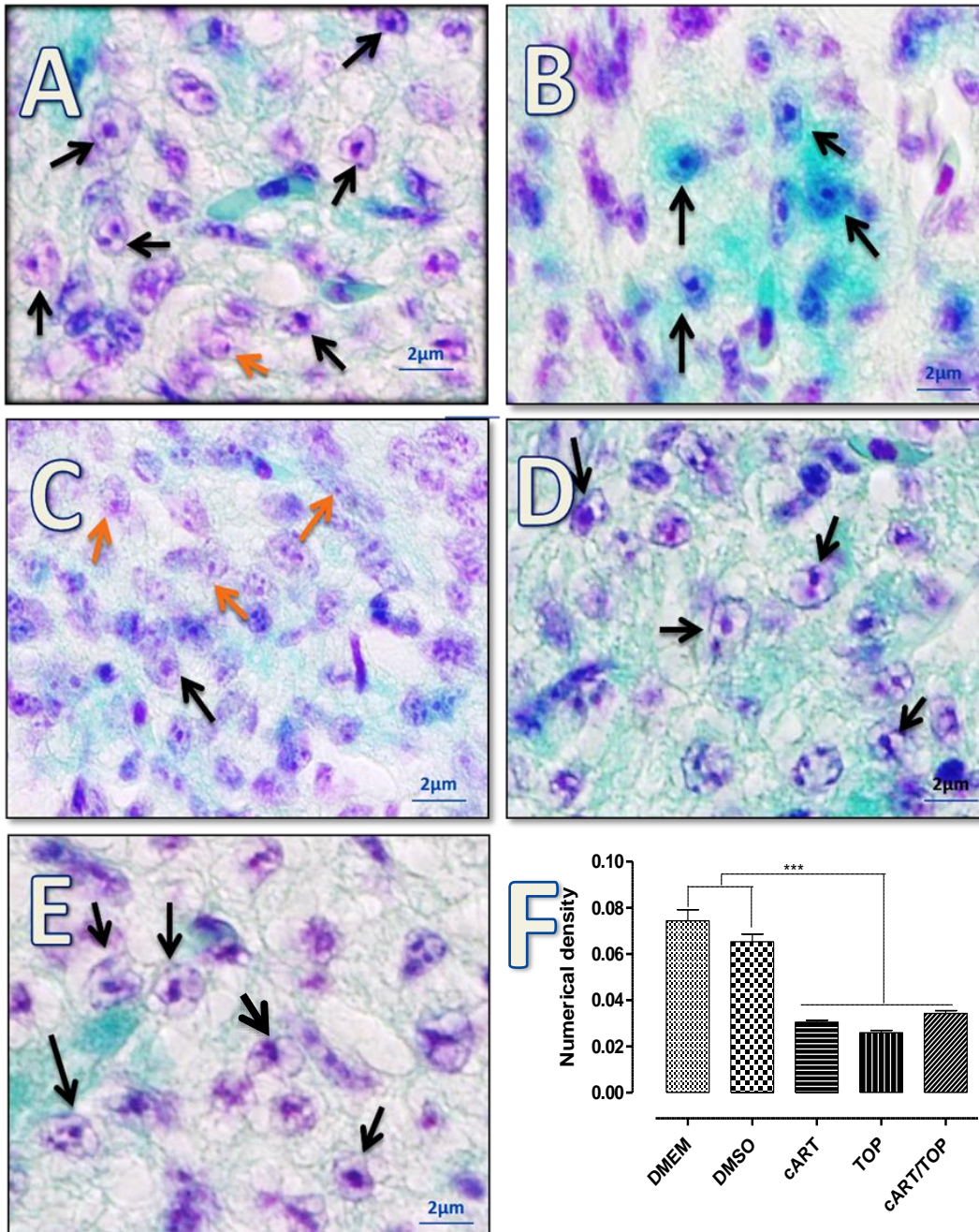


Figure 4.9. Photomicrographs stained with the Feulgen-Rossenbeck method showing quail cardiac neural crest cells injected into chick hosts embryos (black arrows), while the orange arrows show the nuclei of chick hosts embryo. 4.9 A shows neural crest cells which were cultured in DMEM only, while 4.9 B shows neural crest cells cultured in DMSO only. 4.9C shows neural crest cells cultured in TOP, while 4.9 D and E show neural crest cells cultured in cART only and cART/TOP respectively (Mag 1000X, Oil immersion). 4.9F shows the numerical density of injected quail cardiac neural crest cells into chicken host embryos. The numerical density in the treated-samples was significantly reduced when compared to the controls.

4.4.0 Discussion

The current study investigated the effect of the cART and TOP on the migration of cardiac neural crest as a potential mechanism (amongst others) for VSD formation. The involvement of neural crest cells in the formation of specific heart structures was first established by Kirby and his colleagues (Kirby *et al.*; 1983). In their investigation, the ablation of neural crest cells (which they later called cardiac neural crest cells) resulted in the absence of the aortico-pulmonary septum. It therefore suggests that, the absence of cardiac neural crest cells and the subsequent failure of the truncal ridges to form will result in a VSD (Valle and Hadley, 2018).

The results showed that the two main techniques which were employed in the current study to determine if cART and TOP inhibit the migration of neural crest cells were successfully applied. The observed quail neural crest cells in the chick host interventricular system (IVS) in this study suggest that isolation of neural tubes at cardiac levels and the subsequent migration of neural crest cells *in vitro* in the presence of antiretroviral and antiepileptic drugs and secondarily the microinjection of cultured quail cardiac neural crest cells into the cardiac region of a chick embryo hosts *in vivo* (chick-quail chimaera system) were successful. The chick-quail chimaera system was devised by Nicole Le Douarin, who noticed that the interface nuclei of all embryonic and adult cells in the Japanese quail (*Coturnix coturnix japonica*) contained a large amount of heterochromatin which was concentrated in the nucleolus (Le Douarin, 1969 cited in Le Douarin *et al.*, 2004) as opposed to the heterochromatin of chicken cells which is evenly distributed within the nucleoplasm (Le Douarin *et al.*, 2004). This feature allowed the quail cells to be distinguished from chick embryonic cells in tissue grafts performed *in vivo* and was successfully applied in the present study with identification of quail neural crest cells in the IVS of the chick embryo.

Our findings in the *in vitro* and *in vivo* studies showed that cART and TOP inhibit the migration of cardiac neural crest cells when administered at concentration of peak plasma levels. This was represented by the significant reduction in the radius ratio of neural crest cells cultured in cART and TOP, and cART/TOP applications. In addition, the significantly decreased numerical density of cells found at the septum in the treated groups indicated that fewer treated neural crest cells migrated to the interventricular septum in the heart of chicken host embryos. These inhibitions imply the absence or reduced number of cardiac neural crest cells at the IVS of the embryo and therefore failure of their contribution toward complete development of IVS. It further suggests the inhibition of migration may amongst others be associated with the development of VSDs and highlights possible link to the development of VSDs observed in children who are born to mothers on TOP and cART therapy during the first trimester (Hunt *et al.*, 2008; Margulis *et al.*, 2012).

In addition, the current study evaluated the cell cytoskeleton of cultured neural crest cells which were treated with cART, TOP, and cART/TOP. The observed disarrayed arrangement of actin cytoskeleton of treated neural crest cells and as a result, the significant reduction in CTCF value, suggest that structural arrangement of actin cytoskeleton may be crucial and play significant role in the inhibition of neural crest cells migration and subsequent specific organ defect. As has been previously reported, the actin cytoskeleton is very central to the migration of cells, and if perturbed, can disturb the migration of neural crest cells (Lee, 2013; Tang and Gerlach, 2017, Svitkina, 2018).

The results inform caution on co-administration of cART and TOP to pregnant HIV positive women who require treatment for seizures. The study suggests that the occurrence of VSDs involves abnormal migration of cardiac neural crest cells in the presence of cART and TOP, individually and in combination. The teratogenic effects appear to be in third week of development as neural crest cells are known to be migrating out of the neural tube in humans during this period (Copp, 2005).

Unfortunately, the challenge is that most women are unaware that they are pregnant during the third week of gestation; therefore, the prevention of such defects may be intricate and place management burden on clinicians.

The actin filaments in treated neural crest cells (cART only, TOP only and cART/TOP) were more concentrated at the periphery of the cells as opposed to uniform distribution pattern observed in the controls. This formation of a cortical layer of actin filaments just below the plasma membrane is indicative of transformation from a motile, undifferentiated cell into a non-motile differentiated cell (Haendel *et al*; 1996), suggesting its possible role in the rounding of cells (Haendel *et al*; 1996) and consequent influence on cell migration. Previous report indicated that the cell may use this feature to apply tension on the cell membrane in order to facilitate the addition of extra cell membrane into the cell (Haendel *et al*, 1996). Although the actin filaments in the cART-treated cells were confined to the extremities of the cells, the CTCF in these cells was not significantly different to that of the controls. This suggests that cART doesn't reduce the quantity of cellular actin, but disorders its distribution within the cell.

The cytoskeleton of neural crest cells is designed to contribute to cell division and motility. The structural and shape changes seen in the cytoskeleton of treated neural crest cells may hamper cell motility and subsequently interrupt cell division according to Haendel *et al*; (1996) leading to malformations. These alterations of the cytoskeletal morphology could be due to the gathering of new filaments and the displacement of original actin filaments from one location in the cell to another as was previously reported (Cramer & Mitchison, 1995). Cultured neural crest cells are motile, flattened and actively dividing, while differentiated cells are non-motile and rounded, suggesting that the treatment may influence the differentiation of cardiac neural crest cells, and the consequent failure to reach their destinations in the interventricular septum.

Drug-drug interactions (DDIs) are defined as adjustments in the efficacy or toxicity of an individual drug when it is co-administered with another drug at the same time (Farooqui *et al*; 2018; Zaporozhan *et al*; 2019). These interactions may occur due to competitive inhibition, if they are metabolized by the same enzyme or arise if the two drugs have an effect on the same target (Farooqui *et al*; 2018; Shetty *et al*; 2018) or may be antagonistic or synergistic. Topiramate (TOP) and Efavirenz both induce the cytochrome p450 (CYP3A4) enzymatic system (Nallani *et al*; 2003; Xu and Desta; 2013). In addition to the CYP3A4 system, efavirenz is metabolized by CYP2B6 (Xu and Desta; 2013). Our findings in the *in vitro* and *in vivo* studies suggest that TOP does not affect the activity of cART as there was no significant difference in the differences in the radius ratio and numerical density between the cART-only and cART/TOP-treated samples. This suggests that there is no competitive inhibition taking place between cART and TOP. It is probable that the ability of cART to be metabolized by CYP2B6 in addition to CYP3A4 is what prevents the competitive inhibition between the two classes of drugs. However, the results from the CTCF evaluation suggest that cART could have antagonistic effects to the cytotoxicity of TOP as the combination of cART and TOP seems to negate the decrease in CTCF by TOP. It is also crucial to note that Emtricitabine and Tenofovir, other components of cART, are not metabolized by the cytochrome P450 system (Masho *et al*; 2007).

4.4.1 Conclusion

The results of the current study show that both cART and TOP, individually and in combination, inhibit the migration of cardiac neural crest cells, and this could be the basis for the development of VSDs and other associated cardiac anomalies in cART and TOP teratogenicity. In addition, TOP doesn't seem to affect the activity of Atripla. This is a crucial finding as it suggests that the

combination of Atripla and TOP may be suitable for the treatment and management of HIV and seizures which may arise due to viral infection.

CHAPTER 5: The effect of cART and TOP on neurogenesis (neuritogenesis) and the expression of DCX on neural tube-derived neurons

5.1.0 Introduction

Neuronal migration disorders (NMDs) are birth defects which involve the abnormal migration of neurons during the development of the nervous system (Ayanlaja *et al*; 2017; Zare *et al*; 2019; Pan *et al*; 2019). Most NMDs involve genes which are associated with the regulation of the cell cytoskeleton in the cerebral cortex (Ayanlaja *et al*; 2017; Zare *et al*; 2019). During the development of the cerebral cortex, neuroblasts and glioblasts in the mantle layer of the neural tube differentiate into neurons and glial cells. The newly differentiated neurons migrate from their place of origin along the periventricular region where they will ultimately colonize the cortical plate (Ayanlaja *et al*; 2017). When the neurons reach the cortical plate migration will cease and the non-motile neurons will arrange themselves into a precise pattern within the plate (Zare *et al*; 2019). The neurons are directed to specific regions within the cortex by particular signaling pathways (Reiner, 2013). There are two ways in which neurons migrate, namely radial and tangential migration (Ayanlaja *et al*; 2017; Zare *et al*; 2019). In radial migration excitatory pyramidal neurons migrate along the radial glial cells from the cortical ventricular zone whereas tangential migration involves the migration of interneurons to the cortical plate (Ayanlaja *et al*; 2017). These interneurons originally migrate from the dorsal telencephalon before their path is altered in order for them to reach their destination in the cortex (Ayanlaja *et al*; 2017).

The formation of cortical layers takes place in an inside-out fashion (Ayanlaja *et al*; 2017). The earlier forming pyramidal cells are out-paced by the later forming pyramidal cells such that the former become deeper layers of the cortex, whereas the latter form superficial layers

(Ayanlaja *et al*; 2017; Stouffer *et al*; 2016). Thus, the positioning of developing neurons into specific cortical layers is determined by specific events which involve neuronal migration (Ayanlaja *et al*; 2017; Stouffer *et al*; 2016). Therefore, the normal coordination of the production and migration of excitatory and inhibitory neurons is very crucial in the development and normal function of the cortex (Ayanlaja *et al*; 2017; Zare *et al*; 2019; Pan *et al*; 2019). Abnormal migration can result in neurons stopping prematurely along their migratory pathways or migration to ectopic destinations (Zare *et al*; 2019; Pan *et al*; 2019).

If the neurons are inhibited in their migration a myriad of abnormalities such as epilepsy, cognitive impairments and other neurological disorders could occur (Ayanlaja *et al*; 2017; Zare *et al*; 2019; Pan *et al*; 2019).

Lissencephaly is a neuronal migration disorder which is characterized by a smooth cerebral surface due to cortical thickening and lack of gyri and sulci (Zare *et al*; 2019; Pan *et al*; 2019; Stouffer, 2016). In this anomaly the cortex consists of four layers which are characterized by larger than normal and disorganized pyramidal cells (Kato, 2015). In subcortical band heterotopia, strands of gray matter are found among the white matter between the cortex and the lateral ventricles (Ayanlaja *et al*; 2017). In some cases, patients present with microcephaly which is characterized by a small brain and head circumference. Lissencephaly may involve defects in axonal outgrowth and guidance (Ayanlaja *et al*; 2017; Kato, 2015). The aforementioned are features are also associated with the absence of the corpus callosum (Ayanlaja *et al*; 2017).

Research has shown that mutations in the Doublecortin (DCX) gene result in lissencephaly and other neuronal migration disorders (Stouffer, 2016). DCX is a microtubule associated protein which is involved in the development and normal migration of neuronal cells (Ayanlaja *et al*;

2017). DCX is expressed mainly in embryonic neurons and neuron precursor cells (Zare *et al*; 2019; Kato, 2015). In the adult brain DCX is expressed in the hippocampus. The involvement of DCX in neuronal migration disorders was first established in 1998 (Gleeson *et al*; 1998) in the lissencephaly and double cortex syndrome. Because DCX is on the X chromosome, a double cortex is more common in females (Ayanlaja *et al*; 2017; Hehr *et al*; 2007). Therefore, in female individuals with a mutated genotype, one of the X chromosomes will be affected while the other chromosome is normal. The normal X chromosome will result in the normal migration of cells into the cortex, while the mutated chromosome will result in the premature cessation of neuronal migration (Ayanlaja *et al*; 2017; Hehr *et al*; 2007). This will create strands of grey matter between the cortex and the ventricle. Lissencephaly is more common in males because male mutants do not have a functional copy of DCX; therefore, male subjects show more symptoms with a thickened four layered cortex (Pan *et al*; 2019; Ayanlaja *et al*; 2019; Gleeson, 2000). In addition to abnormal neuronal migration DCX has been shown to also play a role in the proliferation of progenitor cells during neurogenesis in mutant mice (Seki *et al*; 2020; Pramparo *et al*; 2010). In knockout mice the number of neuronal progenitor cells was reduced during the development of the cortex (Pramparo *et al*; 2010). This indicates that DCX is not only important in neuronal migration but also proliferation of neurons during cortical development. Therefore, the combination of abnormal migration and proliferation of progenitors of neurons is central to neuronal migration disorders. Research has shown that the expression of DCX in these cells is co-expressed with BRDU, indicating a relationship between migration and proliferation of developing neurons (Seki *et al*; 2020; Pechnick *et al*; 2008).

Apart from the proliferation of neurons, it has been shown that the regulatory and structural interactions between microtubules and actin are also crucial in the formation and migration of

neurons (Tang and Gerlach, 2017). Microtubules attach to actin filaments which are linked to focal adhesions (Tang and Gerlach, 2017). Spinophilin, an actin associated protein which is commonly found in dendrites of neurons which receive impulses, facilitates the interaction of actin with DCX (Cheerathodi *et al*; 2016; Ayanlaja *et al*; 2017). The colocalization of DCX and spinophilin results in the interaction of DCX with both microtubules and f-actin. Without spinophilin DCX only interacts with microtubules and not actin (Cheerathodi *et al*; 2016; Ayanlaja *et al*; 2017).

The polarization of the actin cytoskeleton therefore provides the force necessary for neuronal migration (Tang and Gerlach, 2017). The polarization of actin cytoskeleton is regulated by small GTPases of the Rho family, namely Rac, Rho and cdc 42 (Clayton and Ridley, 2020; Govek *et al*; 2005). Rac and Rho are two GTPases which have been shown to have a distinct effect on the actin cytoskeleton of neurons and a myriad of other migrating cells and may control many functions such as adhesion, motility and morphology of cells (Lyda *et al*; 2019; Margiotta *et al*; 2019; van Aelst and D'Souza-Shorey, 1997). These GTPases act as molecular switches which can be activated by a number of extracellular stimuli in order to generate specific gradients for actomyosin contractility and substrate adhesion (Margiotta *et al*; 2019). Rho A generates contractile actin bundles and large focal adhesions to the substrate, while Rac1 induces actin polymerization to drive lamellipodial protrusion and the formation of small focal adhesions (Lyda *et al*; 2019). Cdc42 generates and induces the formation of filapodia. An increase in the formation of lamellapodia occurs following the microinjection of Rac into cultured cells, while Rho causes the formation of stress fibres and the augmentation of focal contacts (Govek *et al*; 2005).

Xu *et al*; (2019) reported that if Rho A is genetically deleted a disarray in the cortical distribution of neuronal progenitor cells will occur. In addition, the cell junctions in these progenitor cells will

be interrupted. Also, a downregulation of Rho A negatively affects neurogenesis and increases the number mitotic cells and hence these cells remain in the phase of proliferation (Xu *et al*; 2019). This delay in neurogenesis and the subsequent increase in number of progenitor cells in the proliferative phase leads to exencephaly (Xu *et al*; 2019). The downregulation of Rac1 results in the decline in the pool of cortical neuronal progenitor cells with the subsequent formation of microcephaly (Govek *et al*; 2005; Xu *et al*; 2019). This microcephaly is the result of increased apoptosis and hastened cell cycle exit (Govek *et al*; 2005; Xu *et al*; 2019). This fast-tracked exit of the cell cycle by neuronal progenitor cells may reduce the size of the forebrain (Xu *et al*; 2019).

5.1.1 The development of neurons

During development *in vivo*, neurons are first seen as round, non-process-bearing cells (Miller and Suter 2018; Sainath and Gallo, 2015; Gordon-Weeks., 2000). They will eventually become assembled into functional networks, where they will continue to grow in response to environmental cues and subsequently extend processes, collectively known as neurites (Miller and Suter 2018; Sainath and Gallo, 2015; Gordon-Weeks., 2000). The process of neuritogenesis begins at the surface of the neuron as an active, localised protrusion that develops into an entity called a growth cone (Flynn, 2013; Gordon-Weeks., 2000).

Growth cones are motile dilatations at the ends of both growing dendrites and axons (Tamariz and Varela-Echavarria, 2015). They are also found in regenerating mature axons and dendrites when nerves are damaged due to trauma such as crushing or cutting (Tamariz and Varela-Echavarria, 2015; Gordon-Weeks., 2000). During development of the nervous system, growth cones have three important functions: they control migration by guiding the neurite through the

developing embryo in order to locate the cell with which they will form a synapse. Secondly, they build the extending neurite behind them as they migrate; and lastly, they form the pre- or postsynaptic element of the synapse (Tamariz and Varela-Echavarria, 2015; Flynn, 2013; Gordon-Weeks., 2000). Hence, growth cones are important for establishing the process-bearing morphology characteristic of neurons (Flynn, 2013; Gordon-Weeks., 2000). Proper neurite outgrowth, as well as axonal and dendritic morphogenesis is essential for neuronal maturation, synaptic formation and neuronal function (Frank and Tsai, 2009; Merot *et al.*, 2009; Hong *et al.*, 2013).

Once neuritogenesis is initiated, the developing processes become invaded by cytoplasm and microtubules, where they will eventually develop into either axons or dendrites (Miller and Suter 2018). Neuritogenesis *in vivo* usually begins with the extension of a single neuron that will become the axon, while the later emerging neurites develop into dendrites (Gordon-Weeks., 2000).

Neurite extension is a special case of cellular motility that depends on the integrity of microtubules (Tamariz and Varela-Echavarria, 2015). While a number of similarities exist between neurite extension and cellular translocation, there are two important differences. First, newly synthesised components of the neurite are added onto the existing neurite resulting in neurite extension and second, neurite extension is not associated with movement of the cell body and hence the nucleus of the neuron (Hsieh *et al.*; 2006). The formation of neurites therefore begins with the increase in number and the organization of actin filaments and microtubules.

Microtubules act as regulators of neurite outgrowth by acting as the structural substrate for the transport of membrane bound organelles (Calogero *et al.*; 2019; Hsieh *et al.*; 2006; Gordon-

Weeks., 2000). Microtubules also regulate the assembly and disassembly of focal adhesion in migrating cells in a process regulated by the Rho family of GTPases (Zinn *et al*; 2019).

Microtubules have two main functions in neuritogenesis: Firstly, they provide a structural basis for the transport of membrane-bound organelles and secondly, they contribute to the maintenance of the structural integrity of the neurite (Calogero *et al*; 2019; Hsieh *et al*; 2006; Gordon-Weeks., 2000). Hence, microtubules play an important role in neurite growth. Other evidence for the role played by microtubules in the development of neurons is seen in studies that show an inhibition of neurite elongation by neurons in culture, in the presence of agents that depolarise microtubules (Calogero *et al*; 2019; Hsieh *et al*; 2006; Gordon-Weeks., 2000). However, it has also been observed that when substrate adhesion is increased, microtubule depolymerisation results in the formation of additional growth cones along the shaft of the neurite rather than resulting in neurite retraction (Calogero *et al*; 2019; Kelliher, 2019; Hahn *et al*; 2019; Gordon-Weeks., 2000). This would, therefore result in increased branching of the neurite.

Observations of neurites under the electron microscope showed abundant smooth endoplasmic reticulum, mitochondria, vesicles, neurofilaments and microtubules in the terminal enlargements of axons (Gordon-Weeks., 2000). As mentioned previously, growth cones are highly motile entities and would therefore require large amounts of ATP. A large number of mitochondria would therefore be predictable in the cytoplasm of the neurites (Gordon-Weeks., 2000).

Studies have shown that the administration of cART to pregnant HIV positive women results in neuronal migration disorders. The reported neurological defects observed were ventricular dilatation, partial agenesis of corpus callosum, subependymal cyst and pachygyria (Sibiude *et al*., 2014). The mechanism by which cART causes these defects is unclear and therefore the current study seeks to unravel some of the possible mechanisms of action by examining the structural

and molecular development of neurons. This study suggests that cART causes neuronal migration disorders by altering the morphology and proliferation of neurites during the embryonic neurogenesis. In addition, the study postulates that cART affects the neuronal expression of the Rho family of GTPases which regulate the organization of the actin cytoskeleton and microtubules in the migrating neurons.

The aim of the study was therefore to investigate the effect of cART and TOP on the neural tube-derived neurite outgrowth and the gene expression of the Rho family of GTPases.

5.2.0 Material and methods

5.2.1 Drugs

cART and Topiramate, and the relevant controls were prepared as previously described in chapter 3.

5.2.2 Ethical clearance

All experimental procedures were approved by the University of the Witwatersrand, Animal Research Ethics Committee (Animal Ethics Clearance Number 2019/01/2/A).

5.2.3 Preparation of equipment

Glassware and solutions were sterilized as previously prescribed in chapter 3.

5.2.4 Embryos

Fertile Japanese quail (*Cortunix Cortunix japonica*) eggs were used in this study. The quail eggs were incubated for 36 hours at 37°C in a humidified incubator in order to obtain neural tubes at cranial levels. All experimentation was carried out in a laminar flow hood under aseptic conditions.

5.2.5 Neural tube cultures

Neural tubes were dissected from the blastoderm of quail embryos as previously described in chapter 3.

The explants were randomly allocated to the following treatments: as controls (Groups A & B) the neural tube explants were cultured in 1 ml of DMEM only, (n=16), and 1 ml of 0.05% DMSO reconstituted in DMEM (DMSO only, n=14). As experimentals, the explants were cultured in a

1ml DMEM solution containing 3 μ M topiramate (TOP only, Group C, n=13), 5 μ M of Atripla® (cART only Group D, n=12) and the combination of the two concentrations of Atripla® and Topiramate (cART/TOP Group E, n=13). The neural tubes containing neural crest cells were cultured for 24 hours after which the migrating neural crest cells were removed in order to allow for neurite outgrowth from the neural tube. The neural crest cells were removed with tungsten needles under a stereomicroscope. The neural crest cells, which are the primordium of the peripheral nervous system were excluded in order to allow only the neural tube, the primordium of the central nervous system, in the culture dish. The cultures were allowed to grow for a further 72 hours (for a total of 96 hours). In order to maintain the concentrations of the drugs the culture medium was replaced every 24 hours. For the quantitative PCR study the neural tubes were removed from the culture dishes in order to harvest the neurites only. Both the neural tubes and the growing neurites were left in the culture dish for immunohistochemistry (DCX and Rhodamine phalloidin).

The cultures were photographed at 96 hours using an Olympus inverted phase contrast microscope (Olympus, South Africa) at specific magnifications.

5.2.6 Immunocytochemistry

Neural tubes and neurites which had been cultured in DMEM only (n=6), DMSO only, cART, TOP, and cART/TOP were stained with DCX in order to study the structure of the neurites. The neural tubes and neurites were washed with warm phosphate-buffered saline before being fixed with 4% paraformaldehyde in phosphate-buffered saline (PBS) for 20 min. The neurons were permeated with 0.1% Triton X-100 in PBS for 5 minutes. Following permeation with triton X the

explants were blocked with 3% bovine serum albumin in PBS for 1-hour min at room temperature. The cultures were incubated with a primary antibody (DCX 1:500) in 1% BSA-PBS overnight on a shaker at 4°C. Following incubation with the primary antibody the cultures were incubated with a secondary antibody in 1% BSA-PBS for 1 h at room temperature. The secondary antibody used was anti-rabbit Alexa Fluor 488 goat anti-mouse IgG. The primary and secondary antibodies were omitted in the negative control, while the developing quail brain was used as a positive control. The neurites were viewed on a fluorescence microscope and pictures were taken at specific magnifications.

5.2.7 Neurite measurements

The relative thickness of neurites was measured using systematic sampling and Image J software. A double square lattice system and a table of random numbers were used to determine the measurements. A total of 125 measurements were made (n=25 for each treatment). In addition, the corrected total cell fluorescence was determined in the neurites using the following formula:

CTCF = Integrated Density – (Area of selected cell X Mean fluorescence of background readings).

5.2.8 Rhodamine Phalloidin staining

Neural tubes and neurites (n=39) which had been cultured in plain DMEM only (n=8), DMSO only (N=8), cART (n=8), TOP (N=7), and cART/TOP (n=8) were stained with Rhodamine phalloidin in

order to evaluate the cell cytoskeleton of the neural tube-derived neurons. In order to determine the level of fluorescence the corrected total cell fluorescence (CTCF) was calculated using image J® software (National Institutes of Health, USA) as follows:

CTCF= Integrated density- (Area of selected cell X Mean fluorescence of background reading). A student t-test was used to investigate if the differences between the control and experimental cultures were significant

5.2.9 MTT assay for cell proliferation

Neural tubes (n=30, n=6 for each treatment) which were cultured for 96 hours in a 96-well plate were used to investigate the effect of cART and TOP on the proliferation and viability of neural crest cells. Following 96 hours of culture, the cells were incubated with 10 µl of the MTT solution for 4 hours at 37°C in a humidified incubator. Following this, the cultures were incubated with 100 µl of the solubilisation buffer overnight in a humidified incubator at 37°C. The plate was then placed on an orbital shaker at room temperature for 5 minutes. The absorbances were measured at 600 nm using a BioTek® Power Wave 340 microplate spectrophotometer (Analytical and Diagnostic Products, South Africa).

5.2.10 RNA extraction

The RNeasy® Micro kit (Qiagen, South Africa) was used to extract RNA from neural crest derived neurites which were cultured in DMEM only (n=5), DMSO only (n=4), cART (n=6), TOP (n=5), and cART/TOP (n=5) after 96 hours. In order to maximise the quantity of RNA, the samples from

each treatment were pooled, as a single culture could not yield enough cells for RNA extraction. As an example all 5 DMEM only neurite culture samples were combined and were considered as one biological sample. The experiment was repeated 3 times in order to obtain 3 biological replicates for each treatment.

The neural tubes were removed and the neurites were brought into suspension by adding 150µl of 0.25% trypsin solution for 5 minutes at room temperature. An equal volume of the culture medium was added to each well in order to stop the action of trypsin. The suspended neurons together with the culture medium was transferred into a 2ml Eppendorf tube and centrifuged at 5000 rpm for 15 minutes. The supernatant was discarded and RNA was extracted from the cell pellet using the following protocol.

The cell pellet was resuspended in 750µl of buffer RLT® (Qiagen, South Africa) in the eppendorf tube. In order to complete the homogenization, process the lysis was transferred into a QIA shredder Spin Column™ (Qiagen, South Africa) and centrifuged at 14000rpm for 2 minutes. In order to precipitate any protein or DNA the homogenate was pipetted into a new 2ml collection tube after which 750µl of 70% ethanol was added. Following this, the homogenate was transferred into an RNeasy® MiniElute Spin Column and centrifuged at 14000rpm for 15 seconds. The flow-through was discarded and 700 µl of buffer RW1 was added to the column. Following the addition of the buffer, the column was micro-centrifuged for 15 seconds at 14000rpm. Following this the lysate was transferred into a new 2ml collection tube and 500 µl of buffer RPE® (Qiagen, South Africa). The spin column was micro-centrifuged at 14000rpm 15 seconds. 500 µl of 70% ethanol was used to dry the column. The flow through and the collection tube were discarded. The 2ml collection tube was substituted with a new 1.5ml eppendorf tube. In order to elute the RNA from the Spin Column, 40µl of RNase-free water was added to the

column and spun for 2 minutes at 14000rpm. A Nano-Drop® spectrophotometer, Series ND-100 was used to determine the RNA concentration and purity. The RNA samples were stored in a -80°C freezer.

RNA was diluted with RNase free water using the equation $c_1V_1=c_2V_2$ with the final concentration of 50 ng and a volume of 10 µl in preparation for reverse transcription.

5.2.11 Reverse Transcription (cDNA synthesis)

Applied Biosystems high capacity Reverse Transcription Kit (Cat # 4368814) was used to reverse-transcribe the extracted RNA. Standard Minimum information for publication of quantitative Real-time PCR experiments (MIQE) guidelines were followed. The reaction samples, including the inter-plate calibrator, and other relevant controls were organized in triplicates using MicroAmp™ 0.1mL 48-wells white plates (Applied Biosystems).

Quantitative PCR reaction was set up and run on the PCR machine (One Step Thermocycler, Applied Biosystems). The mRNA level of AQP4 was normalized to GAPDH and β-Actin and was calculated using $2^{-\Delta\Delta Ct}$

5.2.12 Statistical analysis

The One way Anova test was carried out using IBM SPSS Statistics 20 (IBM, Chicago, IL) in order to determine if there was a significant difference between the treated and untreated samples. This was followed by Bonferroni's multiple comparison test for post hoc analysis. A Student's "t"-test (using a 5% level of significance), was carried out to determine if there was a

significant difference in the thickness between the neurites of the control groups and the treatment cultures. The level of significance was set at $p < 0.05$.

5.2.13 Primer design

The mRNA sequences for the genes of interest (RhoB, Rac 1 and Slug) were sourced from the following sites and subsequently synthesized by Inqaba biocom:

RhoB: [http://www.ncbi.nlm.nih.gov/nucore/118090145?log\\$=seqview_refseq_mRNA](http://www.ncbi.nlm.nih.gov/nucore/118090145?log$=seqview_refseq_mRNA)

Rac 1: http://www.ncbi.nlm.nih.gov/nucore/NM_205017.1

Slug: http://www.ncbi.nlm.nih.gov/nucore/XM_001236568.1?ordinalpos=2&itool=EntrezSystem2.PEntrez.Sequence.Sequence_ResultsPanel.Sequence_RVDocSum

The primer sequences of the genes of interest and house-keeping genes were as follows:

Gallus β -Actin Forward	5'ACCCCAAAGCCAACAGA3'
Gallus β -Actin Reverse	5'CCAGAGTCCATCACAATACC3'
Gallus GAPDH Forward	5'GTTCTGTTCCCTTCTGTCTC3'
Gallus GAPDH Reverse	5'GTTTCTATCAGCCTCTCCCA3'
Gallus Rac 1 Forward	5'ACGAAGCTATCCGAGCAGTTCTGT3'
Gallus Rac 1 Reverse	5'TTCTGAGCAAAGCACAGGGTTTGG3'
Gallus Rho B Forward	5'TCTTTGAGAACTACGTGGCCGACA3'
Gallus Rho B Reverse	5'TGTCCACTGAGAAGCACATGAGGA3'

5.2.14 Quantitative PCR data analysis

The relative quantity (RQ) of the gene of interest was calculated using the following equation: 2-

$\Delta\Delta Ct = \text{relative quantity}$

$\Delta\Delta Ct = \Delta Ct - Ct$ (Internal calibrator, IPC)

$\Delta Ct = Ct$ (sample) – Ct (Reference gene)

The reference genes were Beta actin and GAPDH.

5.3.0 Results

The migration of neural crest cells was viewed after 24 hours of culture when the migrating neural crest cells were removed from the culture plate. After 48 hours of culture sparse neurite outgrowth was seen in cultures which had been cultured in peak plasma concentrations of cART, TOP and cART/TOP. In contrast, the control cultures were devoid of these neuronal processes. However, after 96 hours of culture neurite outgrowth was evident in all the explants irrespective of whether they were treated or control cultures (Figure 5.1A-E). Most of the neurites which were cultured in cART (Figure 5.1C, white arrows) appeared to be shorter and thicker than the control cultures (Figure 5.1A, B). Interspersed between the thick neurites were thin neurites of similar length. In contrast, the neurites which were cultured in TOP (Figure 5.1D) were thinner and longer. Neurites which were cultured in cART/TOP appeared to be of similar length to that of the control cultures (Fig. 5.1E). The treated cultures (cART, TOP and cART/TOP) showed more branching and anastomosing of neurites compared to the control cultures. Some control cultures had a mixture of thick and thin neurites (Figure 5.1A); however, most of the neurites were thin (Figures 5.1 A, B, white arrows).

5.3.1 DCX Staining

Alexa Fluor 488 with a green fluorescent was used to highlight the migrating DCX-positive neurons in neural tube cultures after 96 hours of culture. The majority of the neurites which were seen with the phase contrast microscope stained positive for DCX, a feature which is indicative of migrating neurons (Fig. 5.2 A-E). The cART-treated cultures (Fig. 5.2C) were thicker and shorter

(white arrows), while the TOP-treated cultures (Fig. 5.2D) and the control cultures (Fig. 5.2 A, B) appeared longer and thinner. Figure 5.2F shows that the neurites cultured in cART were significantly thicker than the other experimental cultures ($p < 0.05$) as well as the control cultures ($p < 0.05$). The neurites cultured in TOP were thinner than the control cultures as well as other treated cultures, but the results were not significant ($P > 0.05$). In addition, the TOP-treated, cART/TOP-treated and control cultures exhibited more arborisation than the cART treated cultures. The CTCF of the cART-treated neurites was significantly lower than that of the controls ($p < 0.05$) and other experimental cultures ($p < 0.05$) indicating decreased expression of DCX in these cultures (Figure 5.4). Neurites were absent in the negative control cultures in which the primary and secondary antibodies were omitted during immunohistochemistry (Fig. 5.3 A, B). Only DAPI-positive nuclei which stained a blue colour could be seen in these cells (Fig. 5.3 A, B).

5.3.2 Actin staining

Neural tube-derived neurons were stained with rhodamine phalloidin in order to evaluate the distribution and structure of the actin cytoskeleton. The actin filaments in the control cultures (Figures 5.5A and 5.5B) and TOP-treated cultures (Figure 5.5D) were distributed throughout the entire perimeter of the cell. However, the actin filaments in cART treated cells were irregularly arranged and confined more towards the periphery (Figures 5.5C, blue arrows). The stress fibres of the TOP and cART/TOP-treated cultures were thicker and were separated from each other (Fig 5.5 D, E, blue arrows). A number of vacuoles were observed in the cell bodies of most of the treated cultures and some control cultures (Figs 5.5 B-E, blue circles). Apart from cART-treated cultures, actin filaments were prominent in the axons and dendrites of all cultures. In addition, the

dendrites in cART-and cART/TOP-treated cultures appeared shorter and fewer than those of control cultures (white arrows). The amount of actin fluorescence (CTCF) in the treated neurons was significantly lower than that of control cultures (Fig. 5.5 F), with cART and TOP-treated cultures the most affected. The CTCF of the cART/TOP-treated cultures was higher than that of the cART only and TOP only-treated cultures individually (Fig 5.5F).

5.3.3 MTT proliferation assay

Both treated and untreated neuronal cells were used to determine the proliferation and viability on the neural tube-derived neurons which were in culture for 96 hours. Figure 5.6 shows that the proliferation in cART-treated and cART/TOP neurons was higher than the control cells as shown by the higher absorbance reading. However, there was no difference in the proliferation rate between the control and the TOP-treated cultures as the absorbance reading between the two treatments was comparable (Figure 5.6).

5.3.4 Gene expression

In order to determine the differences in the expression of Rac1 and RhoB genes in neural tube-derived neurons which had been cultured in cART, TOP and cART/TOP, quantitative PCR was performed on the cDNA of the experimental and control cultures. The amount of gene present in each sample was evaluated through the determination of threshold cycle values from which the relative quantity of the genes was calculated (Figures 5.7 and 5.8). The DMEM only control cultures were used as a reference sample. The upward elevation in these graphs indicates an

increase in expression of the gene of interest relative to the DMEM only control (which is used as a baseline). Figure 5.7 shows that Rac1 was upregulated in the TOP only-treated and cART/TOP-treated neurons, while it was downregulated in the DMSO only control and the cART-treated neurons. In contrast the Rho gene was upregulated in all neuronal culture samples. This was irrespective of whether the cultures were controls or experimental neurons. However, RhoB gene was significantly downregulated in the DMSO only control cultures ($p < 0.05$) when compared to the treated cultures. The treated cultures expressed more RhoB gene compared to the DMSO only control (Figures 5.7 and 5.8). There was no statistical difference in the RQ values between DMEM only and DMSO only control cultures ($p > 0.05$).

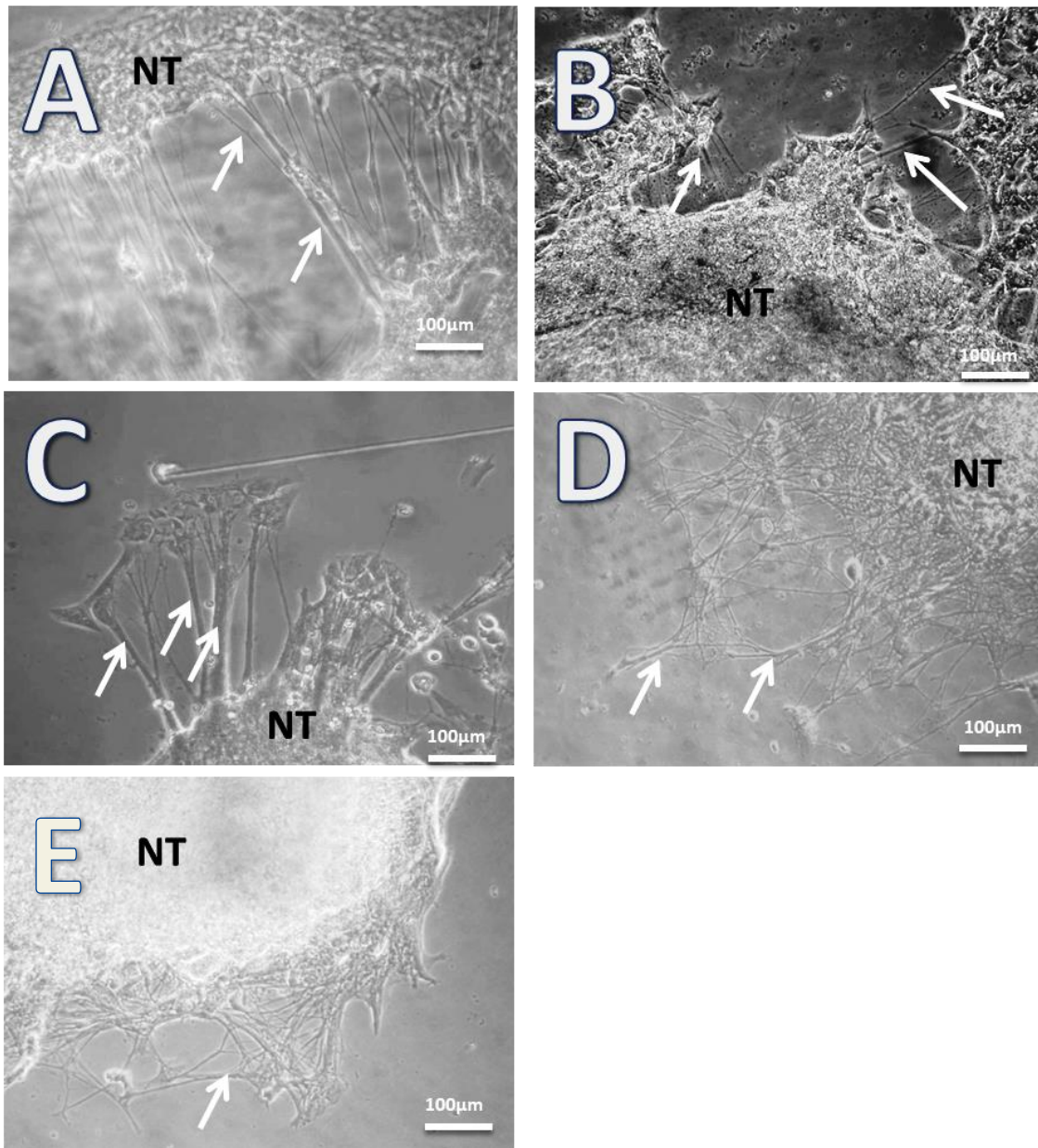


Figure 5.1. Photomicrographs showing neural tubes (NT) and neurites (white arrows) cultured in DMEM only (A), DMSO only (B), cART only (C), TOP only (D) and cART/TOP (E) after 96 hours of culture (Mag 100X). Neurites which were cultured in cART only appeared short and thick, while TOP only-treated neurites appeared long and thin (white arrows). Neurites cultured in CART/TOP were shorter and showed greater arborization.

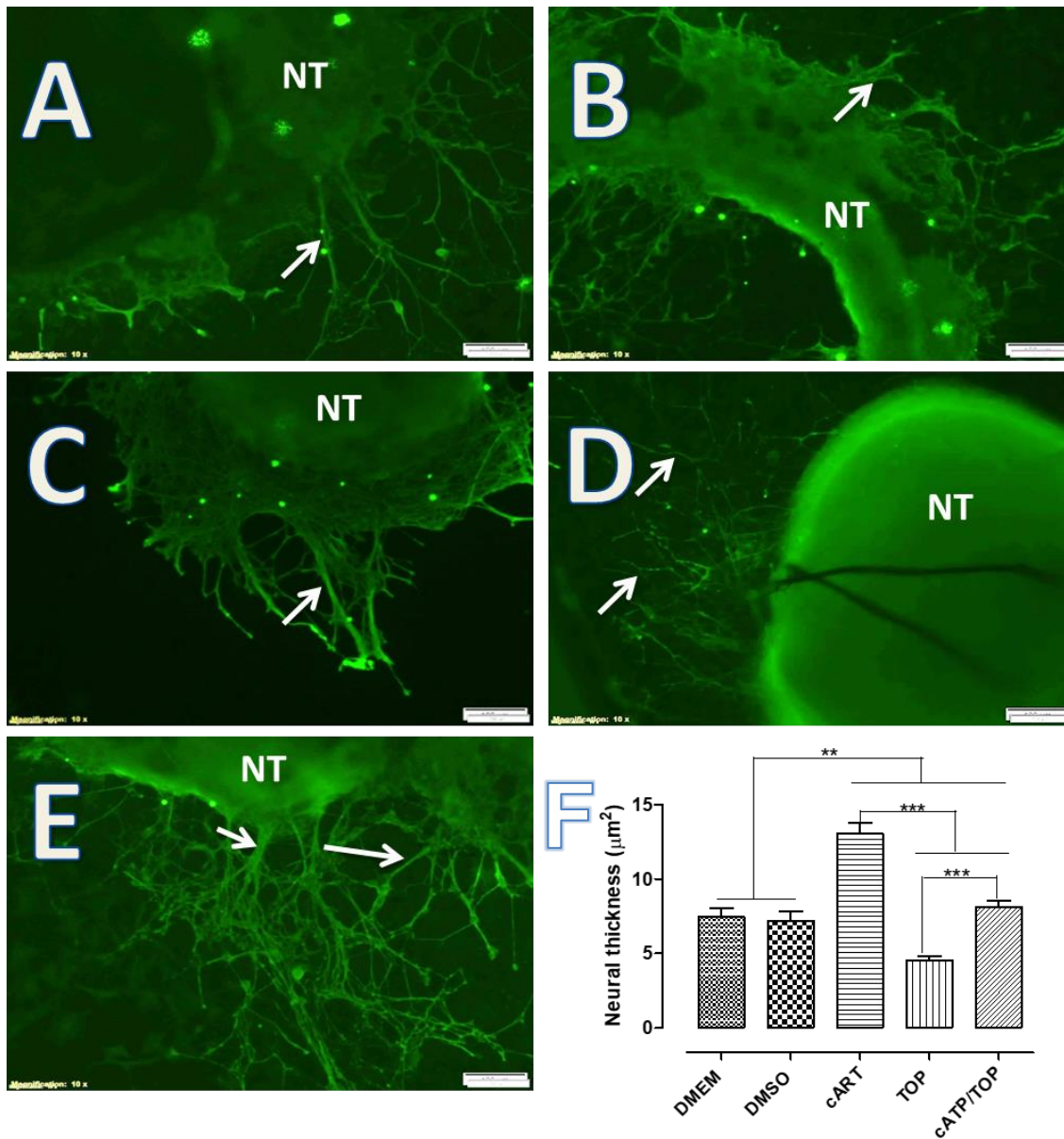


Figure 5.2. Photomicrographs showing DCX-stained neural tubes (NT) and neurites (white arrows) cultured in DMEM only (A), DMSO only (B), cART only (C), TOP only (D) and cART/TOP (E) after 96 hours of culture (Mag 100X). Neurites which were cultured in cART only appeared short and thick, while TOP only-treated neurites appeared long and thin (white arrows). Figure F shows the thickness of DCX-positive neural tube-derived neurons which were cultured in cART, TOP and cART/TOP. The thickness of the cART-treated neurites was significantly greater than that of the controls as well as the other experimental cultures.

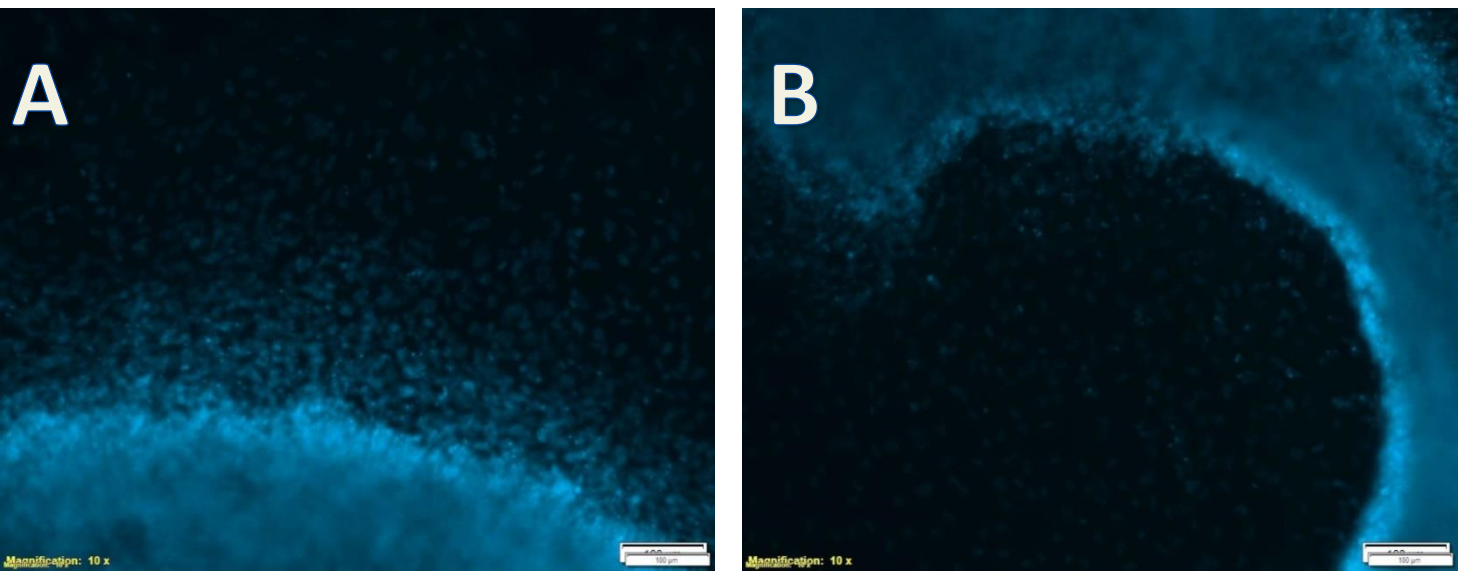


Figure 5.3. Control fluorescent photomicrographs showing DAPI-positive nuclei. Figure A shows a control section where the primary antibody was omitted while Figure B shows a control section where the secondary antibody was omitted. The DAPI-positive cells nuclei stained a blue colour.

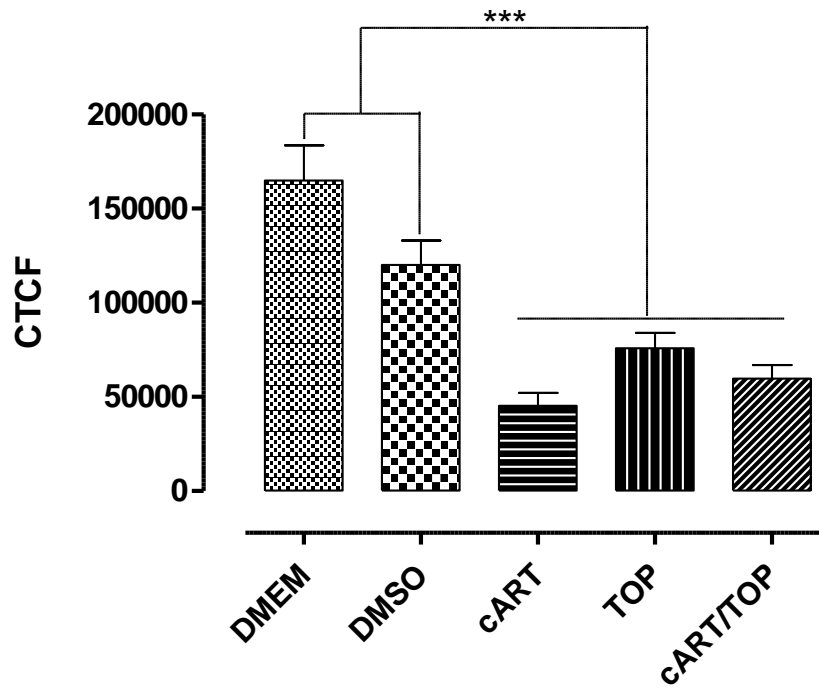


Figure 5.4. A graph showing the CTCF of DCX-positive neural tube-derived neurons which were cultured in cART, TOP and cART/TOP. The CTCF of the cART-treated neurons was significantly lower than the controls as well as the other treated cultures.

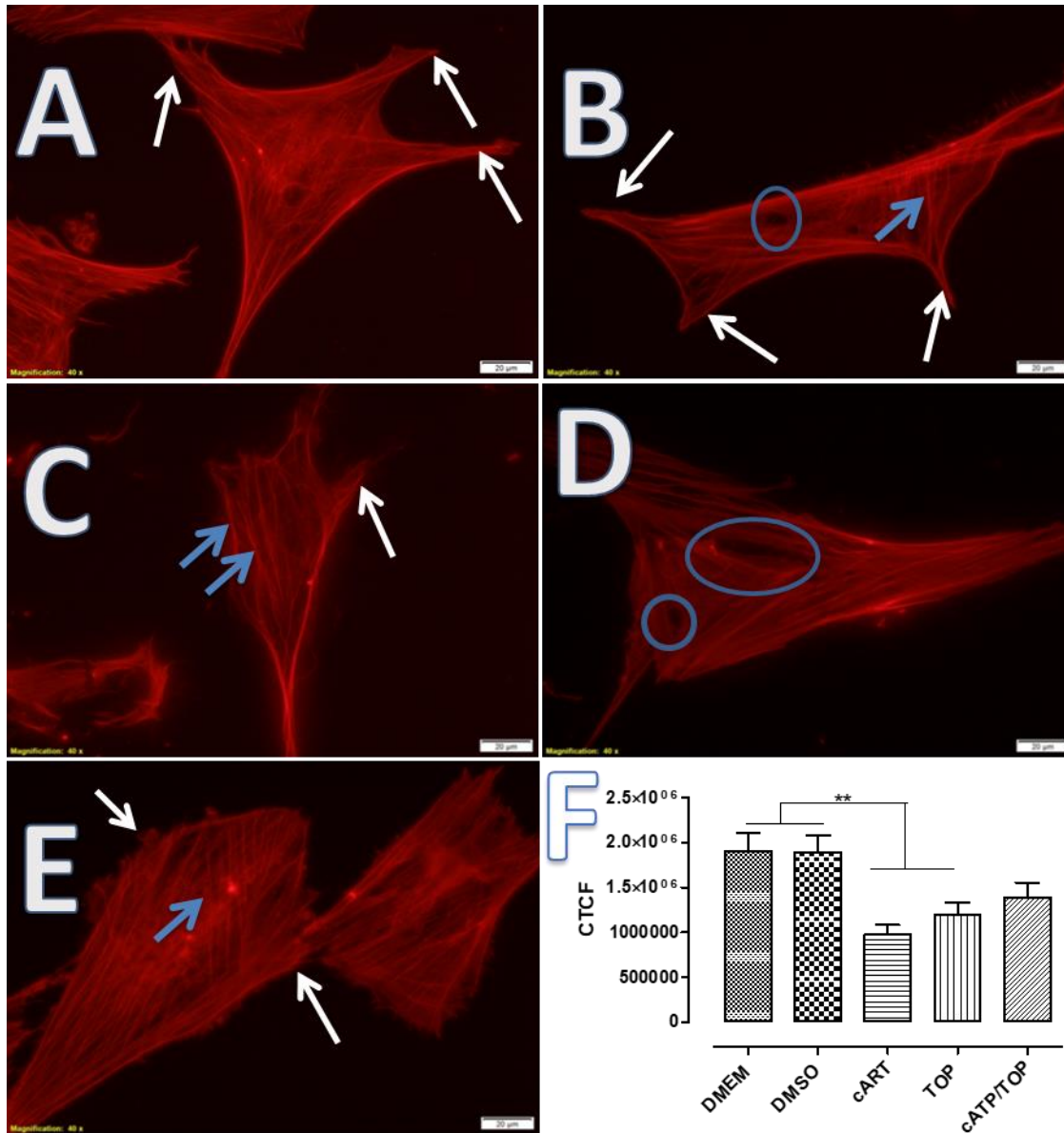


Figure 5.5. Fluorescent photomicrographs showing Rhodamine phalloidin-stained neurons cultured in DMEM only (A), DMSO only (B), cART only (C), TOP only (D) and cART/TOP (E). Cells cultured in cART only, TOP only and cART/TOP showed a disarray in the cytoskeleton (blue arrows) and appeared vacuolated in certain parts of the cell (blue circles). Prominent dendrites were evident in the control cultures (A, B, white arrows), while dendrites were short or absent in the cART only and cART/TOP-treated cultures. Figure F is a graph showing the CTCF of neural tube-derived neurons which were cultured in cART, TOP and cART/TOP and stained with Rhodamine phalloidin. The CTCF of cART only-treated cells was significantly lower than the control cultures and other experimental cultures.

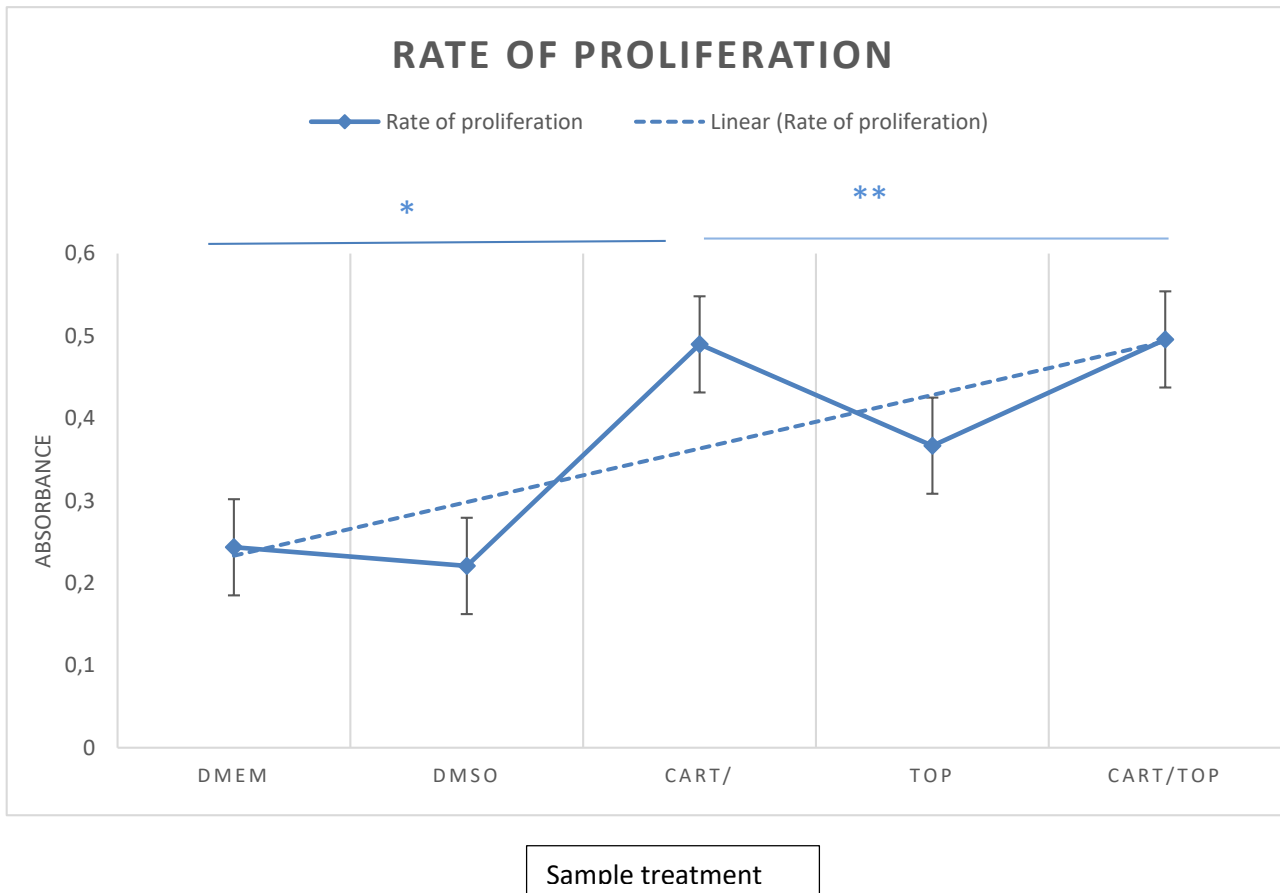


Figure 5.6. An MTT graph showing the rate of proliferation of neural tube-derived neurons in culture. The rate of proliferation was significantly higher compared to the two control cultures ($p < 0.05$). The TOP-treated cultures showed the lowest rate of proliferation out of all the treated cultures.

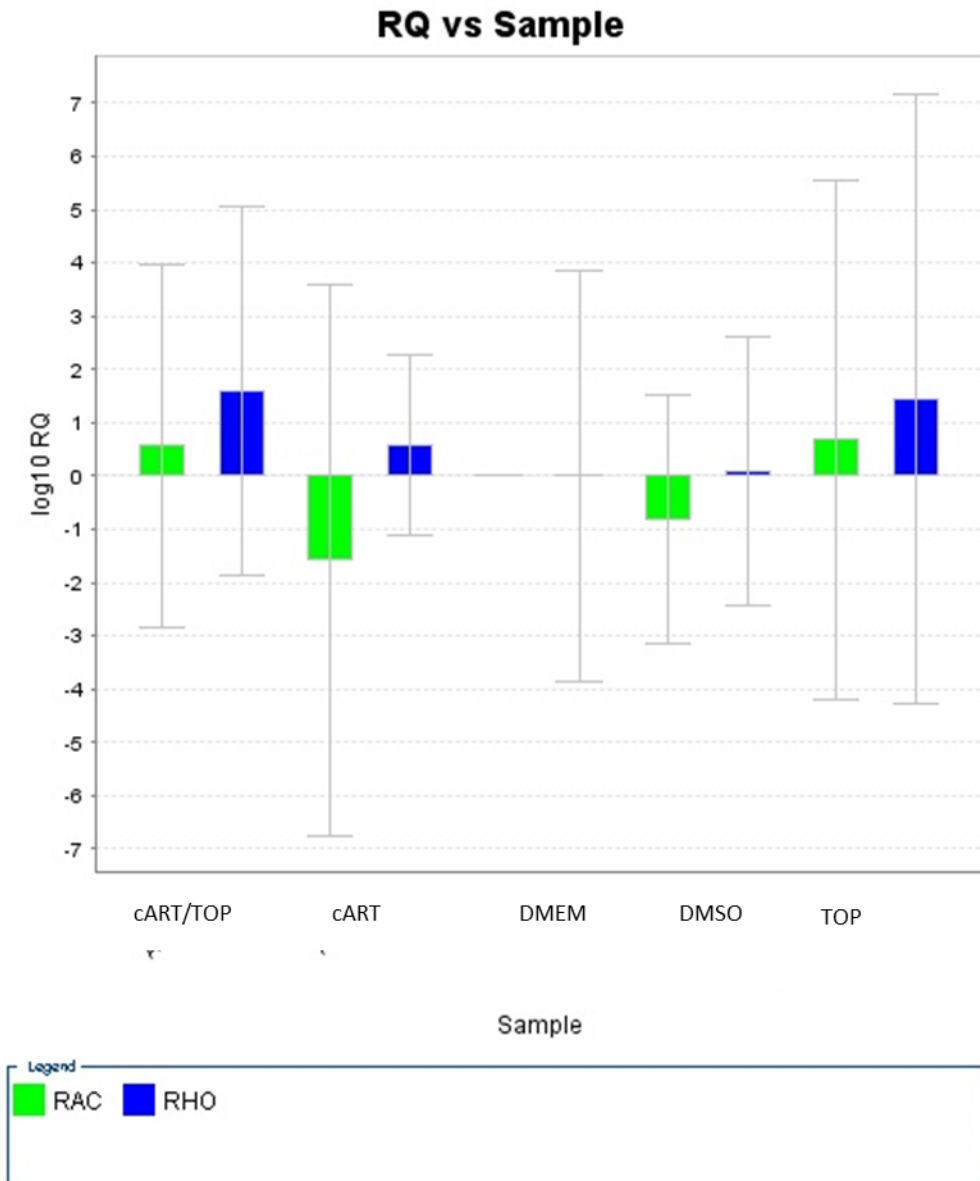


Figure 5.7. A graph showing the relative quantities (RQ) of Rac1 and RhoB in neural tube-derived neurons cultured in cART, TOP and cART/TOP. Rac1 is downregulated in cART and the DMSO control while it is upregulated in TOP and cART/TOP cultures. RhoB is upregulated in all the cultures.

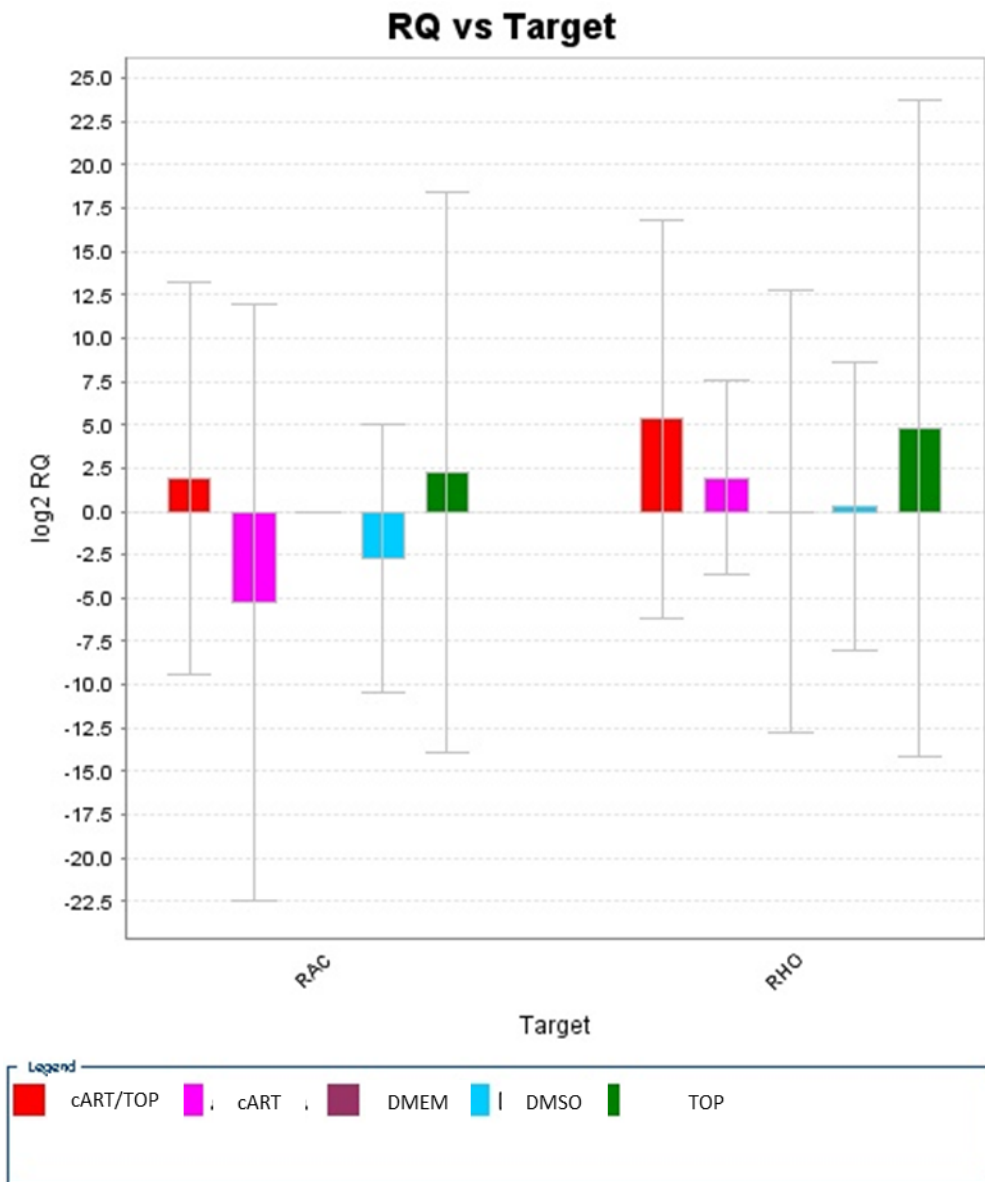


Figure 5.8. A graph showing the relative quantities (RQ) of Rac1 and RhoB in neural tube-derived neurons cultured in cART, TOP and cART/TOP. Rac1 is downregulated in cART and the DMSO control while it is upregulated in TOP and cART/TOP cultures. RhoB is upregulated in all the cultures

5.4.0 Discussion

The current study aimed to investigate the mechanism by which cART and TOP cause neuronal migration disorders in children who are born to mothers who are on this therapy. Neuronal migration disorders such as pachygyria and the partial agenesis of the corpus callosum have been observed in children who are born to HIV patients who had been on cART (Sibiude *et al*; 2014). However, the data on the mechanism by which cART causes these defects has been lacking. The current study sought to unravel the processes associated with neuronal formation and the mechanism by which cART interrupt these processes, with the use of neural tube-derived neurons as a model. These neurons were cultured in the presence of peak plasma levels of cART, TOP and cART/TOP. In order to evaluate neurite outgrowth, the neurons were stained with DCX. The current study shows that cART and TOP alter the growth of neurites when administered at peak plasma levels. The administration of cART resulted in thicker neurites while TOP resulted in longer and thinner neurites. Neurites which were cultured in cART/TOP were shorter, but showed greater arborization. The CTCF evaluation showed that DCX expression was significantly decreased in neurons which were cultured in cART. These results suggest that cART may affect the migration of newly formed neurons by downregulating the expression of DCX. These results are consistent with the findings of other studies that showed that mutation in the DCX gene could lead to neuronal migration disorders (Ayanlaja *et al*; 2017; Stouffer, 2016). In some of the studies, abnormalities were observed in the axonal growth and guidance in DCX mutant neurons (Ayanlaja *et al*; 2017), while other abnormalities involved the arborisation of dendrites (Dioli *et al*; 2019; Das *et al*; 2015). The cART only and TOP only-treated neurons showed greater arborisation when compared to their control counterparts in the current study.

These results are consistent with the findings of Smit-Swintosky (2001) who showed that TOP enhances neurite outgrowth and promotes nerve function after it has been damaged.

DCX promotes the migration of neurons by binding to microtubules (Moslehi *et al*; 2017).

Abnormal relations between microtubules and DCX result in the alteration in the organization of the actin cytoskeleton (Moslehi *et al*; 2019). The disarray in the cell cytoskeleton will result in the abnormal migration of neurons (Moslehi *et al*; 2019). For this reason, the study sought to correlate the organization of actin filaments to the expression of DCX in these neurons. In the cART-treated neurons the actin filaments were irregularly distributed within the cell body. These results confirm the findings that a disarray of the actin cytoskeleton is associated with an abnormal DCX expression (Moslehi *et al*; 2017). Also, research has shown that DCX is involved in the proliferation of neurons in addition to its role in migration (Ayanlaja *et al*; 2017). Migration and proliferation of neurons was deterred in DCX mutant mice indicating the importance of DCX in these processes (Moslehi *et al*; 2017). The current study employed the MTT technique in order to evaluate the proliferation rate of neural tube-derived neurons in the presence of cART and TOP. The MTT assay is a colorimetric assay based on the principle that mitochondrial succinate dehydrogenase reduces soluble yellow MTT to form insoluble purple formazan crystals (Kumar *et al*; 2018). The absorbances are a measure of the number of viable cells present since the soluble MTT can only be reduced to an insoluble formazan precipitate by metabolically active cells (Kumar *et al*; 2018). The results of the MTT assay in the current study showed an increase in the proliferation of neuronal cells cultured in cART and cART/TOP. In this instance the proliferation of the neurons was negatively correlated to the expression of DCX in the treated group, an observation which was contrary to the findings of Ayanlaja and his colleagues (Ayanlaja *et al*; 2017). Research shows that DCX plays a role in the proliferation of neurons and that its loss

could result in the reduction of the progenitor group of cells (Pramparo *et al*; 2010). The increase in proliferation of neurons in the current study suggests that cART increases the proliferation of cells despite the decrease in the expression of DCX. These results coupled with the results of the actin cytoskeleton suggest that cART increases the proliferation of neurons which then cease to migrate prematurely and subsequently differentiate into abnormally thicker neurites.

The current study also evaluated the expression of migratory genes Rac and Rho, which play a role in the formation of stress fibers and focal adhesions. Focal adhesions anchor the actin filaments to the extracellular matrix to allow cells to migrate on the substratum to which they are bound (Burrige and Guilluy, 2016). More importantly, the actin filaments give the cell its shape and structure and they are the major component of the cell projection that allows motility (Burrige and Guilluy, 2016; Sugawara *et al*; 2016).

The Rho family of GTPases plays a major role in the formation of neurites since they are involved in actin and microtubule dynamics (Stankiewicz and Linseman, 2014; Hall and Lalli, 2010; Govek *et al*; 2005). In order to define the structure of neurons the Rho family of GTPases function negatively proportional to each other (Stankiewicz and Linseman, 2014; Govek *et al*; 2005). Rac1 has been shown to express at the distal half on the tips of neurites (Stankiewicz and Linseman, 2014; Govek *et al*; 2005). It has been shown that the presence of Rac1 at the surfaces of the cells as they get involved in the formation of filapodia and lamellipodia is associated with the decline in the expression of Rho. Similarly, if Rho is activated the formation of neurites will be delayed or subdued (Stankiewicz and Linseman, 2014; Govek *et al*; 2005). The aforementioned findings are consistent with the results of the current study which showed that an increase in the expression of the Rho gene was correlated with a decline with DCX expression in the treated

neurons. Similarly, the expression of Rac1 gene was downregulated in these neurons, a finding which may explain the alteration in the morphology of these neurites.

Research shows that the activation of Rho results in the accumulation of actin filaments at the periphery of cells thereby forming a thick band of actin filament at the lateral cortices of the cells (Govek, 2005). This finding is consistent with the results of the current study which showed that the increase in the expression of the Rho gene is correlated with a decline in the Rac gene and actin filaments becoming vacuolated in the centre. Research also shows that Rac1 promotes the formation of neurites and associated filapodia and lamellipodia while Rho prevents the formation of neurites (Xu *et al*; 2019; Govek, 2005). Rac1 gene was significantly reduced in the cART only-treated neurons in the current study while the neurites were thicker and exhibited less branching. These results were further correlated with a decrease in the expression of DCX. Thus the activation and deactivation of Rac and Rho are required for the normal formation and development of neurites (Xu *et al*; 2019; Gonzalez-Billault, 2012). Growth factors, receptors and GTPases regulatory molecules are involved in the antagonistic regulation of Rac1 and Rho during the formation of neurites (Govek, 2005). These include NGF and the Ras-linked tyrosine kinase receptor (Auer *et al*; 2011). This tyrosine kinase receptor regulates the activation of Rac1 by NGF and the downregulation of Rho (Auer *et al*; 2011). CD47 (integrin-associated protein) of immunoglobulin family is another protein which has been shown to induce Rac1 and cdc42 and thereby promoting the formation of neurites and filapodia (Murata *et al*; 2006). The increased contractility in actomyosin is thought to be responsible for the neurite retraction due to the RhoA and Rho-kinase activation (Stankiewicz and Linseman, 2014; Govek *et al*; 2005). Therefore, RhoA activation is associated with the assembly of F-actin filaments, the rounding of cells and the retraction of neurites (Stankiewicz and Linseman, 2014; Govek *et al*; 2005). These findings

are consistent with the increase in Rho expression and the concentration of actin filaments at the periphery of the cells in the cART-treated neurons.

Due to the reliance of neurons on the Rho GTPase family for the regulation of cytoskeletal elements, Rac and Rho genes have been shown to be involved in the formation of dendrites (Stankiewicz and Linseman, 2014). Dendrites grow when the level of retraction declines and with subsequent increase of branching (Govek, 2005; Negishi *et al*; 2005). It is thought that these dendrites are mainly made up of actin close to the cell membrane while the mature branches are predominantly made up of microtubule (Stankiewicz and Linseman, 2014). Studies have shown that Rho results in the decreased arborisation of dendrites in its active form in a myriad of species (Stankiewicz and Linseman, 2014; Govek, 2005). These results are consistent with the findings of the current study where the upregulation of the Rho gene in the TOP-treated and control neurons was correlated with the increase in the arborisation of neurites and dendrites.

5.4.1 Conclusion

Although cART is teratogenic when administered during pregnancy, it remains a viable option to many pregnant women who are HIV positive. As highlighted in the current study, cART causes a myriad of abnormalities when administered during gestation. The results of the current study suggest that cART causes neuronal migration disorders by altering the expression of the DCX, Rac and Rho genes in the neurons of the neural tube, the primordium of the central nervous system. In addition, cART results in the disarray of the cytoskeleton, increased proliferation, and an alteration in the structure of neurites of migrating neurons. The results of cART/TOP were not conclusive as TOP seemed to affect the activity of cART in certain parameters only, but in other

occasions TOP appeared not to alter the action of cART as the results between the cART-treated neurons and cART/TOP neurons were not significantly different.

CHAPTER 6 The effect of cART and TOP on the expression of AQP4 and RPS17 in developing *gallus gallus domesticus* brains

6.1.0 Introduction

Hydrocephalus is a disorder caused by the abnormal formation, flow and absorption of the cerebrospinal fluid (CSF), with resultant CSF volume increase and consequently increased intracranial pressure in the ventricular systems of the brain (Isaacs *et al*; 2018; Delbigio and Di Curzio, 2016). The accumulation of CSF results in the abnormal expansion and increased intracranial pressure in the ventricular cavities of the brain (Kahle *et al*; 2016; Fletcher *et al*; 2000). CSF is produced by the ependymal cells of the choroid plexus in the cerebral ventricles, after which it enters into the subarachnoid spaces, and eventually moves into the cerebral venous system through the arachnoid granulations (Isaacs *et al*; 2018; Delbigio and Di Curzio, 2016). During its flow, CSF will pass through the third and fourth ventricles of the brain with the use of the interventricular foramina and the cerebral aqueduct (Isaacs *et al*; 2018; Delbigio and Di Curzio, 2016). In other occasions hydrocephaly occurs due to the hypersecretion of CSF by the ependymal cells of the choroid plexus (Chu *et al*; 2016).

The two main categories of hydrocephalus are the communicating and non-communication types (Chu *et al*; 2016; Delbigio and Di Curzio, 2016; Fletcher *et al*; 2000). Worldwide, the incidence of congenital hydrocephalus is approximately one case per 1000 births; while in sub-Saharan Africa over 200 000 new cases are recorded every year due to neonatal infection (Scott-Emmert, 2019; Di Curzio, 2016).

Reports link the use of combined antiretroviral therapy (cART) by HIV positive mothers during the first trimester of pregnancy to the formation of CNS anomalies including hydrocephalus and

cerebral edema (Ford *et al*; 2014; Sibiude *et al*; 2014, Mehta *et al*; 2019). Congenital hydrocephalus can also result from enteric gram-negative bacteria such as Gammaproteobacteria, Betaproteobacteria and Acinetobacter (Padhi *et al*; 2011). Other studies have reported the failure of cerebellar vermis to develop (known as Dandy-Walker malformation) following the use of cART due to enlargement of fourth ventricle and the posterior fossa (Chersich *et al*; 2006; Saitoh *et al*; 2005; Des Santis *et al*; 2002). However, from available literature, the mechanism by which cART causes this congenital anomaly remain poorly understood, but since HIV infection is unabating and requiring the continuous cART therapy in many countries of the world, there is a need to study and document the possible mechanisms of cART teratogenicity.

Since Aquaporin 4 (AQP4) gene is the main AQP in the brain and significantly affects water homeostasis in the brain and implicated in the development of hydrocephalus, the study investigated the effects of cART and TOP on the expression of this gene during brain development. Aquaporins are integral membrane proteins which function to transport water across cell membranes in response to osmotic gradients produced by the presence of solutes (Brown, 2017; Verkman *et al*; 2014). Some AQPs also function in the passage of glycerols and are thus called aquaglyceroporins (Brown, 2017; Verkman *et al*; 2014; Nielsen *et al.*, 2002). There are different types of AQPs, and these have been classified as AQP 0 to AQP 13 (Huret, 2020; Verkman *et al*; 2014; Verkman, 2013. AQPs 1,2,4,5 and 8 are exclusively designated to function in water transport whereas AQPs 3, 7 and 9 are involved in the passage of both water and glycerol (Verkman *et al*; 2014; Verkman, 2013). Some of the functions of AQPs include a role in concentrating urine, transporting of glandular fluid discharges associated with lubrication of the eyes and skin (Hara-Chikuma & Verkman, 2008; Tradtrantip, 2009, Verkman, 2013).

AQP4 is located mainly in the cell membranes of astrocytes and ependymal cells (Verkman, *et al*; 2014; Kruse *et al*; 2006) and has a myriad of functions in the brain which include the migration of glial cells, communication between astrocytes, seizures, brain edema, and brain tumors (Verkman, *et al*; 2014; Kruse *et al*; 2006).

Furthermore, in cerebral edema formation, AQP4 is reported to enable astrocyte swelling (“cytotoxic swelling”) and reabsorption of extracellular edema fluid (“vasogenic edema”) due to leaky blood brain barrier (BBB) allowing passage of intravascular proteins and fluid into the extracellular space (Chu *et al*; 2016).

6.1.1 AQP4 Structure

Aquaporin 4 is 30-kDa in size, and has cytosolic amino and carboxy terminal ends (Huret, 2019; Verkman, *et al*; 2014; Kruse *et al*; 2006). The amino and carboxy terminal ends span the cell membrane 6 times, thereby resulting in the formation of 5 interhelical loops (Huret, 2019; Verkman, *et al*; 2014; Kruse *et al*; 2006). These loops are located on both the extracellular and intracellular surfaces (Huret, 2019; Papadopoulos and Saadoun, 2015; Verkman, *et al*; 2014; Kruse *et al*; 2006). The loops are known as loops A, C, and E on the external surfaces, while on the internal surface they are called loops B and D (Huret, 2019; Verkman, *et al*; 2014; Kruse *et al*; 2006), (Figure 1).

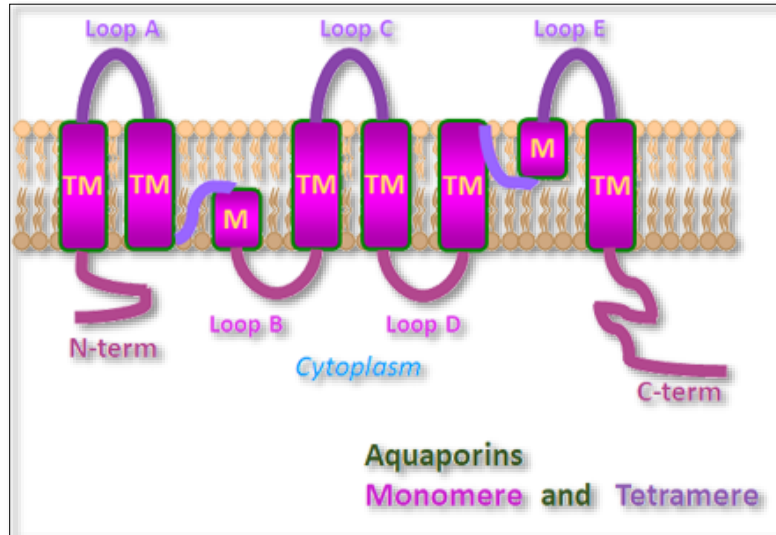


Figure 6.1. A diagram showing the general structure and the interhelical loops of aquaporins (Huret, 2019)

Changes in the expression or localization, and the resulting imbalance in water homeostasis of AQP 4, have been associated with neurological conditions such as traumatic brain injury and stroke (Mader and Brimberg, 2019; Chu *et al*; 2016). AQP 4 is also implicated in brain inflammation, lymphatic fluid clearance, synaptic plasticity and memory formation (Chu *et al*; 2016).

6.1.2 Cerebral edema and Hydrocephalus

Two main types of cerebral edema exist; these are cytotoxic and vasogenic edema (Mader and Brimberg, 2019; Chu *et al*; 2016). The former causes the buildup of water across a normal blood-brain barrier (BBB), while vasogenic edema forms as a result of fluid percolating from a leaky BBB (Mader and Brimberg, 2019; Chu *et al*; 2016; Verkman, 2005, 2008; Papadopoulos and Verkman, 2007). It is thought that brain swelling forms due to a change in the processes involved in the modification of water transport. These changes will result in the hypertrophy of the cerebral cortex (Mader and Brimberg, 2019; Chu *et al*; 2016).

The accumulation of water in cytotoxic edema is due to the deficiency of energy which occurs as a result of the damage of the sodium and potassium pump (Mader and Brimberg, 2019; Chu *et al*; 2016). Astrocytes are the main cells which are central to cytotoxic edema (Mader and Brimberg, 2019; Chu *et al*; 2016). The leaky BBB in vasogenic edema allows the passage of intravascular proteins and fluid into the extracellular space (Chu *et al*; 2016). Vasogenic edema is mostly prevalent in brain tumors, focal inflammation, abscesses and late ischemia (Chu *et al*; 2016). Manley *et al* (2000) showed that brain edema was decreased remarkably in mice which were deficient in AQP4. In addition, others studies reported that AQP4-deficient mice had significantly lower brain water accumulation in acute bacterial meningitis (Verkman *et al*; 2014; Papadopoulos *et al*; 2005). Research in cytotoxic edema indicates that mice lacking AQP4 were unlikely to have cellular enlargement and had enhanced neurological effect (Yao *et al.*, 2015). In contrast vasogenic edema increases in AQP4-deficient mice (Chu *et al*; 2016; Papadopoulos *et al.*, 2004).

Hydrocephalus, a specialized form of vasogenic edema, results from the obstruction of CSF drainage (Mader and Brimberg, 2019; Chu *et al*; 2016). Research shows that the progression of hydrocephalus, intracranial pressure, and enlargement of ventricles increases in AQP4-deficient mice (Mader and Brimberg, 2019; Chu *et al*; 2016; Verkman *et al.*, 2006). In contrast, Castaneyra-Ruiz *et al*, (2013) and Mao *et al*, (2006) showed that the levels of AQP 4 are increased in subjects with hydrocephalus. The findings of Guo *et al* (2018) are consistent with the finding that the development of hydrocephalus is proportional to the increase of AQP4 levels. However, in their study, Guo and his colleagues (2018) discovered that if AQP 4 was silenced with the use of SiRNA, hydrocephalus was intensified. In addition, the silencing of AQP 4

disrupted the BBB and the integrity of the ependymal layer. These finding suggests that AQP 4 has a protective role during hydrocephalus (Guo *et al*; 2018).

Although aquaporins have been implicated in cerebral edema, it has been shown that these membrane water channels play a role in the removal of water because of their bidirectional nature (Guo *et al*; 2018; Chu *et al*; 2016). The pathway of the water removal is along the extracellular space and the glial limitans. From here water will flow into the ventricles, and finally into the blood stream with the use of AQP4 which is situated in the endfeet of the astrocytes (Chu *et al*; 2016; Smith *et al.*, 2015; Thrane *et al.*, 2015).

The present study therefore aimed to investigate the effect of cART and TOP on the expression of AQP 4 during the development of *gallus gallus* domesticus brains. The altered expression of AQP4 levels due to the administration of cART would be indicative or suggestive of its teratogenicity during brain development. In addition, the timing of altered expression of AQP4 in the developing brain could also be indicative of the critical period in which the *gallus gallus domesticus* brain is particularly susceptible to the toxicity of cART. In this way, it could be determined if the factors responsible for the development of hydrocephalus and other related CNS anomalies due to the administration of cART are confined to the early stages of development, or if these factors are exerted during the later stages of brain development. While the function of AQP4 in the adult brain has been established, very little data exists on the role of AQP4 during development and therefore the current study aimed to contribute to the scant developmental research which has been done to date.

6.1.3 Antiretroviral therapy and Ribosomal Proteins

Several reports have shown that cART inhibits protein synthesis in normal tissues by decreasing ribosomal proteins (RPs) (Bertrand and Toborek; Tan *et al*; 2017) which has been associated with myriad of congenital defects (Engidaye *et al*; 2019; Wan *et al*; 2016; Zhang *et al*; 2014) which include hydrocephalus among others.

Ribosomes are cytoplasmic units that are involved in protein synthesis and the translation of mRNA (Zhou *et al*; 2015; de la Cruz *et al*; 2015; Sonenberg and Hinnebusch, 2009). Ribosomes comprise of 4 ribosomal species and 79 RNA-binding proteins called ribosomal proteins (RPs) (Zhou *et al*; 2015). The main functions of RPs are to stabilize the rRNA structure in the ribosome and to ensure that protein synthesis occurs (Zhou *et al*; 2015; de la Cruz *et al*; 2015; Nissen *et al.*, 2000). Research has shown that if certain ribosomal protein genes are mutated, physiological defects become inevitable (Goudarzi and Lindstrom; 2016; Kakehi *et al*; 2015; Szakonyi and Byrne, 2011), suggesting a regulatory role in these proteins. Because the biogenesis of ribosomes and the translation of mRNA are required for growth, proliferation and differentiation of cells; abnormal defects could occur if these processes are impaired. In *Drosophila* a number of defects which include delayed larval development, small body size, malformation of eyes and wings and recessive lethality were observed when the number of ribosomes and the subsequent protein synthesis were reduced (Lee *et al*; 2018; Lambertsson, 1998; Saeboe-Larssen *et al.*, 1998). The absence of RPS6 has been shown to prevent the proliferation of hepatocytes in mice following partial hepatectomy (Chauvin *et al*; 2014; Volarevic *et al.*, 2000). Low birth weight and reduced skeletal growth defects were also observed in RPL29-knockout mice with reduced cell proliferation and protein synthesis (Kirn-Safran *et al.*, 2007).

Research has shown that the mutation of specific ribosomal proteins such as RPS7, RPS 10, RSP 17 and RPS19 has been shown to cause a myriad of congenital defects (Engidaye *et al*; 2019; Wan *et al*; 2016; Zhang *et al*; 2014). The impairment of these RPs, particularly RPS17 and RPS19, is related to congenital bone marrow failure syndrome known as Diamond–Blackfan anemia (DBA) (Engidaye *et al*; 2019; Wan *et al*; 2016; Zhang *et al*; 2014). This condition exhibits a wide variety of symptoms, which include hydrocephalus among others (Engidaye *et al*; 2019; Wan *et al*; 2016; Kubik-Zahorodna *et al*; 2016; Zhang *et al*; 2014). The current study aimed to investigate the possible involvement of RPS17 in the development and progression of hydrocephalus, which has been observed in cART toxicity. The study therefore postulates that as one of the mechanism of action in the development of hydrocephalus, cART impairs the expression of the RPS17 gene.

Therefore, the aim of the study was to investigate the effect of cART and TOP on the gene expression of AQP 4 and RPS17 in developing *gallus gallus domesticus* brain.

6.2.0 Material and Methods

6.2.1 Drugs

A generic tablet of Atripla® (Bristol-Myers Squibb & Gilead Sciences LLC, South Africa) containing 600 mg of efavirenz (EFV), 200 mg of emtricitabine (FTC) and 300 mg of tenofovir disoproxil fumarate (TDF) was used as combination antiretroviral therapy (cART). The tablet was crushed into powder and dissolved in Dimethyl sulfoxide (DMSO, sigma). Topiramate (sigma, CAS NO: 97240-79-7, T0575) was also dissolved in DMSO. A hundred percent solution of 1g/ml in DMSO was made for both drugs.

6.2.2 The *in vivo* administration of drugs into chicken embryos.

Fertile chicken eggs (*Gallus gallus domesticus*) were used in this experiment. These eggs (n=36) were obtained from the animal unit, University of the Witwatersrand. The average weight of the eggs was $51.5\text{g} \pm 0.6$. The chicken eggs were incubated for three days at a temperature of 37°C in a humidified incubator. The eggs were turned twice daily to prevent the embryos from adhering to the shell membrane, and consequently dying. After three days, the blunt end of the egg was punctured using a hack-saw blade to release air from the air sac. Following this, 1ml of albumen was removed by penetrating the pointed end of the egg slightly below the equator of the shell with the hypodermic needle and a syringe.

The needle was pointed downward, almost vertically, as it passes into the shell to avoid damage to the yolk. To avoid leakage of albumen, the entry point was sealed with clear tape. The injection

was made into the blunt side of the egg using a 1ml hypodermic needle. The injection of cART, TOP, and the combination of the two drugs (cART/TOP) was made into the blunt side of each experimental egg using a 1ml hypodermic needle. The administered doses of the two drugs were determined from the dosages of the two drugs and the established weight of 20mg for a 3rd and 4th days old developing embryo when the egg weight is approximately 50mg (Mortola, 2010). For cART and TOP, a stock solution of 1mg Atripla (cART) and 1mg TOP in 1ml DMSO was separately freshly prepared. Subsequently, a single dose of 200µl cART and 0.02mg TOP per embryo were respectively administered to the appropriate embryos. The concentration of the cART/TOP was the combination of the individual concentrations of cART and TOP. Control embryos were treated with equal volume of saline (C1), while the second set of controls received 0.05% of DMSO reconstituted in saline (C2). The treatments were administered by microinjecting directly into the blunt side of the egg. Twelve (n=12) eggs were used for each treatment, with 4 eggs designated to a specific developmental stage.

After drug administration, the eggs were sealed with clear tape and returned to the humidified incubator at 37°C. The method of candling was used throughout gestation in order to check the viability of the embryos. The embryos were sacrificed by decapitation, and subsequently harvested from the blunt side of the egg and washed in saline. The brains were dissected out at days 7, 14 and 20, weighed and stored in RNAlater at 4°C. RNA was extracted from whole brains.

6.2.3 RNA extraction

RNA extraction was performed using the standard Trizol-chloroform-isopropanol method. The concentration and the purity (A_{260}/A_{280}) of RNA were determined using a NanoDrop 2000

Spectrophotometer (Thermo Scientific, Waltham, Ma). The RNA was then stored at -80°C until use.

6.2.4 Reverse Transcription and Quantitative PCR

Applied Biosystems high capacity Reverse Transcription Kit. (Cat # 4368814) was used to reverse-transcribe the extracted RNA. Standard MIQE guidelines were followed. The reaction samples, including the inter-plate calibrator, were organized in triplicates using MicroAmp™ 0.1mL 48-wells white plates (Applied Biosystems).

Quantitative PCR reaction was set up and run on the PCR machine. The mRNA level of AQP4 and RPS17 was normalized to GAPDH and β -Actin and was calculated using $2^{-\Delta\Delta Ct}$

6.2.5 Evaluation of AQP 4 and RPS17 genes expression

The expression of AQP 4 and RPS17 genes in day 7, 14 and 20 *gallus gallus domesticus* brains of control and treated samples (cART, TOP and cART/TOP) was determined using quantitative PCR. The level of expression of the genes in each sample was obtained through the determination of threshold cycle values from which the relative quantity (RQ) of the genes was calculated. The C1 control cultures were used as a reference sample, and in cases where the gene of interest was not detectable in the control samples, the IPC control sample was used as a reference sample.

6.2.6 Statistical analysis

One way Anova test was carried out using IBM SPSS Statistics 20 (IBM, Chicago, IL) in order to determine if there was a significant difference between the RQ values of the treated and untreated samples. The level of significance was set at $p < 0.05$.

6.2.7 Genes and Primers

The primers for genes of interest were designed online using Eurofins genomics tool (<https://www.eurofinsgenomics.com>) and analyzed on IDT OligoAnalyzer tool (<https://eu.idtdna.com/calc/analyzer>) available online. The primers were purchased from Inqaba Biotechnical Industry (Pretoria, South Africa).

The primer sequences of the genes of interest and house-keeping genes were as follows:

Gallus β -Actin Forward	5'ACCCCAAAGCCAACAGA3'
Gallus β -Actin Reverse	5'CCAGAGTCCATCACAATACC3'
Gallus GAPDH Forward	5'GTTCTGTTCCCTTCTGTCTC3'
Gallus GAPDH Reverse	5'GTTTCTATCAGCCTCTCCCA3'
Gallus AQP4 Forward	5'ACGAAGCTATCCGAGCAGTTCTGT3'
Gallus AQP4 Reverse	5'TTCTGAGCAAAGCACAGGGTTTGG3'
Gallus RPS17 Forward	5'TCTTTGAGAACTACGTGGCCGACA3'
Gallus RSP17 Reverse	5'TGTCCACTGAGAAGCACATGAGGA3'

6.3.0 Results

The mean brain weights of the control group at 7, 14 and 20 -day old were $0.79\text{g} \pm 0.7$; $1.92\text{g} \pm 0.6$; and $4.03\text{g} \pm 0.8$ respectively. The mean brain weights of the cART-treated group were slightly increased, but not significantly different in all the stages, 7 ($0.88\text{g} \pm 0.7$) 14 ($2.11\text{g} \pm 0.6$), 20 ($4.27\text{g} \pm 0.8$) day of development ($p > 0.05$). The mean brain weights of the TOP-treated brains were 7 ($0.72\text{g} \pm 0.2$), 14 ($1.98\text{g} \pm 0.6$) and 20 ($3.88\text{g} \pm 0.4$), while the mean brain weights of the and cART/TOP-treated brains were 7($0.86\text{g} \pm 0.5$), 14 (1.76 ± 0.3), 20(3.96 ± 0.8)

6.3.1 Survival rates

All the embryos survived at 7 day of development in all the 4 groups. With regard to the day-14 embryos, the survival rate was 83% with recorded death of 2 of the embryos (1 control and 1 TOP-treated). The survival rate at day 20 was 75% with 3 recorded deaths (1 control, 1 cART, 1 cART/TOP). Ultimately, three biological samples were obtained for each treatment.

6.3.2 Aquaporin 4 and RPS17 gene expression in Day 7 brains

AQP4 was not expressed at all in day 7 control brain samples as it was undetected with quantitative PCR (Fig. 6.3), but was expressed in all treated brain samples of same developmental stage with cART-treated brains showing the highest expression. The expression in cART was statistically significant ($p < 0.05$) when compared to TOP-treated samples ($p < 0.05$), but there was no significant difference in the AQP4 expression in the cART- and the cART/TOP-treated brains ($p > 0.05$). Conversely, the RPS17 gene was downregulated in the treated samples when compared to the controls.

6.3.3 Aquaporin 4 and RPS17 gene expression in Day 14 brains

Figure 6.6 shows the expression levels of AQP4 and RPS17 levels in the developing day- 14 brains of *gallus gallus domesticus*. The expression of AQP4 was detectable for the first time in the control brains during this stage. AQP4 expression was significantly downregulated in the cART-treated brains. The two other experimental brain samples (TOP and cART/TOP-treated) showed an increased expression of AQP4. The AQP4 expression in the TOP-treated and cART/TOP-treated brain samples was statistically higher compared to the control brains ($p < 0.05$), however there was no significant difference in RQ between TOP only and cART/TOP-treated brain samples. The expression of the RPS17 gene was the highest in the cART and cART/TOP-treated brains. The expression of RPS17 gene in these brains was statistically higher than in the control brain sample. There was no significant difference in the RQ between the two control brain samples ($p > 0.05$).

6.3.4 Aquaporin 4 and RPS17 gene expression in Day 20 brains

Figure 6.7 shows the expression levels of AQP4 and RPS17 in the developing day 20 brains of *gallus gallus domesticus*. The expression of AQP4 was increased remarkably in the 20-day old brain samples. This was irrespective of whether the brain samples were experimental or controls. There was no statistical difference in the expression of AQP4 between the treated and control brain samples ($p > 0.05$). In addition, there was no significant difference in RQ between cART only, TOP only and cART/TOP treated brain samples. Conversely, the expression levels of RPS17 in the treated sample were all significantly downregulated when compared to the control brain samples ($p < 0.05$). There was no statistical difference in the RQ between the two control brain samples ($p > 0.05$).

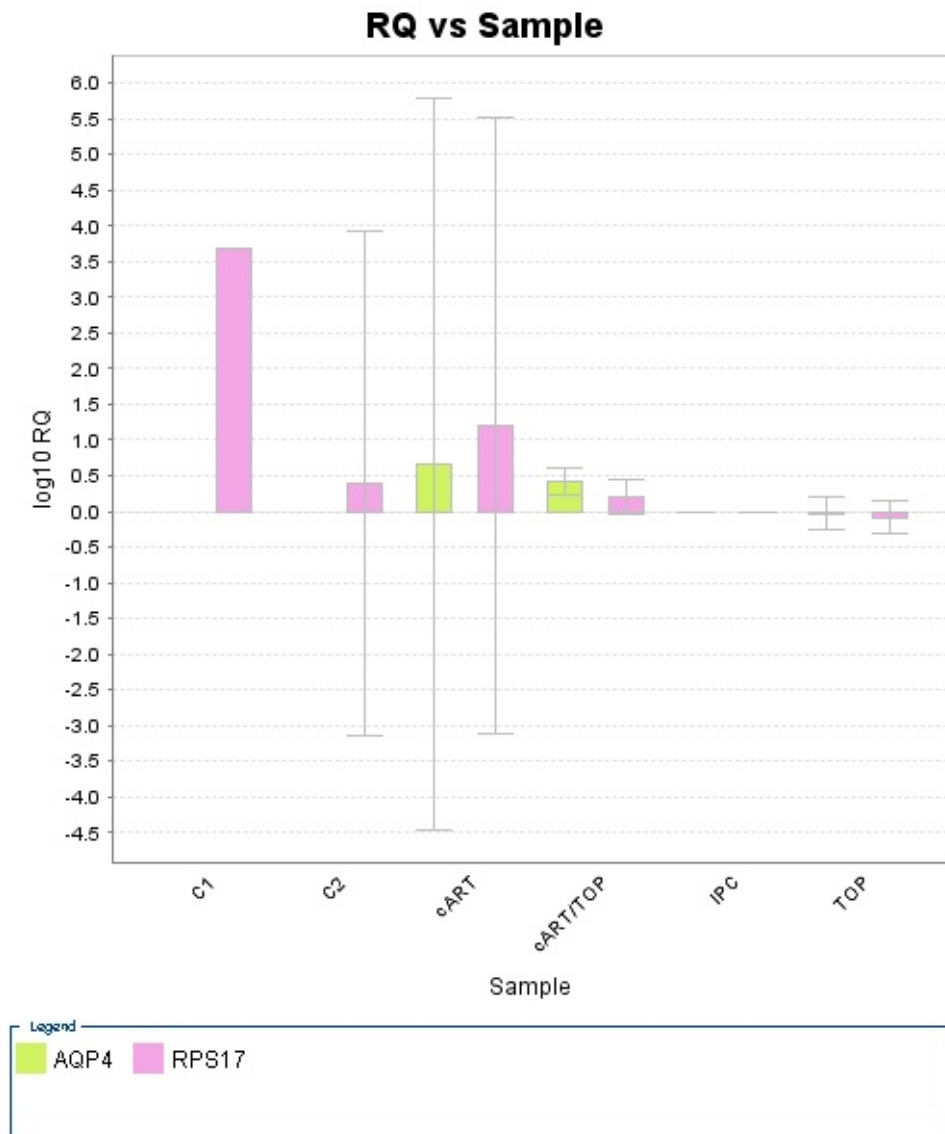


Figure 6.3 Relative quantities (RQ vs Sample) of AQP4 and RPS17 in 7-day-old chick brains which were exposed to cART, TOP and cART /TOP. AQP4 is not expressed in the control cultures; however, its expression is induced by cART, TOP and ATP/TOP. However, the expression of RPS17 is downregulated by the administration with the treatment drugs.

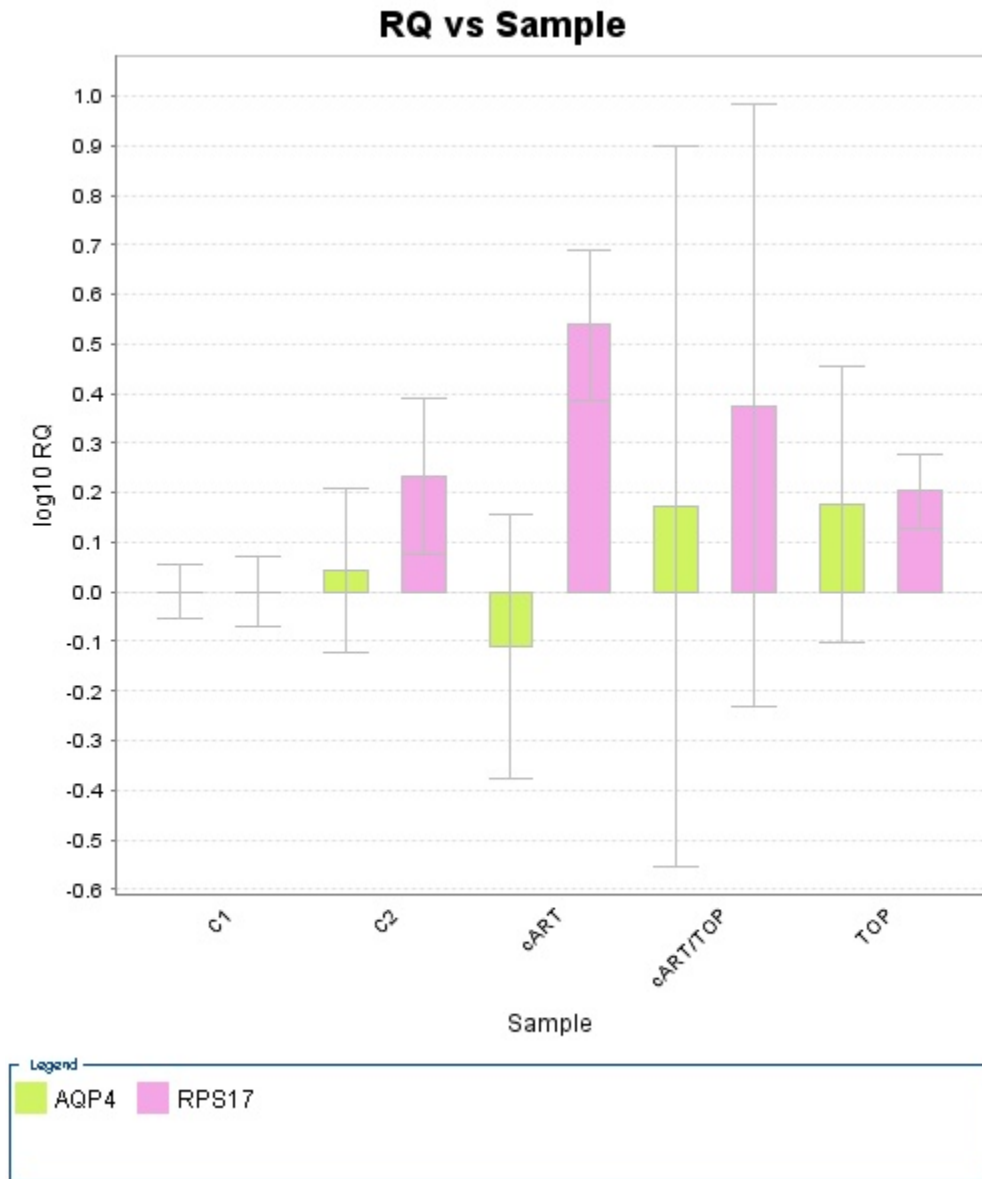


Figure 6.4 Relative quantities (RQ vs Sample) of AQP4 and RPS17 in 14-day-old chick brains which were exposed to cART, TOP and cART /TOP. The expression of AQP4 is reduced in the cART -treated brain samples, while the other treated samples are little affected. The expression levels of RPS17 are increased remarkably in the cART and cART /TOP-treated brain samples.

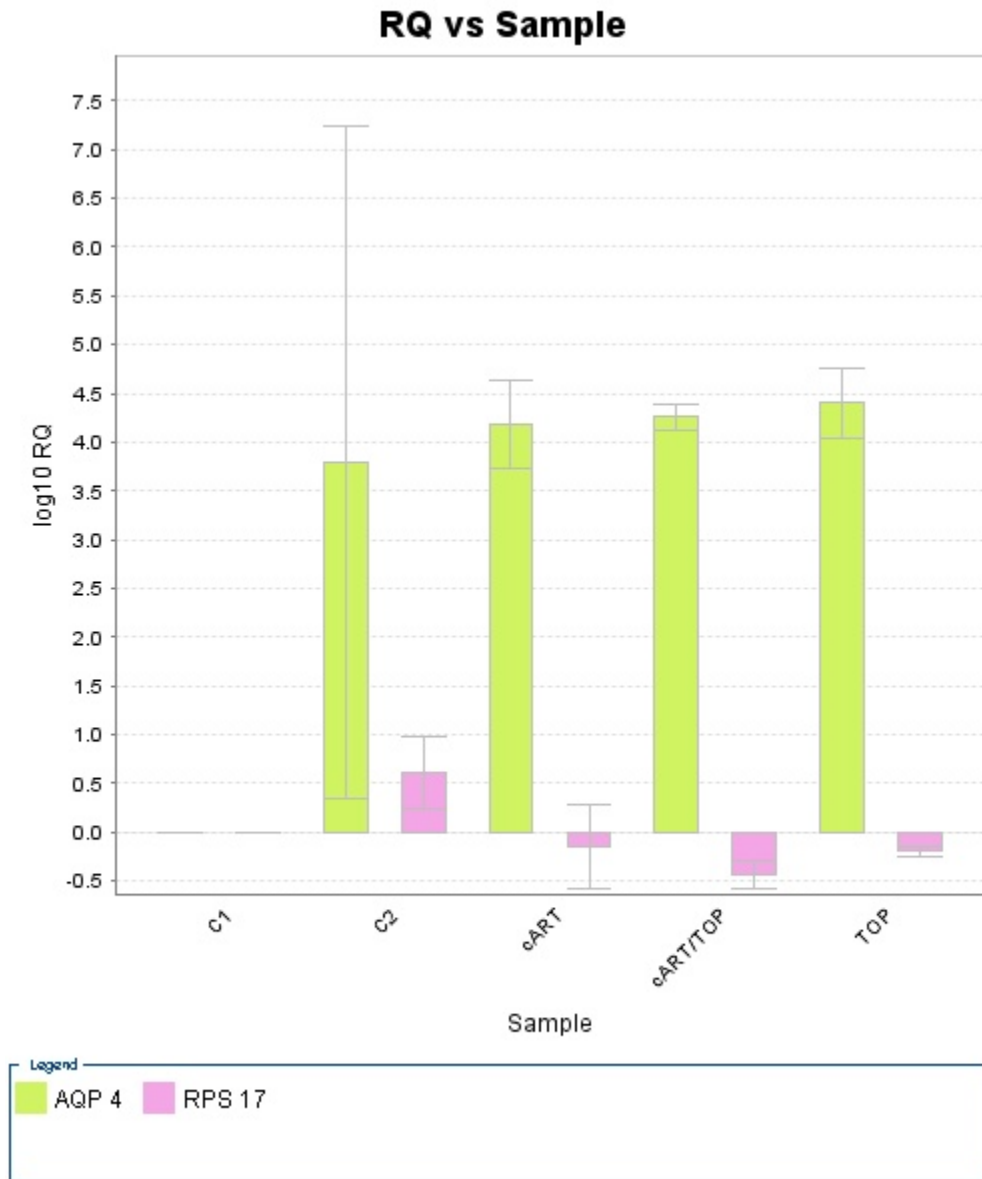


Figure 6.5. Relative quantities (RQ vs Sample) of AQP4 and RPS17 in 20-day-old chick brains which were exposed to cART, TOP and cART /TOP. The level of expression of AQP4 is remarkably high in all the brain samples. The expression levels of RPS17 are downregulated in all the treated brain samples.

6.4.0 Discussion

Since the introduction of cART, the prognosis and outcome of HIV have improved remarkably in people living with HIV with significantly increases survival rate, but associated with teratogenic effects, such as hydrocephalus (Apostolova *et al*; 2015) when administered during the first trimester of pregnancy (Delicio *et al*; 2018; Alemu *et al*; 2015). The mechanism by which cART causes hydrocephalus is unknown, and the present study on the level of AQP4 gene expression is designed to unravel its involvement in fluid homeostasis within the developing brain of *gallus gallus domesticus* under TOP and cART treatment.

The results of the current study show that AQP4 is not detectable in the control brain samples of *gallus gallus domesticus* but expressed in brain samples exposed to TOP and cART during day 7 of development, suggesting that AQP4 is not expressed during the first week of normal development in *gallus gallus domesticus* brains; but its expression in the treated groups may have been activated by the administration of cART and TOP (more significantly by cART followed and minimally by TOP). There was a statistically significant difference between cART only and TOP only treated brains, suggesting that cART induces the production of AQP4 more during this stage. However, there was no significant difference between cART only and cART/TOP treated brains, suggesting that TOP does not affect the activity of cART. The results of the control group are consistent with a study by Nico and his colleagues (Nico *et al*; 2002) who reported that AQP4 is first detectable in developing chicken brain samples during the 9th day of development.

Furthermore, the significant down regulation observed in the second week of development may be attributed to inhibitory effects of cART on the expression of AQP4 gene, which was absent on TOP and cART/TOP treated groups. The expression of AQP4 due to cART treatment on day 7

represents about 10,000-fold increase compared to the expression levels in the control brain samples on day 14 and as well in the down regulation on day 14 by cART. In addition, AQP4 levels increased in the control and experimental groups in day 20 brain samples, but more in TOP treated group suggesting that the developing brain may not be susceptible to the teratogenicity of cART and TOP and both combined during the latter stages of development. Furthermore, AQP4 levels were shown to have increased by more than 20 000 fold in 20-day-old brain samples of the control and treated groups, suggesting that the brain may not be susceptible to the teratogenicity due to cART during the latter stages of development.

These results are consistent with the findings of Nico *et al*; (2002) in which the expression of AQP4 in day-9 embryos was approximated to be 7% of the total adult AQP4 level; however, this expression was elevated to nearly 16% in day-14 embryos. Similar to the findings of the current study, an abrupt surge in AQP4 expression was observed between day-14 and day-20 embryos. In addition, the level of expression observed in day-20 embryos was not significantly different to 2-day-old chicken embryos in Nico *et al*; (2002). This suggests that AQP4 expression reaches its embryonic maximum in day 20 *gallus gallus domesticus* brains.

Research shows that vasogenic edema occurs due to the depletion of AQP4 in brain samples (Huang *et al*; 2019; Tang and Yang, 2016; Papadopoulos *et al*; 2005, Verkman *et al*; 2014) during development, while the present study shows that the early expression of AQP4 was activated by cART during the first week of development in *gallus gallus domesticus* brain. These results may imply that cART induces the early formation of astrocytes and the subsequent expression of AQP4. Once formed, astrocytes will be involved in the formation of the BBB. It is probable that the premature formation of astrocytes leads to the formation of a premature and impaired BBB. It is also likely that the presence of premature AQP4 at this stage is the cause of

premature accumulation of fluid in the primordial ventricular system of the brain and consequently hydrocephalus. The slight increase in the average weights of cART-treated brains suggests the probable accumulation of water in the brain.

It is worth noting that AQP4 is a bidirectional water channel, and therefore it is involved in both the inflow and the outflow of water (Guo *et al*; 2018; Chu *et al*; 2016; Verkman *et al*; 2013). The plausible scenario during the second week of development is that the downregulation of the AQP4 gene by cART in the current study coincided with the normal process of water removal. In this way, the downregulation of the AQP4 gene resulted in the failure of water removal with the subsequent accumulation of fluid in the ventricular cavities. The extensive increase of AQP4 during the third week of development in the 20-day old embryos reflects the important angiogenic role (Kitchen *et al*; 2020; Mader and Brimberg, 2019) played by this gene during the later stages of development.

6.4.1 AQP and the Blood-Brain barrier

Also, linked to the early expression of AQP4 is the development of BBB. As variously reported AQP4 is involved in the formation and maintenance of structural integrity of BBB in the adults and embryonic stages (Mader and Brimberg, 2019; Chu *et al*; 2016; Deng *et al*; 2014; Verkman *et al*; 2014) and the resultant development of vasogenic edema and hydrocephalus in impairment of the BBB (Mader and Brimberg, 2019; Chu *et al*; 2016; Deng *et al*; 2014; Verkman *et al*; 2013). It is therefore possible that both the inhibition and induction of AQP4 by cART as recorded may lead to premature and abnormal formation of the BBB (in the second week of development, (Nico *et al*; 2001)) during the early activation which consequently may incorporate structural defects in BBB especially during the inhibition and reduction of the AQP4 gene, resulting in a leaky BBB.

Additionally, the observed activation of AQP4 expression during the first week of development in *gallus gallus domesticus* developing brains by TOP and cART suggests that both drugs may have similar mechanisms in causing hydrocephalus, as TOP has previously been associated with hydrocephalus in children born to mothers on TOP therapy during pregnancy (de Jong *et al*; 2016; Tennis *et al*; 2015; Hernandez-Diaz *et al*; 2012). Moreover, unlike cART, TOP did not inhibit the expression of AQP gene post day-7 and did affect the activity of cART as there were no significant differences in expression of AQP4 gene between the cART and cART/TOP-treated brain samples.

The effect of cART and TOP on the expression of the RPS17 gene was also investigated. RPs are involved in protein synthesis from messenger mRNA; and also play a role in the occurrence of ribosomal-derived diseases called ribosomopathies (Wang *et al.*, 2015). In the current study, the RSP17 gene was expressed throughout gestation. However, this gene was downregulated in the treated day-7 *gallus gallus domesticus* brain samples. The expression of RPS17 was little affected by the expression of cART and TOP in day 14 brain samples as there was no significant difference between the experimental and control brain samples. However, there was a remarkable reduction in expression of RPS17 gene in the experimental samples of day-20 brains. These findings suggest that cART and TOP inhibit protein synthesis in developing *gallus gallus domesticus* brains during the early and latter stages of development. This reduction of the RPS17 gene has been shown in previous investigations to be responsible for a number of CNS anomalies which may include hydrocephalus (Engidaye *et al*; 2019; Wan *et al*; 2016; Zhang *et al*; 2014).

Conclusion

Previous reports have indicated that both cART and TOP cause hydrocephalus when administered during pregnancy. The mechanism of this teratogenicity is unknown, but the current study shows that both cART and TOP induce the expression of AQP4 during the first week of development, while cART inhibits the expression of AQP4 during the second week of development in *gallus gallus domesticus* brains. These findings suggest the mechanism by which water is retained in the ventricular cavities, causing hydrocephalus. In addition, the study shows that both cART and TOP, individually and in combination downregulate the RPS17 gene in 20 day old brains, suggesting that these drugs inhibit protein synthesis.

7.1.0 Concluding Discussion

The thesis investigated the mechanisms by which cART and TOP result in specific congenital malformations in children born to women who are taking the two drugs individually, and in combination. Research has shown that both cART and TOP cause a variety of congenital malformations during pregnancy when administered individually (Green *et al*; 2012; Ford *et al*; 2014). Birth defects such as VSDs, cleft lip and palate, neuronal migration disorders and hydrocephalus have been reported in both antiretroviral and antiepileptic therapy when administered during pregnancy (Green *et al*; 2012; Ford *et al*; 2014). However, the mechanism of their teratogenicity is unclear. The current study therefore employed the avian model in order to unravel some of the possible mechanism of action. In addition, most of these congenital anomalies have been shown to occur during the first trimester. The findings of this study suggest that perhaps the migration and differentiation of neural crest cells is central to most of the anomalies observed in antiretroviral and antiepileptic cytotoxicity.

In the current study, the administration of both cART and TOP inhibited the migration of both the cardiac and cranial neural crest cells when administered both individually and in combination. The inhibition of neural crest cells has previously been correlated with a myriad of congenital craniofacial and cardiac abnormalities (Keyte and Hutson, 2012) due to their involvement in the formation of a vast number of structures of the craniofacial region, the peripheral nervous system, and the cardiovascular systems. In addition, the current study shows that cART and TOP exert adverse effects on the development of neurites in the developing neural tube when administered at peak plasma levels. Furthermore, cART and TOP reduced the quantity of actin and the expression of DCX in neural tube-derived neurons. Research has shown that neuronal migration disorders involve genes which are associated with the cell cytoskeleton; therefore, these findings

may explain anomalies which are associated with neuronal migration disorders that have been observed in cART and TOP cytotoxicity. In addition, the current study showed that cART induces the premature expression of AQP4, a gene which is involved in the transportation of fluids within the ventricular cavities of the brain (Brown, 2017; Verkman *et al*; 2014). The early expression of this gene could explain the accumulation of fluid in the ventricular cavities in children who are born to mothers who are on cART and TOP.

7.1.1 Efavirenz as a choice for women of child bearing age

The current study investigated the mechanisms of teratogenicity of efavirenz-based combination antiretroviral drug, Atripla. Although South Africa may change to the Dolutegravir-based combination antiretroviral therapy due to some patients developing resistance with efavirenz, research shows that efavirenz is the more favourable drug for women of child bearing age who are not on contraceptives (van der Wijer *et al*; 2019; Kintu *et al*; 2020). This is because the incidence of birth defects is lower with the use of efavirenz than it is with Dolutegravir. For this reason, many countries still prefer the use of efavirenz (Kintu *et al*; 2020). Therefore, in order to avoid the occurrence of congenital anomalies it is important to understand the mechanism of action of efavirenz.

The use of cART during pregnancy is inevitable for many young women who are dependent on this therapy for survival, particularly those women who come from developing countries (Zash *et al*; 2018; Wijer *et al*; 2019; Kintu *et al*; 2020). This poses challenges as these women have to continue taking these drugs even though they are known to be teratogenic. However, most of the studies showed that the significance of efavirenz to cause congenital disorders is very low and

the benefits of the drug outweigh the risks, therefore WHO changed its guidelines which prohibited the use of efavirenz by pregnant women and women of child bearing age (Ford et al; 2010; WHO, 2018). Prior to the introduction of efavirenz, the NNRTIs which were approved by the FDA were nevirapin, delavirdine, etravirine and rilpivirine. However, efavirenz was favored due to its efficiency and lower risk profile (Gulick *et al*; 2004; Riddler *et al*; 2008; Robbins *et al*; 2003). Although efavirenz has the same efficacy as nevirapin, their benefits and side effects differ. Efavirenz has a greater ability to suppress the virus and is less resistant to the virus than nevirapin (Gulick et al; 2004; Riddler et al; 2008; Robbins et al; 2003). Atripla is highly recommended by WHO because it is aligned with the organization's goal to provide simpler, safer, single dose treatment that can be used by a variety of populations and age groups (WHO, 2019). In addition, efavirenz regimen is co-active with rifamycin which is used to treat tuberculosis (Bhatt, 2014). Also, efavirenz is able to pass through the blood-brain barrier (Tozzi et al; 2007; Marra et al; 2009), penetrating the cerebrospinal fluid and preventing viral replication. Efavirenz is used as a first-line treatment across the world especially in developing countries where there is few or no other alternative for treatment (UNAIDS, 2018). In developed countries such as Italy (Baroncelli et al; 2009), patients have a variety of choices when it comes to antiretroviral treatment. Patients can choose a drug that is suitable for their viral characteristics. Research shows that the majority of people using ARVs are women (Mayosi *et al*; 2012), therefore the use of efavirenz is inevitable for many women who are dependent on the drug for survival, particularly those who come from developing countries (WHO, 2016).

7.1.2 Dolutegravir vs Efavirenz for women of child bearing age

Dolutegravir-based antiretroviral therapy (cART) has been shown to be more efficient and tolerable to HIV patients (van der Wijer *et al*; 2019; Kintu *et al*; 2020) and it is not surprising that

South Africa has resolved to stop using the previously recommended efavirenz-based cART. The eagerness to use Dolutegravir-based cART received a setback for women of child bearing age when a study in 2018, now referred to as the Tsepamo study (Zash *et al*; 2018) discovered a higher risk of neural tube defects with the use of Dolutegravir. The risk of neural tube defects in women who conceived while taking Dolutegravir was 0.94%, compared to 0.05% in infants born to mothers who conceived receiving efavirenz. Due to this finding, WHO recommended the use of Dolutegravir-based cART as a general first-line regime (WHO 2019). However, due to its lower risk in neural tube defects, efavirenz was endorsed as a safer option for women of child bearing age. However, these findings pose a great challenge in the choice of the preferred drug as a first-line regime. The adverse effects of Dolutegravir during pregnancy should be compared to its overall benefit against efavirenz. Dolutegravir is likely to improve the overall outcome in patients by increasing sustained virologic suppression (Zash *et al*; 2018; van der Wijer *et al*; 2019; Kintu *et al*; 2020). Currently Dolutegravir is recommended for women of child bearing age who are on contraceptives, however, the inability to access reproductive health services could be a challenge to women in developing countries (Zash *et al*; 2018; van der Wijer *et al*; 2019; Kintu *et al*; 2020). Therefore, it may not be possible to implement the WHO guidelines in countries such as Kenya and Malawi (Zash *et al*; 2018; van der Wijer *et al*; 2019; Kintu *et al*; 2020). Efavirenz in these countries will be the choice for first-line treatment in women of child-bearing age, however, other countries such as south Africa and Zimbabwe may prescribe Dolutegravir.

Dugdale *et al*; (2019) showed that the use of efavirenz would result in more deaths among HIV positive women than prevented pediatric deaths. The present WHO guidelines would prevent approximately 4100 pediatric deaths which are related to neural tube defects, however this would increase the number of deaths by about 8000 in HIV positive women of child bearing age.

However, a recent study performed by NAMSAL in Cameroon showed that there was no difference in 48 week virologic suppression between dolutegravir- and efavirenz-based cART (Cournil *et al*; 2018).

7.1.3 Choice of AED for HIV patients

The current study sought to investigate if TOP would affect the activity of cART if administered in combination. This is because there is considerable concurrent use of AEDs and ARVs worldwide because some HIV patients develop seizures which arise as a result of CNS infection from HIV-based opportunistic infections (Siddiqi and Birbeck 2013). However, there are no established guidelines for antiepileptic drug treatment for PLWHIV (Siddiqi and Birbeck 2013). This is particularly important as the possible interactions between the two drugs may have adverse effects on the management of HIV and seizures. In particular, the P450 enzymatic system is of interest as it is activated by the two drugs (Zaporojan *et al*; 2019). AEDs which activate the P450 system may decrease the efficiency of the NNRTIs and PIs which likewise activate the P450 system. Therefore, it is important that the aforementioned are taken into consideration because a wrong choice of AEDs may result in the reduction of plasma levels of AEDs and subsequent viral progression, immunologic decline, clinical disease progression, and ARV resistance (Zaporojan *et al*; 2019). Similarly, ARVs may decrease plasma levels of AEDs, resulting in the worsening of seizures (Zaporojan *et al*; 2019). The results of the current study show that TOP does not affect the activity of cART, suggesting that TOP could be an appropriate antiepileptic drug to combat seizures in HIV patients who are taking Atripla.

7.1.4 Neural crest cells in congenital anomalies

The results of this study show that cART and TOP exert adverse effects on the migration of both cardiac and cranial neural crest cells. These findings could help explain features of Cardio-facio-cutaneous syndrome (CFC) as the symptoms of this syndrome involve structures which are derived from both the cardiac and cranial neural crest cells (Pierpont *et al*; 2014). Interestingly, anomalies observed in children born to women who are on cART and TOP include those of cardiac and the craniofacial region (Ford *et al*; 2014). Therefore, it is probable that both cART and TOP result in the development of CFC, and that this condition may be caused by the inhibition of cardiac and cranial neural crest cell migration. This syndrome is a multiple congenital anomaly disorder which comprises malformations of the craniofacial region and heart defects (Pierpont *et al*; 2014). Other anomalies of CFC include growth delays and neurocognitive deficits. CFC is classified under a group of disorders called RASopathies, which also include neurofibromatosis type 1 as one of the anomalies (Pierpont *et al*; 2014). The craniofacial characteristics of CFC include macrocephaly, bitemporal narrowing, convex facial profile, and hypoplastic supraorbital ridges and high-arched palate (Goodwin *et al*; 2013), gastrointestinal dysfunction, neurocognitive delay, and seizures (Pierpont *et al*; 2014).

For a very long time neurofibromatosis and neurocutaneous melanosis were the only neurocutaneous syndromes known to be caused by the ailing neural crest (Sarnat and Flores-Sarnat, 2005; Sarnat and Flores-Sarnat, 2013). During this period, clinicians looked to identify the common pathogenic theme among a myriad of neurocutaneous syndromes. However, this has been challenging as most of these neurocutaneous syndromes are clinically and genetically different from each other. In addition, neurocutaneous syndromes were regarded as abnormalities of ectoderm; however, the fact that some of the tissues involved in these

abnormalities were mesodermal and endodermal in origin was confusing to researchers (Sarnat and Flores-Sarnat, 2005; Sarnat and Flores-Sarnat, 2013). Numerous studies have conjured on a probable involvement of neural crest cells in the pathogenesis of neurocutaneous syndromes.

Common characteristics of neurocutaneous syndromes comprise vascular malformations of the integument among other organs, altered pigmentation in cutaneous lesions, peripheral nerve lesions, asymmetry and abnormal growth in several tissues and organs(Sarnat and Flores-Sarnat, 2005; Sarnat and Flores-Sarnat, 2013). In addition, it has been shown the ailing neural crest has been attributed to the lipomas which are related to neurocutaneous syndromes.

Neurofibromatosis is an autosomal dominant disease which occurs as a result of an abnormal neural crest. The café-au-lait and depigmented spots appear due to the abnormal differentiation of melanocytes from neural crest cells (Sarnat and Flores-Sarnat, 2005; Sarnat and Flores-Sarnat, 2013). In addition, neurofibromas and schwannomas of peripheral nerves are derived from the abnormal growth and differentiation of neural crest cells (Sarnat and Flores-Sarnat, 2005; Sarnat and Flores-Sarnat, 2013). Other characteristics of Neurofibromatosis include pheochromocytoma, hypertelorism and meningiomas of the cerebral cortex (Sarnat and Flores-Sarnat, 2005; Sarnat and Flores-Sarnat, 2013). The results of this study are consistent with the aforementioned points as these findings suggest that neural crest development could play an important role in the development of congenital anomalies of pigmentation and peripheral nerves which are observed in cART cytotoxicity. In this study, cART altered the thickness of developing neurites and pigment production in the cranial neural crest.

7.1.5 The probable mechanism of cART and TOP cytotoxicity on the actin cytoskeleton

In order to mitigate against the limitations of the determination of the radius ratio (extent of migration), the current study evaluated the actin cytoskeleton of cultured neural crest cells which were treated with cART, TOP, and cART/TOP. The results were correlated with the migration assay as research has shown that adverse effects on neural crest cell actin cytoskeleton results in the inhibition of migration (Haendel *et al*; 1996).

The mechanism by which cART and TOP affect the actin cytoskeleton in migrating neural crest cells is not clear. However, three actin-associated proteins which are involved in the regulation of actin assembly in migrating neural crest cells have been discovered (Vermillion *et al*; 2014) and could therefore provide the basis for the adverse effects of cART and TOP on the actin cytoskeleton. Doublecortin, a member of a family of microtubule associated proteins is involved in the stabilization of actin by facilitating its binding to the microtubules (Vermillion *et al*; 2014). Tropomyosin I stabilizes actin filaments by forming the tail and head polymers in the filament major groove. In addition, Tropomyosin I is involved in the formation of stress fibers and focal adhesions. Actin depolymerizing factors are permissive of actin-associated migration of neural crest cells (Vermillion *et al*; 2014).

In addition, it is plausible that the mechanism of cART and TOP could encompass the accumulation of acetylated histones, as TOP has been shown to be a histone deacetylases (HDAC) inhibitor (Eyal *et al*; 2004). In addition, a study by Bruning *et al*; (2016) showed that efavirenz, a component of cART is able to induce DNA damage and apoptosis in human leukemia cells by regulating the phosphorylation of p53 and H2AX, a subtype of histone protein H2A, suggesting its possible function as an HDAC inhibitor. H2AX is involved in the gathering of DNA repair proteins to the

areas of DNA double-strand break damage. HDACs are a group of proteins which are involved in the removal of acetyl groups from lysine residues (Li and Seto, 2016). The acetyl groups are removed from the histone tails lysine residues, resulting in basic histones (Suraweera *et al*; 2018). This alteration enables the histones to bind more firmly around DNA, resulting in a change in the nuclear signaling pathways which regulate cell proliferation and survival (Li and Seto, 2016). However, it has been shown that some HDACs can deacetylate proteins which are not histones (Valenzuela-Fernández *et al*; 2008). These include proteins which are associated with the cytoarchitecture (Valenzuela-Fernández *et al*; 2008). Histone deacetylase 6 (HDAC6) is mostly found in the cytoplasm and is involved in the deacetylation of α -tubulin, a component of microtubules which form a major element of the cytoskeleton (Valenzuela-Fernández *et al*; 2008). Microtubules are involved in a cyclic activity of polymerization and depolymerization to regulate cell morphology and motility. It has been shown that HDAC6 regulates cell motility by increasing the acetylation of cortactin, a protein which is localized at the periphery of cells where dynamic actin assembly is occurring (Valenzuela-Fernández *et al*; 2008). In association with F-actin, cortactin increases actin polymerization and branching thereby increasing cell motility. Cortactin is permissive of migration is upregulated; however, motility is hindered when cortactin is downregulated (Valenzuela-Fernández *et al*; 2008).

7.1.6 Rationale for the choice of neural crest cell migration assay

The current study used the determination of the radius ratio in order to resolve the extent of migration of neural crest cells. Generally, specific and specialized methods are employed to evaluate the migration of neural crest cells. These methods include time-lapse video image

analysis of neural crest cells, which are fluorescence tagged (Kawakami et al. 2011). Other techniques involve scratch assays associated with human neural crest cells (Zimmer *et al.* 2012). According to Usami *et al* (2014 and 2016), these methods are not ideal for investigating the effects of teratogens in a normal toxicity laboratory. As a result, Usami *et al* (2014) established an *in vitro* assay which enables the quantification of migration following the administration of exogenous chemicals. This method involves the determination of the radius ratio which is calculated from the circular spread of migrating neural crest cells. The limitation of this method is that the increase in migration in the circular spread may be partly due to the increase in numbers of neural crest cells. Similarly, the decrease in number of neural crest cells could in part decrease the distance of migration (spread). However, this migration assay is more accurate than measuring the linear migration of neural crest cells as these cells do not migrate in a linear fashion. According to Li et al, (2019), migrating neural crest cells display a range of contrasting cellular behavior. While some neural crest cells are committed to “persistent and directional migration”, some cells are involved in migration from dorsal to ventral and some cells even migrate backwards before proceeding forward again. In addition, most of the neural crest cells migrate individually, however, some neural crest cells migrate in groups and the latter group may be involved in contact inhibition. Also, while some neural crest cells migrate in a zig-zagged manner, these cells also show a spreading behavior (Li et al; 2019) and hence this choice of migration assay (cellular spread). All the aforementioned factors make the determination of the distance of migration a challenge.

These factors mean that cells that are found at the migration front do not necessarily migrate the fastest. As a result, the linear measurement of migration which in this instance is referred to as vector displacement, is not a true determination of neural crest migration. The determination of the

radius ratio (spread) is therefore more accurate as neural crest cells have been shown to migrate in that manner.

7.1.7 The choice of the avian model for the study

The current study employed the use of the avian model in order to explain the mechanism of cART and TOP teratogenicity. The use of avian models has contributed immensely towards the understanding of the embryonic development of vertebrates. Most of what is currently known regarding vertebrate morphology was first established using chicken and quail models. The growth patterns of avians are preserved and comparable to those observed in mammals, and this enables extrapolation of results to humans (Smith et al, 2012). Because avian embryos are predisposed to a wide-range of toxic substances such as medicinal, ecological, manufactural chemicals, and dietary components, they are preferable for first-line screenings as they are unlikely to give false negatives (Harris and Hansen, 2012). A myriad of processes such as organogenesis and cell differentiation can be studied in the embryo during gestation and in hatched chicken.

The use of avian models in toxicology research is more favourable as chicken and quail eggs are inexpensive, allowing for large samples. The incubation of eggs is economical and short, as chickens have an incubation period of 21 days, while the gestation period in quail embryos is eighteen days (Smith et al, 2012). In addition, the embryo can be easily observed and monitored by making a window through the shell which can be resealed to resume growth. (Smith et al, 2012). The shell and the consistent size of the eggs allows for the administration of precise doses of test drugs or teratogens (Smith et al, 2012). When the effects of toxicants and teratogens are

studied at specific periods of embryonic development for treatment and exposure purposes, based on the route, it is much easier when using avian models as dose-response relations can be established (Hill and Hoffman, 1984).

Avians are more associated to mammals, and less related to amphibians, reptiles, and fish with regard to embryonic development. This is because avians, like mammals develop an allantois (Starck and Ricklefs, 1998). Even though avians are devoid of a placenta, the maternal transmission of environmental toxicants can occur prior to laying of eggs (Russell et al, 1999). Toxins such as selenium can be accrued by avians and maternally conveyed to their eggs during oogenesis, with the subsequent development of congenital anomalies (Bryan et al, 2003). The process of oogenesis involves the transportation of lipoproteins from the maternal tissues to the eggs, and because organic chemicals generally reside in lipids, they can be transferred concurrently during this process (Russell et al, 1999). Other toxins such as methylmercury are largely transmissible through maternal transfer, and it has been shown that methylmercury concentrations in eggs are comparable with maternal blood levels (Ackerman et al, 2020).

7.1.8 Cytochrome P450 activity in avian neural crest cells

Although cytochrome P450 enzymes have been shown to be present in developing chicken and quail avian models, only few have been characterized (Reijntjes *et al*; 2004; Li et al; 2017). CYP1A1 and CYP26A1 are expressed in anterior neural folds and neural plates of developing avian models. It has been shown that CYP 26A1 enzyme is localized in cardiogenic precursors (Reijntjes *et al*; 2004; Li et al; 2017). It is thought that CYP26A1 could be involved in the formation of neural crest cells as it is expressed in the neural folds during neurulation. These enzymes as well as CYP 26

C1 have also been shown to be expressed in migrating avian neural crest cells (Reijntjes *et al*; 2004; Li *et al*; 2017). Topiramate and Efavirenz are metabolized by the CYP3A4 enzymatic system (Nallani *et al*; 2003; Xu and Desta; 2013). Although this specific enzyme has not been characterized specifically in avian neural crest cells, Diaz *et al*; (2010) showed that both chicken and quail have CYP1A1, CYP1A2, CYP2A6, and CYP3A4 enzymatic activity. A study by Fuller *et al*; (2002) showed that valproic acid, which uses the CYP3A4 system, is metabolized by avian neural crest cells, suggesting that neural crest cells have the CYP3A4 enzymatic system.

7.1.9 Limitations and Future studies

The current study used the migration assay in order to determine the distance of migration of neural crest cells. This assay measures the radius of the circle occupied by migrated neural crest cells. However, this assay doesn't indicate whether a larger radius translates to an increased number of neural crest cells or whether the large radius is due to increased migration. In addition, a number of drugs which induce the P450 cytochrome enzymatic system have been assayed using avian neural crest cells in previous and current studies, suggesting that these cells express receptors for this system. However, there is no data which shows a wide range of receptor types which are present in these cells. Therefore, a study which will show the expression of these receptors is necessary. While the present study involved only the administration of drugs in animal models without HIV virus infection, future studies which include viral mimetics as an additional intervention would be considered as the inclusion of HIV may influence the outcome. However, sampling of adult cadavers relative to embryological study of this nature may not be feasible. Though, it will be interesting to consider the sampling of neonatal

cadavers born to mothers who were placed on antiretroviral and antiepileptic therapy, but a such study will be ethically problematic.

References

- Abdulaziz, A.T.A., Li, J. & Zhou, D. The prevalence, characteristics and outcome of seizure in tuberculous meningitis. (2020). **Acta Epileptologica** 2, 1.
- Ahmed, M., Bui, A., Taioli, E. (2017). Epidemiology of Cleft Lip and Palate. DOI: 10.5772/67165
- Alemu, F. M., Yalew, A. W., Fantahun, M., & Ashu, E. E. (2015). Antiretroviral Therapy and Pregnancy Outcomes in Developing Countries: A Systematic Review. **International journal of MCH and AIDS**, 3(1), 31–43.
- Anderson RH, Cook AC. 2004. Morphology of the functionally univentricular heart. *Cardiology Young* 14(1):3–12.
- Anderson, R.H., Spicer, D.E., Mohun, T.J., Hikspoors, J.P. and Lamers, W.H. (2019), Remodeling of the Embryonic Interventricular Communication in Regard to the Description and Classification of Ventricular Septal Defects. *Anat Record journal*, 302: 19-31.
- Apostolova N, Funes HA, Blas-Garcia A, Galindo MJ, Alvarez A, Esplugues JV. (2015). Efavirenz and the CNS: what we already know and questions that need to be answered. *J Antimicrobial Chemotherapy*. 70:2693–708.
- Auer M, Hausott B, Klimaschewski L. (2011). Rho GTPases as regulators of morphological neuroplasticity. *Annals of Anatomy*.193(4):259-66.
- Aukrust P, Haug C, Ueland T, Lien E, Müller F. et al. (1999). Decreased bone formative and enhanced resorptive markers in human immunodeficiency virus infection: indication of normalization of the bone-remodeling process during highly active antiretroviral therapy. *Journal of Clinical Endocrinology Metabolism*; 84:145-50.

- Ayanlaja, A. A., Xiong, Y., Gao, Y., Ji, G., Tang, C., Abdikani Abdullah, Z., & Gao, D. (2017). Distinct Features of Doublecortin as a Marker of Neuronal Migration and Its Implications in Cancer Cell Mobility. *Frontiers in molecular neuroscience*, 10: 199.
- Baroncelli S, Tamburrini E, Ravizza M, Dalzero S, Tibaldi C, Ferrazzi E, Anzidei G, Ficon M, Alberico S, Martinelli P, Placido G, Guaraldi G, Pinnetti C, Florida M. (2009). Italian Group on Surveillance on Antiretroviral Treatment in Pregnancy. Antiretroviral treatment in pregnancy: a six-year perspective on recent trends in prescription patterns, viral load suppression, and pregnancy outcomes. *AIDS Patient Care STDS*. 23:513-20.
- Barrell William B., Griffin John N., Harvey Jessica-Lily, HipSci Consortium, Danovi Davide, Beales Philip, Grigoriadis Agamemnon E., Liu Karen J., Durbin Richard, Gaffney Daniel, Agu Chukwuma, Alderton Alex (2019). Induction of Neural Crest Stem Cells from Bardet–Biedl Syndrome Patient Derived hiPSCs. 12: 39
- Battino D, Tomson T, Bonizzoni E, Craig J, Lindhout D, Sabers A, Perucca E, Vajda F; EURAP Study Group. (2013). Seizure control and treatment changes in pregnancy: observations from the EURAP epilepsy pregnancy registry. *Epilepsia*. 54(9):1621-7.
- Bertrand, L., & Toborek, M. (2015). Dysregulation of endoplasmic reticulum stress and autophagic responses by the antiretroviral drug efavirenz. *Molecular Pharmacology*, 88: 304-315.
- Bhatt NB, Barau C, Amin A, Baudin E, Meggi B, Silva C, Furlan V, Grinsztejn B, Barrail-Tran A, Bonnet M, Taburet AM; ANRS 12146-CARINEMO Study Group. (2014). Pharmacokinetics of rifampin and isoniazid in tuberculosis-HIV-coinfected patients receiving nevirapine- or efavirenz-based antiretroviral treatment. *Antimicrobial Agents Chemotherapy*. 58(6):3182-90.

- Biro M, Romeo Y, Kroschwald S, Bovellan M, Boden A, Tcherkezian J, Roux P, Charras G, Paluch E K. (2013). Cell cortex composition and homeostasis resolved by integrating proteomics and quantitative imaging. *Cytoskeleton*. Hoboken 2013; 70: 741-754.
- Brittain, K., Mellins, C. A., Phillips, T., Zerbe, A., Abrams, E. J., Myer, L., & Remien, R. H. (2017). Social Support, Stigma and Antenatal Depression Among HIV-Infected Pregnant Women in South Africa. *AIDS and behavior*, 21(1), 274–282.
- Brogly, S., Abzug, M., Heather Watts, D., Cunningham, C., Williams, P., Oleske, J., Conway, D., Rhoda S. Sperling, Hans Spiegel, Russell B. Van Dyke, R. (2010). Birth defects among children born to HIV-infected women: Pediatric AIDS Clinical Trials Protocols 219 and 219C. *Journal of the Pediatric Infectious Diseases Society* 29: 721–727.
- Brown D. (2017). The Discovery of Water Channels (Aquaporins). *Annals of Nutrition and Metabolism*. 1:37-42.
- Brown T, Chen Y, Judith S, Currier M, Ribaud H, Rothenberg J. et al. (2013). Body Composition, Soluble Markers of Inflammation, and Bone Mineral Density in Antiretroviral Therapy-Naïve HIV-1 Infected Individuals. *J Acquired Immune Deficiency Syndrome*; 63: 323–330.
- Brüning, A., Jückstock, J., Kost, B., Tsikouras, P., Weissenbacher, T., Mahner, S., & Mylonas, I. (2017). Induction of DNA damage and apoptosis in human leukemia cells by efavirenz. *Oncology Reports*, 37, 617-621.
- Burrige K, Guilluy C. (2016). Focal adhesions, stress fibers and mechanical tension. *Exp Cell Research*. 343(1):14-20. doi: 10.1016/j.yexcr.2015.10.029.

- Bush JO, Jiang R. (2012). Palatogenesis: morphogenetic and molecular mechanisms of secondary palate development. *Development*. 139(2):231-43.
- Calogero AM, Mazzetti S, Pezzoli G, Cappelletti G. (2019). Neuronal microtubules and proteins linked to Parkinson's disease: a relevant interaction? *Journal of biological chemistry*. 400(9):1099-1112.
- Carrol, A., Brew, B. (2017). HIV-associated neurocognitive disorders: recent advances in pathogenesis, biomarkers, and treatment. *F1000Research*. 6:312.
- Cartsos VM, Palaska PK, Zavras AI. (2012). Antiretroviral prophylaxis and the risk of cleft lip and palate: preliminary signal detection in the food and drug administration's adverse events reporting system database. *Cleft Palate Craniofacial Journal*. 49: 118– 121.
- Castañeyra-Ruiz, L., González-Marrero, I., González-Toledo, J. M., Castañeyra-Ruiz, A., de Paz-Carmona, H., Castañeyra-Perdomo, A., & Carmona-Calero, E. M. (2013). Aquaporin-4 expression in the cerebrospinal fluid in congenital human hydrocephalus. *Fluids and barriers of the CNS*. 10: 18.
- Chabaud M, Heuzé ML, Bretou M, Vargas P, Maiuri P, Solanes P, Maurin M, Terriac E, Le Berre M, Lankar D. et al. (2015). Cell migration and antigen capture are antagonistic processes coupled by myosin II in dendritic cells. *Nature Communications*; 6, 7526.
- Chai Y, Jiang X, Ito Y, Bringas Jr P, Han J, Rowitch D. (2000). Fate of the mammalian cranial neural crest during tooth and mandibular morphogenesis. *Development*; 127:1671-9.
- Chandran R, Feller L., Lemmer J, Khammissa R. (2016). HIV-Associated Oral Mucosal Melanin Hyperpigmentation: A Clinical Study in a South African Population Sample. *AIDS Research and Treatment*; doi: 10.1155/2016/8389214

- Cheerathodi, M., Avci, N. G., Guerrero, P. A., Tang, L. K., Popp, J., Morales, J. E., Chen, Z., Carnero, A., Lang, F. F., Ballif, B. A., Rivera, G. M., & McCarty, J. H. (2016). The Cytoskeletal Adapter Protein Spinophilin Regulates Invadopodia Dynamics and Tumor Cell Invasion in Glioblastoma. *Molecular cancer research: MCR*, 14(12), 1277–1287.
- Chersich, M. F., Urban, M. F., Venter, F. W., Wessels, T., Krause, A., Gray, G. E., Luchters, S., & Viljoen, D. L. (2006). Efavirenz use during pregnancy and for women of child-bearing potential. *AIDS research and therapy*, 3, 11.
- Christiansen, E.G. Coles, D.G. Wilkinson (2000). Molecular control of neural crest formation, migration and differentiation. *Current. Opinion in Cell Biology.*, 12: 719-724
- Chu, H., Huang, C., Ding, H., Dong, J., Gao, Z., Yang, X., Tang, Y., & Dong, Q. (2016). Aquaporin-4 and Cerebrovascular Diseases. *International journal of molecular sciences*, 17(8), 1249.
- Chugh, P, Paluch E. (2018). The actin cortex at a glance. *Journal of Cell Science* 2018;131: jcs186254
- Clay, P. G., Taylor, T. A., Glaros, A. G., McRae, M., Williams, C., McCandless, D., & Oelklaus, M. (2008). "One pill, once daily": what clinicians need to know about Atriplatrade mark. *Therapeutics and clinical risk management*, 4(2): 291–302.
- Clayton NS, Ridley AJ. (2020). Targeting Rho GTPase Signaling Networks in Cancer. *Frontiers in Cell Developmental Biology*. 3; 8:222.
- Conesa-Buendía FM, Llamas-Granda P, Larrañaga-Vera A, Wilder T, Largo R, Herrero-Beaumont G, Cronstein B, Mediero A. (2019). Tenofovir Causes Bone Loss via Decreased Bone Formation and Increased Bone Resorption, Which Can Be Counteracted by Dipyridamole in Mice. *Journal of Bone Mineral Research*. 34(5):923-938.

- Copp, A. (2005). Neurulation in the cranial region – normal and abnormal. *Journal of Anatomy*. 207: 623-635.
- Cordero D, Brugmann, S, Chu Y, Bajpai R, Jame M, Helms J. (2011). Cranial neural crest cells on the move: their roles in craniofacial development. *American Journal of Medical Genetics A*; 155A:270-9.
- Cournil A et al. Dolutegravir- versus an efavirenz 400mg-based regimen for the initial treatment of HIV-infected patients in Cameroon: 48-week efficacy results of the NAMSAL ANRS 12313 trial. International Congress on Drug Therapy in HIV Infection (HIV Glasgow), Glasgow, UK, abstract 0342.
- Cramer, L., Mitchison, T. (1995). Myosin is involved in postmitotic cell spreading. *Journal of Cell Biology*. 131(1):179-89.
- Crane JF, Trainor PA. Neural crest stem and progenitor cells. *Annual Review in Cell Developmental Biology*. 2006; 22:267-86.
- Crane JF, Trainor PA. Neural crest stem and progenitor cells. *Annual Review in Cell Developmental Biology* 2006; 22:267-86. doi: 10.1146/annurev.cellbio.22.010305.103814.
- Dakkak, W., Oliver, T. (2019). *Ventricular Septal Defect*. STAT Pearls Publishing, Treasure Island (FL).
- Dalakas MC. (2001). Peripheral neuropathy and antiretroviral drugs. *Journal of the Peripheral Nervous System*; 6(1):14–20.
- Das R, Bhattacharjee S, Patel AA, Harris JM, Bhattacharya S, Letcher JM, Clark SG, Nanda S (2017). Dendritic cytoskeletal architecture is modulated by 795 combinatorial transcriptional regulation in *Drosophila melanogaster*. *Genetics* 207:1401–1421.

- de Jong, J., Garne, E., de Jong-van den Berg, L.T.W. et al (2016). The Risk of Specific Congenital Anomalies in Relation to Newer Antiepileptic Drugs: A Literature Review. *Drugs - Real World Outcomes* 3, 131–143.
- De Santis M, Carducci B, De Santis L, Cavaliere AF, Straface G. (2002). Periconceptual exposure to efavirenz and neural tube defects. *Archives of Internal Medicine*. 2002; 162:355.
- De Sousa, A. D., Devare, S., & Ghanshani, J. (2009). Psychological issues in cleft lip and cleft palate. *Journal of Indian Association of Pediatric Surgeons*, 14(2), 55–58.
- Del Bigio MR, Di Curzio DL. (2016). Nonsurgical therapy for hydrocephalus: a comprehensive and critical review. *Fluids Barriers CNS*. 5; 13:3.
- Delicio, A. M., Lajos, G. J., Amaral, E., Lopes, F., Cavichioli, F., Myoshi, I., & Milanez, H. (2018). Adverse effects of antiretroviral therapy in pregnant women infected with HIV in Brazil from 2000 to 2015: a cohort study. *BMC infectious diseases*, 18(1), 485.
- Deng J, Zhao F, Yu X, Zhao Y, Li D, Shi H, et al. (2014). Expression of Aquaporin 4 and Breakdown of the Blood-Brain Barrier after Hypoglycemia-Induced Brain Edema in Rats. *PLoS ONE* 9(9): e107022.
- Diaz, H.W. Murcia, S.M. Cepeda. (2010). Cytochrome P450 enzymes involved in the metabolism of aflatoxin B1 in chickens and quail. *Poultry Science*. 89 (11): 2461-2469,
- Diego Franco, Sigolène M. Meilhac, Vincent M. Christoffels, Andreas Kispert, Margaret Buckingham, Robert G. Kelly (2006). Left and right ventricular contributions to the formation of the interventricular septum in the mouse heart. *Developmental Biology*. 294 (2): 366-375

- Dietrich P, Dragatsis I. (2016). Familial Dysautonomia: Mechanisms and Models. *Genetics Molecular Biology* 2016; 39:497-514.
- Dioli, C., Patrício, P., Sousa, N. et al. (2019). Chronic stress triggers divergent dendritic alterations in immature neurons of the adult hippocampus, depending on their ultimate terminal fields. *Translational Psychiatry* 9: 143.
- Duan J., Lai J, Wang D, Zhou W. et al. (2019). Topiramate precipitating a manic episode in a bipolar patient comorbid with binge eating disorder. *Medicine (Baltimore)* 2019; 98(17): e15287.
- Dugdale CM, Ciaranello AL, Bekker LG, Stern ME, Myer L, Wood R, Sax PE, Abrams EJ, Freedberg KA, Walensky RP. (2019). Risks and Benefits of Dolutegravir- and Efavirenz-Based Strategies for South African Women With HIV of Child-Bearing Potential: A Modeling Study. *Annals of Internal Medicine.* 7;170(9):614-625.
- Eggleton JS, Nagalli S. Highly Active Antiretroviral Therapy (HAART) [2020]. In: StatPearls [Internet]. Treasure Island
- Emmert, A. S., Iwasawa, E., Shula, C., Schultz, P., Lindquist, D., Dunn, R. S., Fugate, E. M., Hu, Y. C., Mangano, F. T., & Goto, J. (2019). Impaired neural differentiation and glymphatic CSF flow in the *Ccdc39* rat model of neonatal hydrocephalus: genetic interaction with *L1cam*. *Disease models & mechanisms*, 12(11), dmm040972.
- Emoto K. (2011). Dendrite remodeling in development and disease. *Development, growth and differentiation*; 53: 277-286
- Engidaye, G., Melku, M., & Enawgaw, B. (2019). Diamond Blackfan Anemia: Genetics, Pathogenesis, Diagnosis and Treatment. *EJIFCC*, 30: 67–81.

- Etchevers H, Dupin E, Le Douarin N. (2019). The diverse neural crest: from embryology to human pathology. *Development*; 146: 169821.
- Eyal S, Yagen B, Sobol E, Altschuler Y, Shmuel M, Bialer M. (2004). The activity of antiepileptic drugs as histone deacetylase inhibitors. *Epilepsia*. 45(7):737-44.
- Farooqui, R., Hoor, T., Karim, N., Muneer, M. (2018). Potential Drug-Drug Interactions among Patients prescriptions collected from Medicine Out-patient Setting. *PAKISTAN JOURNAL OF MEDICAL SCIENCES*34(1):144-148.
- Fletcher JM, Dennis M, Northrup H, Yeates KO, Ris MD, Taylor HG (2000). Pediatric neuropsychology: Research, theory and practice. *Hydrocephalus* 25–46.
- Flynn KC. (2013). The cytoskeleton and neurite initiation. *Bioarchitecture*. 3(4):86-109.
- Ford N, Mofenson L, Shubber Z, Calmy A, Andrieux-Meyer I, Vitoria M, Shaffer N, Renaud F. (2014). Safety of efavirenz in the first trimester of pregnancy: an updated systematic review and meta-analysis. *AIDS*. 2: S123-31.
- Ford, N; Migone, C; Calmy, A; Kerschberger, B; Kanters, S; Nsanzimana, S. et al (2018). Benefits and risks of rapid initiation of antiretroviral therapy. *AIDS*. 32(1):17-23.
- Frank C. L., Tsai L. H. (2009). Alternative functions of core cell cycle regulators in neuronal migration, neuronal maturation, and synaptic plasticity. *Neuron* 62 312–326.
- Ghosh, A. K., Rao, K. V., Nyalapatla, P. R., Osswald, H. L., Martyr, C. D., Aoki, M., Hayashi, H., Agniswamy, J., Wang, Y. F., Bulut, H., Das, D., Weber, I. T., & Mitsuya, H. (2017). Design and Development of Highly Potent HIV-1 Protease Inhibitors with a Crown-Like Oxotricyclic Core as the P2-Ligand to Combat Multidrug-Resistant HIV Variants. *Journal of medicinal chemistry*, 60(10), 4267–4278.

- Gibb, D. M., Kizito, H., Russell, E. C., Chidziva, E., Zalwango, E., Nalumenya, R., Spyer, M., Tumukunde, D., Nathoo, K., Munderi, P., Kyomugisha, H., Hakim, J., Grosskurth, H., Gilks, C. F., Walker, A. S., Musoke, P. (2012). Pregnancy and infant outcomes among HIV-infected women taking long-term ART with and without tenofovir in the DART trial. *PLoS medicine*, 9(5), e1001217.
- Gleeson, J.G., K.M. Allen, J.W. Fox, E.D. Lamperti, S. Berkovic, I. Scheffer, E.C. Cooper, W.B. Dobyns, S.R. Minnerath, M.E. Ross, and C.A. Walsh. (1998). doublecortin, a brain-specific gene mutated in human X-linked lissencephaly and double cortex syndrome, encodes a putative signaling protein. *Cell*. 92:63–72.
- Goodwin AF, Oberoi S, Landan M, Charles C, Groth J, Martinez A, Fairley C, Weiss LA, Tidyman WE, Klein OD, Rauen KA. (2013). Craniofacial and dental development in cardio-facio-cutaneous syndrome: the importance of Ras signaling homeostasis. *Clinical Genetics*. 83(6):539-44.
- Gordon-Weeks, P. (2000). *Neuronal Growth Cones (Developmental and Cell Biology Series)*. Cambridge: Cambridge University Press. doi:10.1017/CBO9780511529719
- Govek EE, Newey SE, Van Aelst L. (2005). The role of the Rho GTPases in neuronal development. *Genes and Development*.19(1):1-49.
- Graham, A., Jo Begbie Imelda McGonnell (2003). Significance of the cranial neural crest. 229:5-13
- Green, M; Seeger, J; Peterson, C; Bhattacharyya A. (2012). Utilization of Topiramate During Pregnancy and Risk of Birth Defects. *American headache society*. 52:1070-1084
- Gulick RM, Ribaud HJ, Shikuma CM, Lustgarten S, Squires KE, Meyer WA 3rd, Acosta EP, Schackman BR, Pilcher CD, Murphy RL, Maher WE, Witt MD, Reichman RC, Snyder

- S, Klingman KL, Kuritzkes DR; AIDS Clinical Trials Group Study A5095 Team. (2004). Triple-nucleoside regimens versus efavirenz-containing regimens for the initial treatment of HIV-1 infection. *The New England Journal of Medicine*. 350(18):1850-61.
- Guo, J., Mi, X., Zhan, R., Li, M., Wei, L., & Sun, J. (2018). Aquaporin 4 Silencing Aggravates Hydrocephalus Induced by Injection of Autologous Blood in Rats. *Medical science monitor: international medical journal of experimental and clinical research*, 24, 4204–4212.
- Hadianfard MJ, Ashraf A. (2012). Hip dysplasia associated with a hereditary sensorimotor polyneuropathy mimics a myopathic process. *Annals of Indian Academy of neurology*;15: 211-213
- Haendel, M., Bollinger, K., Baas, P. (1996). Cytoskeletal changes during neurogenesis in cultures of avian neural crest cells. *Journal of Neurocytology* 25, 289-301
- Hall A, Lalli G. (2010). Rho and Ras GTPases in axon growth, guidance, and branching. *Cold Spring Harbor perspectives in biology*.2 (2): a001818.
- Hamburger, V., Hamilton, H. (1951). A series of normal stages in the development of the chick embryo. *Journal of Morphology* 88: 49-92.
- Hehr U, Uyanik G, Aigner L, Couillard-Despres S, Winkler J. (2007). DCX-Related Disorders. In: Adam MP, Ardinger HH, Pagon RA, Wallace SE, Bean LJH, Stephens K, Amemiya A, editors. *GeneReviews®* [Internet]. Seattle (WA): University of Washington, Seattle.
- Hehr U, Uyanik G, Aigner L, et al. DCX-Related Disorders. (2019) In: Adam MP, Ardinger HH, Pagon RA, et al., editors. *Seattle: University of Washington, Seattle; 1993-2021.*

- Helms JA, Cordero D, Tapadia MD. (2005). New insights into craniofacial morphogenesis. *Development*. 132:851–861.
- Hernandez-Diaz S, Huybrechts KF, Desai RJ, Cohen JM, Mogun H, Pennell PB, Bateman BT, Patorno E. (2018). Topiramate use early in pregnancy and the risk of oral clefts: A pregnancy cohort study. *Neurology*. 23;90(4): e342-e351.
- Hileman O, Eckard A, McComsey G. (2015). Bone loss in HIV—a contemporary review. *Current Opinion in Endocrinol Diabetes and Obesity*; 22: 446–451.
- Holmes LB, Harvey EA, Coull BA, Huntington KB, Khoshbin S, Hayes AM, Ryan LM. (2001). The teratogenicity of anticonvulsant drugs. *The New England Journal of Medicine*. 12;344(15):1132-8.
- Hong, J., Zhang, H., Kawase-Koga, Y., & Sun, T. (2013). MicroRNA function is required for neurite outgrowth of mature neurons in the mouse postnatal cerebral cortex. *Frontiers in cellular neuroscience*, 7, 151.
- Hou L, Pavan WJ. (2008). Transcriptional and signaling regulation in neural crest stem cell-derived melanocyte development: do all roads lead to Mitf? *Cell Research*. 18(12):1163-76.
- Hsieh S. H., Ferraro G. B., Fournier A. E. (2006). Myelin-associated inhibitors regulate cofilin phosphorylation and neuronal inhibition through LIM kinase and Slingshot phosphatase. *Journal of Neuroscience*. 26: 1006–1015.
- Hu D, Helms JA. (1999). The role of sonic hedgehog in normal and abnormal craniofacial morphogenesis. *Development*. 126:4873–4884.

- Huang Yuan, Li Sheng-nan, Zhou Xiu-ya, Zhang Li-xin, Chen Gang-xian, Wang Ting-hua, Xia Qing-jie, Liang Nan, Zhang Xiao (2019). The Dual Role of AQP4 in Cytotoxic and Vasogenic Edema Following Spinal Cord Contusion and Its Possible Association with Energy Metabolism via COX5A. *Frontiers in Neuroscience*. 13: 584
- Hunt, S., Russell, A., Smithson, W., Parsons, L., Robertson, I., Waddell, R., et al. (2008). Topiramate in pregnancy. *Neurology*. 71(4), p. 272 – 276.
- Huret, JL. (2020). AQP1 (aquaporin 1 (Colton blood group)). *Atlas of Genetics and Cytogenetics in Oncology and Haematology*. DOI: 10.4267/2042/70645
- Hutson M., Kirby M. (2003). Neural crest and cardiovascular development: a 20-year perspective. *Birth Defects Research C Embryo Today*. 69(1):2-13.
- Isaacs AM, Riva-Cambrin J, Yavin D, Hockley A, Pringsheim TM, et al. (2019). Correction: Age-specific global epidemiology of hydrocephalus: Systematic review, meta-analysis and global birth surveillance. *PLOS ONE* 14(1): e0210851.
- Ito Y, Yeo J, Chytil A, Han J, Bringas P, Nakajima A. et al. (2003). Conditional inactivation of *Tgfb β 2* in cranial neural crest causes cleft palate and calvaria defects. *Development* 2003; 130: 5269-5280.
- Matthias Starck, J. Matthias Starck R.E. Ricklefs (1998). Avian growth and development. *Evolution in the altricial precocial spectrum*
- James A, Oluwatosin B, Njideka G, et al. (2014). Cleft palate in HIV-exposed newborns of mothers on HIGHLY ACTIVE ANTIRETROVIRAL THERAPY. *Oral Surgery*; 7:102-106.
- Jessica K. Lyda, Zhang L. Tan, Abira Rajah, Asheesh Momi, Laurent Mackay, Claire M. Brown, Anmar Khadra. (2019). Rac activation is key to cell motility and directionality: An
-

experimental and modelling investigation, Computational and Structural Biotechnology Journal. 17:1436-1452,

- Ji JD, Park-Min KH, Shen Z, Fajardo R, Goldring S, McHugh KP, Ivashkiv LB (2009). Inhibition of RANK expression and osteoclastogenesis by TLRs and IFN-gamma in human osteoclast precursors. *Journal of Immunology*; 183:7223-33.
- Jiang R, Bush JO, Lidral AC. (2006). Development of the upper lip: morphogenetic and molecular mechanisms. 235:1152–1166.
- Joao EC, Calvet GA, Krauss MR, Freimanis Hance L, Ortiz J, Ivalo SA, Pierre R, Reyes M, Heather Watts D, Read JS. (2010). Maternal antiretroviral use during pregnancy and infant congenital anomalies: the NISDI perinatal study. *J Acquired Immune Deficiency Syndrome*; 53:176-85.
- Julg B, Bogner JR. (2008). Atriplatrade mark - HIV therapy in one pill. *Therapeutic Clinical Risk Management*. 4(3):573-7. Horberg, M. A., & Klein, D. B. (2010). An update on the use of Atripla in the treatment of HIV in the United States. *HIV/AIDS* 2: 135–140.
- Jungmann, E., Mercey, D., DeRuiter, A., Edwards, S., Donoghue, S., Tamsin Booth, T. et al; (2001). Is first trimester exposure to the combination of antiretroviral therapy and folate antagonists a risk factor for congenital abnormalities? *Sexually Transmitted Infections* 2001; 77:441-443.
- Kahle KT, Kulkarni AV, Limbrick DD Jr., Warf BC (2016). Hydrocephalus in children. *Lancet*. 2016;387: 788–99.
- Karunamuni G, Gu S, Doughman Y, Peterson LM, Mai K, McHale Q., et al. (2014). Ethanol exposure alters early cardiac function in the looping heart: a mechanism for congenital heart defects? *American Journal of Physiology and Heart Circulation Physiology* 2014; 306, H414–H421.

- Kato M. (2015). Genotype-phenotype correlation in neuronal migration disorders and cortical dysplasias. *Frontiers in Neurosciences*. 9:181.
- Kawakami, K., G. Abe, T. Asada, K. Asakawa, R. Fukuda, A. Ito, P. Lal, N. Mouri, A. Muto, M.L. Suster, et al. (2010). zTrap: zebrafish gene trap and enhancer trap database. *BMC Developmental Biology*, 10: 105
- Keays DA, Tian G, Poirier K, Huang GJ, Siebold C, Cleak J, Oliver PL, Fray M, Harvey RJ, Molnár Z, Piñon MC, Dear N, Valdar W, Brown SD, Davies KE, Rawlins JN, Cowan NJ, Nolan P, Chelly J, Flint J. (2007). Mutations in alpha-tubulin cause abnormal neuronal migration in mice and lissencephaly in humans. *Cell*. 128(1):45-57.
- Keyte, A., & Hutson, M. R. (2012). The neural crest in cardiac congenital anomalies. *Differentiation; research in biological diversity*, 84(1), 25–40.
- Kim HK, Chin BS, Shin HS. (2015). Clinical features of seizures in patients with human immunodeficiency virus infection. *Journal of Korean medical science*. 30: 694-699.
- Kintu, K., Thokozile R Malaba, Jesca Nakibuka, Christiana Papamichael, Angela Colbers, Kelly Byrne, Kay Seden, Eva Maria Hodel, Tao Chen (2020). Dolutegravir versus efavirenz in women starting HIV therapy in late pregnancy (DOLPHIN-2): an open-label, randomised controlled trial. *The Lancet HIV*. 7: e332-e339,
- Kirby M, Gale T, Stewart D. (1983). Neural crest cells contribute to aorticopulmonary septation. *Science*; 220:1059–1061.
- Kitchen P., Salman M.M., Halsey A.M., Clarke-Bland C., MacDonald J.A., Ishida H., Vogel H.J., Bill R.M. (2020). Targeting Aquaporin-4 Subcellular Localization to Treat Central Nervous System Edema. *Cell*, 181: 784-799.

- Knapp KM, Brogly SB, Muenz DG, et al. (2012). Prevalence of congenital anomalies in infants with in utero exposure to antiretrovirals. *The Pediatric Infectious Disease Journal*. 31(2):164-170.
- Knight R, Schilling T. (2006). Cranial Neural Crest and Development of the Head Skeleton. *Advances in Experimental Medicine and Biology*; 589:120-33.
- Krause M, Gautreau A. (2014). Steering cell migration: lamellipodium dynamics and the regulation of directional persistence. *Nature Reviews Molecular Cell Biology*. 15(9):577-90.
- Kruse E, Uehlein N, Kaldenhoff R. (2006). The aquaporins. *Genome Biol*. 7(2):206. doi: 10.1186/gb-2006-7-2-206.
- Kulesa P, Bailey M, Kasemeier-Kulesa C, McLennana R. Cranial neural crest migration: New rules for an old road. *Developmental Biology* 2010; 344: 543-554.
- Kumar P, Nagarajan A, Uchil PD. (2018). Analysis of Cell Viability by the MTT Assay. *Cold Spring Harb Protocol*. 2018(6).
- Lai, Y. H., Ding, Y. J., Moses, D., & Chen, Y. H. (2017). Teratogenic Effects of Topiramate in a Zebrafish Model. *International journal of molecular sciences*, 18(8), 1721.
- Le Douarin, N. (2004). The avian embryo as a model to study the development of the neural crest: a long and still ongoing story. *Mechanisms of Development*. 129: 1089-1102.
- Lee J. (2013). The Actin Cytoskeleton and the Regulation of Cell Migration. *Colloquium Series on Building Blocks of the cell. Cell Structure and Function [Internet]* 2013; 1:1-71.
- Li et al., (2019). In Vivo Quantitative Imaging Provides Insights into Trunk Neural Crest Migration. *Cell Reports* 26: 1489–1500
- Li Y, Seto E. (2016). HDACs and HDAC Inhibitors in Cancer Development and Therapy. *Cold Spring Harbor perspectives in biology*. 6(10): a026831.

- Li, G., Simmler, C., Chen, L., Nikolic, D., Chen, S. N., Pauli, G. F., & van Breemen, R. B. (2017). Cytochrome P450 inhibition by three licorice species and fourteen licorice constituents. *European journal of pharmaceutical sciences: official journal of the European Federation for Pharmaceutical Sciences*, 109: 182–190.
- Lumsden A, Sprawson N, Graham A. (1991). Segmental origin and migration of neural crest cells in the hindbrain region of the chick embryo. *Development*.113(4):1281-91.
- Mader, S., & Brimberg, L. (2019). Aquaporin-4 Water Channel in the Brain and Its Implication for Health and Disease. *Cells*, 8(2), 90. <https://doi.org/>
- Makoto Usami, M., Katsuyoshi Mitsunaga, K., Tomohiko Irie, T., Atsuko Miyajima, A., and Osamu Doi, O. (2014). Simple in vitro migration assay for neural crest cells and the opposite effects of all-trans-retinoic acid on cephalic- and trunk-derived cells. *Congenital Anomalies* 2014; 54, 184–188.
- Mao X, Enno TL, Del Bigio MR. (2006). Aquaporin 4 changes in rat brain with severe hydrocephalus. *European Journal of Neuroscience*. 23:2929–2936.
- Margiotta A, Bucci C. (2019). Coordination between Rac1 and Rab Proteins: Functional Implications in Health and Disease. *Cells*. 8(5):396.
- Margulis, A., Mitchell, A., Gilboa, S., Werler, M., Mittleman, M., Glynn, R. (2012). Use of topiramate in pregnancy and risk of oral clefts. *American Journal of Obstetrics and Gynecology*, [online] volume 207(5): 405.e1 – 405.e7.
- Martinez de Tejada B, Gayet-Ageron A, Winterfeld U, Thorne C, Favarato G. (2019). European Pregnancy and Paediatric HIV Cohort Collaboration Study Group. Birth Defects After Exposure to Efavirenz-Based Antiretroviral Therapy at Conception/First Trimester of

Pregnancy: A Multicohort Analysis. *Journal of Acquired Immune Deficiency Syndrome*. 80(3):316-324. Erratum in: *J Acquir Immune Defic Syndr*. 2020 Feb 1; 83(2): e15.

- Masho, S., Wang, C., Nixon, D., (2007). Review of tenofovir-emtricitabine. *Therapeutic Clinical Risk Management*. 3(6): 1097–1104
- McCormack, S. A., & Best, B. M. (2014). Protecting the fetus against HIV infection: a systematic review of placental transfer of antiretrovirals. *Clinical pharmacokinetics*, 53(11), 989–1004.
- Meador K.J., Pennell P.B., Harden C.L., Gordon J.C., Tomson T., Kaplan P.W., et al. (2008) Pregnancy registries in epilepsy: a consensus statement on health outcomes. *Neurology* 71: 1109–1117
- Mehta U, Van Schalkwyk C, Naidoo P, Ramkisson A, Mhlongo O et al (2019). Birth outcomes following antiretroviral exposure during pregnancy: Initial results from a pregnancy exposure registry in South Africa. *Southern African Journal of HIV Medicine*: 1608-9693.
- Merot Y., Retaux S., Heng J. I. (2009). Molecular mechanisms of projection neuron production and maturation in the developing cerebral cortex. *Seminar. Cell and Developmental. Biology*. 20: 726–734
- Miller, K. E., & Suter, D. M. (2018). An Integrated Cytoskeletal Model of Neurite Outgrowth. *Frontiers in cellular neuroscience*, 12: 447.
- Mishina Y, Snider TN. (2014). Neural crest cell signaling pathways critical to cranial bone development and pathology. *Experimental cell research*; 325: 138-147.
- Mishra, S., Sabhlok, S., Panda, P. K., & Khatri, I. (2015). Management of Midline Facial Clefts. *Journal of maxillofacial and oral surgery*, 14(4), 883–890.

- Molgaard-Nelsen, D., & Hviid, A. (2011). Newer-Generation Antiepileptic Drugs and the Risk of Major Birth Defects. *JAMA*. 305(19), p. 1996 – 2002.
- Moran C, Weitzmann N, Ofotokun I. (2017). Bone Loss in HIV Infection. *Current Treatment Options in Infectious Diseases* 2017; 9:52–67.
- Moret F., Renaudot C., Bozon M., Castellani V. (2007). Semaphorin and neuropilin co-expression in motoneurons sets axon sensitivity to environmental semaphorin sources during motor axon pathfinding. *Development* 134, 4491–4501
- Moslehi, M., Ng, D.C.H. & Bogoyevitch, M.A. (2017). Dynamic microtubule association of Doublecortin X (DCX) is regulated by its C-terminus. *Scientific Reports* 7, 5245.
- Murata, T., Ohnishi, H., Okazawa, H., Murata, Y., Kusakari, S., Hayashi, Y., Miyashita, M., Itoh, H., Oldenborg, P.A., Furuya, N., et al. (2006). CD47 promotes neuronal development through Src- and FRG/Vav2-mediated activation of Rac and Cdc42. *Journal of Neuroscience*. 26, 12397–12407.
- Mutlib AE, Chen H, Nemeth GA, Markwalder JA, Seitz SP, Gan LS, Christ DD. (1999). Identification and characterization of efavirenz metabolites by liquid chromatography/mass spectrometry and high field NMR: species differences in the metabolism of efavirenz. *Drug Drug Metabolism and Disposition*. 1999 Nov; 27(11):1319-1333.
- Nagarajan R, Savitha VH, Subramaniyan B. (2009). Communication disorders in individuals with cleft lip and palate: An overview. *Indian Journal of Plastic Surgery*. S137-43. doi: 10.4103/0970-0358.57199.

- Nallani, S., Glauser, T., Hariparsad, N., Setchell, K., Buckley, D., Buckley, A., Desai, P. (2003). Dose-dependent Induction of Cytochrome P450 (CYP) 3A4 and Activation of Pregnane X Receptor by Topiramate. *Epilepsia*. 44: 1521-1528.
- Negishi M. and Katoh, H. (2002). Rho family GTPases as key regulators for neuronal network formation. *Journal of Biochemistry*. (Tokyo) 132: 157–166.
- Nico B, Frigeri A, Nicchia GP, et al. (2001). Role of aquaporin-4 water channel in the development and integrity of the blood-brain barrier. *Journal of Cell Science*. 114:1297–307.
- Nico, Beatrice & Ribatti, Domenico & Frigeri, Antonio & Nicchia, Grazia & Corsi, Patrizia & Svelto, Maria & Roncali, Luisa. (2002). Aquaporin-4 expression during development of the cerebellum. *Cerebellum* (London, England). 1: 207-212.
- Nie X, Luukko K, Kettunen P. (2006). BMP signalling in craniofacial development. *Int. Journal of Developmental Biology*; 50: 511-52
- Ornoy, A., Zvi, N., Arnon, J., Wajnberg, R., Shechtman, S., & Diav-Citrin, O., (2008). The outcome of pregnancy following topiramate treatment: A study on 52 pregnancies. *Reproductive Toxicology*, volume 25(3): 388 – 389.
- Padhi A, Ranjeva SL, Donaldson SC, Warf BC, Mugamba J, Johnson D, Opio Z, Jayarao B, Kapur V, Poss M, Schiff SJ. (2011). Association of bacteria with hydrocephalus in Ugandan infants. *Journal of neurosurgery. Pediatrics*. 7(1):73-87.
- Pallocca G, Nyffeler J, Dolde X, Grinberg J, Gstraunthaler G, Waldmann T, Rahnenführer J, Sachinidis A, Leist M. (2017). Impairment of human neural crest cell migration by prolonged exposure to interferon-beta. *Archives of Toxicology* 2017; 91: 3385–3402.

- Pan, Y. H., Wu, N., & Yuan, X. B. (2019). Toward a Better Understanding of Neuronal Migration Deficits in Autism Spectrum Disorders. *Frontiers in cell and developmental biology*. 7: 205.
- Papadopoulos, M. C., and Verkman, A. S. (2005). Aquaporin-4 gene disruption in mice reduces brain swelling and mortality in pneumococcal meningitis. *Journal of Biological Chemistry*. 280: 13906–13912.
- Park JH, Lee NK, Lee SY (2017). Current Understanding of RANK Signaling in Osteoclast Differentiation and Maturation. *Molecule and cells*; 40: 706–713.
- Pau AK, George JM. (2014) Antiretroviral therapy: current drugs. *Infectious Disease Clinics of North America*. 28(3):371-402.
- Pechnick R. N., Zonis S., Wawrowsky K., Pourmorady J., Chesnokova V. (2008). p21Cip1 restricts neuronal proliferation in the subgranular zone of the dentate gyrus of the hippocampus. *Proceedings of the National Academy of Sciences of the United States of America* 105, 1358–1363.
- Phiri K, Hernandez-Diaz S, Dugan KB, et al. (2020). First trimester exposure to antiretroviral therapy and risk of birth defects. *Journal of the Pediatric Infectious Diseases Society*. 2014; 33(7):741-746.
- Phiri, K., Sonia Hernandez-Diaz, S., Dugan, K., Williams, P., Dudley, J. et al (2014). First Trimester Exposure to Antiretroviral Therapy and Risk of Birth Defects. *Journal of the Pediatric Infectious Diseases Society*. 33(7): 741–746.
- Pierpont ME, Magoulas PL, Adi S, Kavamura MI, Neri G, Noonan J, Pierpont EI, Reinker K, Roberts AE, Shankar S, Sullivan J, Wolford M, Conger B, Santa Cruz M, Rauen KA.

- (2014). Cardio-facio-cutaneous syndrome: clinical features, diagnosis, and management guidelines. *Pediatrics*. 134(4): e1149-62.
- Pramparo T, Youn YH, Hirotsume S, Wynshaw-Boris A. (2010). Novel embryonic neuronal migration and neurogenesis defects in *Dcx* mutant mice are exacerbated by *Lis1* reduction. *Journal of Neuroscience*. 30:3002–3012.
- Prieto, L, González- Tomé, M., Muñoz, E., Fernández-Ibieta, M., Soto, B., Ana Álvarez, Navarro, M., Roa, M., Beceiro, J., Isabel de José, M., Iciar Olabarrieta, Lora, D., José Tomás Ramos and the Madrid Cohort of HIV-Infected Mother-Infant Pairs. (2014). Birth defects in a cohort of infants born to HIV-infected women in Spain, 2000-2009. *BMC Infectious Diseases*.14:700.
- Privitera, F., Monte, I. P., Indelicato, A., & Tamburino, C. (2017). A Membranous Septal Aneurysm Causing Right Ventricular Outflow Tract Obstruction in an Adult. *Journal of cardiovascular echography*, 27(4), 145–148.
- Radhakrishna U, Albayrak S, Zafra R, Baraa A, Vishweswaraiah S, Veerappa AM, et al. (2019). Placental epigenetics for evaluation of fetal congenital heart defects: Ventricular Septal Defect (VSD). *PLoS ONE* 14(3): e0200229.
- Radisky DC, Levy DD, Littlepage LE, Liu H, Nelson CM, Fata JE, Leake D, Godden EL, Albertson DG, Nieto MA, Werb Z and Bissell MJ. (2005). *Rac1b* and reactive oxygen species mediate MMP-3-induced EMT and genomic instability. *Nature*, 436, 123–127.
- Rakhmanina NY, van den Anker JN. (2010). Efavirenz in the therapy of HIV infection. *Expert Opinion in Drug Metabolism and Toxicology*.6(1):95-103.

- Reijntjes S, Gale E, Maden M. (2004). Generating gradients of retinoic acid in the chick embryo: Cyp26C1 expression and a comparative analysis of the Cyp26 enzymes. *Developmental Dynamics*. 2004; 230:509–17.
- Riddler SA, Haubrich R, DiRienzo AG, Peeples L, Powderly WG, Klingman KL, Garren KW, George T, Rooney JF, Brizz B, Lalloo UG, Murphy RL, Swindells S, Havlir D, Mellors JW; AIDS Clinical Trials Group Study A5142 Team. (2008). Class-sparing regimens for initial treatment of HIV-1 infection. *The New England Journal of Medicine*. 358(20):2095-106.
- Roh M, Eliades P, Gupta S, Tsao H. (2015). Genetics of melanocytic nevi. *Pigment cell and melanoma*; 28:661-672.
- Russell, I., Randall, R., Zimmerman, D., & Govender, D. (2019). Outbreak of avian botulism and its effect on waterbirds in the Wilderness Lakes, South Africa. *Koedoe*, 61(1):1-13
- Sainath R., Gallo G. (2015). Cytoskeletal and signaling mechanisms of neurite formation. *Cell Tissue Research*. 359: 267–278.
- Saitoh A, Hull AD, Franklin P, Spector SA. (2005). Myelomeningocele in an infant with intrauterine exposure to efavirenz. *Journal of Perinatology*. 25:555–556.
- Sakai T, Larsen M, Yamada KM. (2003). Fibronectin requirement in branching morphogenesis. *Nature*. 423(6942):876-81.
- Sarnat HB, Flores-Sarnat L. (2005). Embryology of the neural crest: its inductive role in the neurocutaneous syndromes. *Journal of Child Neurology*. 20(8):637-43.

- Sarnat HB, Flores-Sarnat L. (2013) Genetics of neural crest and neurocutaneous syndromes. *Handbook of Clinical Neurology*. 111:309-14.
- Seki T. (2020). Understanding the Real State of Human Adult Hippocampal Neurogenesis from Studies of Rodents and Non-Human Primates. *Frontiers in neuroscience*, 14, 839.
- Shetty, V., Chowta, M., Chowta, N., Shenoy, A., Kamath, A., Kamath, P. (2018). Evaluation of Potential Drug-Drug Interactions with Medications Prescribed to Geriatric Patients in a Tertiary Care Hospital. *Journal of Aging Research*. DOI: 10.1155/2018/5728957
- Sibiude J, Mandelbrot L, Blanche S, Le Chenadec J, Boullag-Bonnet N, Faye A, Dollfus C, Tubiana R, Bonnet D, Lelong N, Khoshnood B, Warszawski J. (2014). Association between prenatal exposure to antiretroviral therapy and birth defects: an analysis of the French perinatal cohort study. *PLoS Med*. 29;11: e1001635.
- Siddiqi O, Birbeck GL. (2013). Safe Treatment of Seizures in the Setting of HIV/AIDS. *Current Treatment Options in Neurology*. 15(4):529-43.
- Siddiqi, O., Elafros, C.M., Bositis, I.J., Koranik, W.H., Theodore, J.F. Okulicz, J. (2017). New-onset seizure in HIV-infected adult Zambians: a search for causes and consequences. 88: 477-482.
- Smarius B, Loozen C, Manten W, Bekker M, Pistorius L, Breugem C. (2017). Accurate diagnosis of prenatal cleft lip/palate by understanding the embryology. *World Journal of Methodology*. 7(3):93-100.
- Smith A. J., Jin B., Verkman A. S. (2015). Muddying the water in brain edema? *Trends in Neuroscience*. 20 1–2.

- Smith, S. M., Flentke, G. R., & Garic, A. (2012). Avian models in teratology and developmental toxicology. *Methods in molecular biology* (Clifton, N.J.), 889, 85–103.
- Smith-Swintosky VL, Zhao B, Shank RP, Plata-Salaman CR. (2001). Topiramate promotes neurite outgrowth and recovery of function after nerve injury. *Neuroreport*. 12(5):1031-4.
- Snider, T., Mishina, Y. (2014). Cranial neural crest cell contribution to craniofacial formation, pathology, and future directions in tissue engineering. *Birth Defects Research Part C: 102* (3): 324-332
- Sommer L. (2011). Generation of melanocytes from neural crest cells. *Pigment cell and melanoma*. 24:411-421.
- Sonia Hernandez-Diaz, Krista F. Huybrechts, Rishi J. Desai, Jacqueline M. Cohen, Helen Mogun, Page B. Pennell, Brian T. Bateman, Elisabetta Patorno. (2018). Topiramate use early in pregnancy and the risk of oral clefts: A pregnancy cohort study. *Neurology*. 90 (4) e342-e351
- South African national aids council, (2019). <https://sanac.org.za>
- Ssentongo P. (2019). Prevalence and incidence of new-onset seizures and epilepsy in patients with human immunodeficiency virus (HIV): Systematic review and meta-analysis. *Epilepsy behavior*. 93: 49-55.
- Stankiewicz TR, Linseman DA. (2014). Rho family GTPases: key players in neuronal development, neuronal survival, and neurodegeneration. *Frontiers in Cell Neuroscience*. 7; 8:314.
- Stouffer, M. A., Golden, J. A., & Francis, F. (2016). Neuronal migration disorders: Focus on the cytoskeleton and epilepsy. *Neurobiology of disease*, 92(Pt A), 18–45.

- Suraweera, A., O'Byrne, K. J., & Richard, D. J. (2018). Combination Therapy with Histone Deacetylase Inhibitors (HDACi) for the Treatment of Cancer: Achieving the Full Therapeutic Potential of HDACi. *Frontiers in oncology*, 8, 92.
- Svitkina, T. (2018). Ultrastructure of the actin cytoskeleton. *Current Opinion in Cell Biology*: 54:1-8.
- Takahashi, Y, DOUGLAS Sipp, D., HIDEKI Enomoto, H. (2013). Tissue Interactions in Neural Crest Cell Development and Disease. *Science* 23: 860-863
- Tamariz E, Varela-Echavarría A. (2015). The discovery of the growth cone and its influence on the study of axon guidance. *Frontiers in Neuroanatomy*. 9:51.
- Tang G, Yang GY. (2016). Aquaporin-4: A Potential Therapeutic Target for Cerebral Edema. *International Journal of Molecular Science*. 29;17(10):1413.
- Tang, D., Gerlach, B. (2017). The roles and regulation of the actin cytoskeleton, intermediate filaments and microtubules in smooth muscle cell migration. *Respiratory Research*. 18: s12931-017-0544-7.
- Tarantal AF, Castillo A, Ekert JE, Bischofberger N, Martin RB. (2002). Fetal and maternal outcome after administration of tenofovir to gravid rhesus monkeys (*Macaca mulatta*). *Journal of Acquired Immune Deficiency Syndrome*. 29(3):207-20.
- Tarr, J. T., Lambi, A. G., Bradley, J. P., Barbe, M. F., & Popoff, S. N. (2018). Development of Normal and Cleft Palate: A Central Role for Connective Tissue Growth Factor (CTGF)/CCN2. *Journal of developmental biology*, 6(3), 18.

- Taylor CP, Meldrum BS. Na⁺ channels as targets for neuroprotective drugs. *Trends Pharmacol Sci.* 1995 Sep;16(9):309-16. doi: 10.1016/s0165-6147(00)89060-4. PMID: 7482996.
- Tennis P, Chan A, Curkendall M, Li K, Mines D, Peterson C, Andrews B, Calingaert B, Chen Y, Deshpande G, Everage N, Holick N, Meyer M, Nkhoma T, Quinn S, Rothman J, Esposito B. (2015). Topiramate use during pregnancy and major congenital malformations in multiple populations. *Birth Defects Research A Clinical Molecular Teratology.* 103:269-75.
- Theveneau E, Mayor R. (2012). Neural crest delamination and migration: from epithelium-to-mesenchyme transition to collective cell migration. *Developmental Biology.* 1; 366(1):34-54.
- Thrane A. S., Thrane V. R., Plog B. A., Nedergaard M. (2015). Filtering the muddied waters of brain edema. *Trends in Neuroscience.* 38 1–3.
- Tobin JL, Di Franco M, Eichers E, May-Simera H, Garcia M, Yan J, Quinlan R, Justice MJ, Hennekam RC, Briscoe J, Tada M, Mayor R, Burns AJ, Lupski JR, Hammond P, Beales PL. (2008). Inhibition of neural crest migration underlies craniofacial dysmorphology and Hirschsprung's disease in Bardet-Biedl syndrome. *Proceedings of the National Academy of Sciences of the United States of America* 105(18):6714-9.
- Tomson T, Battino D. (2012). Teratogenic effects of antiepileptic drugs. *Lancet Neurology.* 11(9):803-13. doi: 10.1016/S1474-4422(12)70103-5.

- Townsend CL, Cortina-Borja M, Peckham CS, de Ruiter A, Lyall H, Tookey PA. (2008). Low rates of mother-to-child transmission of HIV following effective pregnancy interventions in the United Kingdom and Ireland, 2000-2006. *AIDS*. 11;22(8):973-81.
- Tozzi V, Balestra P, Bellagamba R, Corpolongo A, Salvatori MF, Visco-Comandini U, Vlassi C, Giulianelli M, Galgani S, Antinori A, et al. (2007) Persistence of neuropsychologic deficits despite long-term highly active antiretroviral therapy in patients with HIV-related neurocognitive impairment: prevalence and risk factors. *J Acquired Immune Deficiency Syndrome* 45:174–182
- Trainor PA. (2010). Craniofacial birth defects: The role of neural crest cells in the etiology and pathogenesis of Treacher Collins syndrome and the potential for prevention. *American Journal of Medical Genetics*; 152A:2984–2994.
- Tumusiime DK, Venter F., Musenge E, Stewart A. (2014). Prevalence of peripheral neuropathy and its associated demographic and health status characteristics, among people on antiretroviral therapy in Rwanda. *BMC Public Health*; 1471-2458-14-1306
- Usami, M., Mitsunaga, K., Irie, T., Miyajima, A., Doi, O. (2014). Simple in vitro migration assay for neural crest cells and the opposite effects of all-trans-retinoic acid on cephalic- and trunk-derived cells. *Congenital Anomalies*; 54:184–188.
- Valenzuela-Fernández A, Cabrero JR, Serrador JM, Sánchez-Madrid F. (2008). HDAC6: a key regulator of cytoskeleton, cell migration and cell-cell interactions. *Trends in Cell Biology*. 18(6):291-7.
- Valle, C., Hadley, M. (2018). Truncus Arteriosus. *Adult Congenital Heart Disease in Clinical Practice* 319-330.

- Van Aelst L. and D'Souza-Schorey, C. (1997). Rho GTPases and signaling networks. *Genes & Development*. 11: 2295–2322.
- van de Wijer, L., Garcia, L.P., Hanswijk, S.I. et al. (2019). Neurodevelopmental and behavioral consequences of perinatal exposure to the HIV drug efavirenz in a rodent model. *Translational Psychiatry* 9, 84.
- Vannappagari, V., Koram, N., Albano, J., Tilson, H., Gee, C. (2016). Association between in utero zidovudine exposure and nondefect adverse birth outcomes: analysis of prospectively collected data from the Antiretroviral Pregnancy Registry. *BJOG*. 123(6): 910–916.
- Verkman, A. S., Anderson, M. O., & Papadopoulos, M. C. (2014). Aquaporins: important but elusive drug targets. *Nature reviews. Drug discovery*, 13(4), 259–277.
- Vermillion, K. L., Lidberg, K. A., & Gammill, L. S. (2014). Cytoplasmic protein methylation is essential for neural crest migration. *The Journal of cell biology*, 204(1), 95–109.
- Vlot MC, Grijsen ML, Prins JM, de Jongh RT, de Jonge R, den Heijer M, et al. (2018). Effect of antiretroviral therapy on bone turnover and bone mineral density in men with primary HIV-1 infection. *PLoS ONE*;13(3): e0193679.
- Waldo, K., Miyagawa-Tomita, S., Kumiski, D., Kirby, M. (1998). Cardiac Neural Crest Cells Provide New Insight into Septation of the Cardiac Outflow Tract: Aortic Sac to Ventricular Septal Closure. *Developmental Biology*. 196: 129-144.
- Walton NY, Treiman DM. (1992). Valproic acid treatment of experimental status epilepticus. *Epilepsy Research*. 12(3):199-205. doi: 10.1016/0920-1211(92)90074-4.
- Walubo, A. (2007). The role of cytochrome P450 in antiretroviral drug interactions. *Expert Opinion in Drug Metabolism and Toxicology*.4:583-598.

- Wang Q, Kurosaka H, Kikuchi M, Nakaya A, Trainor P, Yamashiro T. (2019). Perturbed development of cranial neural crest cells in association with reduced sonic hedgehog signaling underlies the pathogenesis of retinoic-acid-induced cleft palate. *Disease Models & Mechanisms*; 12: dmm040279
- Wang R, Yoshida K, Toki T, Sawada T, Uechi T, Okuno Y, et al. (2015). Loss of function mutations in RPL27 and RPS27 identified by whole-exome sequencing in Diamond-Blackfan anaemia. *British Journal of Haematology*. 168:854-864
- Watt, K., Paul A. Trainor, P. (2014). Neurocristopathies. The Etiology and Pathogenesis of Disorders Arising from Defects in Neural Crest Cell Development. *Evolution, Development and Disease*: 361-394
- Watts DH. (2020) Treating HIV during pregnancy: an update on safety issues. *Drug Saf*. 2006; 29(6):467- 490.
- Watts, D; Covington, D., Beckerman, K., Susan, S., Chavers, S., Tilson, H. (2004). Assessing the risk of birth defects associated with antiretroviral exposure during pregnancy. *Fetal Medicine* 191: 985-992.
- Williams PL, Crain MJ, Yildirim C, Hazra R, Van Dyke RB, Rich K, Read JS, Stuard E, Rathore M, Mendez HA, Watts, DH. (2015). Congenital anomalies and in utero antiretroviral exposure in human immunodeficiency virus–exposed uninfected infants. *JAMA pediatrics*; 169:48-55.
- Wilner, A. (2012). Antiepileptics and HIV: An Evidence-Based Guideline. *Epilepsy Notes*
- Xu, C., Desta, Z. (2013). In vitro Analysis and Quantitative Prediction of Efavirenz Inhibition of Eight Cytochrome P450 (CYP) Enzymes: Major Effects on CYPs 2B6, 2C8, 2C9 and 2C19. *Drug Metabolism Pharmacokinetics*. 28(4): 362–371.

- Xu, Z., Chen, Y., & Chen, Y. (2019). Spatiotemporal Regulation of Rho GTPases in Neuronal Migration. *Cells*, 8(6), 568.
- Yang F, Yang L, Wataya-Kaneda M, Tanemura A, Tsuruta, D et al. (2018). Dysregulation of autophagy in melanocytes contributes to hypopigmented macules in tuberous sclerosis complex; 89:155-164.
- Yu K., Ornitz D. M. (2011). Histomorphological study of palatal shelf elevation during murine secondary palate formation. *Developmental Dynamics*. 240, 1737-1744
- Zaporozhan PH, Mcnamara JA, Williams C, Bergin J, Redmond CP, Doherty. (2019). Seizures in HIV: the case for special consideration. *Epilepsy Behavioral Case Report*. 19: 38-43.
- Zare I, Paul D, Moody S. (2019). Doublecortin Mutation in an Adolescent Male. *Child Neurology Open*. 6:2329048X19836589.
- Zash, R, Denise L Jacobson, Modiegi Diseko, Gloria Mayondi, Mompoti Mmalane, et al. (2018). Comparative safety of dolutegravir-based or efavirenz-based antiretroviral treatment started during pregnancy in Botswana: an observational study. 7: 804-810
- Zhang JY, Jia M, Zhao HZ, Luo ZB, Xu WQ, Shen HP, et al. (2016). A new in-frame deletion in ribosomal protein S19 in a Chinese infant with Diamond-Blackfan anemia. *Blood Cells, Molecules and Diseases*; 62:1-5.
- Zhang X., Velumian A., Jones O., Carlen P. (2000) Modulation of high-voltage-activated calcium channels in dentate granule cells by topiramate. *Epilepsia* 41(Suppl. 1): S52–S60
- Zimmer, B., Lee, G., Balmer, N. V., Meganathan, K., Sachinidis, A., Studer, L., & Leist, M. (2012). Evaluation of developmental toxicants and signaling pathways in a functional test

- based on the migration of human neural crest cells. Environmental health perspectives, 120(8), 1116–1122.

APPENDIX A



Mr T TSHABALALA

13 March 2020

University of Witwatersrand

ACCEPTANCE OF ABSTRACT

**48th Annual Conference of the Anatomical Society of Southern Africa, Durban, South Africa
19-22 April 2020**

Dear Mr T Tshabalala,

We are pleased to inform you that your abstract entitled “**The effect of Atripla and Topiramate on the migration of avian neural crest cells**” has been accepted as an ORAL presentation at the ASSA 2020 conference. *Please kindly see attached abstract for minor comments from the Abstract review committee.*

Please ensure that you have registered for the conference before 31 March 2020 to confirm your participation. Registration must be conducted online through the link on the conference. If you are no longer planning to attend, kindly inform the local organizing committee and we will withdraw your abstract.

For administrative purposes, kindly ensure that you have completed the payment in full by the 31 March 2020 in order for you to be included in the final program.

For more information regarding the conference, kindly consult the following website:

<https://www.dut.ac.za/assa-2020/>

Kindly send us your updated abstract for our conference proceedings booklet to soobramoney@ukzn.ac.za by 16 March 2020

Thank you and we look forward to seeing in Durban

Yours sincerely


Professor L Lazarus

Co- Chairperson of Local Organizing Committee
Department of Clinical Anatomy
University of KwaZulu Natal
Email: ramsaropl@ukzn.ac.za

Professor JD Pillay

Co- Chairperson of Local Organizing Committee
Basic Medical Sciences
Durban University of Technology
Email: pillayjd@dut.ac.za

Coadministration of ARV (Atripla) and Topiramate disrupts quail cardiac neural crest cell migration

Thabiso Tshabalala¹  | Pilani Nkomozezi² | Amadi Ogonda Ihunwo¹ | Felix Mbajjorgu¹

¹Divisions of Histology and Embryology and Morphological Anatomy, School of Anatomical Sciences, Faculty of Health Sciences, University of the Witwatersrand, Johannesburg, South Africa

²Department of Anatomy and Physiology, University of Johannesburg, Johannesburg, South Africa

Correspondence

Thabiso Tshabalala, School of Anatomical Sciences, Faculty of Health Sciences, University of the Witwatersrand, 7 York Road, Parktown, 2193, Johannesburg, South Africa.

Email: thabiso.tshabalala@wits.ac.za

Funding information

Faculty of Health Sciences, University of the Witwatersrand

Abstract

Introduction: Congenital anomalies such as ventricular septal defects and truncus communis have been reported with the prenatal use of antiretroviral therapy. The mechanism of antiretroviral therapy teratogenicity is unclear and is therefore the focus of this study. Some human immunodeficiency virus patients on antiretrovirals are placed on antiepileptic drugs which are also teratogenic. The interactive effects arising from this therapeutic combination may affect their teratogenic propensity through their effects on neural crest cell migration.

Methods: Appropriately cultured neural crest cells from dissected neural tubes of 32-hr old quail embryos exposed to culture media containing peak plasma levels of Atripla, Topiramate and the combination of both were studied. Distance of migration of neural crest cells was measured using the migration assay and the cells were stained with rhodamine phalloidin to evaluate the cell actin. Also quail neural crest cells were brought into suspension and microinjected into chick hosts to determine the migration of the cells to the interventricular septum.

Results: Migration of cultured neural crest cells was extensive in the control cultures, but inhibited in the treated groups. The experimental cultures showed a disarray of actin cytoskeleton contrary to normal distribution of actin filaments in controls. Significantly, few quail neural crest cells migrated to the interventricular septum of chick host embryos compared to the control cultures. The coadministration of topiramate with antiretroviral therapy does not seem to affect the activity of the antiretroviral drug.

Conclusion: These results indicate that Atripla and Topiramate cause ventricular septal defects by inhibiting the migration of cardiac neural crest cells.

1 | INTRODUCTION

The introduction of combined antiretroviral therapy (cART) has significantly improved the life span and quality of life of people living with human immunodeficiency virus (PLWHIV) by decreasing the viral loads to undetectable levels, with resultant reduction in the incidence of HIV related opportunistic infections (Ford et al., 2018). In addition, the use of cART in the treatment of HIV-infected pregnant women and in the prevention of mother-to-child transmission of HIV has occasioned a significant reduction in the number of infants born with HIV (Williams et al., 2015). However, the safety of intrauterine exposure to cART remains a concern, particularly as an increasing number of women are becoming pregnant while already receiving cART (Watts, 2006). While previous studies assessing the risk of congenital anomalies (CAs) related to intrauterine exposure to cART seem to report absence of CAs (Jungmann et al., 2001; Watts et al., 2004), recent evidence suggests that intrauterine exposure to cART could increase the risk of CAs (Knapp, Brogly, Muenz, et al., 2012; Mehta et al., 2019; Phiri et al., 2014; Williams et al., 2015).

Apart from possible cART-related CAs, another complication associated with cART is epileptic seizures which has been reported in as many as a tenth of PLWHIV and may therefore require treatment with antiepileptic drugs (AEDs; Siddiqi & Birbeck, 2013; Siddiqi et al., 2017; Ssentongo, 2019; Zaporozhan et al., 2019). Causes of seizures among these patients include drugs, opportunistic infections; and the HIV itself (Carroll & Brew, 2017). Furthermore, HIV patients who exhibit symptoms of peripheral neuropathy may be treated with AEDs (Siddiqi et al., 2017; Birbeck et al., 2012). Peripheral neuropathy affects more than 50% of PLWHIV (Birbeck et al., 2012). Thus, HIV infected patients who present with either seizures or peripheral neuropathy may require co-treatment with AEDs and cART (Kim, Chin, & Shin, 2015; Ssentongo, 2019). Co-treatment with these drugs is a great concern since both undergo cytochrome P450 metabolism (Zaporozhan et al., 2019), raising the possibility of drug-to-drug interactions. These interactions may result in the attenuation, increase or otherwise the adverse and/or the desired and beneficial effects of one or both of the drugs (Walubo, 2007; Zaporozhan et al., 2019) and consequently increased viral progression or amplification of seizures (Zaporozhan et al., 2019) as the case may be.

Topiramate (TOP) is one of the AEDs used in the management of patients with epilepsy. In addition to seizures, TOP is also used in the treatment of migraines, bipolar mood disorders and peripheral neuropathy (Margulis et al., 2012; Molgaard-Nelsen &

Hviid, 2011; Ornoy et al., 2008). Despite its therapeutic benefits in epilepsy, TOP has been shown to be teratogenic when administered during pregnancy, particularly during the first trimester (Hunt et al., 2008; Margulis et al., 2012). A myriad of craniofacial and cardiovascular abnormalities have been attributed to the administration of TOP during early pregnancy (Margulis et al., 2012; Tennis et al., 2015). The cardiovascular effects of TOP teratogenicity include coarctation of the aorta, patent ductus arteriosus, atrial and ventricular septal defects (ASD and VSD) (Tennisset al., 2015). Remarkably, some of the aforementioned cardiovascular defects such as VSDs have also been reported in cART teratogenicity (Brogly et al., 2010; Prieto et al., 2014; Vannappagari, Koram, Albano, Tilson, & Gee, 2016; Williams et al., 2015).

VSDs are known to be the most common type of cardiovascular CAs (Dakkak & Oliver, 2019). The most common VSDs occur due to failure of the interventricular foramen to close, resulting in an open communication between the two ventricular chambers (Radhakrishna et al., 2019). Ablation studies have shown that the failure of migration of cardiac neural crest cells to the truncal ridges and their subsequent failure to contribute toward the closure of the interventricular foramen results in VSDs (Hutson & Kirby, 2003; Waldo, Miyagawa-Tomita, Kumiski, & Kirby, 1998) which underscore the important role of cardiac neural crest cells in the development of an normal interventricular septum in the embryo and subsequently in a definitive adult heart.

Although studies have established a link between the use of cART or TOP during the first trimester of pregnancy and the development of VSDs, the mechanism through which this association occurs remains unclear. Since the burden of HIV/AIDS is still very much in the society, and the use of cART and TOP is continuing, there is a need to study the possible mechanisms of their teratogenicity. In this regard, this study aims to investigate the individual and combined effects of cART using a combination antiretroviral therapy (cART) drug and TOP on the migration of quail cardiac neural crest cells *in vitro*. The study will further determine the *in vivo* migration of *in vitro* cART and TOP-treated quail neural crest (QNC) cells, microinjected into chick embryo *in vivo*.

2 | MATERIALS AND METHODS

2.1 | Drugs

A generic tablet of Atripla (Bristol-Myers Squibb & Gilead Sciences LLC, South Africa) containing 600 mg of

efavirenz (EFV), 200 mg of emtricitabine (FTC) and 300 mg of tenofovir disoproxil fumarate (TDF) was used as cART. The tablet was crushed into powder and dissolved in dimethyl sulfoxide (DMSO, Sigma). TOP (Sigma, CAS No. 97240-79-7, T0575) was also dissolved in DMSO. A hundred percent solution of 1 g/ml in DMSO was prepared for both drugs.

2.2 | Embryos and ethical clearance

Sixty (60) fertile Japanese quail (*Cortunix Cortunix japonica*) and 60 chicken (*Gallus gallus domesticus*) eggs were used in this study. The quail eggs were incubated for 32 hr at 37°C in a humidified incubator. The chicken eggs were used as hosts and were also incubated at 32 hr in a humidified incubator. All experimentation was carried out in a laminar flow hood under aseptic conditions. All experimental procedures were approved by the University of the Witwatersrand, Animal Ethics Committee (Animal Ethics Clearance Number 2019/01/2/A).

2.3 | Preparation of equipment

Glassware was dry-heat sterilized at 180°C for 2 hr. Solutions were autoclaved at 121°C at 100 kPa for 30 min. Four-well Nunc culture multidishes (Nunc, Denmark) were layered with fibronectin (Sigma) which was made up in distilled water (1:40 dilution). The dishes containing fibronectin were incubated for 1 hr at 37°C in a humidified incubator. After incubation, excess fibronectin was removed using a fine pipette. Dulbecco's minimal essential medium (DMEM, 30 µl) was added to each well, and the dishes were incubated for a further 1 hr at 37°C until use.

2.4 | Neural tube cultures

In order to determine the extent of migration of neural crest cells, quail neural tubes were cultured in the presence of the two drugs as follows: The shell of each quail egg was wiped with cotton wool dipped in 70% alcohol. The egg was cut open, and emptied into an oval dish containing chick Ringer's solution (sodium chloride, potassium chloride, calcium chloride and sodium bicarbonate). The blastoderm of Stage 8 quail embryos (staging according to Hamburger & Hamilton, 1951) was removed from the underlying yolk. The blastoderm was pinned out firmly on the black wax dish. In order to obtain cardiac neural crest cells, the neural tube together with adjacent somites, was dissected out between the level of the mid-otic placode and the third somite (Figure 1a). The tissue was placed in 0.0004% collagenase in calcium and magnesium-free Tyrode's solution for 20 min at room temperature. The tissue was then removed from the collagenase solution and rinsed in Ringer's solution. The neural tube, including neural crest, was separated from the surrounding tissues by microdissection and pipetted on to a fibronectin-coated well (1:40, Sigma) of a four-well Nunc culture dish (Figure 1a).

The explants were randomly allocated to the following treatments: as controls (a and b) the neural tube explants were cultured in 1 ml of DMEM only, ($n = 12$), and 1 ml of 0.05% DMSO reconstituted in DMEM (DMEM only, $n = 12$). As experimental, the explants were cultured in a 1 ml DMEM solution containing 3 µM TOP (Group C, TOP only, $n = 12$), 5 µM of Atripla (Group D, cART only, $n = 12$) and the combination of the two concentrations of Atripla and TOP (Group E, cART/TOP, $n = 12$). The culture medium was made up of the DMEM solution containing 15% chick embryo extract and 10% horse serum (Bronner-Fraser, 1996). The cultures were then placed in an incubator (with 5% CO₂)

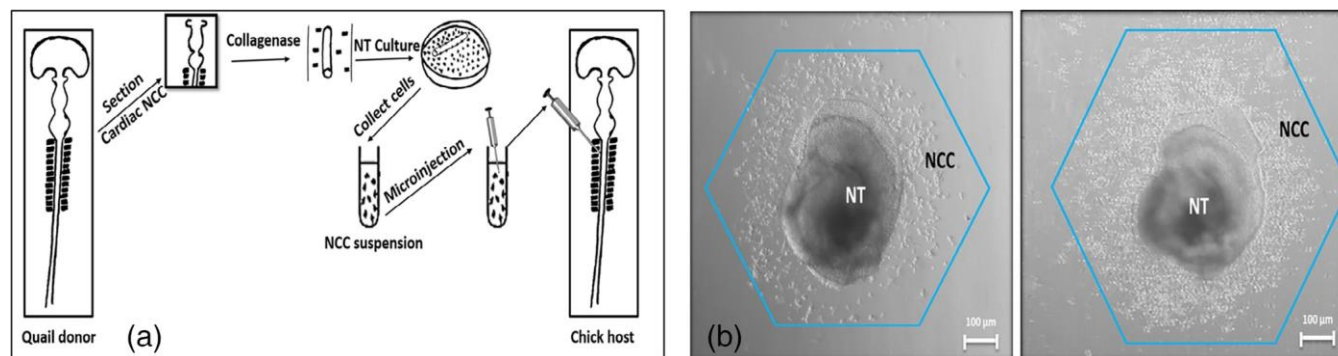


FIGURE 1 (a) shows a summary diagram illustrating the in vitro neural tube culture technique and the microinjection of quail cardiac neural crest cells into chicken host embryos, while (b) shows photomicrographs of the control neural tube (NT) and migrating neural crest cells (NCC) after 24 (a) and 48 hr (b) in culture. A polygon tool (blue) was used to measure the area migrated by cardiac neural crest cells

at 37°C in a humidified atmosphere and were viewed after 8 and 24 hr. The cultures were photographed at 24 and 48 hr using an Olympus inverted phase contrast microscope (Olympus, South Africa) at specific magnifications. In order to maintain the concentrations of the drugs the culture medium was replaced after 24 hr.

2.5 | Measurement of QNC cell migration

Only cell cultures where neural crest cells had migrated out around the entire circumference of the neural tube were used to analyze migration. Only four cultures (one DMEM only, one DMSO only, and two TOP only) did not have neural crest cells completely surrounding the neural tube, and were thus excluded from the migration assay. In order to determine the effect of cART and TOP on the extent of migration, the distance migrated by the neural crest cells was calculated as the difference in the radius of the circular spread of the cells between 24 and 48 hr of culture (Usami, Mitsunaga, Irie, Miyajima, & Doi, 2014). The outermost NCCs in each of the cultured neural tubes were connected with the polygon tool in a circular fashion, and the pixel count inside the polygon was measured (Figure 1b). The radius (R) of the polygon was calculated as follows:

$$R = \sqrt{\frac{\text{number of pixels in a polygon}}{\pi}} \quad (1)$$

In order to evaluate the extent of neural crest migration (Figure 1b), the radius ratio (RR) was calculated using the following formula:

$$RR = \frac{R_{48h} - R_{24h}}{R_{24h}} \quad (2)$$

2.6 | Actin staining and quantification

In order to evaluate the effects of cART and TOP on the actin cytoskeleton of neural crest cells control and experimental neural crest cells, which were cultured for 48 hr in vitro, were washed with prewarmed phosphate-buffered saline (PBS) at pH 7.4. After rinsing, the cells were fixed in 3.7% formaldehyde solution in PBS for 10 min at room temperature. After washing extensively in PBS, the cells were layered with 0.1% triton-X in PBS for 5 min, and washed in PBS thereafter. To reduce non-specific background, the fixed cells were preincubated with PBS containing 1% BSA for 25 min prior to adding the staining solution (rhodamine phalloidin, Sigma) to stain for actin. The cells were covered with a solution of rhodamine phalloidin (1:40) in PBS for 20 min at room

temperature. After extensive rinsing in PBS, the cells were viewed using a Zeiss Axioscope fluorescence microscope (Zeiss, South Africa).

In order to determine the level of fluorescence the corrected total cell fluorescence (CTCF) was calculated using ImageJ software (National Institutes of Health) as follows:

$$CTCF = \text{Integrated density} - (\text{area of selected cell} \times \text{mean fluorescence of background reading}).$$

This technique enables the evaluation of microscopic fluorescent images into more reliable quantitative manner. Thus, image analysis techniques are applied to quantify the total fluorescence in a stained cell using ImageJ software. The equation enables the CTCF (level of fluorescence) of the background to be equalized against the mean CTCF of neighboring interphase cells which are in the vicinity (in the same field of view). The final CTCF therefore represents a fold increase over interphase levels (McCloy et al., 2014).

2.7 | Suspension of cultured neural crest cells to obtain cells for microinjection

In order to obtain NCCs for microinjection, migrating QNC cells which had been cultured on fibronectin for 24 hr were brought into suspension using 2.5% trypsin as follows. Both the culture medium and the neural tube were removed from each well, and the neural crest cells were washed with prewarmed PBS. A 150 µl of trypsin (Highveld Biological, South Africa, Gauteng) was added to each well and the adhering neural crest cells were then incubated at 37°C for 3–5 min. The trypsin was used neat (undiluted). The action of trypsin was stopped by adding 500 µl of DMEM to each well. The suspended cells were transferred into a sterile centrifuge tube and spun for 5 min at 1,500 rpm. The supernatant was poured off and the pelleted cells were used for microinjection into the cardiac regions of chick embryo hosts which had been incubated for 32 hr. To test for cell viability, a TC20 automated cell counter (BIO-RAD, Country) was used. In addition, neural crest cells were replated onto a clean fibronectin-coated four-well Nunc culture multidish. The cells were viewed hourly to determine if they are able to adhere to the fibronectin.

2.8 | Transfer of cultured and suspended QNC cells into a chick host

2.8.1 | The QNC cell experiment

Out of 60 chick host embryos, 12 died and 48 embryos (80%) were used for this part of the study and were distributed as follows: DMEM only ($n = 8$); DMSO only

($n = 9$); cART only ($n = 10$); TOP only ($n = 11$); and cART/TOP ($n = 10$). For the microinjections of quail cardiac neural crest cells into the cardiac region of chick hosts, fertile 32 hr chicken host embryos were used. The chick-quail chimaera technique was used because the large quail nucleoli are easily distinguishable from the small nucleoli of chick cells, and hence any neural crest cell which had migrated from the quail donor neural tubes could be easily identified in the chicken host embryo.

In this procedure, each chicken egg (Stages 8–9) was wiped with 70% alcohol and placed horizontally onto an egg holder. The blunt end of the egg was punctured using a hacksaw blade to release air from the air sac, in order to lower the blastoderm and prevent it from adhering to the shell. Following which, 1.5 ml of albumen was aspirated by penetrating the pointed end of the egg, slightly below the equator of the shell with the needle and a syringe. The needle was pointed downward, almost vertically, as it is passed into the shell to avoid damage to the yolk. To avoid leakage of albumen, the entry point was sealed with clear tape. A window was then cut in the shell, overlying the position of the embryo at the highest point of the egg when lying transversely, and the shell membrane was removed. The embryo was then visible through the window. To keep the blastoderm moist, a few drops of chick Ringer's solution with antibiotics (1 μ l penicillin and streptomycin, Sigma) was placed on to the chorioallantoic membrane of the embryo. In order to visualize the different regions of the embryo, 100 μ l of 1% Pelican India ink (diluted in Ringer's solution) was injected below the blastoderm. The cultured, suspended QNC cells were counted using a TC20 automated cell counter (BIO-RAD). Each cell pellet was diluted using the culture medium until a live cell count reached 1×10^{-3} to ensure that an equivalent number of QNC cells are injected into the chicken host. The cells were then backfilled into a sterile-pulled thin glass needle of unknown diameter. The needle was connected to an aspirator tube. The tip of the needle was then inserted into the desired region of the embryo. The QNC cells were then microinjected under the surface ectoderm into the mesenchyme adjacent to the cardiac neural tube (Figure 1a). This procedure was carried out for both the nontreated controls (DMEM only and DMSO only) and the treated groups (cART only; TOP only and cART/TOP). Following microinjection of the neural crest cells, the egg was sealed with clear cellophane tape and returned to the humidified incubator at 37°C for 14 days. The chicken embryos were removed from the egg shells, and the hearts were dissected out, and fixed in 10% formalin, processed in an automatic processor (Shandon Citadel 1000), and embedded in paraffin wax. The heart

tissue was serially sectioned on a Leica microtome (Leica, South Africa) at 5 μ m and stained with the Feulgen–Rossenbeck method to identify the large nucleoli of QNC cells. To avoid loss of tissue during processing, silane-coated slides were used. Light microscopy was used to view the processed tissue.

2.9 | Feulgen reaction

In order to locate the quail cardiac neural crest cells which had migrated to the interventricular septum of chicken hosts the Feulgen reaction method was used to stain the chicken heart samples (Feulgen & Rossenbeck, 1924). This method which allows DNA to be stained *in situ* highlights the big nucleoli of QNC cells which can be distinguished from smaller chicken nucleoli (Ribatti, 2019). This is important in identifying the quail nucleoli in the chicken host as it confirms the migration of the NCCs to the interventricular septum.

The paraffin sections of the chicken hearts samples were brought to distilled water. The sections were briefly rinsed in cold ammonium chloride (NHCL) and transferred to NHCL at 60°C for 8 min. As controls, similar sections of each heart tissue were placed in distilled water at 60°C for the same period of time (8 min). After washing in distilled water, the sections were transferred to Schiff's reagent for 60 min. The sections were rinsed in three changes of sulfite rinse (Bancroft, 2002) solution, and then in water. The sections were counterstained in 1% aqueous light green for 1 min (Bancroft, 2002; Pawitan & Tanzil, 1995), dehydrated, cleared and mounted in entellan. As a positive control for the big quail nucleoli, adult quail liver was used. A developing chicken interventricular septum was used to show the small chicken nucleoli.

The interventricular septum of the chicken host embryo was assessed under the light microscope (Figure 8, $\times 100$, oil immersion) for the presence of QNC cells and the cells were counted using ImageJ software (National Institutes of Health, USA). The cells were counted using systematic sampling. A double square lattice system and a table of random numbers were used to determine the areas of cell counts. Ten sets of counts were randomly made on each interventricular septum of chicken hosts (given a total count of 80 to 100 per treatment group) and the average was used as a count for each group. The numerical density of QNC cells was expressed as:

$$\frac{\text{Number of counts}}{\text{area}}$$

2.10 | Statistical analysis

All statistical analyses were done using graphpad prism software for windows (Version 5.0, GraphPad Software Inc., San Diego, CA). Measurements for each variable (RR, CTCF, and numerical density) were expressed as mean \pm SEM. Group means for each variable were compared using one-way analysis of variance (ANOVA) followed by Bonferroni's multiple comparison test for post hoc analysis. A significance level of $p < .05$ was used.

3 | RESULTS

3.1 | cART and TOP inhibit the migration of cardiac neural crest cells

In order to investigate the effect of cART and TOP on the in vitro migration of cardiac neural crest cells, quail neural tubes (dissected at cardiac levels) were cultured in the

presence of the plasma concentration levels of cART and TOP individually, and in combination for 48 hr. The results indicate that both cART and TOP inhibit the migration of cardiac neural crest cells when administered at peak plasma levels. The qualitative results of neural crest cell migration are as shown in Figures 2 and 5. The neural crest cells started to migrate out of the neural tube after 12 hr of culture in both the treated and control explants and some good migration distance was covered at 24 hr when the pictures were taken. The neural crest cells of the treated groups (TOP only, cART only, and cART/TOP-treated, i.e., groups c, d, and e, respectively) migrated a lesser distance (Figure 2c–e orange double-headed arrows, Figure 5c–e) than the control cultures (Figure 2a,b; orange double-headed arrows, Figure 5a,b). The interruption of migration was pronounced in group where neural crest cells cultured in cART only were clustered around the epithelial sheath as they delaminate from the neural tube (Figure 2d; curly brackets). However, the TOP only-cultured neural crest cells, were sparse and scattered (Figure 2c), and in addition a gap

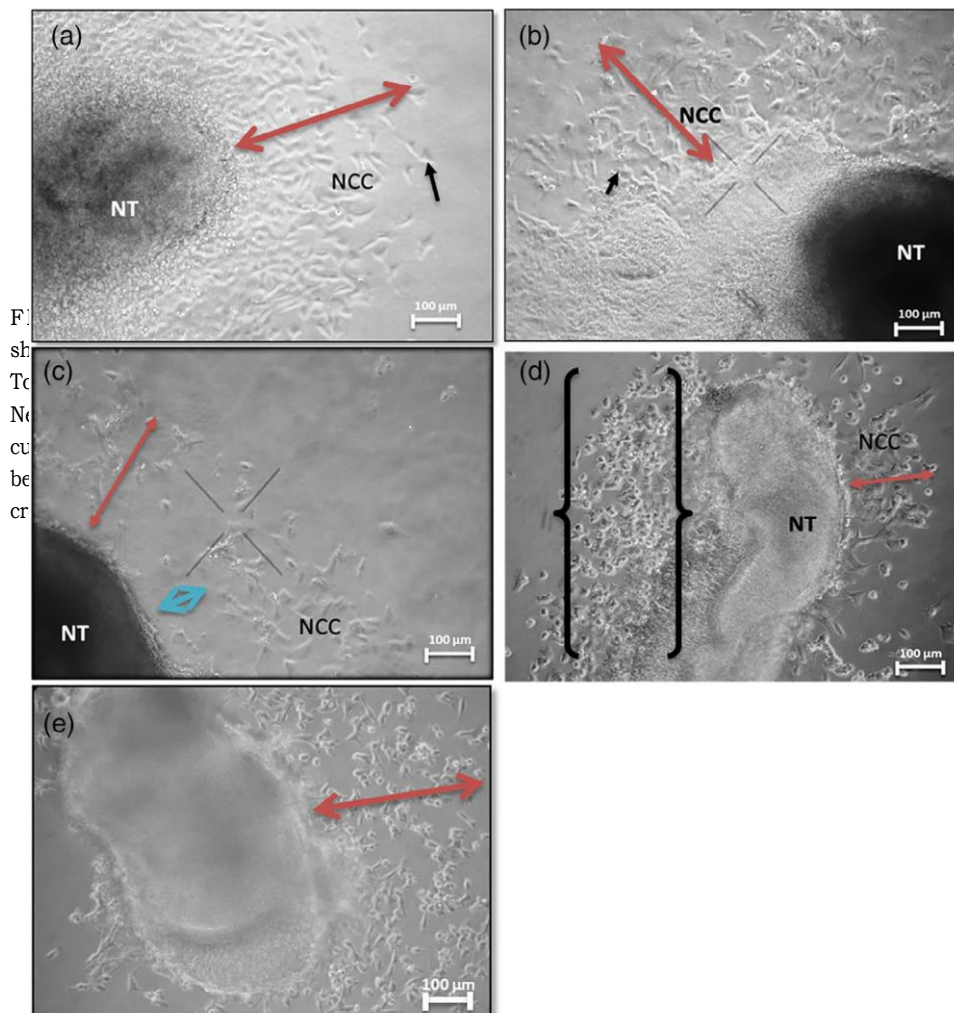


FIGURE 2

Photomicrographs of cardiac neural crest cells cultured in the presence of dimethyl sulfoxide (DMSO) only (b), and TOP (c), cART (d), and cART/TOP (e) for 24 hr. The control explants (a,b) compared to the treated explants (c–e) (orange double-headed arrows), cART-treated cells appeared to migrate a lesser distance than the cART-treated neural

was observed in delaminating process depicted by the blue double-headed arrow (Figure 2c). The distance of migration in cART/TOP-treated neural crest cells was reduced when compared to the control cultures, but was greater than in the cART only-treated neural crest cells (Figure 2e).

In addition, the cART only-treated neural crest cells showed rounded profiles both at low (Figure 2d; curly brackets, $\times 100$) and high magnifications (Figure 3d [$\times 200$] and 4D [$\times 400$]). However, at low (Figure 3a,b) and higher magnification (Figure 4a), the migrating NCC of the control groups exhibited a polygonal/stellate shape with filapodial extensions; depicting typical migrating cells (Figures 2a and 3a,b, black arrows). The cART/TOP-treated neural crest cells also showed

rounded profiles at higher magnification (Figures 3e and 4e). Numerous detached filapodial extensions from the migrating neural crest cells could be seen among the migrating neural crest cells (Figure 3a,b, red arrows). While most of the neural crest cells had a single nucleolus (Figure 4b,d,e, red circle) some exhibited pale vesicular nuclei with two nucleoli (Figure 4a,c, yellow circle).

One-way ANOVA showed a significant effect of treatments on the RRs (Figure 5a–e) of the neural crest cultures, with higher RRs in control cultures (DMEM only and DMSO only, a and b) compared to treated groups (cART only; TOP only and cART/TOP, c–e) (Bonferroni's post hoc test $F(4, 64) = 61.68, p < .0001$, Figure 5f). However, no significant differences were found among the

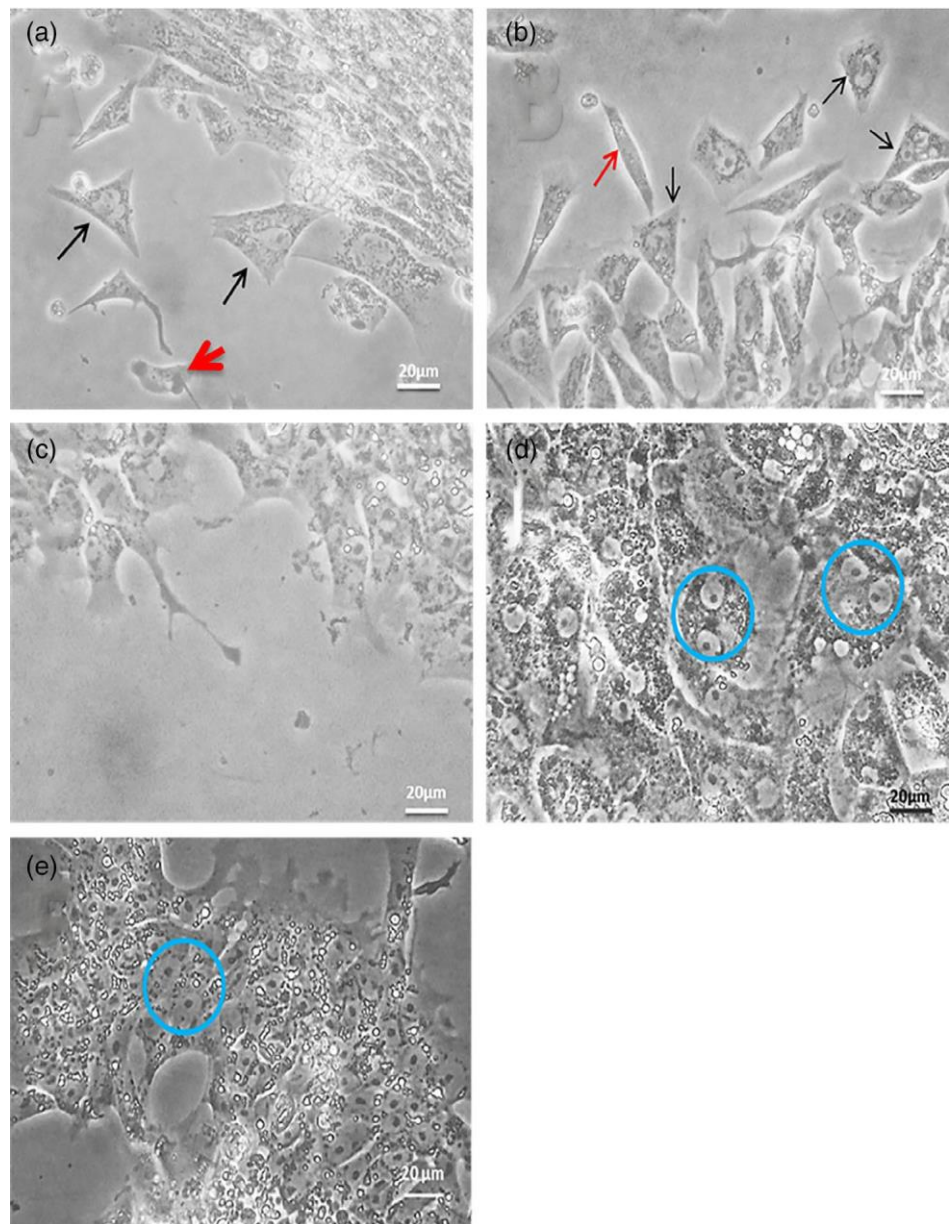
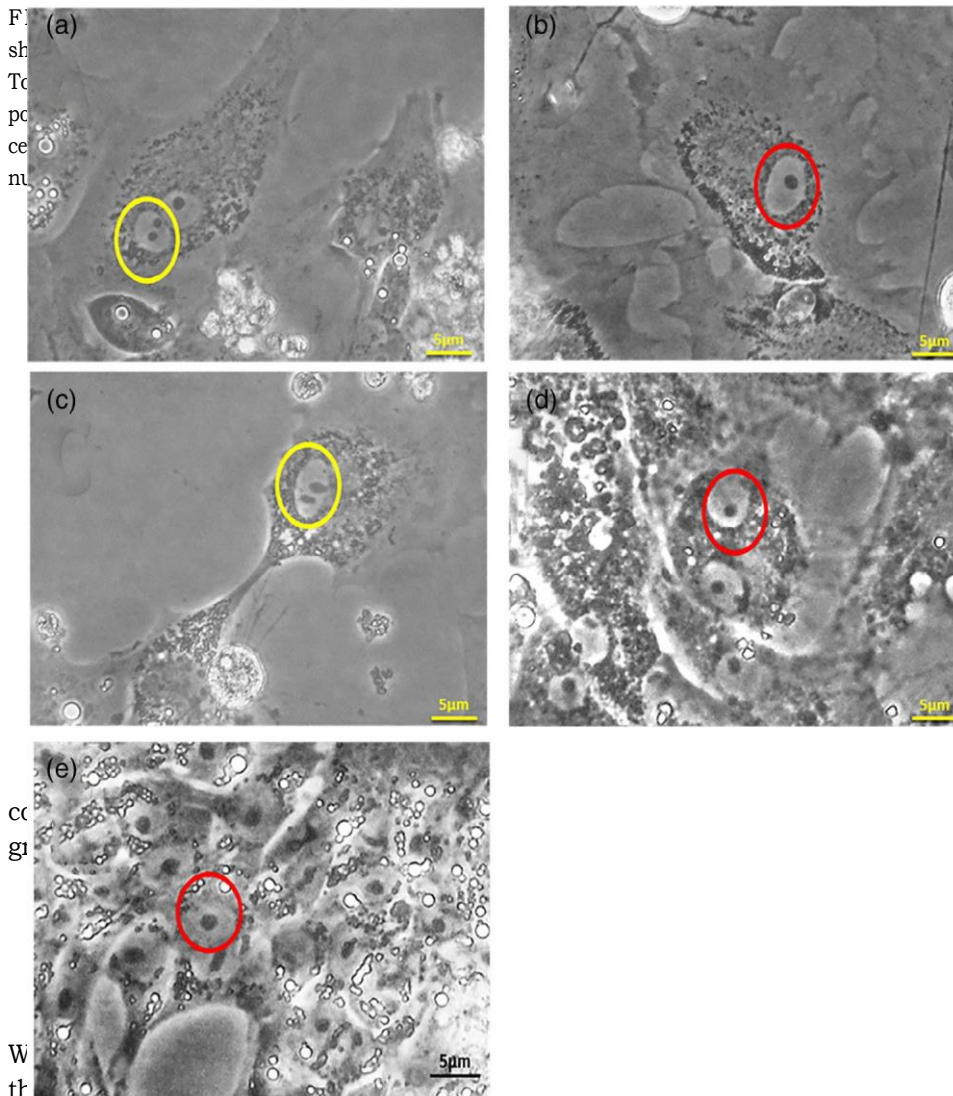


FIGURE 3 Photomicrographs showing neural crest cells cultured in Dulbecco's minimal essential medium (DMEM) only (a), dimethyl sulfoxide (DMSO) only (b), Topiramate (TOP) only (c), combined antiretroviral therapy (cART) only (d), and cART/TOP (e) after 24 hr. Control neural crest cells are mostly polygonal in shape (black arrows) while cART-treated and cART/TOP-treated neural crest cells appear rounded (blue circle). Figure 3a,b (red arrows) shows filapodia which have detached from migrating neural crest cells. (Magnification $\times 200$)



Photomicrographs of neural crest cells cultured in the presence of dimethyl sulfoxide (DMSO) only (b), and in the presence of rhodamine phalloidin for 24 hr of culture. Control cells have polygonal profiles. Neural crest cells with prominent nucleolus (red circles) some had two

actin filaments (a) and DMSO only (b). The actin filaments are seen extending within the processes of all the control cells (Figure 6a,b). The filaments could be seen criss-crossing with each other at right angles (Figure 6a,b, yellow circles). Rhodamine phalloidin staining also revealed the actin filaments in control neural crest cells (Figure 6a,b). The experimental cells showed similar features of the control cells (Figure 6c-e). The cells were more rounded and smaller than the control cells. The actin filaments appeared to be in disarray, concentrated at the lateral cortices and center was devoid of filaments (Figure 6c-e). Filopodial extensions, detached from the migrating cells were observed in both the experimental and control cultures (Figure 6b-e, white arrows) but are more numerous in the control cultures than in the treated cultures. The experimental neural crest cells which remained in the vicinity of the neural tube appeared to be attached to each other (Figure 6c-e).

mechanism of VSD formation in babies born to HIV positive mothers on cART and TOP treatment. In order to achieve this, quail neural tubes (dissected at cardiac levels) were cultured in the presence of the plasma concentration levels of cART and TOP individually, and in combination for 48 hr. The results indicate that both cART and TOP inhibit the migration of cardiac neural crest cells when administered at peak plasma levels. The results as shown in Figure 6a,b reveal that rhodamine phalloidin stained control neural crest cells which were

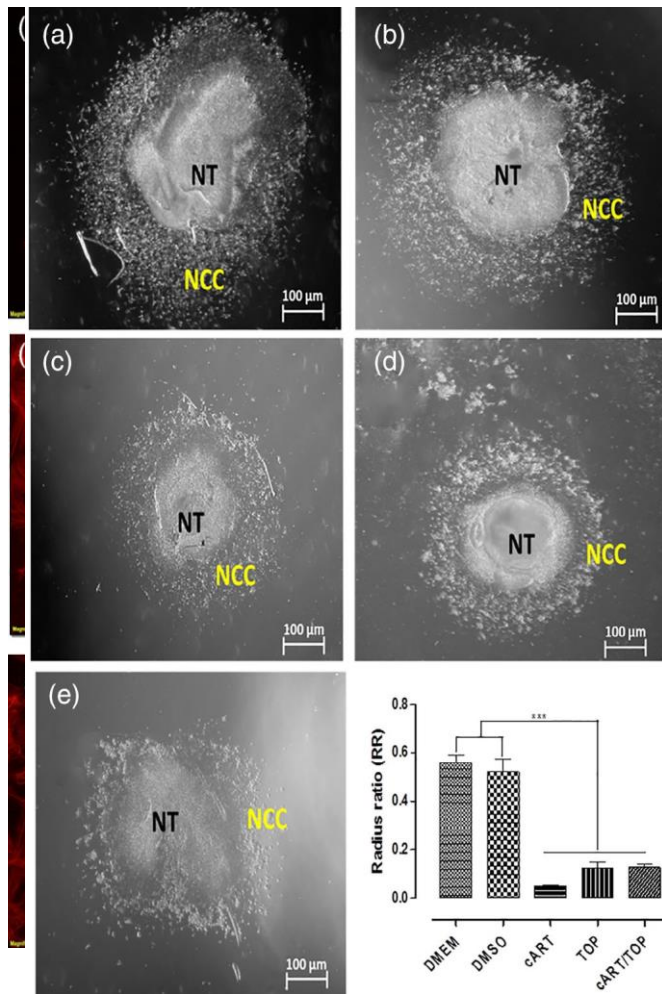


FIGURE 5 Photomicrographs showing neural crest cells cultured in Dulbecco's minimal essential medium (DMEM) only (a), dimethyl sulfoxide (DMSO) only (b), Topiramate (TOP) only (c), combined antiretroviral therapy (cART) only (d) and cART/ TOP (e) after 24 hr. Migration of neural crest cells (NCC) cultured in cART, TOP and cART/TOP appear inhibited to some extent (magnification $\times 40$). (f) The difference in the radius ratio of cardiac neural crest cells. Migration in the treated cultures was significantly lower than in the control cultures

One-way ANOVA showed a significant effect of treatments on the CTCF of actin in the neural crest cultures ($F(4, 120) = 11.41, p < .0001$, Figure 6f). The CTCF values of control cultures (DMEM only and DMSO only) were not significantly different from that of the cART only group ($p > .05$) but significantly different from the TOP only ($p < .0001$) and cART/TOP ($p < .01$) groups. Furthermore, the mean of CTCF for the TOP only group was significantly lower than the cART only or cART/ TOP groups ($p < .05$). However, no significant differences were found between the DMEM only and DMSO only groups or between the cART only and cART/TOP groups ($p > .05$) (Figure 7).

FIGURE 6 Fluorescence photomicrographs showing neural crest cells which were cultured in Dulbecco's minimal essential medium (DMEM) only (a), dimethyl sulfoxide (DMSO) only (b), Topiramate (TOP) only (c), combined antiretroviral therapy (cART) only (d) and cART/TOP (e) after 48 hr. Control neural crest cells show the criss-crossing of actin filaments at right angles (a and b, yellow circles). Filapodial extensions which have detached from migrating neural crest cells appear to be more abundant in the control cultures (b, white arrows). Actin filaments are more confined to the extremities of the cells in treated cultures (c–e). (f) The actin corrected total cell fluorescence (CTCF) of treated and untreated cardiac neural crest cells. The CTCF in TOP only-treated neural crest cells was significantly lower than that of all other cultures

3.3 | cART and TOP inhibits the migration of cardiac neural crest cells to the interventricular septum

We aimed to investigate if QNC cells cultured in peak plasma levels of cART and TOP individually, and in combination will reach the interventricular septum in chicken host embryos, using the quail-chick chimaera technique. In order to achieve this, cultured cranial neural crest cells were brought into suspension and

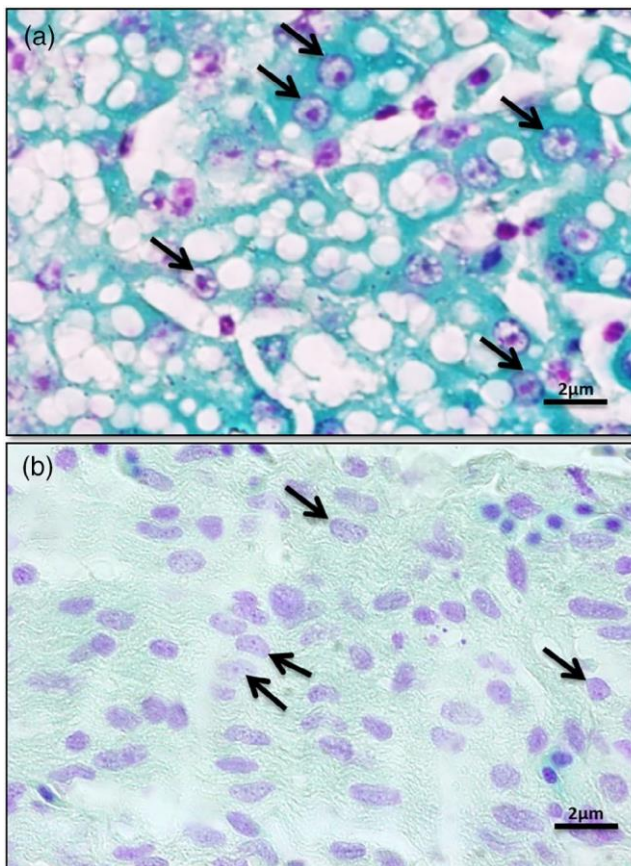


FIGURE 7 A Feulgen-stained photomicrograph showing a section through an adult quail liver (a, positive control) and a chicken interventricular septum (b) showing large and small nucleoli respectively. The nuclei in quail liver are pale and exhibit big prominent nucleoli (black arrows). (Magnification $\times 1,000$, oil immersion)

microinjected into 32-hr-old chicken embryos at cardiac levels. The Feulgen–Rossenbeck method was used to locate the QNC cells on the chicken interventricular septum by their large nucleoli. The results show that both cART and TOP individually, and in combination inhibit the migration of QNC cells as fewer treated cells were located in the chicken interventricular septum. The nucleolus of QNC cells microinjected onto chick hosts (Figures 8 and 9, black arrows), were distinguishable from the chicken nucleolus (Figure 9a,c, orange arrows) by their large size in the interventricular septum of the chick hosts either singly or in groups using the Feulgen stain (Figure 9). The QNC cells were distributed throughout the interventricular septum in the heart of the chicken host, forming part of the septum. Following cell counts (which were expressed as numerical density), both control cardiac neural crest cells (DMEM only and DMSO only, a and b) which were microinjected in chick-host embryos were found to be more numerous compared to the treated cultures (cART only; TOP only and

cART/TOP). All treated cardiac neural cells were fewer, but were also dispersed throughout the interventricular septum (Figure 9c–e). The adult liver section which was used as a positive control (Figure 7a) exhibited large prominent nucleoli (black arrows), while the chicken cells exhibited smaller nucleoli (Figure 7b) with the Feulgen–Rossenbeck method.

One-way ANOVA showed a significant effect of treatments on the numerical density of QNC cells in the chick heart interventricular septum ($F(4, 31) = 67.12; p < .0001$, Figure 9f). The control groups (DMEM only and DMSO only) had significantly higher numerical densities of QNC cells in the chick heart interventricular septum compared to the experimental groups; cART only; TOP only and cART/TOP (Bonferroni's post hoc test $F = 67.12, p < .05$). In addition, no significant difference was found among all the treated groups ($p > .05$) and among the control groups ($p > .05$), Figure 9f).

4 | DISCUSSION

The current study investigated the effect of the cART and TOP on the migration of only cardiac neural crest as a potential mechanism (among others) for VSD formation, which informed the focus on cardiac neural crest cells. The involvement of neural crest cells in the formation of specific heart structures was first established by Kirby and his colleagues (Kirby, Gale, & Stewart, 1983). In their investigation, the ablation of neural crest cells (which they later called cardiac neural crest cells) resulted in the absence of the aorticopulmonary septum. It therefore suggests that, the absence of cardiac neural crest cells and the subsequent failure of the truncal ridges to form will result in a VSD (Valle & Hadley, 2018).

The successful migration of cardiac neural crest cells as recorded indicates that the two main techniques employed in the current study to determine if cART and TOP inhibit the migration of neural crest cells were successfully applied. The observed QNC cells in the chick host interventricular system (IVS), suggest that isolation of neural tubes at cardiac levels and the subsequent migration of neural crest cells in vitro in the presence of antiretroviral and AEDs were successful. Secondly, it showed that the microinjection of cultured quail cardiac neural crest cells into the cardiac region of a chick embryo hosts in vivo (chick-quail chimaera system) was also successful. The chick-quail chimaera system was devised by Nicole Le Douarin, who noticed that the interface nuclei of all embryonic and adult cells in the Japanese quail (*Coturnix coturnix japonica*) contained a large amount of heterochromatin which was concentrated in the nucleolus (Le Douarin, 1969 cited in le

FIGURE 8 A photomicrograph showing a longitudinal section through the heart of a chicken host embryo stained with the Feulgen–Rossenbeck method. The section shows the thick interventricular septum (IVS), the left (LV), right ventricles (RV), and the higher magnification of the interventricular septum where the quail nuclei (black arrows) of microinjected cells were located (magnification $\times 200$, a; $\times 1,000$, b)

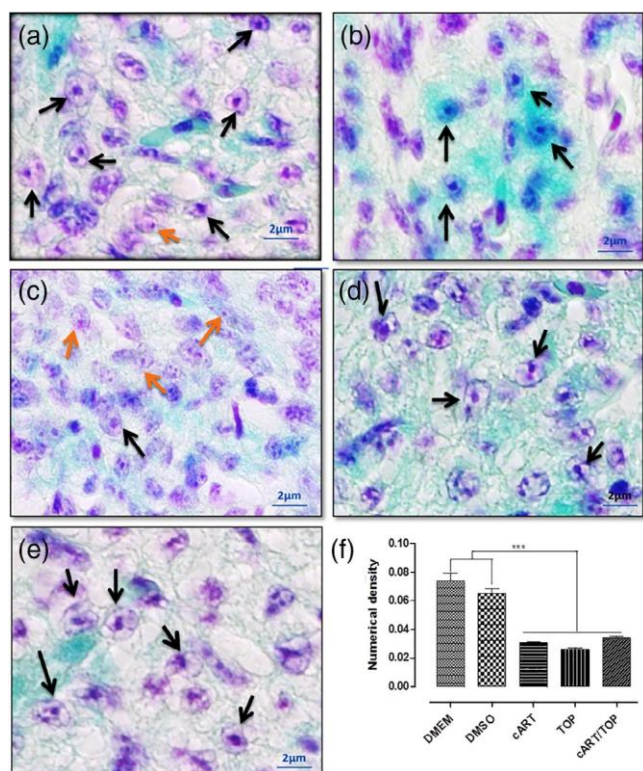
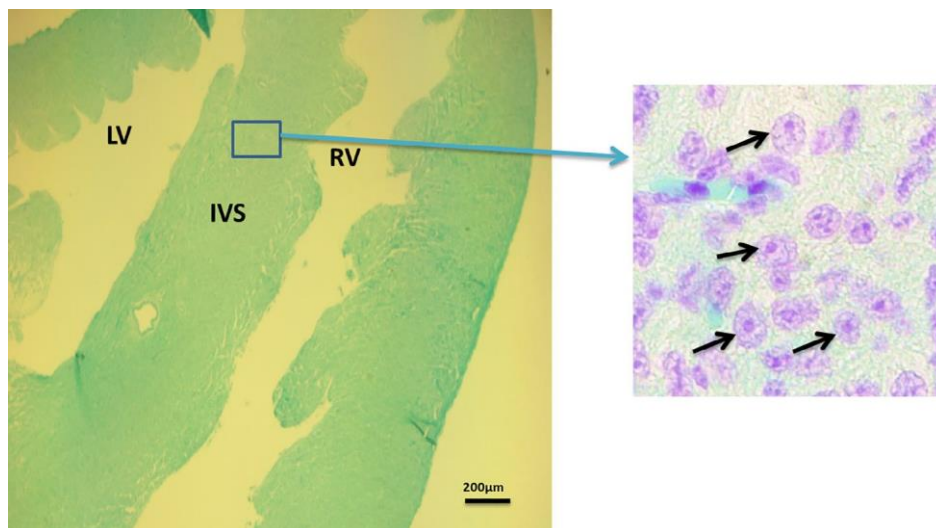


FIGURE 9 Photomicrographs stained with the Feulgen–Rossenbeck method showing quail cardiac neural crest cells injected into chick host embryos (black arrows), while the orange arrows show the nuclei of chick host embryo. (a) Neural crest cells which were cultured in Dulbecco's minimal essential medium (DMEM) only, while (b) shows neural crest cells cultured in dimethyl sulfoxide (DMSO) only. (c) Neural crest cells cultured in Topiramate (TOP), while (d) and (e) show neural crest cells cultured in combined antiretroviral therapy (cART) only and cART/TOP, respectively (magnification $\times 1,000$, oil immersion). (f) The numerical density of injected quail cardiac neural crest cells into chicken host embryos. The numerical density in the treated samples was significantly reduced when compared to the controls

Douarin, 2004) as opposed to the heterochromatin of chicken cells which is evenly distributed within the nucleoplasm (le Douarin, 2004). This feature allowed the quail cells to be distinguished from chick embryonic cells in tissue grafts performed *in vivo* and was successfully applied in the present study with identification of QNC cells in the IVS of the chick embryo.

Our findings in the *in vitro* and *in vivo* studies showed that cART and TOP inhibit the migration of cardiac neural crest cells when administered at concentration of peak plasma levels. This was represented by the significant reduction in the RR of neural crest cells cultured in cART and TOP, and cART/TOP applications. In addition, the significantly decreased numerical density of cells found at the septum in the treated groups indicated that fewer treated neural crest cells migrated to the interventricular septum in the heart of chicken host embryos. These inhibitions imply the absence or reduced number of cardiac NCC at the IVS of the embryo and therefore failure of their contribution toward complete development of IVS. It further suggests the inhibition of migration may be associated with the development of VSDs and highlights the link to the development of VSDs observed in children who are born to mothers on TOP and cART therapy during the first trimester (Hunt et al., 2008; Margulis et al., 2012).

The *in vitro* assay method described by Usami et al. (2014 and 2016), which have been indicated as the ideal method for evaluating the toxicity of chemicals on neural crest cell migration was adopted in this study in cognizance that neural crest cell migration in this assay is determined as a circular spread and cannot be measured linearly. Other methods, such as time-lapse video image analysis of neural crest cells, which are fluorescence tagged (Fuller, Cornelius, Murphy, & Wiens, 2002;

Kawakami, Umeda, Nakagata, Takeo, & Yamamura, 2011) and the scratch assays technique associated with human neural crest cells (Zimmer et al., 2012), have been previously employed (Fuller et al., 2002; Kawakami et al., 2011; Zimmer et al., 2012). However, these are not ideal for investigating the effects of teratogens in developmental toxicity (Usami et al.; 2014 and 2016). To confirm the results of the RR technique, the current study evaluated the actin cytoskeleton of cultured neural crest cells which were treated with cART, TOP, and cART/TOP. The results of the effects of cART, TOP, and cART/TOP were correlated with the migration assay as it has been shown that adverse effects on neural crest cell actin cytoskeleton results in the inhibition of their migration (Haendel, Bollinger, & Baas, 1996). The observed disarrayed arrangement of actin cytoskeleton of treated neural crest cells and the consequent significant reduction in CTCF value, suggest adverse structural effects on the arrangement of actin cytoskeleton which are crucial and play significant role in the inhibition of neural crest cells migration and subsequent specific organ defect. As previously reported, the actin cytoskeleton is very central to the migration of cells, and if perturbed, can disturb the migration of neural crest cells (Lee, 2013; Svitkina, 2018; Tang & Gerlach, 2017).

The results inform caution on coadministration of cART and TOP to pregnant HIV positive women who require treatment for seizures. The study suggests that the occurrence of VSDs involves abnormal migration of cardiac neural crest cells in the presence of cART and TOP, individually and in combination which teratogenic effects appear to be in third week of development as neural crest cells are known to be migrating out of the neural tube in humans during this period (Copp, 2005). Unfortunately, the challenge is that most women are unaware that they are pregnant during the third week of gestation; therefore, the prevention of such defects may be intricate and place management burden on clinicians.

The actin filaments in treated neural crest cells (cART only, TOP only and cART/TOP) were more concentrated at the periphery of the cells as opposed to uniform distribution pattern observed in the controls. This formation of a cortical layer of actin filaments just below the plasma membrane is indicative of transformation from a motile, undifferentiated cell into a nonmotile differentiated cell (Haendel et al., 1996), suggesting its possible role in the rounding of cells (Haendel et al., 1996) and consequent influence on cell migration. Previous report indicated that the cell may use this feature to apply tension on the cell membrane in order to facilitate the addition of extracellular membrane into the cell (Haendel et al., 1996). Although the actin filaments in the cART-treated cells

were confined to the extremities of the cells, the CTCF in these cells was not significantly different to that of the controls. This suggests that cART does not reduce the quantity of cellular actin, but disorders its distribution within the cell.

The cytoskeleton of neural crest cells is designed to contribute to cell division and motility. The structural and shape changes seen in the cytoskeleton of treated neural crest cells may hamper cell motility and subsequently interrupt cell division according to Haendel et al. (1996) leading to malformations. These alterations of the cytoskeletal morphology could be due to the gathering of new filaments and the displacement of original actin filaments from one location in the cell to another as was previously reported (Cramer & Mitchison, 1995). Cultured NCCs are motile, flattened and actively dividing, while differentiated cells are nonmotile and rounded, suggesting that the treatment may influence the differentiation of cardiac neural crest cells, and the consequent failure to reach their destinations in the interventricular septum. An earlier report has shown TOP to be a histone deacetylases (HDAC) inhibitor (Eyal et al., 2004). Another report (Brüning, Jückstock, Kost, Tsikouras, et al., 2017), showed that efavirenz, a component of cART, is able to induce DNA damage and apoptosis in human leukemia cells by regulating the phosphorylation of p53 and H2AX, a subtype of histone protein H2A, suggesting its possible function as an HDAC inhibitor. Furthermore, HDAC 6 (HDAC6) is mostly found in the cytoplasm and is involved in the deacetylation of α -tubulin, a component of microtubules which form a major element of the cytoskeleton (Valenzuela-Fernández, Román Cabrero, Serrador, & Sánchez, 2008). These reports may help to explain the effects of TOP and cART as observed on the actin and cytoskeleton of the treated groups.

Drug–drug interactions are defined as adjustments in the efficacy or toxicity of an individual drug when it is co-administered with another drug at the same time (Farooqui, Hoor, Karim, & Muneer, 2018; Zaporozhan et al., 2019). These interactions may occur due to competitive inhibition, if they are metabolized by the same enzyme or arise if the two drugs have an effect on the same target (Farooqui et al., 2018; Shetty et al., 2018) or may be antagonistic or synergistic. TOP and Efavirenz both induce the cytochrome p450 (CYP3A4) enzymatic system (Nallani et al., 2003; Xu & Desta, 2013). In addition to the CYP3A4 system, efavirenz is metabolized by CYP2B6 (Xu & Desta, 2013). Our findings in the in vitro and in vivo studies suggest that TOP does not affect the activity of cART as there was no significant difference in the RR and numerical density between the cART-only and cART/TOP-treated samples. This suggests that there

is no competitive inhibition taking place between cART and TOP. It is probable that the ability of cART to be metabolized by CYP2B6 in addition to CYP3A4 is what prevents the competitive inhibition between the two classes of drugs. However, the results from the CTCF evaluation suggest that cART could have antagonistic effects to the cytotoxicity of TOP on cardiac NCCs migration, as the combination of cART and TOP seems to negate the decrease in CTCF by TOP. While the present study did not focus on characterization of P450 enzymes involved in the metabolism of TOP and cART, previous reports have indicated that both chicken and quail embryos have the CYP1A1, CYP1A2, CYP2A6, and CYP3A4 cytochrome P450 enzymatic activity; and CYP26C1 being expressed in migrating avian neural crest cells (Diaz, Murcia, & Cepeda, 2010; Li et al., 2017; Reijntjes, Gale, & Maden, 2004). Although TOP and Efavirenz are reported to be metabolized by the CYP3A4 enzymatic system (Nallani et al., 2003; Xu & Desta, 2013), it has not been characterized specifically in avian neural crest cells. Another report indicated that emtricitabine and tenofovir, other components of cART, are not metabolized by the cytochrome P450 system (Masho, Wang, & Nixon, 2007). However, valproic acid, which uses the CYP3A4 system, is metabolized by avian neural crest cells (Fuller et al., 2002), suggesting that neural crest cells have the CYP3A4 enzymatic system.

5 | CONCLUSION

The results of the current study show that both cART and TOP, individually and in combination, inhibit the migration of cardiac neural crest cells, and this could be the basis for the development of VSDs and other associated cardiac anomalies in cART and TOP teratogenicity. In addition, TOP does not seem to affect the activity of Atripla. This is a crucial finding as it suggests that the combination of Atripla and TOP may be suitable for the treatment and management of HIV and seizures which may arise due to viral infection.

ACKNOWLEDGMENT

The study was funded by the enabling grant, Faculty of Health Sciences, University of the Witwatersrand.

DATA AVAILABILITY STATEMENT

The data that support the findings of this study are available from the corresponding author (T. T.) on request.

ORCID

Thabiso Tshabalala  <https://orcid.org/0000-0002-1271-8824>

REFERENCES

- Bancroft, J. (2002). *Theory and practice of histological techniques* (5th ed.). China: Churchill Livingstone.
- Birbeck, G. L., French, J. A., Perucca, E., Simpson, D. M., Fraimow, H., George, J. M., ... Levy, R. H. (2012). Evidence-based guideline: Antiepileptic drug selection for people with HIV/AIDS: Report of the Quality Standards Subcommittee of the American Academy of Neurology and the Ad Hoc Task Force of the Commission on Therapeutic Strategies of the International League Against Epilepsy. *Neurology*, *78*(2), 139–145. <http://dx.doi.org/10.1212/wnl.0b013e31823efc8f>.
- Brogly, S., Abzug, M., Heather Watts, D., Cunningham, C., Williams, P., Oleske, J., ... van Dyke, R. (2010). Birth defects among children born to HIV-infected women: Pediatric AIDS clinical trials protocols 219 and 219C. *Journal of Pediatric Infectious Diseases*, *29*, 721–727. <https://doi.org/10.1097/INF.0b013e3181e74a2f>
- Bronner-Fraser, M. (1996). Manipulations of neural crest cells or their migratory pathways. *Methods in Cell Biology*, *51*, 61–79. [https://doi.org/10.1016/s0091-679x44\(08\)06022-6](https://doi.org/10.1016/s0091-679x44(08)06022-6).
- Brüning, A., Jückstock, J., Kost, B., Tsikouras, P., Weissenbacher, T., Mahner, S., & Mylonas, I. (2017). Induction of DNA damage and apoptosis in human leukemia cells by efavirenz. *Oncology Reports*, *37*, 617–621. doi.org/10.3892/or.2016.5243
- Carrol, A., & Brew, B. (2017). HIV-associated neurocognitive disorders: Recent advances in pathogenesis, biomarkers, and treatment. *F1000Res*, *6*, 312. <https://doi.org/10.12688/f1000research.10651.1>
- Copp, A. (2005). Neurulation in the cranial region—Normal and abnormal. *Journal of Anatomy*, *207*, 623–635. <https://doi.org/10.1016/j.jceb.2018.02.007>
- Cramer, L., & Mitchison, T. (1995). Myosin is involved in postmitotic cell spreading. *Journal of Cell Biology*, *131*(1), 179–189. <https://doi.org/10.1083/jcb.131.1.179>
- Dakkak, W., & Oliver, T. (2019). *Ventricular septal defect*. Treasure Island, FL: STAT Pearls Publishing.
- Diaz, G., Murcia, H., & Cepeda, S. (2010). Cytochrome P450 enzymes involved in the metabolism of aflatoxin B1 in chickens and quail. *Metabolism and Nutrition*, *89*, 2461–2469. doi.org/10.3382/ps.2010-00864
- Eyal, S., Yagen, B., Sobol, E., Altschuler, Y., Shmuel, M., & Bialer, M. (2004). The activity of antiepileptic drugs as histone deacetylase inhibitors. *Epilepsia*, *45*, 737–744. <https://doi.org/10.1111/j.0013-9580.2004.00104.x>
- Farooqui, R., Hoor, T., Karim, N., & Muneer, M. (2018). Potential drug-drug interactions among patients prescriptions collected from medicine out-patient setting. *Pakistan Journal of Medical Sciences*, *34*(1), 144–148. <https://doi.org/10.12669/pjms.341.13986>
- Feulgren, R., & Rossenbeck, H. (1924). Mikroskopisch-chemischer Nachweis einer Nucleinsäure vom Typus der Thymonucleinsäure und die darauf beruhende elektive Färbung von Zellkernen in mikroskopischen Präparaten. *Hoppe-Seyler's Zeitschrift für physiologische Chemie*, *135*(5-6), 203–248. <http://dx.doi.org/10.1515/bchm2.1924.135.5-6.203>
- Ford, N., Migone, C., Calmy, A., Kerschberger, B., Kanters, S., Nsanzimana, S., ... Shubber, Z. (2018). Benefits and risks of rapid initiation of antiretroviral therapy. *Aids*, *32*(1), 17–23. <https://doi.org/10.1097/QAD.0000000000001671>

- Fuller, L., Cornelius, S. K., Murphy, C., & Wiens, D. (2002). Neural crest cell motility in valproic acid. *Reproductive Toxicology*, *16*, 825–839.
- Haendel, M., Bollinger, K., & Baas, P. (1996). Cytoskeletal changes during neurogenesis in cultures of avian neural crest cells. *Journal of Neurocytology*, *25*, 289–301.
- Hamburger, V., & Hamilton, H. (1951). A series of normal stages in the development of the chick embryo. *Journal of Morphology*, *88*, 49–92. doi.org/10.1002/jmor.1050880104
- Hunt, S., Russell, A., Smithson, W., Parsons, L., Robertson, I., Waddell, R., ... UK Epilepsy and Pregnancy Register. (2008). Topiramate in pregnancy. *Neurology*, *71*(4), 272–276. https://doi.org/10.1212/01.wnl.0000318293.28278.33
- Hutson, M., & Kirby, M. (2003). Neural crest and cardiovascular development: A 20-year perspective. *Birth Defects Research. Part C, Embryo Today*, *69*(1), 2–13. https://doi.org/10.1002/bdrc.10002
- Jungmann, E., Mercey, D., DeRuiter, A., Edwards, S., Donoghue, S., Booth, T., ... Taylor, G. (2001). Is first trimester exposure to the combination of antiretroviral therapy and folate antagonists a risk factor for congenital abnormalities? *Sexually Transmitted Infections*, *77*, 441–443. https://doi.org/10.1136/sti.77.6.441
- Kawakami, M., Umeda, M., Nakagata, N., Takeo, T., & Yamamura, K. (2011). Novel migrating mouse neural crest cell assay system utilizing P0-Cre/EGFP fluorescent time-lapse imaging. *BMC Developmental Biology*, *11*, 68.
- Kim, H. K., Chin, B. S., & Shin, H.-S. (2015). Clinical features of seizures in patients with human immunodeficiency virus infection. *Journal of Korean Medical Science*, *30*, 694–699. https://doi.org/10.3346/jkms.2015.30.6.694
- Kirby, M., Gale, T., & Stewart, D. (1983). Neural crest cells contribute to aorticopulmonary septation. *Science*, *220*, 1059–1061. https://doi.org/10.1126/science.6844926
- Knapp, K. M., Brogly, S. B., Muenz, D. G., Spiegel, H. M., Conway, D. H., Scott, G. B., ... Read, J. S. (2012). Prevalence of congenital anomalies in infants with in utero exposure to antiretrovirals. *Journal of Pediatric Infectious Diseases*, *31*(2), 164–170.
- le Douarin, N. (2004). The avian embryo as a model to study the development of the neural crest: A long and still ongoing story. *Mechanisms of Development*, *129*, 1089–1102. https://doi.org/10.1016/j.mod.2004.06.003
- Le Douarin, N., & Houssaint, E. (1969). Mise en évidence des cellules phéochromes dans le mésenchyme métanéphritique de Poulet évoluant en l'absence de l'uretère. *C. R. Soc. Biol*, *163*, 505–508.
- Le Douarin, N. M., & Teillet, M.-A. M. (1974). Experimental analysis of the migration and differentiation of neuroblasts of the autonomic nervous system and of neuroectodermal mesenchymal derivatives, using a biological cell marking technique. *Developmental Biology*, *41*(1), 162–184. http://dx.doi.org/10.1016/0012-1606(74)90291-7.
- Lee, J. (2013). The actin cytoskeleton and the regulation of cell migration. Colloquium series on building blocks of the cell. *Cell Structure and Function*, *1*, 1–71.
- Li, G., Simmler, C., Chen, L., Nikolic, D., Chen, S., Pauli, G. F., & van Breemen, R. B. (2017). Cytochrome P450 inhibition by three licorice species and fourteen licorice constituents. *European Journal of Pharmaceutical Sciences*, *109*, 182–190. https://doi.org/10.1016/j.ejps.2017.07.034
- Margulis, A., Mitchell, A., Gilboa, S., Werler, M., Mittleman, M., & Glynn, R. (2012). Use of topiramate in pregnancy and risk of oral clefts. *American Journal of Obstetrics and Gynecology*, *207*(5), 405.e1–405.e7. https://doi.org/10.1001/jama.2011.624
- Masho, S., Wang, C., & Nixon, D. (2007). Review of tenofovir-emtricitabine. *Therapeutics and Clinical Risk Management*, *3* (6), 1097–1104.
- McCloy, R. A., Rogers, S., Caldon, C. E., Lorca, T., Castro, A., & Burgess, A. (2014). Partial inhibition of Cdk1 in G2 phase overrides the SAC and decouples mitotic events. *Cell Cycle*, *3*, 1400–1412. https://doi.org/10.4161/cc.28401
- Mehta, U., van Schalkwyk, C., Naidoo, P., Ramkissoon, A., Mhlongo, O., Maharaj, N., ... Moran, N. (2019). Birth outcomes following antiretroviral exposure during pregnancy: Initial results from a pregnancy exposure registry in South Africa. *Southern African Journal of HIV Medicine*, *20*(1), 971–982.
- Molgaard-Nelsen, D., & Hviid, A. (2011). Newer-generation antiepileptic drugs and the risk of major birth defects. *Journal of the American Medical Association*, *305*(19), 1996–2002. https://doi.org/10.1001/jama.2011.624
- Nallani, S., Glauser, T., Hariparsad, N., Setchell, K., Buckley, D., Buckley, A., & Desai, P. (2003). Dose-dependent induction of cytochrome P450 (CYP) 3A4 and activation of pregnane X receptor by Topiramate. *Epilepsia*, *44*, 1521–1528. https://doi.org/10.1111/j.0013-9580.2003.06203
- Ornoy, A., Zvi, N., Arnon, J., Wajnberg, R., Shechtman, S., & Diav-Citrin, O. (2008). The outcome of pregnancy following topiramate treatment: A study on 52 pregnancies. *Reproductive Toxicology*, *25*(3), 388–389. https://doi.org/10.1016/j.reprotox.2008.03.001
- Pawitan, J., & Tanzil, R. (1995). Application of Feulgen-light green staining method to show the micronuclei in fetal rat blood. *Medical Journal of Indonesia*, *4*, 280. https://doi.org/10.13181/mji.v4i4.928
- Phiri, K., Hernandez-Diaz, S., Dugan, K. B., Williams, P. L., Dudley, J. A., Jules, A., ... Cooper, W. O. (2014). First trimester exposure to antiretroviral therapy and risk of birth defects. *The Pediatric Infectious Disease Journal*, *33*(7), 741–746. https://doi.org/10.1097/INF.0000000000000251
- Prieto, L., González-Tomé, M., Muñoz, E., Fernández-Ibieta, M., Soto, B., Álvarez, A., ... the Madrid Cohort of HIV-Infected Mother-Infant Pairs. (2014). Birth defects in a cohort of infants born to HIV-infected women in Spain, 2000–2009. *BMC Infectious Diseases*, *14*, 700. https://doi.org/10.1186/s12879-014-0700-3
- Radhakrishna, U., Albayrak, S., Zafra, R., Baraa, A., Vishweswaraiyah, S., Veerappa, A. M., ... Bahado-Singh, R. O. (2019). Placental epigenetics for evaluation of fetal congenital heart defects: Ventricular septal defect (VSD). *PLoS One*, *14*(3), e0200229.
- Reijntjes, S., Gale, E., & Maden, M. (2004). Generating gradients of retinoic acid in the chick embryo: Cyp26C1 expression and a comparative analysis of the Cyp26 enzymes. *Patterns and Phenotypes*, *230*, 509–517. doi.org/10.1002/dvdy.20025
- Ribatti, D. (2019). Nicole Le Douarin and the use of quail-chick chimeras to study the developmental fate of neural crest and hematopoietic cells. *Mechanism of Development*, *158*, 103557. https://doi.org/10.1016/j.mod.2019.103557
- Shetty, V., Chowta, M., Chowta, N., Shenoy, A., Kamath, A., & Kamath, P. (2018). Evaluation of potential drug-drug

interactions with medications prescribed to geriatric patients in a tertiary care hospital. *Journal of Aging Research*, 2018, 1–6. <https://doi.org/10.1155/2018/5728957>

Siddiqi, O., & Birbeck, G. L. (2013). Safe treatment of seizures in the setting of HIV/AIDS. *Current Treatment Options in Neurology*, 15(4), 529–543. <https://doi.org/10.1007/s11940-013-0237-6>

Siddiqi, O., Elafros, C. M., Bositis, I. J., Korálnik, W. H., Theodore, J. F., & Okulicz, J. (2017). New-onset seizure in HIV-infected adult Zambians: A search for causes and consequences. *Neurology*, 88, 477–482. <https://doi.org/10.1212/WNL.0000000000003538>

0000000000003538

Ssentongo, P. (2019). Prevalence and incidence of new-onset seizures and epilepsy in patients with human immunodeficiency virus (HIV):

Systematic review and meta-analysis. *Epilepsy Behavior*, 93, 49–55. <https://doi.org/10.1016/j.yebeh.2019.01.033>

Opinion in Cell Biology, 54, 1–8.

Tang, D., & Gerlach, B. (2017). The roles and regulation of the actin cytoskeleton, intermediate filaments and microtubules in smooth muscle cell migration. *Respiratory Research*, 18(1), 54–65. <https://doi.org/10.1186/s12931-017-0544-7>

Tennis, P., Chan, A., Curkendall, M., Li, K., Mines, D., Peterson, C.,

... Esposito, B. (2015). Topiramate use during pregnancy and major congenital malformations in multiple populations. *Birth Defects Research. Part A, Clinical and Molecular Teratology*, 103, 269–275. <https://doi.org/10.1002/bdra.23357>

Usami, M., Mitsunaga, K., Irie, T., Miyajima, A., & Doi, O. (2014). Simple in vitro migration assay for neural crest cells and the opposite effects of all-trans-retinoic acid on cephalic- and trunk-derived cells. *Congenital Anomalies*, 54, 184–188. <https://doi.org/10.1111/cga.12059>

Usami, M., Mitsunaga, K., Miyajima, A., Takamatu, M., Kazama, S., & Irie, T. (2016). Effects of 13 developmentally toxic chemicals on the migration of rat cephalic neural crest cells in vitro. *Congenital Anomalies*, 56, 52–59. <https://doi.org/10.1111/cga.1212>

Valenzuela-Fernández, A., Román Cabrero, J., Serrador, J., & Sánchez, F. (2008). HDAC6: A key regulator of cytoskeleton, cell migration and cell–cell interactions. *Trends in Cell Biology*, 18, 291–297. doi.org/10.1016/j.tcb.2008.04.003

Valle, C., & Hadley, M. (2018). Truncus arteriosus. In D. DeFaria Yeh & A. Bhatt (Eds), *Adult Congenital Heart Disease in Clinical Practice* (pp. 319–330). Cham: Springer. https://doi.org/10.1007/978-3-319-67420-9_24

Vannappagari, V., Koram, N., Albano, J., Tilson, H., & Gee, C. (2016). Association between in utero zidovudine exposure and nondefect adverse birth outcomes: Analysis of prospectively

Waldo, K., Miyagawa-Tomita, S., Kumiski, D., & Kirby, M. (1998). Cardiac neural crest cells provide new insight into septation of the cardiac outflow tract: Aortic sac to ventricular septal closure. *Developmental Biology*, 196, 129–144. <https://doi.org/10.1006/dbio.1998.8860>

Walubo, A. (2007). The role of cytochrome P450 in antiretroviral drug interactions. *Expert Opinion on Drug Metabolism & Toxicology*, 4, 583–598. <https://doi.org/10.1517/17425225.3.4.583>

Watts, D., Covington, D., Beckerman, K., Susan, S., Chavers, S., & Tilson, H. (2004). Assessing the risk of birth defects associated with antiretroviral exposure during pregnancy. *Fetal Medicine*, 191, 985–992. <https://doi.org/10.1016/j.ajog.2004.05.061>

Watts, D. H. (2006). Treating HIV during pregnancy: An update on safety issues. *Drug Safety*, 29(6), 467–490. <https://doi.org/10.2165/00002018-200629060-00002>

Williams, P. L., Crain, M. J., Yildirim, C., Hazra, R., vanDyke, R. B., Rich, K., ... Watts, D. H. (2015). Congenital anomalies and in utero antiretroviral exposure in human immunodeficiency virus-exposed uninfected infants. *JAMA Pediatrics*, 169(1), 48–55.

Xu, C., & Desta, Z. (2013). In vitro analysis and quantitative prediction of efavirenz inhibition of eight cytochrome P450 (CYP) enzymes: Major effects on CYPs 2B6, 2C8, 2C9 and 2C19. *Drug Metabolism and Pharmacokinetics*, 28(4), 362–371.

Zaporojan, L., PH, M. N., Williams, J. A., Bergin, C., Redmond, J., & Doherty, C. P. (2019). Seizures in HIV: The case for special consideration. *Epilepsy & Behavior Case Reports*, 10, 38–43.

Zimmer, B., Lee, G., Balmer, N. V., Meganathan, K., Sachinidis, A., Studer, L., & Leist, M. (2012). Evaluation of developmental toxicants and signaling pathways in a functional test based on the migration of human neural crest cells. *Environmental Health Perspectives*, 120, 1116–1122.

How to cite this article: Tshabalala T, Nkomozezi P, Ihunwo AO, Mbajjorgu F. Coadministration of ARV (Atripla) and Topiramate disrupts quail cardiac neural crest cell migration.

Birth Defects Research. 2021;1–15. <https://doi.org/10.1002/bdr2.1871>

ftNGQ5OS05MjU4LWM3NjY2MTE3NzQ4YQAAH8NQ9Ywa4pCpVR8mx7%2FDmM%3D?state=0

Categorize ▾ ...

Congenital Anomalies - Manuscript ID CGA-12-2020-128

CA Congenital Anomalies <onbehalf@manuscriptcentral.com>
>

Mon 12/7/2020 3:24 PM
To: Thabiso Tshabalala
Cc: Thabiso Tshabalala; Amadi Ihunwo; Pilanin@uj.ac.za; Ejikeme Mbajorgu

07-Dec-2020

Dear Mr. Tshabalala:

Your manuscript entitled "The effects of co-administration of combination antiretroviral therapy and Topiramate on cranial neural crest cell migration: impact on congenital craniofacial anomalies" by Tshabalala, Thabiso; Ihunwo, Amadi; Nkomozepe, Pilani; Mbajorgu, Ejikeme, has been successfully submitted online and is presently being given full consideration for publication in Congenital Anomalies.

Co-authors: Please contact the Editorial Office as soon as possible if you disagree with being listed as a co-author for this manuscript.

Your manuscript ID is CGA-12-2020-128.

Please mention the above manuscript ID in all future correspondence or when calling the office for questions. If there are any changes in your street address or e-mail address, please log in to Manuscript Central at <https://mc.manuscriptcentral.com/cga> and edit your user information as appropriate.

You can also view the status of your manuscript at any time by checking your Author Center after logging in to <https://mc.manuscriptcentral.com/cga>.

Address for the Editorial Office
Professor Toshihisa Hatta, Editor-in-Chief, Congenital Anomalies
c/o Department of Anatomy, Kanazawa Medical University



STRICTLY CONFIDENTIAL

ANIMAL RESEARCH ETHICS COMMITTEE (AREC)

CLEARANCE CERTIFICATE NO. 2019/01/2/A

APPLICANT: Mr T Tshabalala

SCHOOL: Anatomical Sciences

DEPARTMENT:

LOCATION:

PROJECT TITLE: The effect of Atripla and Bedaquiline and Topiramate on the migration of quail neural crest cells in vitro

Number and Species

80 eggs X2 =160 Quail Eggs

Approval was given for the use of animals for the project described above at an AREC meeting held on 2019/01/29. This approval remains valid until 2021/02/20.

Unreported changes to the application may invalidate the clearance given by the AREC

An annual progress report must be provided

The use of these animals is subject to AREC guidelines for the use and care of animals, is limited to the procedures described in the application form and is subject to any additional conditions listed below:

Signed: [Signature] Date: 09th May 2019
(Chairperson, AREC)

I am satisfied that the persons listed in this application are competent to perform the procedures therein, in terms of Section 23 (1) (c) of the Veterinary and Para-Veterinary Professions Act (19 of 1982)

Signed: [Signature] Date: 09 May 2019
(Registered Veterinarian)

cc: Supervisor: N/A
Director: CAS

Works 2000/In0015/AESCCErt.wps

ORIGINALITY REPORT

25%

SIMILARITY INDEX

3%

INTERNET SOURCES

22%

PUBLICATIONS

3%

STUDENT PAPERS

PRIMARY SOURCES

-
- | | | |
|----------|--|------------|
| 1 | Thabiso Tshabalala, Pilani Nkomozepe, Amadi Ogonda Ihunwo, Felix Mbajiorgu. "Coadministration of (Atripla) and Topiramate disrupts quail cardiac neural crest cell migration", Birth Defects Research, 2021
Publication | 22% |
| 2 | Submitted to University of Witwatersrand
Student Paper | 2% |
| 3 | wiredspace.wits.ac.za
Internet Source | 2% |
-
-

Appendix B

Instruments

1 fine forceps

1 fine scalpel

Insect pins

1 spoon

Coarse scissors

Other equipment

1 bottle 70% alcohol

1 bottle 90% alcohol

Gill soap

Towel, plastic sheeting

Alcohol burner + matches

Solutions

Chick Ringer's solution

8.5g sodium chloride

0.42g potassium chloride

0.25g calcium chloride

1000 ml distilled water

100 μ l pen-strep antibiotic

Tyrode's solution

Solution A

500 ml distilled water

2.0g sodium chloride

0.05 potassium chloride

0.012g $\text{N}_2\text{H}_2\text{PO}_4\text{H}_2\text{O}$

Solution B

480 ml distilled water

0.025g NAHCO_3

1g glucose was mixed in 20 ml distilled water in a 100 ml bottle and placed in the fridge. Solutions A and B were autoclaved separately, and the swinnexed glucose mixture was added to the solutions. 100 μl pen-strep antibiotic was added to the final solution.

Collagenase

0.0025g collagenase + 6 ml Tyrode's solution

The mixture was refrigerated before use

Culture medium

75 % Dulbecco's minimal essential medium (DMEM)

15 % Embryo extract

10 % Horse serum

DMSO

DMSO was dissolved in DMEM (concentration 10^{-5}M)

Rhodamine Phalloidin

5 μl rhodamine phalloidin + 300 μl PBS

Fibronectin

25 μl in 1ml sterile distilled water

Solubilization buffer pH 8.0

To make 250 ml of the solution

5.0g deoxycholate

0.3g Tris

Tris buffer, pH 7.1

To make 50 ml of the solution

0.01g Tris

Stacking Gel Solution (4% Acrylamide): (for testing PCR product)

H₂O	3.075 ml
0.5 M Tris-HCl, pH 6.8	1.25 ml
20% (w/v) SDS	0.025 ml
Acrylamide/Bis-acrylamide (30%/0.8% w/v)	0.67 ml
10% (w/v) ammonium persulfate (APS)	0.025 ml
TEMED	0.005 ml

Silane dipped slides

Soak slides in 10 % Contrad or Super 10 overnight

Rinse in hot running water-minimum-2 hours

Dry in oven at 60°C

Dip in acetone

Dip in 2% silane in acetone for 30 minutes (6ml silane + 294 ml acetone)

Wash in two changes of acetone

Wash briefly in distilled water

Dry in 42°C incubator overnight.

Phosphate Buffered Saline (PBS)

8g NaCl

0.2g KCl

1.15g Na₂HPO₄

0.2g KH_2PO_4

Embryo extract preparation

Glassware and solutions were sterilized the preceding day. Eleven-day-old chick eggs were cleaned with 70% alcohol, and broken into a glass dish containing a small amount of chick Ringer's solution. The head was cut off, and both the head and body were placed into another sterile glass dish, and washed. Four embryos were prepared in this manner. The prepared embryos were inserted into a 20ml syringe. Five ml was then expressed into a sterile graduated centrifuge tube. Five ml Ringer's solution was added, and the contents were stirred with a glass rod. The contents were covered and left to stand at room temperature for one hour. Following this, the suspension was spun for 20 minutes at 2000g. After spinning, the supernatant was poured into sterile bijoux bottle and frozen until use.

India ink

1ml in 99mls Chick Ringer's solution

Feulgen reaction (Feulgen and Rossenbeck, 1924)

The paraffin sections of the chick heads or whole embryos were brought to distilled water. The sections were briefly rinsed in cold NHCL and transferred to NHCL at 60°C for 8 minutes. As controls, similar sections of each embryo were placed in distilled water at 60°C for the same period of time. After washing in distilled water, the sections were transferred to Schiff's reagent for 60 minutes. The sections were rinsed in three changes of sulphite rinse solution (see appendix), and then in water. The sections were counterstained in 1% aqueous light green for 1 minute, dehydrated, cleared and mounted in entellan. As a positive control, for the Feulgen-Rossenbeck method, six day old quail embryos were used.

Alizarin Red Solution:

Alizarin Red S (C.I. 58005) ----- 2 g

Distilled water ----- 100 ml

Mix well. Adjust the pH to 4.1~4.3 with 10% ammonium hydroxide.

Acetone-Xylene:

Acetone (100%) ----- 50 ml

Xylene ----- 50 ml